Universitat de Girona
Escola Politècnica Superior

Final Year Project

Degree: Chemical Engineering

Title: Contribution of the European Chemical Industry to the Planetary Boundaries

Document: Project report

Student: Irene Barnosell Roura

Tutor: Carlos Pozo Fernandez

Department: Enginyeria Química, Agrària i Tecnologia Agroalimentària (EQATA)

Area: Chemical engineering

Call (month/year): June/2021

INDEX

1 Introduction 13
1.1 Background 13
1.2 Methodology 17
2 Goals of the study 23
3 Chemical Industry 25
4 Characterization of the European chemical sector 26
4.1 Selected chemicals and processes 28
4.1.1 Acrylonitrile 28
4.1.2 Ammonia 29
4.1.3 Benzene 32
4.1.4 Cumene 34
4.1.5 Ethylene 36
4.1.6 Ethylene glycol 38
4.1.7 Ethylene oxide 39
4.1.8 Methanol 41
4.1.9 Xylene 42
4.1.10 Polyethylene 43
4.1.11 Polypropylene 49
4.1.12 Propylene 50
4.1.13 Propylene oxide 51
4.1.14 Styrene 52
4.1.15 Terephthalic acid 54
4.1.16 Toluene 55
4.1.17 Vinyl chloride 55
4.2 Interrelations between processes 58
5 Earth Systems 65
6 Planetary boundaries 68
6.1 Climate change 70
6.2 Ocean acidification 73
6.3 Stratospheric ozone depletion 74
6.4 Biogeochemical flows 78
6.5 Land system change 85
6.6 Freshwater use 87
6.7 Atmospheric aerosol loading 90
6.8 Included planetary boundaries 92

7 Life Cycle Assessment 93
7.1 Phases of LCA 95
7.1.1 Goal and scope definition 95
7.1.2 Life cycle inventory 102
7.1.3 Life cycle impact assessment 104
7.1.4 Interpretation of results 109
8 Application of the PB-LCIA damage assessment model 110
8.1 Collection of data on elementary flows (LCI phase) 110
8.2 Treatment of LCI data 111
8.3 Characterization of LCIs in terms of their contribution to the planetary boundaries (LCIA phase). 113
8.4 Modelling impacts 115
8.5 Allocation of the safe operating space 116
8.5.1 Definition of the safe operating space 116
8.5.2 Assigning the share of safe operating space to the studied sector and region 117
9 Data Quality Analysis 124
9.1 Data Quality Indicators 127
9.1.1 Geographical coverage 127
9.1.2 Technological coverage 127
9.1.3 Temporal coverage 128
9.1.4 Completeness 128
9.1.5 Reliability 130
9.2 Assigned scores for all studied chemicals 130
9.3 Uncertainty study 131
10 Results and discussion 135
10.1 Environmental performance of the European chemical industry 135
10.1.1 Egalitarian allocation 137
10.1.2 Non-egalitarian allocation 151
10.1.3 Criteria for the downscaling of the planetary boundaries 155
10.2 Impact breakdown 162
10.2.1 Climate change and ocean acidification 166
10.2.2 Stratospheric ozone depletion 171
10.2.3 Biogeochemical flows (N and P) 172
10.2.4 Land system change 174
10.2.5 Freshwater use 176
10.2.6 Aerosol loading 178
10.3 Impact distribution 180

10.4 Potential improvement pathways 181
10.4.1 Energy mix 182
10.4.2 Carbon capture and storage (CCS) 188
10.4.3 Green hydrogen production and chlor-alkali electrolysis powered with renewable energy 210
10.4.4 Summary of improvement pathways 214
11 Conclusions 217
12 Planning and budgeting 224
12.1 Planning 224
12.2 Costs 226
12.2.1 Labour force 226
12.2.2 Software 226
12.2.3 Indirect costs 226
12.2.4 Total cost 227
13 Bibliography 228

FIGURE INDEX

Fig. 1-1: Methodology of the study. 17
Fig. 1-2: Figure illustrating the concept of LCIs. 18
Fig. 4-1: Average energy consumption per chemical versus total production volume within EU-28. 27
Fig. 4-2: Average GHG emissions versus production volume per chemical within EU-28. 27
Fig. 4-3: Process flow diagram for the production of acrylonitrile through the SOHIO process (adapted from Cespi et al., 2014). 29
Fig. 4-4: Process flow diagram for the catalytic reforming process (adapted from RBN Energy, 2014; Speight, 2020). . 34
Fig. 4-5: Process flow diagram for production of cumene through alkylation of benzene and propylene (adapted from Alghamdi et al., 2019). 36
Fig. 4-6: Process flow diagram of the steam cracking of naphtha (Haghighi et al., 2013). 38
Fig. 4-7: Process flow diagram for the production of ethylene glycol by the hydrolysis of ethylene oxide (adapted from Rebsdat & Mayer, 2012a). 39
Fig. 4-8: Process flow diagram for the production of ethylene oxide from ethylene (adapted from Rebsdat & Mayer, 2012b). 40
Fig. 4-9: Process flow diagram for the production of methanol by steam reforming (adapted from Douglas & Hoadley, 2006; Udugama, 2017). 42
Fig. 4-10: Main types of PE (Malkan, 2017)..... 43
Fig. 4-11: Process flow diagram for the production of PE by the autoclave process (adapted from Kehinde et al., 2012; Quachio et al., 2012; Lingell, 2015). 45
Fig. 4-12: Process flow diagram for the gas phase polymerization of ethylene (adapted from Fernandes & Lona, 2000; Sun et al., 2020). 47
Fig. 4-13: Process flow diagram of the solution process for the production of polyethyelene (adapted from Encyclopaedia Britannica, 2017). 48
Fig. 4-14: Process flow diagram of the slurry process for the production of PE (adapted from Kosek & Ray, 1999). 49
Fig. 4-15: Process flow diagram of the chlorohydrin process (adapted from Matar & Hatch, 2001; Nijhuis et al., 2006). 52
Fig. 4-16: Process flow diagram of the dehydrogenation of ethylbenzene process (adapted from Chadwick, 2000; Zarubina, 2015). 54
Fig. 4-17: Process flow diagram of the oxidation of p-xylene process (adapted from Han et al., 2003; Sheehan, 2011). 55
Fig. 4-18: Process flow diagram of the combination of the direct chlorination and oxychlorination of ethylene to produce vinyl chloride (adapted from Ferreira et al., 2020). 57
Fig. 4-19: Sankey diagram illustrating the issue with double-counting impacts taking the manufacturing process of polyethylene from ethylene as an example. 58
Fig. 4-20: Example breakdown of the LCIs for PE. 59
Fig. 4-21: Selected chemicals and their interrelationships. 62
Fig. 5-1: Behaviour differences between Earth Systems (Rockström et al., 2009). 66
Fig. 5-2: Current state of the PBs. 67
Fig. 6-1: Distribution of nitrogen (Steffen et al., 2015)..... 80
Fig. 6-2: Distribution of phosphorus (Steffen et al., 2015). 84
Fig. 6-3: Tropical (green), temperate (blue) and boreal (brown) forest biomes distribution..... 86
Fig. 6-4 Current state of the freshwater use risk index (Steffen et al., 2015). 90
Fig. 7-1: Links between LCA phases. 95
Fig. 7-2: Scope definition in LCA. 96
Fig. 7-3: Sankey diagram depicting the comparison between one- and two-echelon chains. 99
Fig. 7-4: Section of the impact pathway for global warming (adapted from Hauschild & Huijbregts, 2015; Li et al., 2019). 105
Fig. 7-5: PB-LCIA methodology linking LCA and the PBs framework. 106
Fig. 7-6: Effect factor approaches zero if the current state is the same or below the target (Huijbregts, 2011). Example for the state of macroinvertebrate communities in freshwater ecosystems depending on the phosphorus concentration. . 109
Fig. 8-1: Methodology of the LCI phase..... 110
Fig. 8-2: Difference in derivation and modelling between conventional LCIA methods and PB-LCIA (Ryberg et al., 2018b). 113
Fig. 8-3: Egalitarian allocation of the SOS narrowing down from global PBs to a European level, then the European chemical industry and finally the chemicals and processes under study. 119
Fig. 8-4: Adjustment of GVA using harmonized consumer price indexes to calculate cumulative inflation. 121
Fig. 9-1: Matrix containing the 100 potential contributions of each of the 23 chemicals in each of the 9 PBs. 133
Fig. 9-2: Matlab figure representing the generated impact scenarios for all PBs. 134
Fig. 10-1: Fractions of deforested and reforested land as a consequence of the chemical industry's activity. 146
Fig. 10-2: Freshwater withdrawal and return as a consequence of the chemical industry's activity. 147
Fig. 10-3: Contributions of chemicals to the nine PBs (EUSoSOS). 148
Fig. 10-4: Contributions of chemicals to the nine PBs (EUCISoSOS). 149
Fig. 10-5: Contributions of chemicals to the nine PBs (FSoSOS). 150
Fig. 10-6: Contributions of chemicals to the nine PBs (SQSoSOS). 154
Fig. 10-7: Predictions on the state of the PBs assuming the current consumption patterns are maintained for the years 2030, 2050 and 2100. 158
Fig. 10-8: Breakdown of the impacts to the nine studied PBs with chemicals sorted according to their production volume. 164
Fig. 10-9: Breakdown of the impacts on the nine studied PBs where the percentages over the total contribution to each threshold are shown for all activities with a burden representing ≤1% of the total. 165
Fig. 10-10: Total GHG emissions (kg) per kg of chemical. 166
Fig. 10-11: CO_2 emissions (kg) per kg of chemical. 168
Fig. 10-12: Total emissions of ODS (kg) and dinitrogen monoxide per kg of chemical. 171
Fig. 10-13: Nitrate emissions to surface water (kg) per kg of chemical. 173

Fig. 10-14: Phosphate emissions to surface water (kg) per kg of chemical. 173
Fig. 10-15: Deforested land (m^2) and reforested land (m^2) per kg of chemical. 176
Fig. 10-16: Total withdrawn water (L) and returned water (L) per kg of chemical. 177
Fig. 10-17: ODS emissions (kg) per kg of chemical. 179
Fig. 10-18: High voltage electricity mix for the European region (average technology mix used by ecoinvent) as compared with the proposed renewable mix. 184
Fig. 10-19: Schematic representation a DACCS system (adapted from Fridahl et. al., 2020). 190
Fig. 10-20: Impact reduction with respect to the current situation achieved by the implementation of DACCS in terms of % over the total contribution to each PB in the current scenario (conservative scenario: BAU mix and cancellation of only CO_2 emissions). 192
Fig. 10-21: Schematic representation of the concept behind BECCS (Fridahl et. al., 2020). 198
Fig. 10-22: Impact reduction with respect to the current situation achieved by the implementation of BECCS in terms of % over the total contribution to each PB in the current scenario (conservative scenario: BAU mix and cancellation of only CO_2 emissions). 200
Fig. 10-23: Carbon capture and storage capacities required to fulfil the goals of the eight modelled scenarios (million tonnes CO2), where RM: renewable mix; BAU: business and usual mix. 205
Fig. 10-24: Land requirements of all BECCS scenarios (land in km^2yr necessary to grow the biomass for the process). 209
Fig. 10-25: Summary of improvement pathways where the % of total improvement or worsening of the occSoSOS is represented for each included scenario. 216
Fig. 12-1: Gantt diagram showing the planning of the study elaborated in Microsoft Project. 225

TABLE INDEX

Table 4-1: Processes used to produce the three main types of PE. 44
Table 6-1: Relationship between the original nitrogen and phosphorus threshold values (in green) and those obtained through the N:P ratio (in black). 84
Table 6-2: Calculated maximum amount of freshwater withdrawal (%). 89
Table 6-3: Briefing of the Earth-system processes linked to a PB considered in the present study. 92
Table 7-1: Interlinks between the studied chemicals. 100
Table 7-2: Data Quality Goals. 101
Table 7-3: Initial phase of LCA. 102
Table 8-1: SOS assigned to each PB considering natural contributions. 117
Table 8-2: Remaining SOS for each PB. 117
Table 8-3: Sectorial and national sharing principles for the allocation of the planetary SOS. 123
Table 9-1: Data Quality Goals. 125
Table 9-2: Pedigree matrix (Weidema et al., 1996 revised by Ciroth et al., 2008). Between brackets is the adapted version by (Ciroth et al., 2016) for ecoinvent v3. 126
Table 9-3: Levels of geographical specificity UN (United Nations, 2013; Weidema & Wesnaes, 1996). 127
Table 9-4: Specifications for the completeness category. 130
Table 9-5: Completed pedigree matrix (RS: Reliability of Source; C: Completeness; TD: Temporal Differences; GD: Geographical Differences; FTD: Further Technological Differences). 131
Table 10-1: Large differences between both values cause a small SoSOS to be assigned to the PB. 152
Table 10-2: Summary heat map of the results (occSoSOS) obtained using the different allocation procedures. 160
Table 10-3: Top contributors to all boundaries. 180
Table 10-4: Final contributions to the PBs when the renewable energy mix is used. 185
Table 10-5: Impact reduction with respect to the current situation achieved by the implementation of DACCS (conservative scenario: BAU mix and cancellation of CO_2 emissions). 191
Table 10-6: Impact reduction with respect to the current situation achieved by the implementation of DACCS (BAU mix and aiming for the fraction of occupied SoSOS for the energy imbalance PB to be equal to zero). 195
Table 10-7: Impact reduction with respect to the current situation achieved by the implementation of DACCS (sustainable mix and cancellation of CO_2 emissions). 196
Table 10-8: Impact reduction with respect to the current situation achieved by the implementation of DACCS (sustainable mix and aiming for the fraction of occupied SoSOS for the energy imbalance PB to be equal to zero). 197
Table 10-9: Impact reduction with respect to the current situation achieved by the implementation of BECCS (conservative scenario: BAU mix and cancellation of CO_2 emissions). 199
Table 10-10: Impact reduction with respect to the current situation achieved by the implementation of BECCS (conservative scenario: BAU mix and cancellation of CO_2 emissions). 201
Table 10-11: Impact reduction with respect to the current situation achieved by the implementation of BECCS (renewable mix and cancellation of CO_2 emissions). 202
Table 10-12: Impact reduction with respect to the current situation achieved by the implementation of BECCS (BAU mix and aiming for the fraction of occupied SoSOS for the energy imbalance PB to be equal to zero). 203
Table 10-13: Impact reduction with respect to the current situation achieved by the implementation of BECCS (sustainable mix and aiming for the fraction of occupied SoSOS for the energy imbalance PB to be equal to zero). 204
Table 10-14: Summary of DACCS scenarios. In each cell the symbol code shows if the boundary was transgressed in the current situation and its state after the implementation of CCS: * denotes the boundary is transgressed while – means it is not. The symbols are expressed as follows: BAU situation/scenario. 206
Table 10-15: Summary of BECCS scenarios. In each cell the symbol code shows if the boundary was transgressed in the current situation and its state after the implementation of CCS: * denotes the boundary is transgressed while – means it is not. The symbols are expressed as follows: BAU situation/scenario. 207
Table 10-16: Occupation of EU-28's geological storage capacity taken up by the proposed scenarios. 208
Table 10-17: Affected processes (green hydrogen and mix change for the chlor-alkali process scenario). 212
Table 10-18: Observed changes on the contributions to the PBs after the switch from grey to green H_2 and the powering of the chlor-alkali process with the renewable mix. 213
Table 12-1: Labour costs. 226
Table 12-2: Software costs. 226
Table 12-3: Total costs. 227

ABSTRACT

As environmental degradation and resource depletion accelerate worldwide risking the stability of the planet and undermining its capacity to maintain its current state (the only geologic epoch able to favour human development), mechanisms for the analysis and enhancement of the sustainability level of human activities are becoming increasingly relevant. Acknowledging the challenge posed by the need for a shift towards a greener future of the European chemical industry, this study assessed the degree of disturbance chemical plants operating with current practices exert on the main environmental processes regulating the Earth's functions through the PB-LCIA framework.

This methodology allows to combine Life Cycle Assessment (LCA) with the Planetary Boundaries (PBs). The former is a tool capable of identifying the impacts associated with the different stages of the life-cycle of a system based on its exchanges with the environment (called Life Cycle Inventories or LCIs). Meanwhile, the latter is a framework developed by *Rockström et al.* (2009) which quantifies the resilience of the principal environmental processes in order to avoid human action to exceed the ecologic carrying capacity of the planet (i.e., the maximum rate of pollution and resource harvesting environments are capable to sustainably support). This framework has been, and still is, gaining interest not only from the scientific community but also from businesses, policymakers, and investors (Lucas et al., 2020). As proved in this work, it allows to portray the severity of the environmental damage caused by the assessed activities and size improvement actions, as well as providing a complete priority assessment (Ryberg et al., 2018). A production-based study of the sustainability level of the chemical industry was developed taking a cradle-to-gate approach, where not only impacts derived from the strict in-plant production but also those related to the obtention of feedstocks, energy, and the treatment of wastes, are included.

Firstly, the boundaries of the study were defined in regard to which PBs were to be quantified, which chemicals were relevant for the study, and which was the level of detail desired. All PBs for which a threshold contribution (a pressure level above which the Earth process is at risk) has been defined to date were selected to be included in the research. Besides, the chemical industry was characterized into a representative range of chemicals and processes, resulting in a model

which considered if the products of a process were used as feedstocks in another, to understand relationships happening within the cradle-to-gate system. Secondary, LCI data was collected from LCA database *ecoinvent v3.5*, and an attributional LCA was conducted following the standards defined by ISO 14044. Afterwards, the contributions on the PBs attributed to the sector were computed through the PB-LCIA framework. A data quality analysis was included to assess the adaptation of the collected data to the goals of the study and to compute the uncertainty carried by the results. Since the PBs are defined at a global scale, their downscale to the sector under study was performed through two different allocation criteria. The results highlighted the relevancy of transparency in the allocation method selected in PB-LCIA assessments.

It was found that the industry is transgressing at least 4 out of the 9 PBs by alarming numbers, including those related to climate change (total imbalance caused at top of atmosphere and CO_2 concentration), ocean acidification, and aerosol loading. Ammonia, PP, HDPE, styrene, benzene, and propylene oxide were found to be the top contributors to the global unsustainability of the sector. However, an additional, significant number of impacts stemmed from sectors beyond the boundaries of the industry, such as the energy sector. In light of the obtained results and besides specific actions targeted at critical processes described along the report, four principal improvement pathways were proposed and modelled: (i) the powering of the processes by a more sustainable electricity mix, the deployment of carbon dioxide capture and storage technologies, including (ii) bioenergy with carbon capture and storage and (iii) direct air capture and storage, and (iv) the production of hydrogen through water electrolysis instead of steam reforming powered by wind energy combined by the powering of the chlor-alkali electrolysis with the sustainable mix presented in scenario (i).

Even if all proposed routes for improvement yielded positive results and palliated the impact of the industry on the PBs, their modelling put in evidence no “silver bullet” exists which would allow to improve the performance of the industry alone, since every action causes burden-shifting (i.e., solving a problem on an environmental category poses a burden on another). Therefore, a combination of measures and technological alternatives is needed to drive the industry towards a sustainable future.

KEYWORDS

Life Cycle Assessment; Planetary Boundaries; Sustainability; Chemical Industry; Climate Change; Carbon Dioxide Removal; Pedigree Matrix; Environmental engineering

ABBREVIATION INDEX

AL – Aerosol Loading

BAU – Business As Usual

BECCS – Bioenergy with Carbon Capture and Storage

CCS – Carbon Capture Storage

CDM – Clean Development Mechanism

CDR – Carbon Dioxide Remvoal

COP – Conference Of Parties

CSTR – Continuous Stirred-Tank Reactor

DACCS – Direct Air Capture with Carbon Storage

DEA – Diethanolamine

DQG – Data Quality Goals

DQI – Data Quality Indicators

ECHA - European Chemicals Agency

EUCISoSOS – European Chemical Industry Share Of Safe Operating Space

EUSoSOS – European Share Of Safe Operating Space

FSoSOS - Final Share Of Safe Operating Space

FU – Functional Unit

FW – Fresh Water

GF – Grandfathering

GHG – Greenhouse Gases

GVA – Gross Value Added

GW – Ground Water

HDPE – High Density Polyethylene

HPV – High Production Volume

IEA – International Energy Agency

LCA – Life Cycle Assessment

LCI – Life Cycle Inventory

LCIA – Life Cycle Impact Assessment

LDPE – Low Density Polyethylene

LLDPE – Linear Low Density Polyethylene

NACE – Statistical Classification of Economic Activities in the European Community

ODS – Ozone Depleting Substances

PB – Planetary Boundary

PB-LCIA – Planetary Boundaries-Life Cycle Impact Assessment

PE – Polyethylene

PFD – Process Flow Diagram

PLA – Polylactic acid

PP – Polypropylene

REACH – Registration, Evaluation, Authorisation and Restriction of Chemicals

SOS – Safe Operating space

SoSOS – Share of Safe Operating Space

SQ – Status Quo

SQSoSOS – Status Quo Share Of Safe Operating Space

TPS – Thermoplastic Starch

ACKNOWLEDGEMENTS

I would first like to thank my tutor, Dr. Carlos Pozo, for his immeasurable dedication, guidance, feedback, and enthusiasm during the development of this project and the writing of this report.

Additionally, I want to gratefully acknowledge the support I have received from my family, my partner Adrià, and from Magalí.

1 Introduction

1.1 Background

Human development is putting unprecedented pressure on the Earth's ability to maintain equilibrium due to rapid population increase, climate modification resulting from the emission of greenhouse gases and loss of biodiversity caused mainly by ecosystem destruction and alteration. Anthropogenic activities have been proved to have triggered many environmental imbalances which threaten not only nature but also the human ecosystem in diverse ways. Some responses to change evidenced by environments undermine our development. Such is the case of the gradual switch to a poorer distribution, productivity, and availability of resources, or how habitable regions of the planet are becoming unhabitable due to extreme climate, flooding, or the spreading of diseases. Climate change, diminishing air and water quality, and biodiversity loss, among others, are also all indicators of a degraded environment (IPCC, 2019). The scale and rate at which the Earth Systems are changing is totally unprecedented, even rising concern on whether we may be entering a geological era where the human species is the primary driver of change on the planet, the so-called Anthropocene (Lewis & Maslin, 2015; Waters et al., 2016).

Amid the environmental crisis we are facing and its associated economic costs, a switch to a more sustainable development model has become urgent from both a technological and a political point of view. In this study, the focus is set on the European chemical sector: a driving factor of the world's economy bringing significant benefits to our welfare, yet at the expense of high environmental costs.

At a global level, the chemical industry has annual revenues worth three trillion euro and is in continuous growth. Precisely, Europe (EU-28) is the second largest chemical manufacturer with sales up to 565 billion € per year, that representing 1.1% of EU's GDP. Moreover, it is the region exporting the most chemicals in the world (CEFIC, 2020). The European chemical sector provides ancillary benefits such as the generation of direct and indirect employment, yet it also has a large environmental footprint associated.

Despite persistent efforts on making processes more sustainable and reducing their energy consumption, even against an increasing demand for chemical products, the chemical and petrochemical industry is still one of the largest energy consumers and greenhouse gas (GHG) emissions producers. In addition, it is also responsible for impacts related to toxic, bioaccumulative and persistent products and is linked to major industrial accidents. Overall, the sector's activity is known to heavily alter the natural functioning of Earth systems (see the sections for the Earth Systems and the Planetary boundaries). Still, there is a significant lack of information on the amount of chemicals released into the environment and their associated impacts, especially in the case of new entities (OECD, 2000).

The main challenges the sector currently faces with respect to environmental performance include the need to reduce emissions, hazardous waste, and energy consumption (Environmental agency, 2016). In order to direct efforts and investment towards new or improved technologies, it is key to identify the critical parts of processes to develop better techniques.

Since BAU is no longer an option, a paradigm change and a strategic review of current production processes are needed to allow the industry to continue covering the needs of society while not compromising its future and by placing the minimum burdens on the planet. Moreover, increasing environmental consciousness and the appearance of many restricting polices will force the sector to transition to a sustainable business model in the upcoming years.

Europe has been one of the regions leading the change towards a more sustainable future, introducing many regulations and polices which aim to reduce human impact on the planet. However, actions so far remain insufficient.

The beginning of European environmental governance dates back from the Paris Summit in October 1972, where the first measures to assess, manage and track human impact on the environment were approved (United Nations, 1972). Worldwide, a focus on sustainability has been set since the emergence of the sustainable development concept during the 1980s (LIFE, 2013). Since then, many environmental management tools have been introduced, such as Life Cycle Assessment (LCA), new institutions have been created, and new regulations (e.g., REACH, ISO), approved. Over time, LCA has gained relevancy since it

allows to find strategies to balance environmental effectiveness and economic efficiency (CEFIC, 2020), compare products, and reduce impacts (even if it is unable to assess the sustainability level of activities considering the ecological capacity of the planet). In many cases, the consequences of the exploitation of the planet are not straightforward: ecosystems may appear to be stable until a critical tipping point is crossed. Once this threshold is surpassed, Earth systems can irreversibly collapse (Lenton et al., 2008; Thomas, 2016; Lenton et al., 2018). Based on this idea and thanks to advances in Earth Systems Science, a new framework which does enable absolute sustainability analysis became possible.

The level of disturbance the Earth Systems can withstand while remaining within safe and stable conditions was quantified for the nine principal Earth systems (i.e., climate change, biodiversity loss, stratospheric ozone depletion, ocean acidification, alteration of the biogeochemical flows, land-system change, freshwater use, atmospheric aerosol loading and the introduction of novel entities). This led to the advent of the Planetary boundaries (PBs), framework which was first defined in 2009 by *Rockström et al*. and has been continuously updated. One of the major revision studies, led by one of the contributing authors to the original paper, was published in *Science* in 2015 (Steffen et al., 2015), and updates the methodology. Their approach is taken as a reference in the present study.

Thanks to the PBs framework, the state of an Earth System (e.g., the nitrogen biogeochemical cycle) can be evaluated by identifying the elements that pose a burden to its natural functioning and quantifying the magnitude of these impacts in terms of adequate control variables (e.g., intended anthropogenic nitrogen fixation expressed in Tg $N*yr^{-1}$). The transgression of several PBs can lead to major environmental risks and drive the Earth Systems' conditions out of the Holocene state, which is the current geological epoch and the only known era able to support human development as it is now (McCartonSean & Reid, 2021).

The PBs allow to determine whether the assessed activity is overall sustainable, therefore providing further insight than the traditional LCA methodology, which is limited to comparison between different options or isolated analysis but does not provide a threshold above which the activity is using more resources than the Earth can provide.

Ryberg et al. (2018b) introduced the PB-LCIA damage assessment model, which connects both frameworks by allowing the expression of LCA data in the metrics of the PBs, taken as impact categories.

Understanding the stressors posed to the Earth's self-regulating mechanisms and using the PB-LCIA methodology, it is possible to provide guidelines and targets for all industrial sectors and nations to revert this planetary emergency. Acknowledging that important contributions can also be made in other regions and sectors, this study develops a production-oriented quantitative assessment of the impacts of the European (EU-28) chemical industry on seven of the nine aforementioned PBs using LCA. The two remaining boundaries are not included since they are still object of debate within the scientific community.

Previous authors have followed similar approaches and quantified the environmental burdens of different human activities in terms of the PBs. *O'Neil et al.*'s research (2018) studied whether society's basic needs can be met while not transgressing the PBs. *Sandin et al.* (2015) assessed the Swedish clothing sector, while *Tunhi-Olayeni et al.* (2019) concluded the construction industry does not remain within all PBs. *Ryberg et al*. (2018b) also focused on the European region by applying the PB-LCIA damage assessment model to the laundry washing industry. However, no assessment of the sustainability of the chemical sector has been published yet.

1.2 Methodology

Fig. 1-1 illustrates the methodological approach followed to assess the sustainability of the chemical industry in the EU-28 region using the PB-LCIA framework.

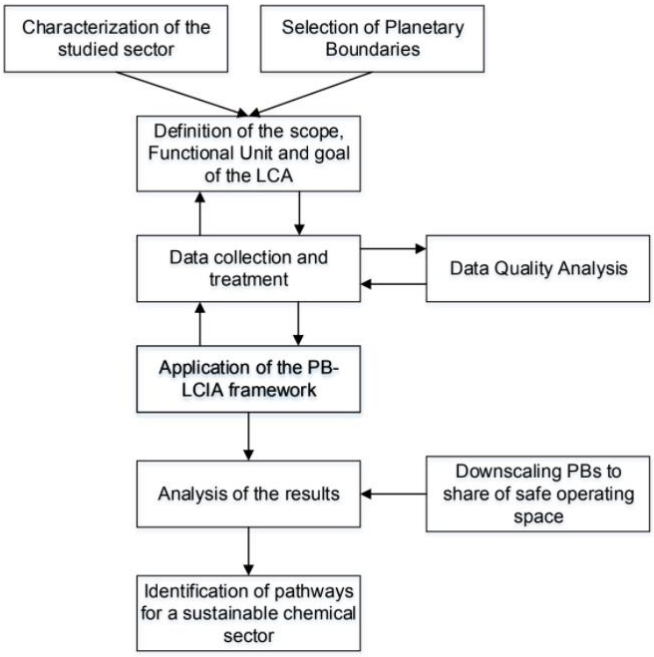

Fig. 1-1: Methodology of the study.

The core step of the methodology is the development of a LCA studying the environmental burdens posed by the chemical industry, and the translation of these to impacts on the PBs using the PB-LCIA framework.

Besides the interpretation of results, the essential steps of LCA are (1) the definition of the study, (2) the Life Cycle Inventory or LCI, and (3) the Life Cycle Impact Assessment or LCIA. Initially, in step 1, the calculation base, scope, and boundaries of study are detailed. Afterwards, in step 2, LCIs are computed. They are the direct environmental stressors and include resource uses, and material and energy flows exchanged between the selected process and *the environment* through all the stages in the life cycle and can be collected from LCA databases (in this case, from *ecoinvent* v3.5 (Wernet et al., 2016)). They are expressed as the amount of each flow exchanged during the production of one unit of product (e.g., kg of nitrates emitted per kg of methanol produced or m^2 of land transformed for the production of 1 kg of ammonia). LCIs describing exchanges between the studied process and *other industrial processes* are also provided by *ecoinvent*

and used in section 4.2. Fig. 1-2 illustrates the concept of LCIs as exchanges between the system and the environment (or other industrial processes). LCIs (i.e., environmental burdens) can leave (e.g., emissions of pollutants, residues to waste treatment) or enter (e.g., those inputs from the environment required to generate the needed energy and raw materials) the system.

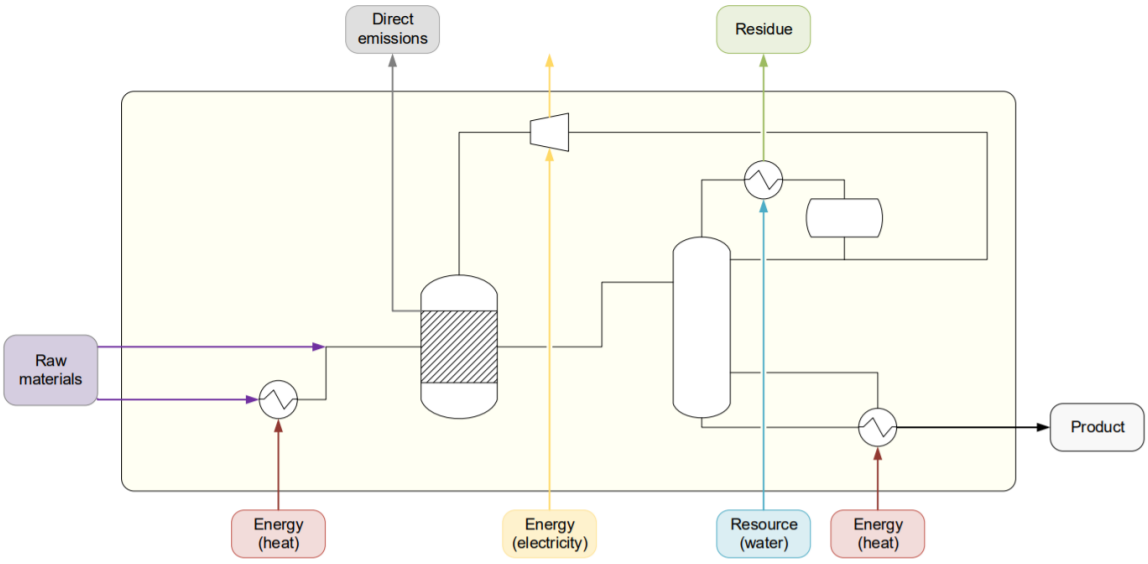

Fig. 1-2: Figure illustrating the concept of LCIs.

In step 3, each stressor (i.e., LCI) is translated to an impact on every selected PB using the PB-Life Cycle Impact Assessment model. Through this framework, the PBs are taken as impact categories in the LCIA phase (PB-LCIA section). LCIs from LCA datasets are connected with the PBs by being multiplied by characterization factors (CFs), which allow their adaptation to the control variables of the PBs. Since impacts on the PBs are quantified in terms of constant fluxes rather than discrete exchanges, the annual production volumes of each chemical are used to obtain the total quantities of each pollutant or resource uptake that are attributed to the activity of the chemical industry during the studied year.

$$Impact_{PB,j} = \sum_{i} LCI_{i,j} * V_j * CF_{i,PB} \quad \forall PB, j \qquad \textit{Eq. 1}$$

Eq. 1 simplifies the calculations needed to obtain the final contribution ($Impact_{PB,j}$) of the manufacturing of *j* on each planetary boundary *PB* [units of *PB*]. Each LCI representing exchange *i* [units *i*/kg *j*] is multiplied by the annual volume of each

chemical *j* [kg *j*/yr] and by the characterization factor linking the LCI *i* and the *PB* [units of *PB**yr/units of *i*]. The impact of all exchanges with the environment stemming from *j* are summed to obtain the total impact. The process is then repeated for each planetary boundary and for all the studied processes and chemicals. For some chemicals, LCIs in ecoinvent include the inputs from the technosphere (i.e., other chemicals needed as feedstock for the manufacture of the chemical assessed). In this study, these LCIs are are labelled as $F_{j,j'}$ and provide the unitary volume of base chemical *j* needed for the manufacture of *j'* [kg *j*/kg *j'*].

It is relevant to note that LCI exchanges include impacts from the manufacturing process itself but also from production of feedstock and energy. Consequently, when quantifying the impacts of a certain process, the impacts from the manufacture of its base reagents are also included. If no further considerations are taken, this can lead to the double counting of the contribution to the PBs of some chemicals. For instance, if both ethylene and polyethylene are studied, the impacts attributed to the fraction of the total volume of ethylene produced annually used to polymerize polyethylene will already be counted when calculating the impacts of polyethylene.

An overview of the sections of the report and how these and other additional issues are tackled is detailed below.

Initially, the scope of the study must be defined based on boundaries established for the following factors: which chemicals and processes are included in the study, which PBs are relevant to the research, and the scope of the LCA. In this regard, some decisions might be affected by data availability.

In the first section, the chemical industry is simplified as a collection of the most representative chemicals and processes, selected based on their production volumes and environmental impact. A high range of compounds, especially some High Production Volume (HPV) chemicals (i.e., those which are introduced to the EU market in more than 1000 tonnes/yr per manufacturer or importer) are used within the industry to produce other chemicals (e.g., ethylene is used to produce polyethylene, ethylene oxide, polypropylene, styrene, and vinyl chloride, all among the selected chemicals). As previously introduced, this could lead to

double counting errors since this study adopts a life cycle perspective, thereby considering not only the environmental risks associated with the strict in-plant production of each chemical but also the impacts derived from the obtention of the necessary feedstocks and energy. To avoid this, it is necessary to disregard the share of the production volume of each chemical that is used as feedstock for other production processes also considered within the scope of the study. Therefore, a model of the studied sector is developed to prevent this error. The studied range of processes is described with the aim of thoroughly identifying the links between chemicals and to better understand and interpret the results.

Secondly, the PBs which are applicable to the studied region and sector are identified and described. On the one hand, some PBs which describe the behaviour of complex Earth dynamics, such as the responses to biodiversity loss, are yet to be defined. On the other hand, some boundaries are specifically developed for a region of the world which is not under study, or their inclusion requires information which is not readily available.

Once the boundaries of the study are correctly defined, the LCA is conducted following the standardized 14044 ISO methodology using an attributional modelling approach, which informs about the impacts associated with the life cycle of a product. In this study, a cradle-to-gate approach is taken, which essentially includes the environmental damage attributed to the obtention, preparation and transport to plant of feedstocks, energy, and resources, as well as the production of the chemicals, and the treatment of wastes. The alternative to attributional modelling is consequential modelling. Consequential LCAs are also carried out in the last section of this study, where Potential improvement pathways are investigated, since the changes on the state of the PBs derived from different actions are assessed.

Acknowledging that the environmental characterization of the chemical industry is not based on real measurements but on datasets and approximations, this study also includes a Data Quality Analysis undertaken to model the uncertainties associated with the consulted datasets. Specifically, each dataset is reviewed and its adjustment to the study's goals is scored employing what is called a *pedigree matrix* designed to assess data quality in LCA through a standardized and objective rubric. This allows to numerically characterize an uncertain

distribution for every LCI of every chemical process considered. Finally, these distributions are discretized into 100 possible scenarios using MATLAB, thus yielding an equivalent number of potential contributions of the chemical industry to the PBs and ultimately providing the reliability level of the results.

Moreover, the downscaling of the PBs to the study's region and sector using different allocation principles is performed. This step is crucial because the level of disturbance the Earth systems can withstand is in most cases presented as a global boundary, but a single activity, region, or process cannot occupy the total room humanity has to manoeuvre (i.e., the so-called safe operating space). Therefore, when assessing a specific activity, it must be assigned a proportional fraction of the total safe operating space defined by the PBs. The results using the principle offering the highest precision level are presented as principal for this study and used as a reference for the modelling of improvement scenarios.

Finally, the interpretation and analysis of the results obtained is carried out, and conclusions and recommendations are drawn. Improvement measures are proposed in light of the obtained results, including specific recommendations for processes with high impacts but also general measures which could globally improve the sector's performance. New models are developed to assess how impacts on the PBs would change if certain improvement scenarios were implemented, paying particular attention to aspects such as whether the state of the would vary (e.g., the fraction of assigned safe operating space that the chemical industry occupies) would vary, if the measures would cause burden-shifting, and the magnitude of the required intervention.

As for predictions about the potential results, the European chemical industry is expected to transgress the climate change boundary, since even when it has been reducing its GHG emissions during the last decades, it is still one of sectors with the highest emissions and responsible for around 145 Mt of CO_2 being emitted annually. Looking towards 2050, CEFIC (European Chemical Industry Council) plans to reduce annual emissions by at least 36% by improving technologies and reducing energy consumption (Boulamanti & Moya, 2017b). The quantification of the impact of the sector on the climate change PBs can be used to assess which processes should be prioritized when updating technologies. As published by the IEA (2013), the processes which account for

the highest GHG emissions are methanol, ammonia, ethylene, propylene, and propylene oxide. Therefore, a special focus should be set towards them when breaking down the results of the contributions to the climate change boundary to see whether their impact is more significant than that of other chemicals once production volumes are considered. The ocean acidification boundary may also be transgressed since it is directly linked with GHG emissions, which cause the increment of pH in marine waters once absorbed.

An additional hypothesis regarding the rest of Earth systems is the consideration of the possibility of the stratospheric ozone depletion and aerosol loading boundaries also being transgressed, since at a global level they are already being surpassed. The impact of the sector could be relevant since a wide variety of ozone-depleting substances (ODS) are used for the manufacture of products of the chemical industry, including polymers, refrigerants, and other agents (European Environment Agency, 2020). In regard to aerosols, according to the *European Commission* (2014b), the use and manufacturing of organic solvents and chemicals is responsible for the majority of Europe's NMVOC emissions. However, when it comes to other aerosols such as SOx and NOx, the energy industry is responsible for 69% and 28% of emissions, respectively. Even if the chemical industry is not one of the main emitters of aerosols, its energy demand may indirectly impact the sector's activity since a cradle-to-gate approach is taken.

Finally, the limits assigned to the biogeochemical flows are also globally transgressed, but the main sector contributing to excess nitrogen and phosphorus is agriculture through fertilizer use (not production) (Blaas & Kroeze, 2016; Ryberg et al., 2018b; Bachari, 2019). Therefore, it may be a possibility that these impacts are not attributed to the chemical sector.

Regarding the land-system-change and freshwater use boundaries, it is also more unlikely that the sector's activity is equally damaging than it is with other boundaries, since their principal threats are agriculture, intensive water and land use stemming from a growing population, general climate degradation, and poor management of resources by the authorities (Arora et al., 2015; Damania et al., 2017; Doell et al., 2009). None of these can be directly attributed to the chemical industry.

2 Goals of the study

The purpose of this research is to identify, quantify and interpret the environmental impacts associated to the activity of the chemical industry in the context of the planetary boundaries using Life Cycle Assessment.

The aims of this research are two-fold: (1) to evaluate whether the current activity of the chemical industry remains within PBs and which are the most endangered Earth cycles, and (2) to identify the processes with higher environmental impact, in order to suggest priorities for action, specific measures, and recommendations to increase the sustainability level of the sector.

To achieve such results, a first objective is to develop a representative model of the chemical industry by identifying the chemicals and processes with higher production volumes and environmental impact in terms of energy demand and greenhouse gas emissions. This selection allows to define the boundaries of the study in terms of scope and level of detail, which must be consistent with that of available data.

Additionally, through this case-study, the implications of the methodology chosen to allocate the impacts (i.e., the results' sensitivity to the principle used for downscaling the PBs) are evaluated by comparing a non-egalitarian and an egalitarian method with three increasing degrees of precision. Results, with their uncertainty ranges obtained from the LCA data quality analysis, are presented, and discussed. The influence of the uncertainties of the collected data on the conclusions drawn are analysed. Additionally, a prediction of how the state of the PBs would change in the future is included.

Finally, improvement scenarios are modelled to assess how the global situation would change if different potential solutions were to be implemented. The efficiency of the proposed measures is evaluated, as well as their feasibility.

The summarized, specific objectives of this study are:

1) To characterize the European chemical sector into a representative range of products and processes in terms of environmental impact and production volume, with a level of detail consistent with available data.
2) To quantify the environmental impacts of the EU-28 chemical industry in terms of their contribution to the PBs using LCA.
3) To allocate the PBs defined at the global level to the European chemical industry according to more than one criterion for the sake of comparison.
4) To analyse whether the sector remains within the PBs and assess its sustainability.
5) To identify which chemicals or processes are contributing the most to the occupation of the allocated safe operating space.
6) To draw specific conclusions and recommendations that, if implemented, would improve the sustainability level of the sector.
7) To calculate the repercussion of the main global improvement measures proposed, assessing the magnitude of the required interventions and whether burden-shifting occurs.
8) To analyse the repercussion of the uncertainty linked to the collected data and how it influenced the results.
9) To make proposals for further research.

According to the standardized ISO methodology for the development of LCA, the definition of goal and scope must be detailed in the project report (Life Cycle Assessment section). Given that one of this study's stages is precisely the development of an LCA, the goals of this specific section are re-visited and expanded during its elaboration.

3 Chemical Industry

Chemicals are needed for the manufacture of around 95% of all man-made products (ICCA, 2010) and provide society with valuable and necessary goods which have a wide range of applications, covering areas as diverse as the agricultural, the transportation or the energy sectors.

The chemical industry can be broken down to three main typologies of products: (i) base chemicals, both organic and inorganic, (ii) speciality chemicals, and (iii) consumer chemicals. The former group are produced at large scales and account for 60% of chemical sales in the EU, despite having lower production costs and selling prices (European Chemical Industry Council: CEFIC, 2020). They are mainly used as feedstock in the production of other chemicals. In the case of speciality chemicals, their production volume is much lower, their uses more specific and their production costs higher, causing them to be high value-added products. From base chemicals and specialities, final products, or consumer chemicals, are produced. Further classifications can be formulated within each of these three categories. Examples of specialities and include active principles, artificial fibres, or pigments, which are used to produce consumer chemicals such as pharmaceutic products, paper, or paints, respectively (Tarrés, Q., 2019). Base chemicals typically include the petrochemical sector.

To assess the level of sustainability of the sector, boundaries defining the scope of the study need to be established. The European chemical industry has been characterized in terms of a representative selection of the most abundant products and processes, together with higher environmental impact.

4 Characterization of the European chemical sector

Following the approach taken in the report by the International Energy Agency (IEA, 2013) on routes to reduce the consumption of energy and GHG emissions in the chemical industry, the top 21 largest-volume chemicals have been included in this study in representation of the European chemical industry. Their manufacture is responsible for 80% of energy consumption and 75% of GHG emissions within the industry (IEA, 2013), owing to both being large-volume chemicals and being produced through processes with high environmental impact. In the industry, each of these 21 chemicals can be manufactured by the means of more than one process. Processes included in this study are all those for which LCI data was available in *ecoinvent*. Caprolactam and phenol were included in the IEA report but neglected in this study, since information on their LCIs or exact production volume could not be found, respectively. Their environmental impact was, however, lower in terms of both GHG emissions and energy consumption (IEA, 2013).

The 19 chemicals and 25 processes finally selected in representation of the chemical industry for this study can be found in Table S1-1 and are further described in Selected chemicals and processes section. Due to their high production volumes and environmental consequences, improvements on any of the studied processes are bound to have substantial impacts.

Among the selected chemicals, IEA suggests a special focus should be set towards three groups, which account for the highest consumption and emissions: olefins (ethylene and propylene), ammonia and BTX aromatics (including benzene, toluene, and xylenes). Fig. 4-1 and Fig. 4-2 provide the average emissions (tCO_2/t) and energy consumption (GJ/t), respectively, of each chemical process in this study vs its corresponding production volumes in Europe (expressed in tonnes to match the units of the y axis). After the adaptation of the data to the processes and region under study, the five highlighted groups by IEA, 2013 still stand out, however, acrylonitrile, LLDPE and propylene oxide should also be given special attention regarding their energy demand and emissions.

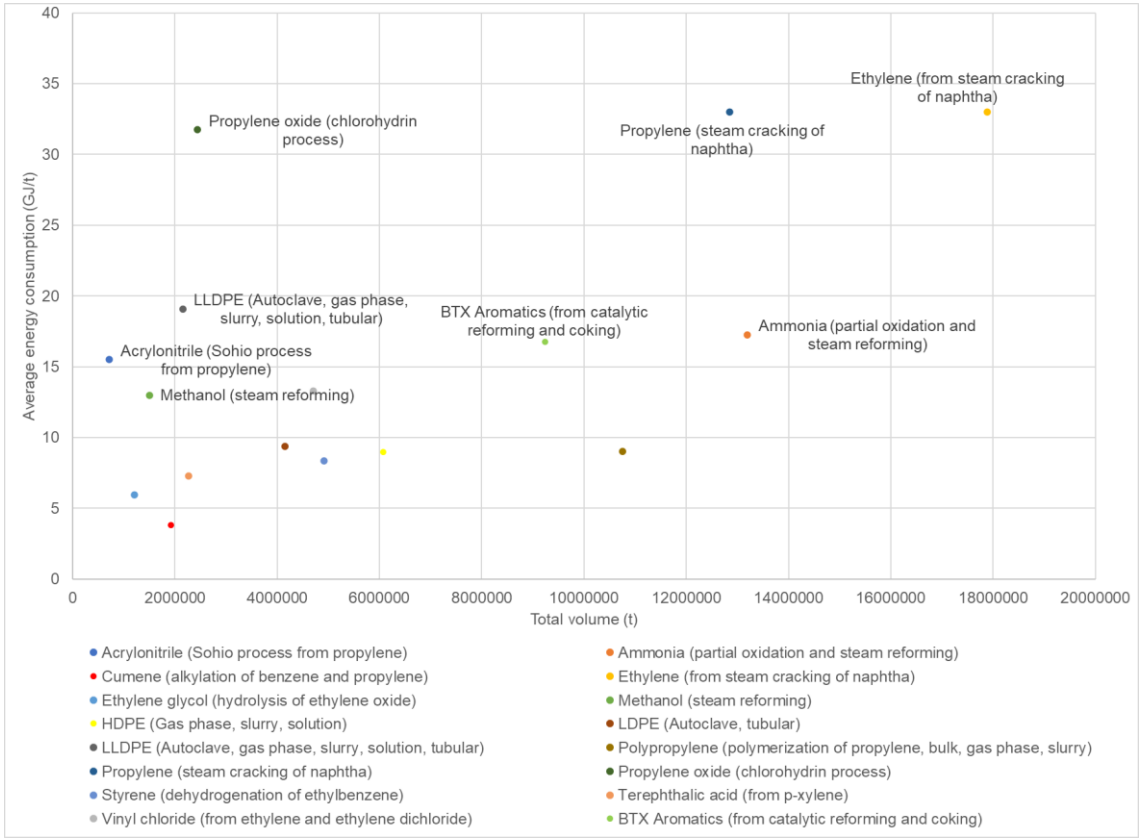

Fig. 4-1: Average energy consumption per chemical versus total production volume within EU-28.

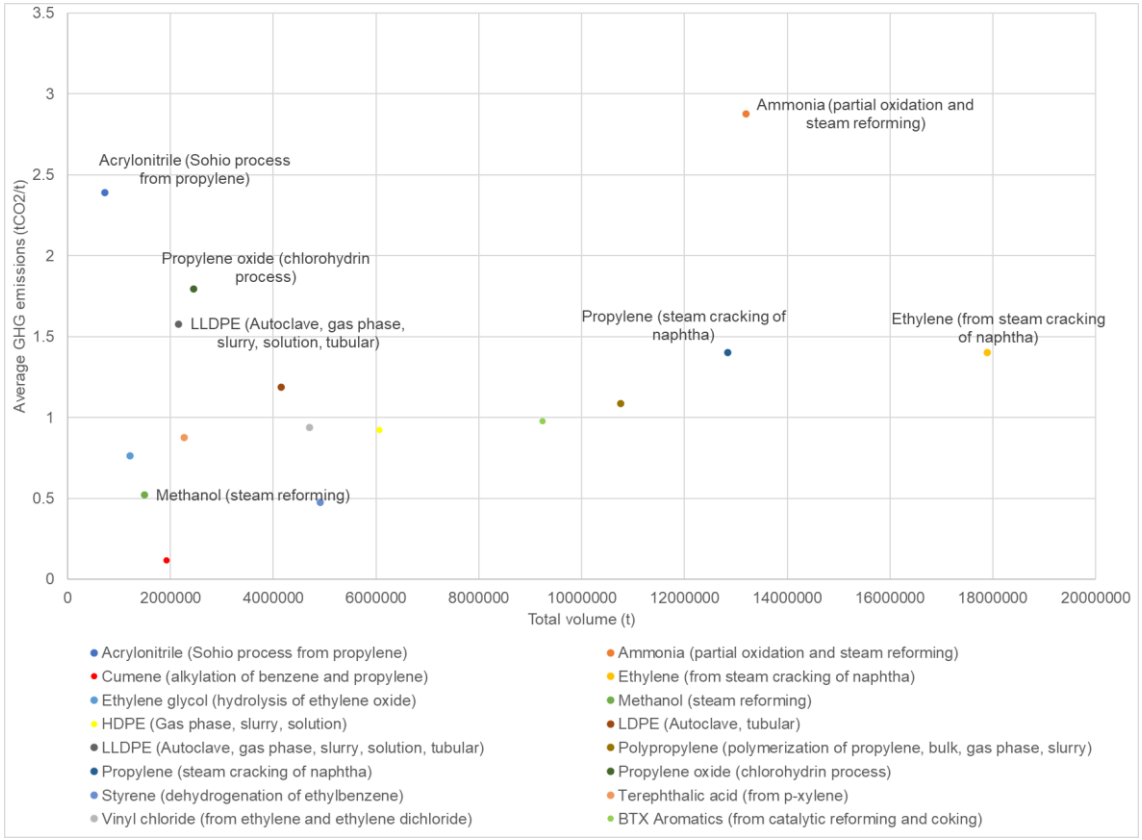

Fig. 4-2: Average GHG emissions versus production volume per chemical within EU-28.

4.1 Selected chemicals and processes

The selected processes are described in this section to ensure the understanding of the assessed activities which facilitates the discussion and comprehension of results. Section 4.2 identifies and models the relationships between the processes described in this section (4.1) to avoid double counting their impacts on the PBs. The knowledge about chemical processes and the representation of process flux diagrams using Microsoft Visio acquired during the degree has been key for the selection and understanding of the chemical processes involved in the degradation of the environment attributable to the chemical industry and the interpretation of the results.

4.1.1 Acrylonitrile

Acrylonitrile (CH_2CHCN) is an organic compound used mainly in the plastics industry. It is needed to produce ABS (acrylonitrile butadiene styrene), which has a wide range of applications thanks to its high resistance to temperature, chemical corrosion, and impacts. Other uses of acrylonitrile include the production of polyacrylonitrile fibres, nitrile butadiene rubber or acrylamide (Mordor intelligence, 2019).

4.1.1.1 Sohio process

Acrylonitrile is mainly produced by the Sohio process, which consists of the catalytic oxidation of propylene in the presence of ammonia (American Chemical Society, 1996), a process called ammoxidation (*Eq. 2*).

$$2\ CH_3\text{-}CH{=}CH_2 + 2\ NH_3 + 3\ O_2 \rightarrow 2\ CH_2{=}CH\text{-}CN + 6H_2O \qquad \textit{Eq. 2}$$

The catalysts for this process are antimonate and multi metal molybdate. The process is energy-intensive since it is conducted at a temperature range of around 400-500ºC, and at a pressure of 30-200 kPa (Cespi et al., 2014). The reaction is conducted in a fluidized-bed reactor, where excess heat from the exothermic reaction must be removed constantly to maintain a constant operation temperature. After the reaction, the purification of the products must be done, usually with a separation sequence of operations consisting of an absorber, which uses sulfuric acid to neutralize unreacted ammonia, and various consecutive

separation columns. As seen in Fig. 4-3, the by-products of the process are acetonitrile and HCN, which are later separated to be used in other processes. Water and other concentrated impurities are also recovered, for re-use and treatment, respectively.

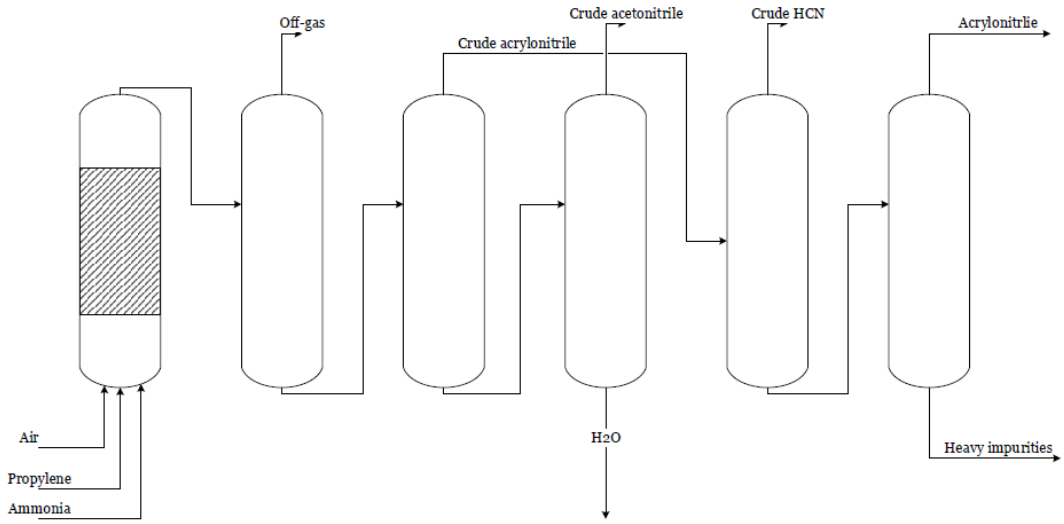

Fig. 4-3: Process flow diagram for the production of acrylonitrile through the SOHIO process (adapted from Cespi et al., 2014).

4.1.2 Ammonia

Ammonia is a very versatile compound which also exists in the environment as part of the biogeochemical cycles. It is mainly used as a feedstock to produce fertilizers and other compounds, such as caprolactam and Acrylonitrile, or as a refrigerant gas. More applications include its use in the production of plastics, dyes, and other chemicals. Only a small fraction of all produced ammonia is given a direct application (Maxwell, 2005). Ammonia has been attracting attention as a potential “green” fuel obtained from hydrogen and able to replace coal and natural gas. Routes for its cleaner production are proposed involving the manufacturing of hydrogen through carbon-free processes. These are explored in the Green hydrogen production and chlor-alkali electrolysis powered with renewable energy section.

Currently, ammonia is mainly produced by means of three different processes, which are described in detail in the ensuing subsections.

4.1.2.1 Partial oxidation

The partial oxidation process is one of the two main routes for the production of ammonia from sythesis gas. It consists of two main steps, including the production of syngas from coal or heavy oils and the sythesis of ammonia itself.

Initially, feedstocks react with oxygen to form carbon monoxide, carbon monoxide and hydrogen in a gasifier, which can be a fixed bed, a fluidized bed or an entrained flow gasifier (*Eq. 3* and *Eq. 4*). The product, in gaseosus form, also contains small fractions of carbon dioxide (CO_2), methane, and soot. The latter must be removed from the gas. There are different methods for extraction, generally using naphtha or light gas oil to separate the soot. Additionally, since the raw material contains impurities in the form of H_2S, the crude gas needs to be further purified, usually though absorption with the addition of a solvent (BAT Nº1, 1995). The removed sulfur and the solvent are reprocessed for re-use.

The partial oxidation process for synthesis gas preparation uses no catalysts and is energy intensive, operating at temperatures of around 1400ºC and pressures of more than 50 bar (The Institute for Industrial Productivity, n.d.). Emissions of nitrogen oxides, CO_2, carbon monoxide and sulfur dioxide may derive from the process.

$$3\,CH_n + O_2 \rightarrow 2\,CO + nH_2 \qquad \textit{Eq. 3}$$

$$CO + H_2O \rightarrow CO_2 + H_2 \qquad \textit{Eq. 4}$$

The obtained hydrogen is then washed with pure nitrogen and used for the shythesis of ammonia through *Eq. 5*. The reaction is conducted at 350-550ºC and 250 bar.

$$N_2 + 3\,H_2 \rightarrow 2\,NH_3 \qquad \textit{Eq. 5}$$

The oxygen and nitrogen used in the process are usually obtained from air in a previous air separation unit. Since the shythesis gas obtained from the partial oxidation process has a high purity, the reation to ammonia is more efficient than that in the steam reforming process, which requires the removal of inerts and treatment of purge gas.

4.1.2.2 Steam reforming

The steam reforming process also produces ammonia from sythesis gas. Its main steps are raw material preparation, syngas production, ammonia synthesis and purification. In this case, natural gas or light carbon fuels are used as raw materials instead of coal or heavy oils. Therefore, the process has a lower energy consumption and also lower CO_2 emissions. It also uses catalysts, while the produciton of synthesis gas thourgh partial oxidation does not.

Since these catalysts are sensitive to the presence of sulfur, the removal of this element from feedstocks through absorption is carried out before the gasification. Firstly, all sulfur is hydrogenated to become H_2S, which is then absorbed on pelleted zinc oxide (SPINE, 1999). After feedstocks are prepared, they go through a primary and a secondary reformer. Sometimes, a pre-reformer is also present to increase the conversion of raw materials to syngas.

In the primary reformer, working at temperatures of around 850ºC and generally using nickel as a catalyst, a gas containing mainly hydrogen, CO_2, and carbon monoxide is obtained (*Eq. 4* and *Eq. 6*). Note that for steam reforming, the compound reacting with the hydrocarbon (in the studied process, natural gas) is water in a vapour phase. In the second reformer, the unreacted raw materials are also converted. Since the reaction is highly endothermic, it is necessary to provide heat in both reformers.

$$CH_4 + H_2O \leftrightarrow CO + 3\,H_2 \qquad \textit{Eq. 6}$$

After the reaction is finished, CO and CO_2 must be removed from the product gas. Firstly, carbon monoxide is converted into CO_2 using iron, copper, chromium and zinc oxide-based catalysts and a temperature change, and secondly, the resulting CO_2 is removed through absorption. To optimise the removal of CO_2, the gas is cooled, and the heat removed can be recovered for use (BAT Nº1, 1995). To ensure no CO_2 reaches the shythesis of ammonia section and deactivates the iron catalyst needed for the reaction that converts syngas to ammonia, a second operation is carried out to remove any residual CO_2 and CO.

These contaminants are removed thourgh their reaction with hydrogen to create mehtane, which does not affect the synthesis, and also water, which needs to be removed before the following stage.

The shythesis of ammonia is similar to that of the partial oxidation process (*Eq. 5*), but it has a lower conversion factor (20-30%). A recirculation of synthesis gas is needed, as well as a purge to avoid the accumulation of inerts in the product (SPINE, 1999). The purged gas is usually sent to a separation section where ammonia and hydrogen are recovered.

An alternative process to steam reforming is the heat exchange autothermal reforming, which uses the heat from the secondary reformer in the primary reformer, reducing both energy demand and emissions. For this to work efficiently, additional air or oxygen-enriched air must be fed to the secondary reformer (BAT Nº1, 1995).

4.1.2.3 Cocamide diethanolamine production

Even if the amount of ammonia coming from this process is a small fraction of the total volume (<0.1% of produced ammonia), it is also included in this study for higher detail as *ecoinvent* provides enough data for its study. Diethanolamine (DEA) is produced from ethylene oxide and ammonia. By-products of the process are ethanolamine and triethanolamine. Cocamide diethanolamine is obtained from the reaction of DEA with oils (International Agency for Research on Cancer, 2013). Cocamide DEA is used as a foaming or an emulsifying agent in bath products or cosmetics.

4.1.3 Benzene

Benzene is widely used within the chemical industry to produce other base chemicals such as cumene (see section for Cumene) or ethylbenzene. Even if this application is currently restricted in some countries due to the carcinogenicity of benzene, it was also used as a solvent (Loomis et al., 2017).

4.1.3.1 Catalytic reforming

There are four main catalytic reforming reactions. These are hydrocracking (combination of catalytic cracking and hydrogenation when paraffins are broken

down into shorter chains, see *Eq. 7*), isomerization (conversion of paraffins to isoparaffins, see *Eq. 8*), dehydrogenation (conversion of naphthenes to aromatics, see *Eq. 9*) and dehydrocyclization (combined dehydrogenation and aromatization of paraffins to aromatics, see *Eq. 10*) (*Texas A&M University, 2012*).

Before feedstocks are fed to the reactor, all metallic contaminants, sulfur, and nitrogen are removed through hydrogenation to improve the efficiency of the platinum and alumina catalysts (Speight, 2020). High operation temperatures can also improve the yields to benzene; thus, the process is carried out at around 500ºC and 8-50 atmospheres in either moving-bed, fluid-bed or fixed-bed reactors. Up to five reactors may be put in series to allow the regeneration of the catalyst in one of them without stopping the production. Additional energy is needed to cool the reactors since dehydrogenation reactions are highly exothermic (McGill School of Computer Science, 2007).

Eq. 7

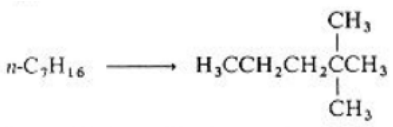

Eq. 8

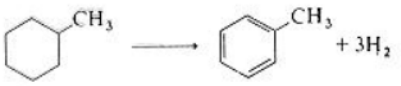

Eq. 9

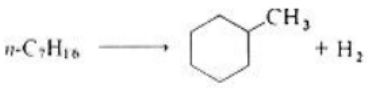

Eq. 10

After reaction, the product must be separated and purified. Generally, this process has two steps, including a first extraction of all aromatics using solvents, and a second separation of benzene by fractionation. Hydrogen resulting from the process can be recovered and re-used. Toluene and xylene are also obtained through the catalytic reforming process, which produces around 70% of the world's BTX aromatics (Nixiolek et al., 2015).

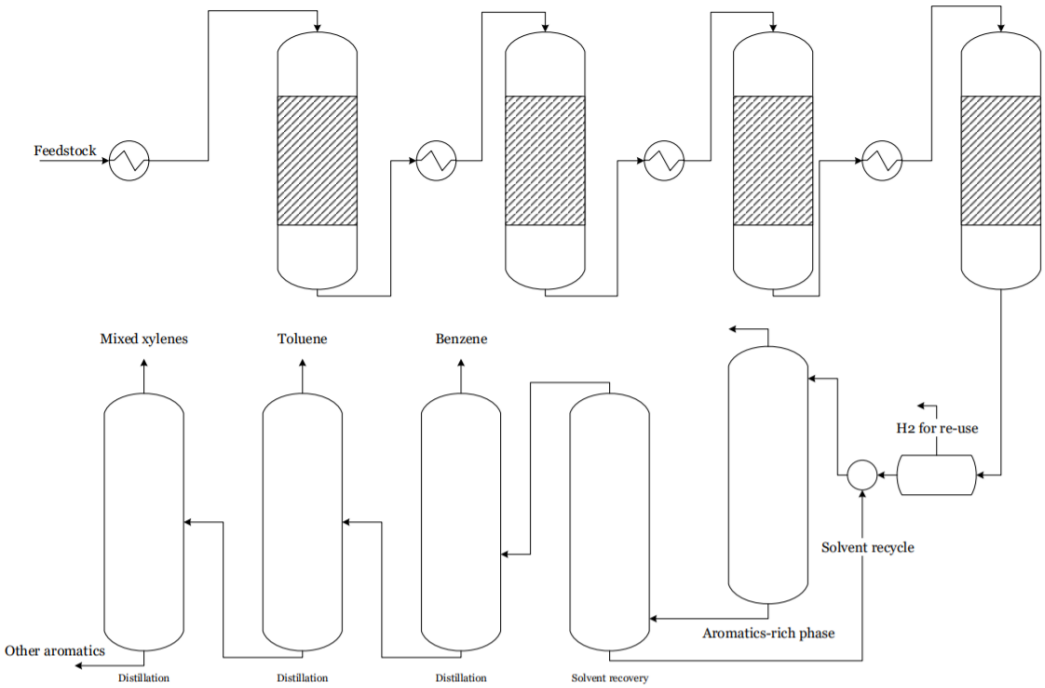

Fig. 4-4: Process flow diagram for the catalytic reforming process (adapted from RBN Energy, 2014; Speight, 2020).

4.1.3.2 From coke production

Historically, benzene was obtained as a refined by-product in the production of coke through coal carbonization. This process consists of the destructive distillation of coal by heating it in the absence of oxygen, an operation that removes light oils, tars, ammonia, water, sulfur compounds, and coke-oven gas. The obtained product is used mainly as a fuel or within the foundry industry, while benzene (and the other two BTX aromatics) can be recovered from coke-oven gas using fractionation (International agency for Research on Cancer, 2012). Even if the fraction of total benzene production obtained from this process is small, it has been included in the study to achieve greater coverage.

4.1.4 Cumene

Cumene (or isopropylbezene) is a volatile compound generally used in the manufacture of other high production volume compounds, such as phenol and acetone. Still, it can also be used to increase octane in fuels (Kugler, 1995).

4.1.4.1 Alkylation of benzene and propylene

The main route for the production of cumene is through the alkylation of benzene and propylene in a reaction unit (*Eq. 11*). A side reaction (*Eq. 12*) of cumene and propylene can from undesired para-isopropylbenzene (DIBP). To recover the lost product, para-isopropylbenzene is reacted back to cumene with benzene in a transalkylation reactor (*Eq. 13*). To do so, a separation sequence at the exit of the reactor is needed. Firstly, unreacted propylene is separated from the heavy stream containing unreacted cumene, DIBP, and benzene in a depropanizer. Afterwards, benzene is separated from the bottom stream through fractionation and recycled to both reactors. Cumene is finally obtained in a third column when it is separated from DIPB (Alghamdi et al., 2019).

Different catalysts such as phosphoric acid, zeolite, or aluminium chloride are used, and the operation temperatures and pressures can vary according to which option is selected, since the optimum conditions for each catalyst must be found. However, both temperatures and pressures of the alkylation reactor are high. As examples, the process operates at around 360ºC/30-40 bar when phosphoric acid is used and at 160-250ºC/30-35 bar when the catalyst is aluminium chloride (Alghamdi et al., 2019). The best available technology for cumene production through alkylation is optimized at 350ºC and 25 bar (Kugler, 1995).

$$C_3H_6 + C_6H_6 \rightarrow C_6H_5\text{-}C_3H_7 \qquad \textit{Eq. 11}$$

$$C_3H_6 + C_9H_{12} \rightarrow C_{12}H_{18} \qquad \textit{Eq. 12}$$

$$C_6H_6 + C_{12}H_{18} \leftrightarrow C_9H_{12} \qquad \textit{Eq. 13}$$

Even if the process flow diagram for this process can vary according to the temperature requirements, and thus, the catalyst used (Kugler, 1995) and the desired composition of the products, Fig. 4-5 depicts a common distribution of all process units needed (Alghamdi et al., 2019).

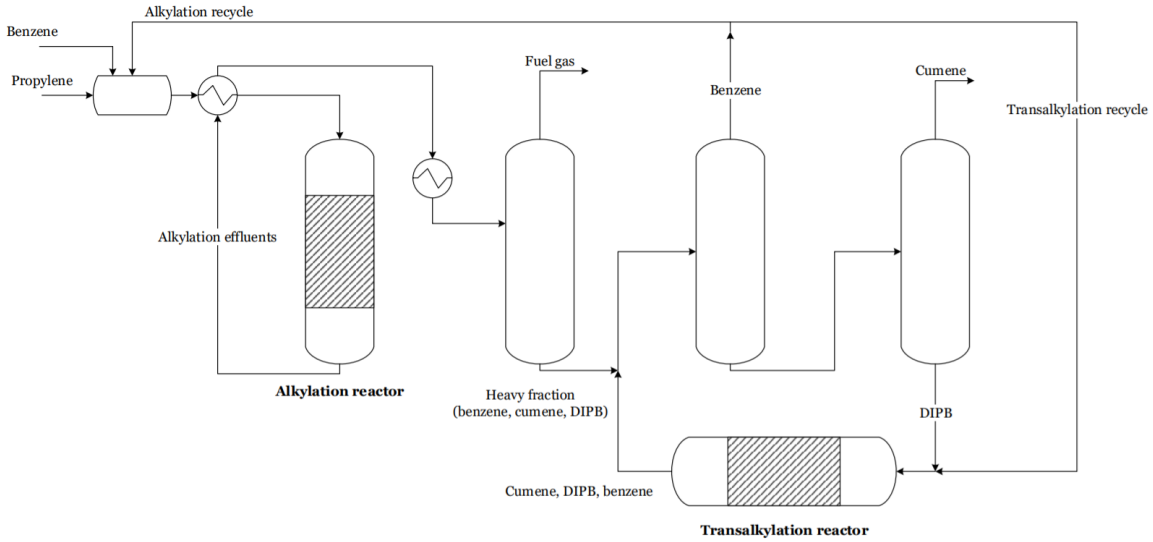

Fig. 4-5: Process flow diagram for production of cumene through alkylation of benzene and propylene (adapted from Alghamdi et al., 2019).

4.1.5 Ethylene

Ethylene is one of the chemicals producing the most GHG emissions and requiring high energy demand. Out of all the studied products, it is also the one with largest total production volume (Fig. 4-1 and Fig. 4-2). Ethylene is in fact positioned as the organic compound with the highest industrial production rate since it is the building block for many other compounds. Around 60% of ethylene production is used for the manufacture of PE of diverse densities (see section for Polyethylene), and it is also used as feedstock in the production processes of vinyl chloride, styrene, ethylene oxide (see sections for Vinyl chloride, Styrene, and Ethylene oxide), and ethylbenzene, among others (The Essential Chemical Industry, 2017). Therefore, special attention is needed in this case to prevent double counting.

Other uses of ethylene include its medical application as an anaesthetic, or its use in the glass, metallurgic, and alimentary industry, as an additive, conservative, and spray gas, respectively (Linde, 2021).

4.1.5.1 Steam (thermal) cracking of naphtha

Ethylene, as other light alkenes (olefins) is produced by the petrochemical industry by steam cracking. In this process, the feedstock can vary according to price or availability, since various saturated hydrocarbons can be used, such as

naphtha, ethane, or LPG, the former being the most widely used raw material and the one considered for this study. During the process, feedstocks are diluted with steam and then lead to a furnace, where the temperature is increased (if naphtha is used as a feedstock, to around 600-900ºC) in the absence of oxygen. In these conditions, hydrocarbons break down into shorter, often unsaturated chains (Posch, 2011). Propylene is obtained as a by-product (see section for Propylene).

The residence time inside the furnace is short (from seconds to milliseconds) to assure the highest possible yield into the desired products, and once their formation is finished, the mixture is sent to a transfer line exchanger (located inside the furnace) to stop the reaction. Besides ethylene, other light alkenes such as propylene and butadiene are obtained as by-products. The product distribution is determined by the selected feed, the temperature, steam ratio, and residence time.

In the BAU process, no catalyst is used. Besides the desired olefins, other compounds, such as cyclic alkanes, diolefins, heavy oils, and coke are also formed by secondary reactions (Mao et al., 2013). The rapid transition from the reactor to the transfer line exchanger and the addition of steam help avoid the formation of coke by stopping the reaction and reducing the partial pressure of hydrocarbons in aims to supress the formation of coke through *Eq. 14* (Song & Tang, 2018).

However, a separation and purification sequence is still needed (a schematic view of a common PFD is presented in Fig. 4-6).

$$C + H_2O \rightarrow CO_2 + H_2 \qquad \textit{Eq. 14}$$

Another route for ethylene production that is being studied is the obtention of the compound by the dehydration of (bio)ethanol vapour in the presence of a silica, alumina, or other, catalyst (The Essential Chemical Industry, 2017).

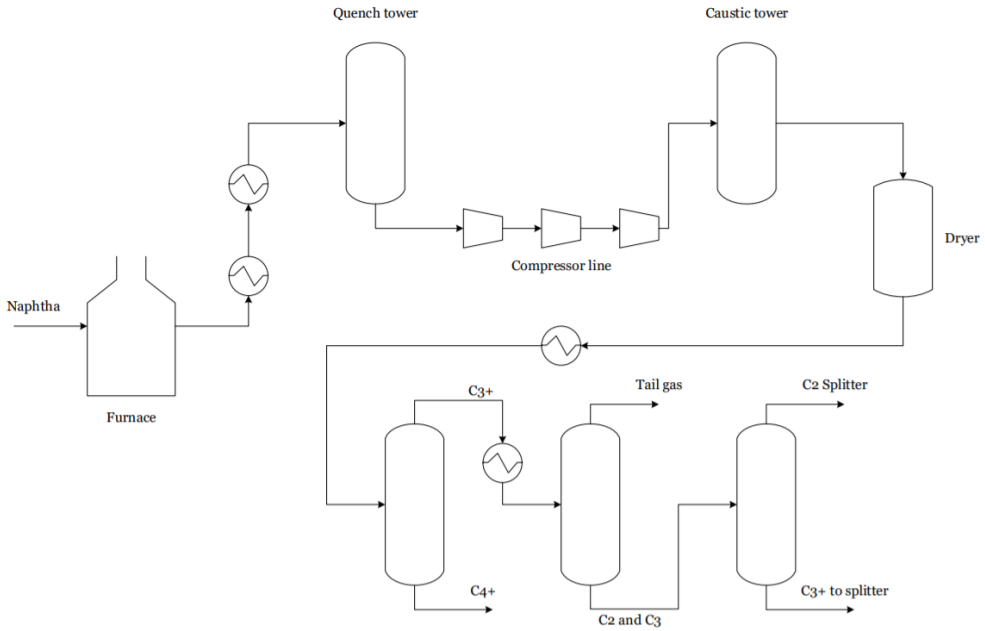

Fig. 4-6: Process flow diagram of the steam cracking of naphtha (Haghighi et al., 2013).

4.1.6 Ethylene glycol

Another high production volume organic compound is ethylene glycol, which is used as a coolant and antifreeze, heat transfer fluid, or to manufacture a wide range of products such as polyester fibres, fiberglass and polyethylene terephthalate (Gulledge, 2021).

4.1.6.1 Hydrolysis of ethylene oxide

Currently, ethylene glycol is solely produced by the thermal hydrolysis of ethylene oxide (*Eq. 15*), which is already the result of the oxidation of ethylene (see section for Ethylene oxide). The process is undertaken in a reactor at high temperatures of around 200ºC and requires a successive separation section since parallel reactions also lead to the formation of di-, tri-, tetra-, and polyethylene glycols. Even if the reaction to these higher homologues cannot be avoided because its kinetics is faster than that of the reaction of ethylene oxide with water, using an excess of water helps optimize the formation of the desired product (Rebsdat & Mayer, 2012a). Unreacted water is separated in a first distillation column and re-used in the reactor.

$$(CH_2CH_2)O + H_2O \rightarrow HO\text{-}CH_2CH_2\text{-}OH \qquad \textit{Eq. 15}$$

The purification can be conducted in a sequence of consecutive distillation columns as seen in Fig. 4-7.

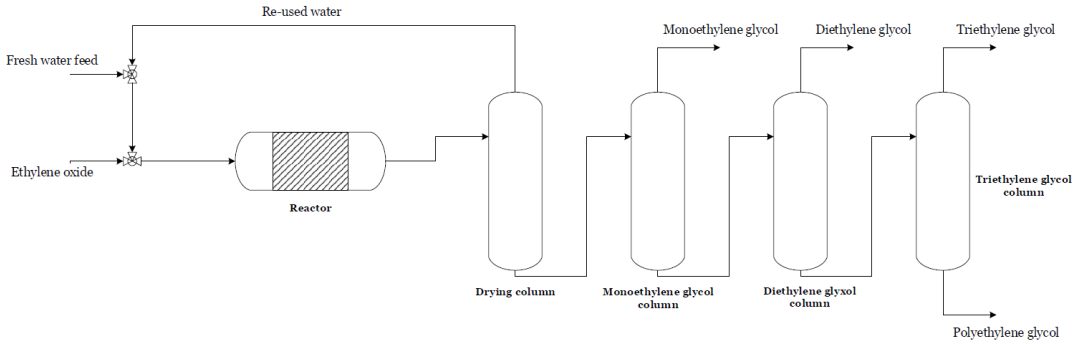

Fig. 4-7: Process flow diagram for the production of ethylene glycol by the hydrolysis of ethylene oxide (adapted from Rebsdat & Mayer, 2012a).

A recently developed alternative to reduce by-product formation is the use of a phosphorous-based catalyst. By introducing a catalyst both operational and capital costs are reduced since less water is used and there is no need for a complex separation section (ICIS, 2010c).

4.1.7 Ethylene oxide

As seen in (section for Ethylene glycol), ethylene oxide is an intermediate used to produce other organics, such as ethylene glycol, but its main application is for sterilization and disinfection in the medical sector. Furthermore, in some cases it is also used as a fumigant (Rebsdat & Mayer, 2012b).

4.1.7.1 Direct oxidation of ethylene

Historically, ethylene oxide was produced by the chlorohydrin process, using this compound as an intermediate, but the process was gradually superseded since it was highly pollutant. Currently, the primary route to produce ethylene oxide is by the oxidation of ethylene usually in a multi-tubular reactor with a fixed bed in each tube since the reaction is catalysed. Refrigeration is needed because the process is highly exothermic (ICIS, 2009).

Ethylene is fed to the reaction unit with oxygen, while silver is used as the catalyst. Two parallel reactions take place at the surface of the catalyst, those being the desired partial oxidation of ethylene (*Eq. 16*) and a complete combustion of

ethylene which results in water and CO_2 (*Eq. 17*). Moreover, the combustion of ethylene oxide once it is formed to give CO_2 and water is also present.

$$H_2C{=}CH_2 + ½\ O_2 \rightarrow C_2H_4O \qquad \textit{Eq. 16}$$

$$H_2C{=}CH_2 + 3\ O_2 \rightarrow 2\ CO_2 + 2\ H_2O \qquad \textit{Eq. 17}$$

At an industrial level, the process operates at temperatures around 200-300ºC and 10-30 bars. A recirculation of gas is used, as well as a purge to prevent the accumulation of inert compounds. After the reaction unit, the mixture is lead through two scrubbing units to separate the ethylene oxide, which is dissolved in water. On the one side, the product-rich aqueous flow is sent to a purification sequence constituted by a desorber (which removes any remaining CO_2, unreacted ethylene, and other contaminants), a stripping column, and a distillation tower (where water is removed, and the product is obtained). On the other side, as for the gas leaving the ethylene oxide scrubber, it is separated in three parts, one is purged, another is recycled, and a small fraction is sent to a second scrubber and a consecutive desorber, which separate the CO_2 contained in the gas. This way, it can be re-used in other applications. The process flow diagram for an oxygen-based process is represented in Fig. 4-8. If ethylene is reacted with air instead of pure oxygen (air-based process), an additional section is required for air purification before it enters the reactor (Rebsdat & Mayer, 2012b).

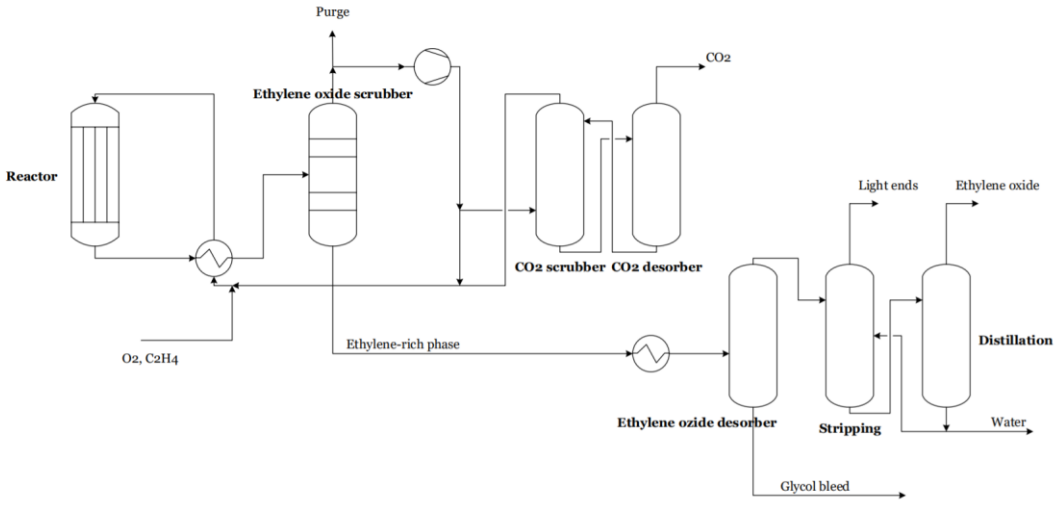

Fig. 4-8: Process flow diagram for the production of ethylene oxide from ethylene (adapted from Rebsdat & Mayer, 2012b).

4.1.8 Methanol

Methanol is the simplest among aliphatic alcohols and one of the most versatile base chemicals. It is used in a variety of applications, ranging from processes within the chemical industry itself, (where methanol is a platform chemical to produce many other chemicals such as acetic acid) to water treatment plants (where it is used in the denitrification process (Foglar & Briski, 2003)). Additionally, as ammonia, it has gained importance as a clean and safe energy source, becoming a potential alternative to fossil fuels (Bertau et al., 2014).

4.1.8.1 Steam reforming of natural gas

As seen in the correspondent section, the Steam reforming process produces synthesis gas from a variety of feedstocks. Nearly 90% of the world's production is from natural gas (Wernet et al., 2016), hence the steam reforming process using natural gas is the methanol production process included in this study. Methanol can be co-produced along with ammonia; however, combined plants are less common and therefore not included in the dataset.

Similar to the production of ammonia through steam reforming, the process consists of four main steps, including feedstock preparation, reforming, methanol synthesis and purification. They are all described in detail in Steam reforming. However, there are some differences in the reforming process if the obtained syngas is aimed to produce methanol instead of ammonia. Since the methanol synthesis reactions are not between nitrogen and hydrogen but between carbon mono- and di- oxide and hydrogen (*Eq. 18* and *Eq. 19*), these compounds do not need to be removed before entering the synthesis loop as in the process for ammonia.

Syngas is directly sent to the methanol synthesis section, where it is converted into methanol through *Eq. 18* and *Eq. 19* in a quench flow reactor containing various catalyst beds. Unreacted gas is recycled as seen in Fig. 4-9 (Udugama, 2017).

$$H_2 + CO \leftrightarrow CH_3OH \qquad \textit{Eq. 18}$$

$$3H_2 + CO_2 \leftrightarrow CH_3OH + H_2O \qquad \textit{Eq. 19}$$

Besides methanol, ethanol is formed in the reactor, as well as butanol, di-methyl ether, tri-methyl amine, and other organic acids and hydrocarbons, even if in lower concentrations than ethanol. An efficient separation section is needed for the produced methanol to reach the purity level established by regulations (< 10 ppm of ethanol).

This purification of the product is carried out by a first topping column which removes the light compounds of the mixture and a distillation column for the final separation of methanol (Udugama, 2017). Depending on the desired purity level or the conditions of the process, one or more additional distillation columns are used.

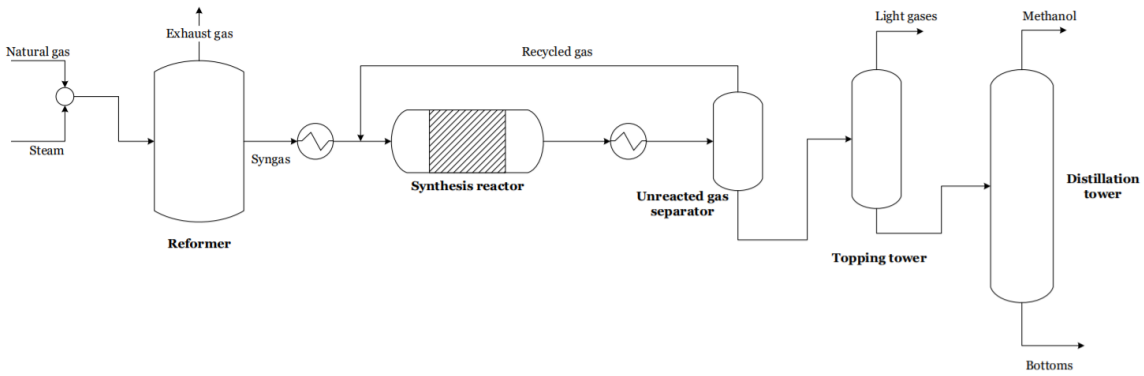

Fig. 4-9: Process flow diagram for the production of methanol by steam reforming (adapted from Douglas & Hoadley, 2006; Udugama, 2017).

4.1.9 Xylene

After benzene, the second included BTX aromatic is xylene, a widely used compound in many different areas despite its toxicity. It is of relevant importance in tissue processing, and also used as a cleaner, a lubricant, a solvent (Kandyala et al., 2010) and an intermediate in the production of other chemicals such as Terephthalic acid.

4.1.9.1 Catalytic reforming

Xylene is mainly obtained by catalytic reforming in the same process as benzene. As discussed in (section for catalytic reforming), xylene is obtained as the top product of the last of the distillation towers in the separation section of the catalytic reforming process for the production of BTX aromatics (Fig. 4-4).

4.1.10 Polyethylene

Polyethylene (PE) is a highly versatile polymer, which makes it the highest production volume plastic worldwide. Its properties vary according to its density and branching, yielding several types of PE. In this study, the three principal grades are be studied, including high density (HDPE), low density (LDPE) and linear low density (LLDPE) polyethylene. Other variations, such as high molecular weight PE or chlorinated PE have much lower production volumes and are often classified as subdivisions of the three previously stated main types (Kupolati et al., 2017).

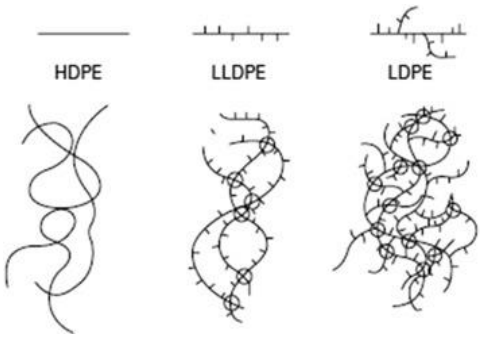

Fig. 4-10: Main types of PE (Malkan, 2017).

On the one hand, HDPE has been classified in this study as PE with a specific density higher than 0.94 g/cc. It is highly malleable but offers high tensile strength. It is resistant to a wide variety of chemicals, and therefore mainly used as a packaging plastic for domestic products such as cleaning products, toys, and food. Another common application of HDPE is in piping (Sadiku et al., 2017; Kumar & Singh, 2020).

On the other hand, all PE with a specific density lower or equal to 0.94 has been classified as LDPE or LLDPE (LDPE's density ranges from 0.91 g/cc to 0.925 g/cc, while LLDPE's slightly higher and typically between 0.915-0.93 g/cc). Both grades of low-density PE have a higher flexibility than HDPE but lower chemical and physical resistance. They have high oxygen and CO_2 permeability and are poor barriers to flavour and smells. However, they are highly impermeable for water and vapour (Kamal et al., 1984).

As seen in Fig. 4-10, LDPE is the most branched polymer in the group, which makes it the lightest type of PE. It is widely used in packaging, especially when thin, light, or flexible plastic is needed, such as in the manufacture of bags,

packaging foam, or in plastic sheeting. The agriculture and construction industries use LDPE quite extensively (Sastry, 2014).

Finally, LLDPE also fins applications in the packaging industry, being the main PE used for the manufacture of plastic films and coatings. As stated before, its density range is similar to that of LDPE. However, at equal density, it offers higher strength, resistance, and elongation (Goswami & Mangaraj, 2011).

PE can be produced by a variety of processes. Table 4-1 shows which of them are used for the manufacture of each type of PE. All production routes can be divided between two categories, those being high-pressure polymerization, which produces LDPE (using autoclave and tubular reactors) and low-pressure polymerization, which produces LLDPE and HDPE (by the solution, slurry, and gas-phase processes). The first group of processes use an initiator to trigger the reaction of ethylene with itself at high pressures. The second group operate at lower pressures but require a co-monomer (such as 1-hexene or 1-butene) and the use of a transition metal catalyst, which can be chromium or molybdenum oxide, metallocene or the Ziegler-Natta catalyst.

Table 4-1: Processes used to produce the three main types of PE.

Polymer	**Processes**
HDPE	Gas phase, Slurry, Solution
LDPE	Autoclave, Tubular
LLDPE	Autoclave, Gas phase, Slurry, Solution, Tubular

Firstly, the two high pressure processes are described. They are used for the industrial manufacture of LDPE and LLDPE.

4.1.10.1 Autoclave

LDPE is mainly produced by two processes using autoclave and tubular reactors. The autoclave process uses high pressures and can also produce LLDPE if an additional alpha olefin comonomer is used (as in the other processes producing LLDPE), which allows for the formation of the side chains that differentiate LLDPE from LDPE. However, only a really reduced fraction of all produced LLDPE is obtained through this process (Nexant, 2008).

Since the autoclave process works at high pressure, the raw materials need to be compressed to reach 1300-2000 bar. Since a pressure increase also leads to a temperature increase, the compression stages are interspersed with cooling stages. Afterwards, the compressed ethylene and the adequate initiator (an organic peroxide) is injected in the autoclave reactor working at temperatures of around 250ºC (Quachio et al., 2012). An autoclave reactor operates as a continuous stirred tank reactor (CSTR), having a varying residence time. Thus, the obtained polymer has a wide molecular weight distribution. Once the reaction is complete, unreacted ethylene is separated from the product and any possible impurities are recycled. As seen in Fig. 4-11, two main separation stages are usually employed, one operating at high pressure and the other at a lower pressure. Additionally, recycled ethylene is treated to remove all contaminants, such as compressor oils and solvents.

As for PE, it is found in liquid form after the second main separator. To make storage easier, it is cooled down and shaped into granules in an extruder (Klimesch et al., 2001; Vetter, 2001; Kehinde et al., 2012).

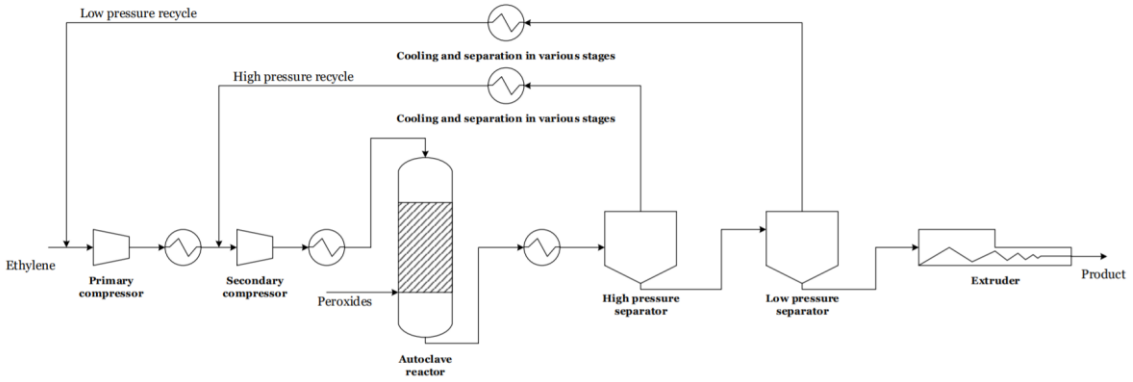

Fig. 4-11: Process flow diagram for the production of PE by the autoclave process (adapted from Kehinde et al., 2012; Quachio et al., 2012; Lingell, 2015).

4.1.10.2 Tubular reactor

The same high-pressure process depicted in Fig. 4-11 can be used to obtain LDPE substituting the autoclave reactor with a tubular reactor (Kval et al., 2013), which offer more flexibility since they usually include lateral injection points, and work as a plug-flow reactor. The polymer obtained from tubular reactors has more homogeneous molecular weight and less long chain branching (Neilen & Bosch, n.d.).

The tubular route is the principal of the two processes for producing LDPE since it offers higher conversion rates (ICIS, 2010a).

The three different processes for low pressure polymerization of ethylene to HDPE and LLDPE are now described. Combinations of these processes in series can also be used (e.g., a slurry process configuration using two consecutive reactors, the second being a gas-phase reactor).

4.1.10.3 Gas phase

The slurry process can produce both HDPE and LDPE and is the most important low-pressure route in terms of plant capacity and production (Nexant, 2008) because it does not use solvents, has short processing times and usually also low capital costs. The process can also produce other polymers, such as polyethylene-vinyl acetate or polypropylene.

The main unit for the gas phase process is a mixed fluidized bed reactor, which offers a residence time distribution similar to that of a CSTR. Purified gaseous ethylene is fed at the bottom of the reactor, while the selected catalyst and pre-polymers, are also injected in the solid phase. Inside the fluidized bed, polymerization takes place at the active sites located at the solids' surface. PE particles grow and sink to the bottom of the reactor, where they are collected. Unreacted ethylene and pre-polymer are collected at the top of the column and re-cycled in the reactor. The gas is also cooled to remove heat from the exothermic polymerization process before being fed back to the reactor in order to control the operation temperature and maintain it around 80-100ºC. The reactor works at a pressure of 30-35 bar (Hulet et al., 2008; Ho et al., 2012; Polymer database, n.d.).

As seen in the simplified process flow diagram in Fig. 4-12, a pre-polymerization reactor is used to increase the conversion inside the reactor. Lastly, a cyclone separates any solids remaining in the recycle gas flow.

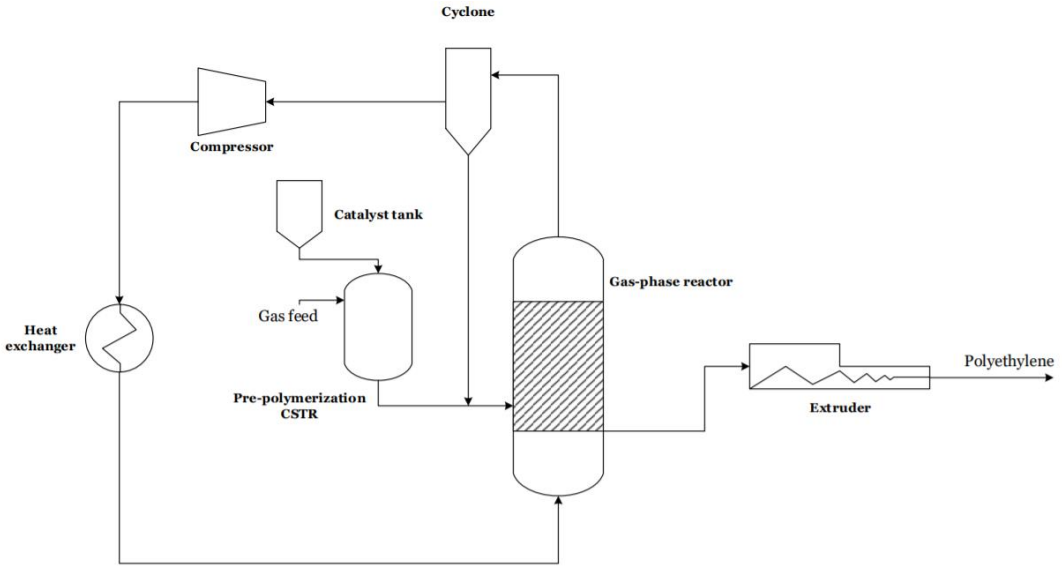

Fig. 4-12: Process flow diagram for the gas phase polymerization of ethylene (adapted from Fernandes & Lona, 2000; Sun et al., 2020).

4.1.10.4 Solution

The solution process also has short residence times and is especially dedicated to the production LLDPE. As stated before, a comonomer must be added to obtain this polymer. In this case, octene-1 comonomer is used (Nexant, 2008).

The process is based on the dissolution of the catalyst in a solvent using a CSTR or a loop reactor operating at around 140ºC and 40-50 bar. The final polymer must be separated from the solvent and purified (Zhong et al., 2017).

Both unreacted ethylene and the solvent must be recovered after the reaction to enable re-use. The separation section has four stages. Initially, unreacted raw material is separated from the mixture and recycled in the reactor. Afterwards, the catalyst is filtered and deactivated with an alcohol, usually methanol. Solvent is then recovered in a hot water bath and a final separation of the product and the added water is needed. As seen in Fig. 4-13, the product is dried and led to an extruder like in the previously described processes (Encyclopædia Britannica, 2017).

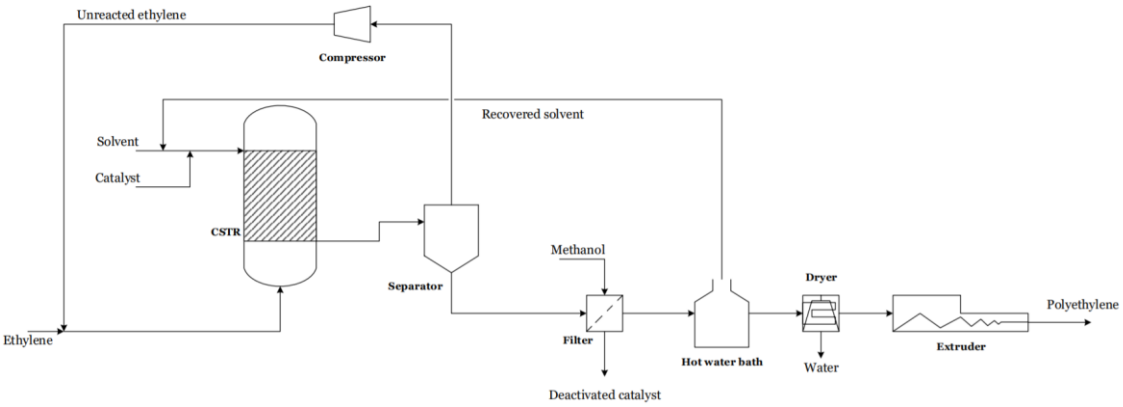

Fig. 4-13: Process flow diagram of the solution process for the production of polyethyelene (adapted from Encyclopaedia Britannica, 2017).

To make the process more environmentally efficient, the solvent can be replaced by water. The process using water instead of solvent is called suspension polymerization.

4.1.10.5 Slurry

The slurry process is especially adequate to produce HDPE, even if only a small fraction of all produced LLDPE is also obtained through this process (Nexant, 2008). Some advantages of slurry-phase polymerization are the high conversion rates obtained and the simplicity of the process, as well as the easier temperature control (Thakur et al., 2020). Usually, two or more reactors are combined in the slurry process in either parallel or series configuration.

As in the solution process, the reactor can be a CSTR or a loop reactor operating at around 110ºC and 31 bars, but in this case the catalyst or the product formed are not dissolved in a solvent but suspended in liquid medium. A pre-polymerization reactor is often also included in the process.

A flash separator and an ethylene recovery unit are placed after the reactor to separate the polymer from the mixture gas containing unreacted ethylene, diluent, and pre-polymers. The obtained PE is dried and cut into pellets (Khare et al., 2002; Zhang et al., 2016).

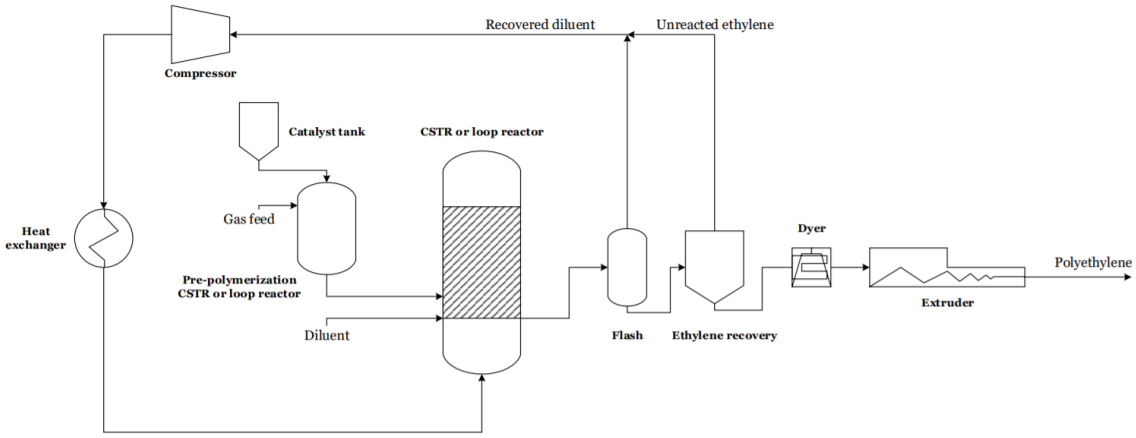

Fig. 4-14: Process flow diagram of the slurry process for the production of PE (adapted from Kosek & Ray, 1999).

4.1.11 Polypropylene

Polypropylene (PP) is the polymer obtained from the polymerization of propylene. It has the second largest production volume after PE, from which it differs in having higher heat resistance, as well a better resistance to fatigue. Its density is lower than that of ethylene and any commodity plastic (from 0.89-0.92 g/cc). Blends between ethylene or other polymers with PE are common, since a final plastic with specific properties can be obtained through tailored combinations (Koerner & Koerner, 2018). PP can be produced in three main structural tactic arrangements, including isotactic (which represents around 95% of all PP), atactic and syndiotactic (Crawford & Quinn, 2017).

PP, as ethylene, is widely used in the packaging industry, but also in the medical, textile, and automotive sectors. Numerous plastic items for domestic, industrial, medical or research purposes are made from PP.

PP is obtained from the polymerization of propylene. Various polymerization routes can be employed. Among them, the gas phase and slurry phase polymerizations have already been described, while details for the remaining process is provided next.

4.1.11.1 Bulk

The bulk (or mass) process uses CSTRs or loop reactors operating at 67-87ºC and 30-40 bars to convert liquid propylene into PP.

Styrene, ethylene terephthalate and other monomers can also be polymerized using the bulk process.

As in other polymerization routes, an initiator and one of the catalysts for low-pressure polymerization is used, and unreacted feed is recycled in the reactor. Since the principal raw material is liquid propylene, it is used as a solvent for the polymer and there is no need to add other substances. Bulk polymerization can be carried out in both batch and continuous operation modes, and its principal challenge is temperature regulation (Netto & Pinto, 2001; Youssef, 2019). There are numerous process configurations, all including a reaction step and several separation and purification stages, as seen in the other polymerization processes.

4.1.11.2 Gas phase

The gas phase process for the production of PP has the same structure as it does when PE is produced (Fig. 4-12). However, in this case, the operation temperature and pressure are around 47-87 ºC and 8-35 bar. The Ziegler-Natta catalyst and metallocene are the principal catalysts used (The Essential Chemical Industry, 2016).

4.1.11.3 Slurry

Slurry-phase polymerization can be used for the manufacture of PP as well as it can for the polymerization of ethylene to PE. The process flow diagram for this route is depicted in Fig. 4-14.

4.1.12 Propylene

Propylene is one of the most relevant base chemicals and serves as a building block for a wide range of products such as Polypropylene, Acrylonitrile, Cumene and Propylene oxide, all included in this study, as well as and different oxo alcohols and halides. Therefore, as with ethylene, special attention is paid to propylene when doing the calculations to avoid double-counting.

Propylene can be manufactured in three different grades, those being polymer grade (the composition of which has 99.5% of propylene), chemical grade (92-96% of propylene) and refinery grade (70% propylene).

While polymer and chemical grade propylene are used within the chemical industry, refinery grade propylene has a thermal use or is employed as an octane-enhancing component in fuels (Bingham et al., 2001; O'Neil, 2013; Zimmerman, 2017). This study focuses on polymer and chemical grade propylene.

The volume of chemical and polymer grade propylene destined to applications other than being a chemical intermediate is negligible if not zero (Kroschwitz et al., 1991; Chenier, 1992; Wittkof & Reuben, 2996; Sawyer, 2015; Maddah, 2016; Plotkin, 2016; Kolb & Field, n.d.). Therefore, special considerations have been made when analysing its total volume (see Interrelations between processes).

4.1.12.1 Steam cracking of naphtha

Most propylene is obtained as a by-product of ethylene in the Steam (thermal) cracking of naphtha process. As the considered feedstock for ethylene production by steam cracking was naphtha, the same liquid is fixed as the raw material for propylene. The ratio between the obtained ethylene and propylene can be modified by changing the feedstock (less propylene is produced from butane and propane than from naphtha or gas oil), or the severity of operation (Nexant, 2009). The process flow diagram for this process is shown in Fig. 4-6.

4.1.13 Propylene oxide

Propylene oxide, mainly manufactured from propylene through the chlorohydrin process, is generally used as a chemical intermediate to produce propylene glycol and other polyethers. Additionally, it has applications as a pesticide and sterilizer, even if it must be manipulated with caution due to its toxicity and flammability (National Center for Biotechnology Information, 2021a).

4.1.13.1 Chlorohydrin process

This process is based on the dehydrochlorination of a chlorohydrin intermediate, which is obtained by the addition of hypochlorous acid to propylene.
The reactions take place in three steps, as seen in *Eq. 20*, *Eq. 21*, and *Eq. 22* (Pilli & Asis, 2018).

$$Cl_2 + H_2O \rightarrow HOCl + HCl \qquad \text{Eq. 20}$$

$$CH_3CH{=}CH_2 + HOCl \rightarrow CH_3\text{-}CHOH\text{-}CH_2Cl \qquad \text{Eq. 21}$$

$$CH_3\text{-}CHOH\text{-}CH_2Cl + NaOH \rightarrow CH_3CHCH_2O + NaCl + H_2O \qquad \text{Eq. 22}$$

The reaction of propylene with hypochlorous acid occurs in an absorber-reactor combination or a bubble column reactor at around 50ºC and 1.5 bar without the need to add a catalyst and offers high conversion rates. Propylene dichloride is formed as a by-product. The mixture is then separated from unreacted gases and led to a stripping column where the reaction of the chlorohydrin with sodium hydroxide takes place. This allows for the product to be stripped from the remaining water, which would cause it to hydrolyse in the presence of the base. Finally, propylene oxide is separated from the by-product and purified by distillation (Nijhuis et al., 2006).

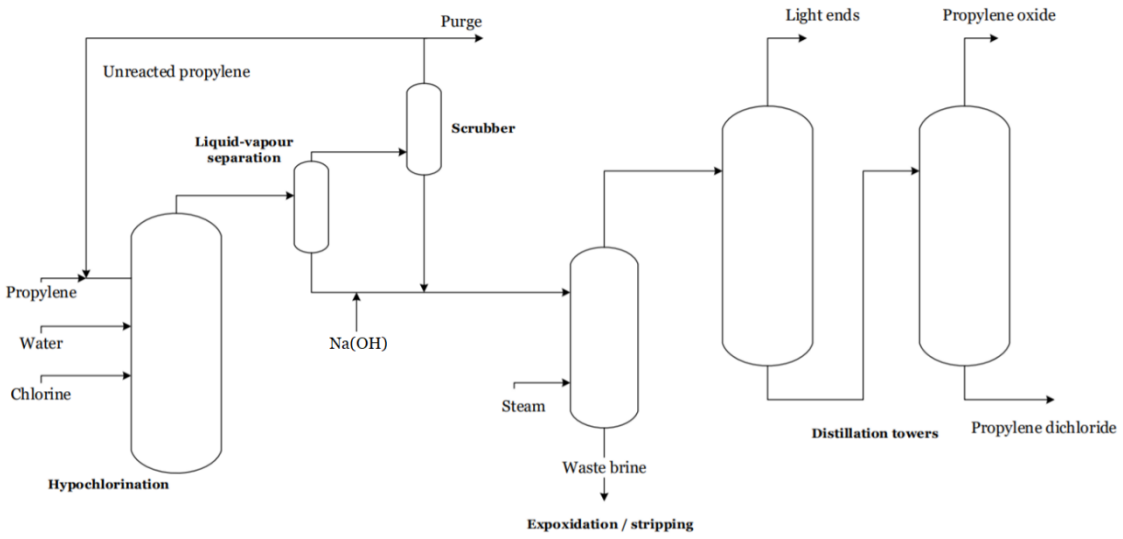

Fig. 4-15: Process flow diagram of the chlorohydrin process (adapted from Matar & Hatch, 2001; Nijhuis et al., 2006).

4.1.14 Styrene

Styrene as a monomer, which is found at a liquid state, is an aromatic hydrocarbon which is often polymerized to produce polystyrene, expanded polystyrene (EPS), styrene-butadiene rubber (SBR), acrylonitrile-styrene-acrylate (ASA), and other various homo- and copolymers. These derivatives of styrene have many applications. As examples, polystyrene is used to make car and household components, and in the packaging industry.

Styrene rubbers are mainly used in the tyre sector but have other applications such as the manufacture of shoe soles or even toys (Mohammad & Simon, 2006). As for ASA resins, they are used in a wide range of sportive, garden, and construction materials since they have high weather resistance and are therefore best suited for exterior uses (McKeen, 2009).

4.1.14.1 Dehydrogenation of ethylbenzene

The process included in the dataset for the production of styrene is the dehydrogenation of ethylbenzene, which follows *Eq. 23*. Since the reaction is endothermic, it is carried out at above 600ºC and atmospheric or lower pressure in one or multiple adiabatic catalytic reactors (ICIS, 2010b). Superheated steam is fed in excess to the reactor with the aim of maintaining such a high temperature. It is also beneficial because it avoids carbon formation and increases the conversion rate to styrene by acting as a diluent (Lee, 2005).

$$C_6H_5CH_2CH_3 \leftrightarrow C_6H_5CH{=}CH_2 + H_2 \qquad \textit{Eq. 23}$$

Benzene and toluene are formed as by-products. To increase the selectivity to styrene, Fe_2O_3 and potassium are used as a catalyst and promoter, respectively. When adding potassium, the stability of the catalyst is also enhanced. Logically, a separation section is still required. Styrene is purified in a distillation column, while the by-products can also be separated for use in other processes. Additionally, vent gas containing by-products is removed from the product mixture in a condenser. To avoid the polymerization of any remaining styrene found in the gas, a polymerization inhibitor is injected to the gas, which can later be further processed (European Patent No. EP0747335B1, 1996). The complete classic process diagram is depicted in Fig. 4-16.

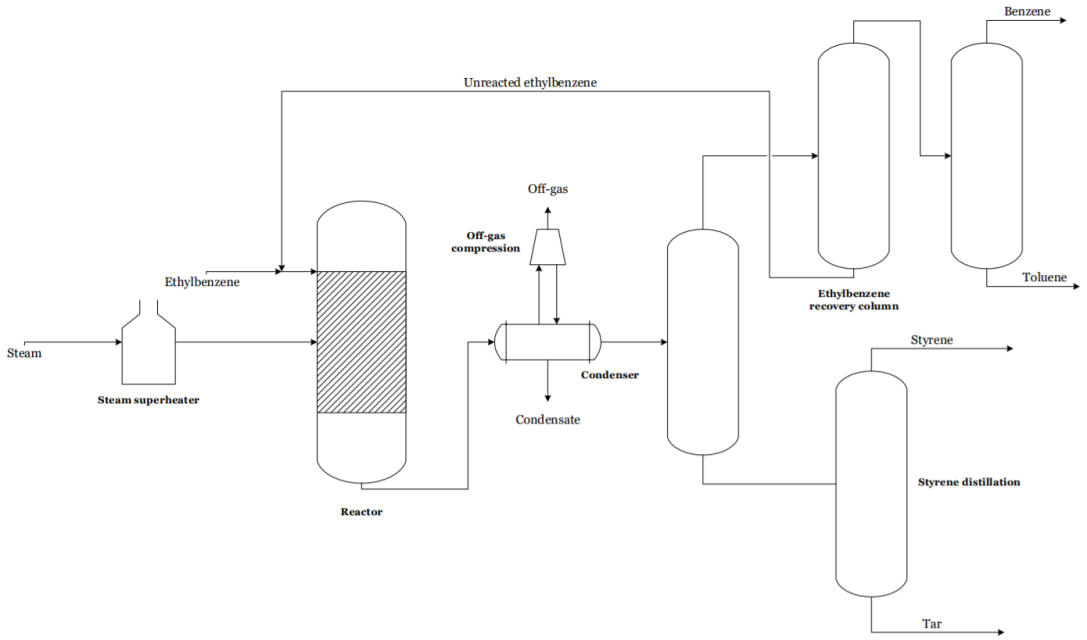

Fig. 4-16: Process flow diagram of the dehydrogenation of ethylbenzene process (adapted from Chadwick, 2000; Zarubina, 2015).

4.1.15 Terephthalic acid

Terephthalic acid (TPA) is one of the most relevant chemicals in terms of production volume and uses. It is mainly used to produce PE terephthalate (PET), which has diverse applications as a packaging plastic, in the textile industry and in the electronics sector (Van Leeuwen, 2003).

4.1.15.1 Oxidation of p-xylene

Terephthalic acid is produced through the oxidation of p-xylene in an acidic medium, using bromide or cobalt/manganese acetate as a catalyst. The reaction follows two steps, as depicted in *Eq. 24*, and is conducted at above 200ºC and 15-30 bars (Hwang et al., 2019).

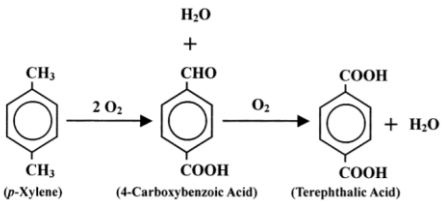

Eq. 24

Various by-products are formed, the most important of which is 4-Carboxybenzaldehyde. The product is purified by filtration (to remove solid contaminants), centrifugation (where the catalyst is separated from the rest of the

mixture in order to be purified and recycled) and digestion (where 4-Carboxybenzaldehyde is further oxidized to terephthalic acid). The final TPA is dried and prepared to be sold. Additionally, the solvent is recovered by distillation (Han et al., 2003).

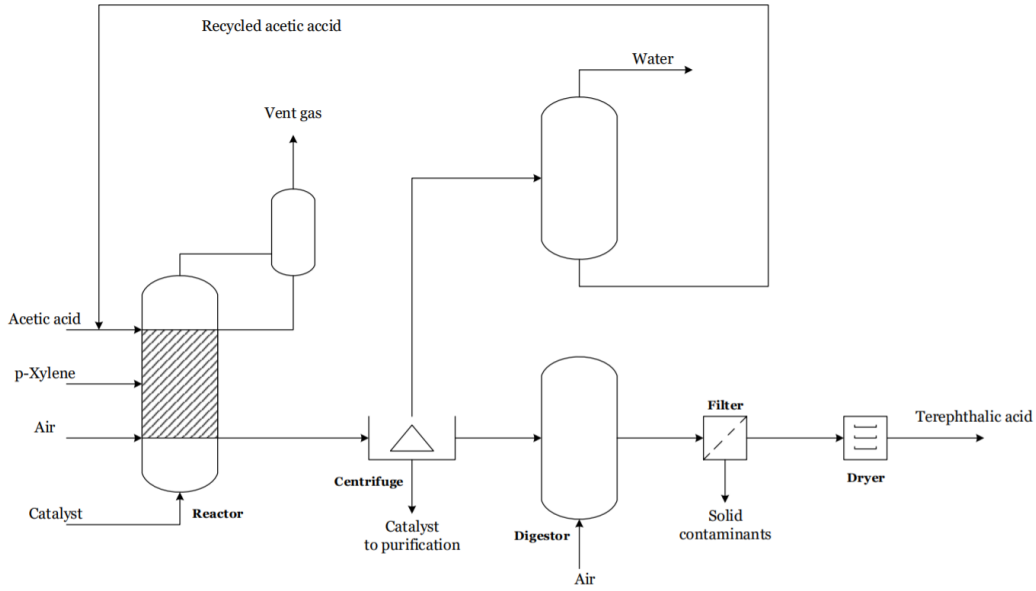

Fig. 4-17: Process flow diagram of the oxidation of p-xylene process (adapted from Han et al., 2003; Sheehan, 2011).

4.1.16 Toluene

Toluene is the third BTX aromatic included in this study. It is used in diverse applications, such as the manufacture of rubber, paints, and coatings, as well as medicines or even model airplanes. It also has a relevant use within the chemical industry as a solvent and chemical intermediate. Various regulations establish the exposure limits to toluene and its use since it can cause narcosis and other numerous health problems (Clough, 2005; National Center for Biotechnology Information, 2021b).

4.1.16.1 Catalytic reforming

As seen in the section dedicated to the production of benzene, toluene is mainly obtained as a by-product in the catalytic reforming process (Fig. 4-4).

4.1.17 Vinyl chloride

Vinyl chloride is mainly destined to the manufacture of polyvinyl chloride (PVC), which is then moulded to produce generally pipes, packaging bottles or materials,

and wires, among other products. PVC is one of the most produced plastics worldwide due to its versatility, low-maintenance, and long lifetime. This last property of PVC creates an environmental concern, just like with other plastics. This environmental issue is thus not caused by the production process but encountered in the end-of-use of the product. Additionally, however, and in contrast with PP or PE, PVC is harder to recycle (Tolman & Dalpiaz, 2013; Abel & DiGiovanni, 2015).

Most industrial vinyl chloride is produced from ethylene. There are two possible routes that can be followed, and both are included in the study.

4.1.17.1 Direct chlorination of ethylene

In the direct chlorination variant, liquid ethylene is reacted with chlorine to produce 1,2-dichloroethane (*Eq. 25*), which is then heated to yield vinyl chloride if a charcoal catalyst is used through the pyrolysis reaction (*Eq. 26*).

$$C_2H_4 + Cl_2 \rightarrow C_2H_4Cl_2 \qquad \textit{Eq. 25}$$

$$C_2H_4Cl_2 + heat \rightarrow C_2H_3Cl + HCl \qquad \textit{Eq. 26}$$

4.1.17.2 Oxychlorination of ethylene

Alternatively, ethylene can be heated together with hydrogen chloride and oxygen to cause its oxychlorination, which also results in 1,2-dichloroethane (*Eq. 27*). For the reaction to succeed, a copper catalyst is employed. Afterwards, *Eq. 26* produces vinyl chloride and water.

$$C_2H_4 + 2\,HCl + \tfrac{1}{2}\,O_2 \rightarrow \quad C_2H_4Cl_2 + H_2O \qquad \textit{Eq. 27}$$

Usually, a combination of both processes is used in vinyl chloride plants, as illustrated in Fig. 4-18. The 1,2-dichloroethane produced by the direct chlorination and oxychlorination is lead to a pyrolysis reactor where it is heated to give the product and hydrogen chloride. Unreacted 1,2-dichloroethane is also recycled back to the reactor. The HCl formed is continuously separated and employed in the oxychlorination reactor, operating at around 350ºC and 4-6 bar. The direct chlorination reactor can operate at either high (around 125ºC) or low (45ºC)

temperatures. The employed reactors are either fixed bed or fluidized bed reactors (Dry et al., 2003; Ma et al., 2020).

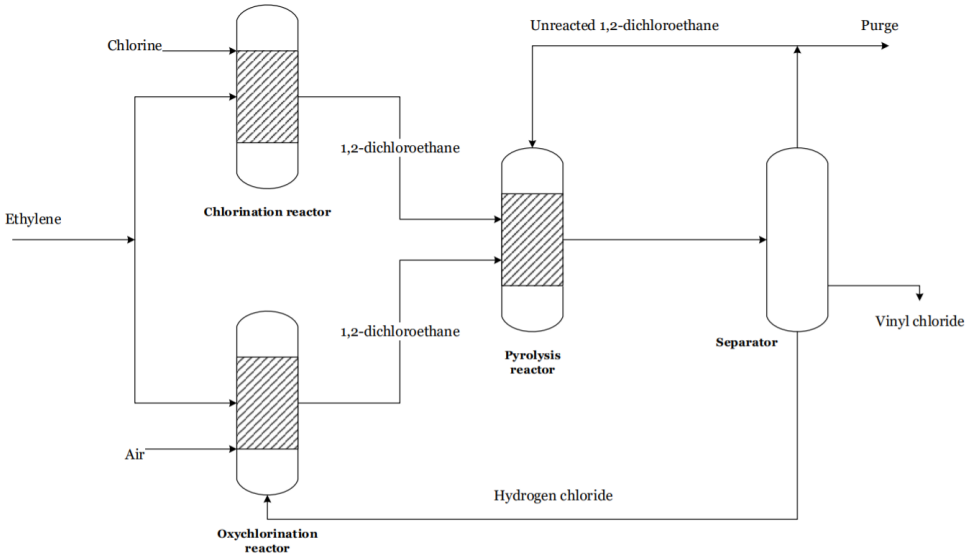

Fig. 4-18: Process flow diagram of the combination of the direct chlorination and oxychlorination of ethylene to produce vinyl chloride (adapted from Ferreira et al., 2020).

4.2 Interrelations between processes

As seen in the previous descriptions, various relationships exist between the chemicals for this study, as a considerable number of them are manufactured from other studied substances. Ethylene and propylene are used as building blocks in the majority of the studied processes. They are used to produce ethylene oxide, PE, styrene, vinyl chloride, cumene, propylene oxide, PP, and acrylonitrile. Indeed, most of all the other chemicals are also interlinked with each other.

These interrelations between processes are of critical importance for this study. The reason is that, following a cradle-to-gate scope, impacts for the manufacture of a given chemical (e.g., PE), include also those caused during the obtention of the necessary energy and raw materials (e.g., ethylene). Therefore, when a chemical studied is also used as feedstock in the production process of another chemical considered, the impacts of the production of the former would be included twice in the calculations. Fig. 4-19 illustrates this concept taking ethylene and PE as examples, and assuming that 0.9 kg of ethylene are needed for the manufacture of 1 kg of PE.

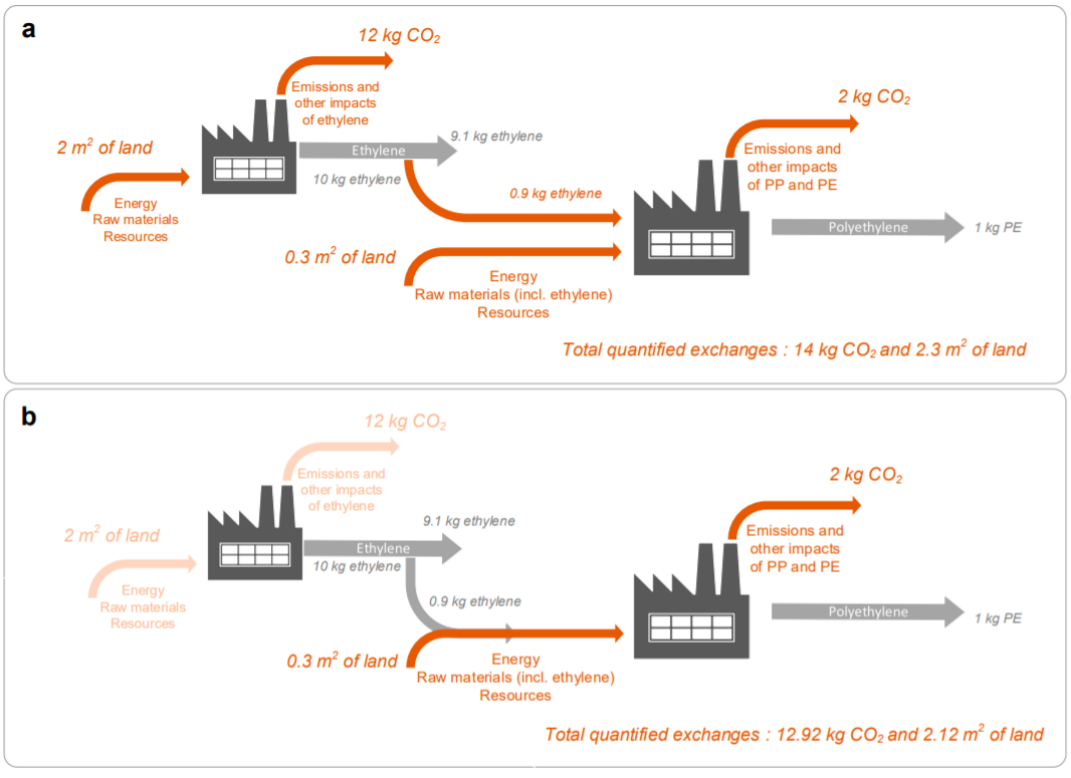

Fig. 4-19: Sankey diagram illustrating the issue with double-counting impacts taking the manufacturing process of polyethylene from ethylene as an example.

Fig. 4-19 takes land use and CO_2 emissions as examples of resource use and pollutant emission. Note that these take the values of 0.3 m^2/kg and 2 kg CO_2/kg, respectively, for PE. For ethylene, LCIs can be calculated as:

$$LCI_{CO_2,ethylene} = \frac{12\ kg\ CO_2}{10\ kg\ ethylene} = 1.2 \frac{kg\ CO_2}{kg\ ethylene} \qquad \textit{Eq. 28}$$

$$LCI_{landuse,ethylene} = \frac{2\ m^2}{10\ kg\ ethylene} = 0.2 \frac{m^2}{kg\ ethylene} \qquad \textit{Eq. 29}$$

In PE's LCIs, the values corresponding to the production of ethylene are already included, as seen in Fig. 4-20.

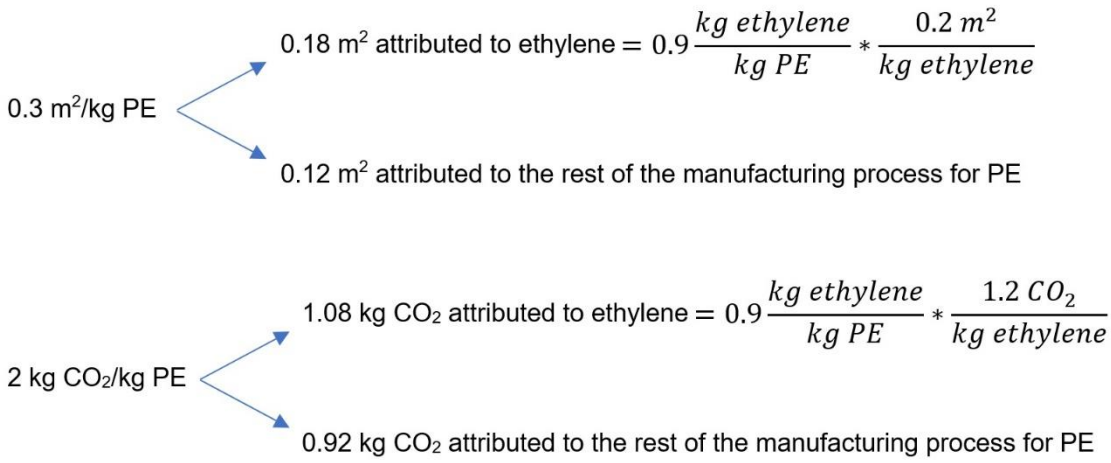

Fig. 4-20: Example breakdown of the LCIs for PE.

Note that in panel a of Fig. 4-19, the volume of ethylene destined to the production of polyethylene is not discarded, and thus the impacts derived from the production of the needed ethylene are counted twice in the final value. Therefore, the total emissions and land use of the system are obtained from the sum of the values both factories.

Meanwhile, in panel b, the 0.9 kg of ethylene used in the second factory are discarded and the total impacts of the system are obtained as follows:

$$CO_2(panel\ b) = (10 - 0.9\ kg\ ethylene) * 1.2 \frac{kg\ CO_2}{kg\ ethylene} + 1\ kg\ PE * \frac{2\ kg\ CO_2}{kg\ PE} = 12.92\ kg\ CO_2 \qquad \textit{Eq. 30}$$

$$Land\ use\ (panel\ b) = 9.1\ kg\ ethylene * \frac{0.2\ m^2}{kg\ ethylene} + 1\ kg\ PE * \frac{0.3\ m^2}{kg\ PE} = 2.12\ m^2 \qquad \textit{Eq. 31}$$

Therefore, as seen in the example, in order to avoid double counting the environmental burdens of any of the selected chemicals, the total production volume of each chemical is recalculated by subtracting the amount of it required as feedstock to any other process considered also within the scope of the study.

This way, the impacts of this production (already quantified in the LCIs of other chemicals) are not included twice. To do so, *ecoinvent* v3.5 data describing the exchanges of each process with other industrial processes is collected and studied.

The volume of base chemical *j* used as feedstock to produce another chemical *j'* ($V_{j,j'}$, in [kg/yr]) is calculated from the product between the total production volume of *j'* ($TPV_{j'}$, in [kg/yr]) and the unitary volume of base chemical *j* needed for the manufacture of *j'* (Fj,j', in [kg *j*/kg *j'*]) as shown in *Eq. 32*. Note that this adjustment is only required for chemicals included within the scope of the study (e.g., not subtracting the amount of toluene used as feedstock for benzene production is not problematic as the manufacture of benzene from toluene is not part of the system under study).

$$V_{j,j'} = LCI_{j,j'} * TPV_{j'} \quad \forall j \qquad \textit{Eq. 32}$$

Production volumes from Eurostat are complemented with import and export trade data from the studied region and time. Since this study is production-centred, import data is neglected to avoid the inclusion of environmental damage that is not happening within the studied area (Lucas et al., 2020). Conversely, export data is included since the production of all exported volume does happen within the European territory and the chemical sector.

The contrary perspective to that of the study's would be a consumption-based approach, where consumers (rather than producers) would be blamed for the associated impacts. In such case, it would be necessary to add imports and exclude exports from production volumes in order to compute the impacts associated with the consumption of products within the EU-28. However, since

the assessed activity is that of an industrial sector, it is adequate to focus on the manufacturing processes carried out by the system under study.

Fig. 4-21 depicts a Sankey diagram providing the interconnections of chemicals within the scope of the study. Nodes represent chemicals (e.g., PP) or chemical/processes pairs (e.g., ammonia from steam reforming, in those cases when there is more than one route included) and the widths of the flows between then are proportional to the volume of the corresponding chemical exchanged [kg/yr]. In this way, the amount of each chemical (*j*) used as feedstock to produce another chemical (*c*) can be identified with a flow connecting node (*j* to *c*). Other inputs which are also necessary to produce each chemical, but which correspond either to compounds or elements not included in the study or other requirements such as energy as neglected in this figure for the sake of simplicity, yet a complete diagram representing all inputs for all second and third stage chemicals can be found in Figure S1-1.

In this figure, nodes denoting exports of chemical *j* are labelled as *j_Exports*, while *j_Other_uses* (OU_j) refers to the fraction of the total production volume of *j* which is given a direct application outside the study [kg/yr], once the calculated consumption of *j* within the study is the sum of the volumes of *j* used for the manufacture of any other included chemical *j'* ($V_{j,j'}$; *Eq. 32*) [kg/yr] (*Eq. 33*).

Data referent to the total production volumes (TPV_j) and exports (EXP_j) are obtained from the *Prodcom* database [kg/yr] (European Union, 2020e).

$$OU_j = TPV_j - EXP_j - \sum_{j'} V_{j,j'} \quad \forall j \qquad \textit{Eq. 33}$$

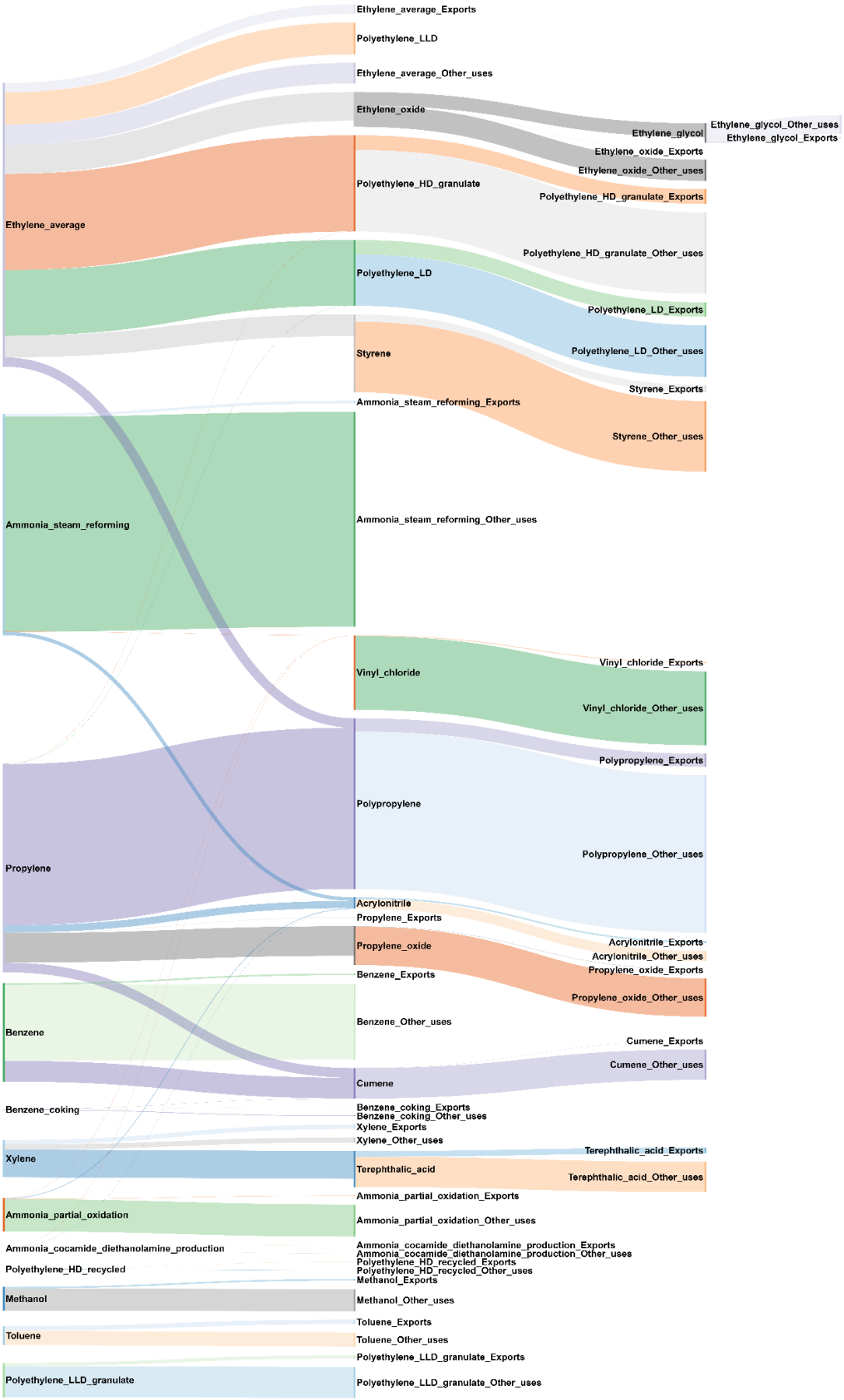

Fig. 4-21: Selected chemicals and their interrelationships.

When *Eq. 32* and *Eq. 33* are used to recalculate production volumes in such a way that no double counting issues can be encountered. In this context, a difficulty is found only in the case of propylene, where the amount of this chemical needed as input for the manufacture of PP, acrylonitrile, propylene oxide, HDPE, LDPE and cumene altogether ($\sum_c V_{polypropylene,c}$) exceeds the total production volume of this chemical after discounting exports ($TPV_{polypropylene} - EXP_{polypropylene}$). This results in the propylene volume dedicated to other uses (*propylene_Other_uses*) to be negative for this compound.

As detailed in *Prodcom*'s user guide, these types of issues can arise when different data collection methods and principles for trade and production are reconciled. For instance, it could be the case that part of chemical *j*'s volume required to produce other compounds, as computed from LCIs using *Eq. 32* (sum of $V_{j,c}$), were indeed imported from other regions and therefore not produced within the territory under study.

To solve this issue, the applications of propylene are researched. The percentage of total volume of propylene used for the manufacture of other chemicals is calculated for this study, and the results are compared with those of other studies. The fractions corresponding to acrylonitrile, cumene and propylene oxide match with all the consulted sources (Sawyer, 2015; Maddah, 2016; Plotkin, 2016). The remaining volume of propylene is destined to the production of PP and *other* chemicals (alcohols including butanol, isopropanol, and 2-ethyl hexanols, acrylic acid, and butyraldehyde). No direct applications are cited in any of the studies (Carr, 2020; Merchant Research & Consulting, 2020).

It must be acknowledged that while this study is focused on the European region, the studies used for comparison show global data, since no regional statistics were available. Thus, changes in the exact shares of propylene destined to each chemical are likely. For instance, in America, a larger volume is destined to propylene oxide (Hocking, 22005; Kolb & Field, n.d.). (Tables S1-2 and S1-3).

However, in all cases, the total propanol production is destined to the manufacture of other chemicals (see section for Propylene). This means that it is no longer necessary to compute cradle-to-gate impacts from propylene production as these are assumed to be already included in those of the derived

chemicals. Consequently, and in view of all the presented information, the total calculated consumption plus the exports for the chemical are set equal to its total production volume.

During the Treatment of LCI data, the calculations undertaken in this section are applied to the PB-LCIA model to avoid the aforementioned replication error.

5 Earth Systems

We define the Earth System as the integration of the planet's spheres, mainly including the hydrosphere, atmosphere, biosphere, cryosphere and geosphere and their interactions through fluxes of both materials (biogeochemical cycles) and energy (radiation, convection, and conduction) (University of London).

Earth Systems are capable of a certain resilience and can hold the consequences of one or more PBs being temporarily surpassed, yet persistent pressure on them can trigger irreversible and severe environmental changes. There are slow and fast feedbacks operating over different time frames depending on the sensitivity of a system, a clear example being the climate change boundary (Zeebe, 2013; Rockstrom et al., 2009). Fast feedbacks in this case include, for example, the loss of sea ice or permafrost over decades due to the transgression of the climate change boundary, while the loss of ice sheets or changes in vegetation and ocean circulation can be described as slow feedbacks since they operate in longer timescales (decades, or even centuries). Even if the larger effects can take millennia to show unacceptable change, it is important to consider that the effects of long-term pressure on the Earth Systems can build up to abrupt and unpredictable, as well as prolonged responses. A similar reference situation would be the Paleocene-Eocene Thermal Maximum, when a massive amount of carbon was released persistently during probably more than 20000 years, but the effects of which lasted for around 200000 years. This caused changes in the carbon cycle, the climate, the distribution and the evolution and extinction of species, among others. This event can be studied to reveal more about the planet responses to environmental changes (Mclnerney et al., 2011).

PBs introduced by *Rockström et al.* in 2009 were defined for the most important Earth System processes. For each of them, control variables which were reliable, robust, and universally applicable to quantify the state of the boundary were identified. For the PBs, the limit is linked to the global perception of what environmental damage is acceptable and what risks and changes we are willing to take and make.

There are Earth system processes that do have a clear threshold where a critical change would happen, while others do not but there is still a point in which

increasing stress upon them would cause growing, and at some point, irreversible damage, and chained effects to other systems. For example, the increase of land transformation (which has no threshold) or deforestation can lead to a decrease of the amount of carbon absorbed by vegetation, which would influence the climate change boundary. These non-linearities in the type of response different Earth Systems can give were considered when defining the PBs. A distinction is made between those PBs that can directly lead to a critical and well-defined threshold and those which operate with slower feedbacks (Fig. 5-1).

Additionally, an uncertainty zone was defined for each boundary, since Earth systems show complex behaviour and interact with each other, making it not realistic to draw an exact threshold. Many analogies can be used to clarify the importance of establishing uncertainty zones. As an example, if we want to make a distinction between hot and cold temperatures, 40ºC would undoubtedly be classified as hot weather, while -5ºC would as cold weather. However, the point where the temperature lowers enough to start being perceived as cold or vice versa is hard to define. Thus, an uncertainty zone helps define the intermediate range of values which would be misleading to classify, or which would even risk being classified from a subjective point of view.

PBs are, therefore, not presented as a unique value below which we can see no affectation of our activities on the environment at all and above which the consequences are unbearable, but rather as thresholds that have an associated uncertainty. All values given for each boundary assume that the rest are not being transgressed (i.e., they are assessed *ceteris paribus*).

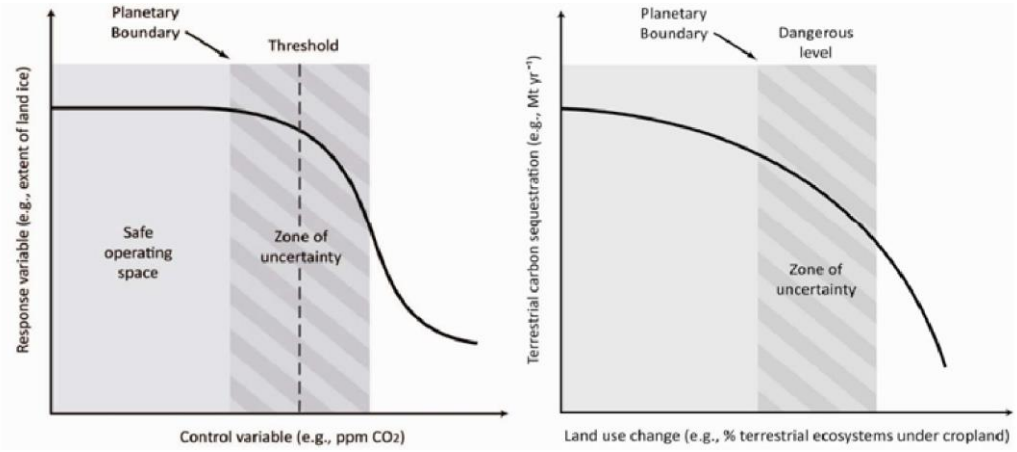

Fig. 5-1: Behaviour differences between Earth Systems (Rockström et al., 2009).

It is known that at least three of the principal PBs have been transgressed to date, including the biodiversity loss, the Phosphorus cycle, and the Nitrogen cycle systems. Additionally, the global impacts on the climate change and land-system change PBs already lie within the zone of uncertainty and the aerosol loading boundary is locally transgressed. Thus, the only totally respected PBs are those for ocean acidification, stratospheric ozone depletion and freshwater use (Steffen et al., 2015). This is already having direct consequences, such as changes in vegetation due to temperature increase (Rockström et al. 2009) or the spreading of pandemic-causing illnesses due to the pressure put on biodiversity. Moreover, further changes can cascade from the transgression of said thresholds, since all boundaries interact, and the lack of stability on one can alter the rest. Therefore, research and action towards maintaining our activities within all PBs is required. Fig. 5-2 shows the concept and current state of the PBs. The yellow region represents the uncertainty range of each boundary, the lower bound of which is where the threshold for each PB lies. If impacts fall within the green zone, the boundary is not transgressed, while the Earth System is under risk if the contributions reach the yellow or red zones. The aerosol loading PB is not represented since its global state has not been quantified yet, and its transgression is regional. Besides, the state of the ozone depletion PB varies seasonally. Even if it is represented as respected it is met annually during spring.

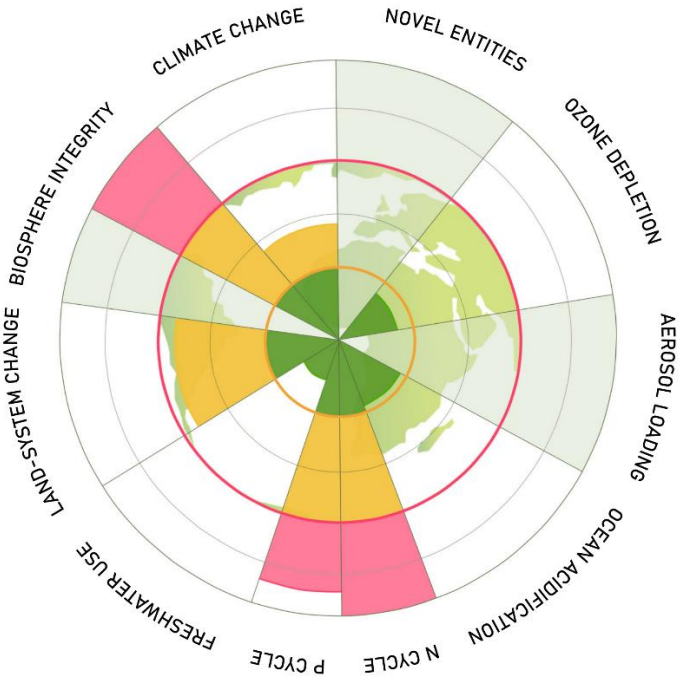

Fig. 5-2: Current state of the PBs.

6 Planetary boundaries

The PBs framework is based on the scientific evidence that the Earth is not a combination of isolated processes but rather a single, integrated system. Interactions between all the processes composing the global system define the epoch the Earth is found in by regulating every aspect of the planet's functioning, e.g., climate, hydric resources, air movements, ocean dynamics or energy exchanges. The elements that compose the Earth system are therefore interlinked, exchange fluxes and depend on each other. The PBs not only have the aim to identify and understand the processes that regulate the stability and capacity of resilience of our planet, but also to provide guidelines for their preservation in order to avoid the destabilization of the Earth and the shift out of the Holocene epoch, which provides us with the suitable conditions for life upon which we depend (McCartonSean & Reid, 2021).

Nine PBs have been defined to date (i.e., energy imbalance at top of atmosphere, atmospheric CO_2 concentration, stratospheric ozone depletion, ocean acidification, the nitrogen and phosphorus cycles, land-system change, freshwater use, aerosol loading, biodiversity integrity, and new entities), even if the definition of two of them (biodiversity integrity, and new entities) is particularly complex and the scientific community has yet to reach an agreement on how to address them. These two boundaries are not included in this study.

In this section, the six PBs considered in this study (see Table 6-3) are discussed, along with how their disturbance can alter the current state of the Earth systems. All criteria playing a role in the definition of the thresholds is explained. Uncertainties are defined around an average value, and the lower-end of the uncertainty range is set as the threshold. As an example, the uncertainty range for the maximum atmospheric CO_2 concentration the climate could withstand is that of 350-500 ppm of CO_2, with 350 ppm being the nominal threshold defined for this PB. The three principal systems which have global-scale thresholds are ocean acidification, climate change, and stratospheric ozone depletion. The rest of PBs, with slower control variables, primarily suffer from major disturbances at regional scales, which may lead to global risks when the impacts aggregate or may trigger other boundaries to be transgressed. CFs provided by the PB-LCIA

methodology for all selected boundaries are global, yet regional CFs are sometimes also available or all slower control variables except for the nitrogen one (i.e., the phosphorus, land system change, freshwater use, and aerosol loading boundaries). If enough information can be collected to assess the boundary at a regional level, the study adopts regional CFs for Europe.

As explained, the impact of the chemical industry on the PBs for the rate of biodiversity loss, and the introduction of novel entities (i.e., heavy metals, endocrine disruptors, biopersistent compounds, etc.) is not quantified. Both are extremely complex systems composed of interactions between species and chemicals, respectively, which cannot be simplified to the control of a single chemical or physical variable (Samper, 2009). Therefore, even if some progress has been made, an agreed conceptual framework for the characterization of these PBs is still lacking.

In the case of the biodiversity loss PB, “extinctions per million species per year” has been proposed as the control variable (Rockström et al., 2009), but no consensus has been reached on where the threshold should lie or on whether the control variable is adequate in the first place. The main issues with the definition of this threshold are the complexity of ecosystems, the lack of knowledge about the state of many populations, how biodiversity should be understood (whether it means species richness or ecosystem diversity in terms of genetic variance) and what does the boundary intend to represent. Biodiversity loss could be measured directly, as in the number of lost species globally or in localized regions which could lead to further large-scale change in ecosystems. However, the boundary could also be addressed as a measure of the level of ecosystem degradation that could lead to this loss of species. The resilience of each group is also different; amphibians, for example, are much more vulnerable to extinction than birds or mammals (Samper, 2009; Montoya et al., 2018; IUCN Red List of Threated Species, 2020). Additionally, the biodiversity boundary is intrinsically tied with the moral issue of how the existence of any species contributes equally to the Earth’s biological richness and should be given the same chances to survive. Alternatives to measuring extinction rates includes setting thresholds for maintaining biome integrity, assuring enough genetic

diversity for future evolutionary purposes, or maintaining functional diversity (Mace et al., 2014).

The introduction of novel entities (or chemical pollution) is included as a PB since it can degrade human health and welfare while also affecting other organisms and triggering the transgression of other boundaries (Rockström et al., 2009). Defining a single threshold for it is, however, difficult, due to the extensive range of chemical substances with associated toxicity, persistence, or radioactivity, among other threatening characteristics. Additionally, compounds may have yet unknown effects on human physiological development or on nature, and their combined effects are also largely unexplored. Approaches to the definition of this boundary would be to develop indicators which could describe global chemical pollution and possibly aid to define the thresholds, or select a representative, known range of chemicals for an initial study of where the threshold would fall (Diamond et al., 2015). However, as in the biodiversity PB, research for better understanding of the systems and action towards protecting the highest number of species and avoiding the adverse effects of chemicals through pollution control are necessary for both environmental and ethical reasons.

6.1 Climate change

The first PB proposed by *Rockström et al.* (2009) and also selected to be included in the study is that of climate change. The climate system is the most well-known Earth system and the one which is the object of the most studies. Hence, numerous sectors, the chemical industry being one of them, have developed roadmaps and goals towards reducing their impact on it. The degradation of the climate system can provoke many undesired outcomes, from the loss of sea ice, to changes in the biosphere and even in the relationships between species (Sekerci, 2020), therefore threatening the well-being of many regions of the world and its balance.

The climate change Earth System boundary was initially proposed considering that the 2ºC guardrail introduced at the UN Conference on the Human Environment held in Stockholm in 1972 (and brought back repeatedly in numerous occasions) had to be respected. According to this, temperature increase due to global warming had to be kept below 2ºC above pre-industrial

temperatures, in average. However, even if the 2ºC limit is respected, polar regions may suffer changes of more than 6ºC due to heterogeneous change around the planet.

In 1995 and 1996 Germany's national advisory council on climate change (WGBU) and the Council of European Ministers revisited the limit and in 2001 the Intergovernmental Panel on Climate Change (IPCC) stated it in its Third Assessment Report (TAR) that even if the 2ºC guardrail is not surpassed, some of the effects of climate change are impossible to reverse. Still, the limit implies a certain security from climate change consequences in most parts of the world (Green car congress, 2009).

In 2007, however, the new IPCC report warned that the 2ºC may not be enough to prevent climate change-induced changes in some parts of the world, and that some effects had not been considered (IPCC, 2007). In fact, various studies identify the necessity of keeping temperatures lower than the 2ºC increase and compare the impacts of this limit to a new 1.5ºC one. By this, we could for example avoid half the risks of global warming for animals and plants (due to range loss) (Watson et al., 2018). The 1.5ºC limit has had political back up, the most recent being the 2015 Paris Agreement, which set the limit to temperature increase well below 2ºC and preferably not surpassing 1.5ºC and defined climate change action from 2020 onwards. It is also necessary to consider that some already triggered responses to climate change, such as the loss of sea ice, may cause the 2ºC guardrail to be crossed sooner if no action is taken, in this case due to the increase of solar heating (Pistone et al., 2019).

There are two different control variables used for the quantification of the impact of anthropogenic activities on climate change, those being atmospheric CO_2 concentration and radiative forcing. Both thresholds are included in this study. While the former focuses on CO_2, the latter describes the effects of all CO_2 and non-CO_2 (e.g., aerosols or methane) greenhouse gases.

Energy imbalance is caused when there is more radiation and heat from the Sun entering than exiting the atmosphere, an effect which is accentuated when high concentrations of gases accumulate at the atmosphere (IPCC, 2013). However, studying the CO_2 emissions in particular is also important because it is the most

relevant greenhouse gas and has a longer lifetime than some other non-CO_2 greenhouse gases (Montzka et al., 2011). Moreover, aerosols have a cooling effect which counteracts global warming caused by non-CO_2 gases, so the CO_2 boundary can be used as the reference threshold for climate change (Rockström et al., 2009).

Initially, the thresholds for the climate change control variables were set at 350 ppm CO_2 for carbon dioxide concentration and one W m^{-2} for radiative forcing, all above the pre-industrial level. The uncertainty band was established for concentrations between 350-550 ppm CO_2 and +1.0-+1.5 W m^{-2} net radiative forcing (Rockstrom et al., 2009). Data from the IPCC climate report in 2007 was employed to observe how the climate responded to the current values of these boundaries, which already exceeded the proposed limit (IPCC, 2007) and studies of the sensitivity and feedbacks of the climate change system under were also considered. For defining the range of uncertainty, paleoclimate records were used. The ppms of CO_2 present in the atmosphere were studied during the time of large-scale glaciation to find the range of concentrations that allowed ice to form and that would allow humanity to maintain the conditions necessary for preserving the planet as we know it today (Hansen et al., 2008).

However, the 550-ppm boundary would leave excessive space for climate to change, since we are already experimenting disbalances, such as abrupt changes in climate, including heatwaves, hailstorms, and heavy rain around the world (Herring et al., 2020), loss of sea ice and permafrost (Nuttall, 2020; Zhongqiong et al., 2020) or reduction of crop yield (Challinor et al., 2019). Therefore, a new range from 350-450 ppm of CO_2 is proposed (Steffen et al., 2015), while the energy imbalance boundary is kept the same.

Both boundaries (i.e., that of atmospheric CO_2 concentration and that of energy imbalance at top of atmosphere) are included in the present study. As explained in the Methodology section, the chemical sector is expected to transgress both boundaries due to its high contribution to GHG emissions (Boulamanti & Moya, 2017b).

6.2 Ocean acidification

The ocean acidification boundary is directly linked with the climate change CO_2 concentration one, since the cause of pH variation in oceans is the absorption of dissolved CO_2 (The Royal Society, 2005). The process is one of the three principal Earth systems and is quantified as a global value which is included in this study.

Oceans hold great importance for various reasons. They contain between 500000 and 10 million described species, with even around 2000 more being discovered each year, therefore contributing enormously to the planet's biodiversity (United Nations, 2017). Furthermore, the absorption of CO_2 by marine vegetation is a key factor for removal of this greenhouse gas from the atmosphere, absorbing up to 25% of anthropogenic emissions (United Nations, 2020a). Nonetheless, this intake of CO_2 is decreasing the pH of the waters by 0.1 units since pre-industrial times and could become even lower and fall by 0.5 units if CO_2 emissions keep increasing by the end of the century. This creates a massive challenge for the fragile marine ecosystem and especially calcifying organisms which create their shells or plates from calcium carbonate ($CaCO_3$, aragonite) (The Royal Society, 2005) or high magnesium calcite (Rockström et al., 2009) since these will dissolve. Affected organisms include different species of plankton, coral and molluscs, and their decline could directly impact other marine life that depends on them for feeding or the wellbeing of coral reefs.

Aragonite saturation (Ω_{arag}) at the surface of the ocean is taken as an indicator for ocean acidification, since $CaCO_3$ is more soluble than calcite (Mucci, 1983). High magnesium calcite can be even more soluble, but it depends on the concentration of magnesium. Therefore, Ω_{arag} indicates the level of saturation of the mineral in the ocean, and its thermodynamic tendency to dissolve.

This saturation, not only for aragonite but for all three minerals (i.e., aragonite, calcite, and magnesium calcite), is influenced by the concentration of carbonate ion in the water, which in turn decreases with pH. Therefore, if the saturation state (Ω) for a mineral is equal to 1, it will not precipitate nor dissolve. Even so, when $\Omega<1$, the seawater will become undersaturated, allowing for further minerals to

dissolve. The reaction of dissolution of aragonite in seawater is the following (*Eq. 34*).

$$Ca^{2+}\,(aq) + CO_3^{2-}\,(aq) \leftrightarrow CaCO_3\,(s) \qquad \textit{Eq. 34}$$

Therefore;

$$\Omega_{arag} = \frac{[Ca^{2+}] * [CO_3^{2-}]}{[CaCO_3]} \qquad \textit{Eq. 35}$$

In *Eq. 35*, concentrations of the dissolved ions are divided by the solubility of aragonite in seawater (SOEST, 2020).

Even though the dissolution of aragonite and therefore also calcite and in many cases high magnesium calcite would give a threshold of $\Omega_{arag} = 1$, it is important to consider that many marine organisms are already threatened at higher values of saturation (Rockström et al., 2009). Many studies suggest marine ecosystems will face low saturation values that can represent a risk in the near future. As an example, if a business-as-usual (BAU) scenario is considered and maintained until 2100 seawater in areas with coral reefs could be totally undersaturated in respect to pre-industrial Ω values, which are argued to have been around $\Omega_{arag} = 3.5$. This could severely threaten the survival of coral reefs and that of organisms depending on them (Ricke et al., 2013). With the aim of both avoiding undersaturation on surface waters while protecting coral, the initially proposed and later confirmed boundary is set at $\Omega_{arag} > 2.752$ (>80% of the average surface ocean aragonite saturation state in pre-industrial levels, $\Omega_{arag} = 3.44$). A variability range was included which considered the seasonal and temporal fluctuation of aragonite saturation (≥80%-≥70%), (Rockström et al., 2009; Steffen et al. 2015; Ryberg et al., 2018b).

6.3 Stratospheric ozone depletion

While an excess of tropospheric ozone is damaging to human health and can cause respiratory diseases, stratospheric ozone (the biggest part of which forms what we refer to as the ozone layer) protects the planet by absorbing UV-B radiation (280-315 nm wavelength) coming from the sun and avoids the

stratosphere to cool down (Steffen et al., 2015). However, it still allows UV-A (315-400 nm) to pass. Without this protection, higher levels of solar radiation would reach the Earth's surface, representing a problem not only for human health but also crops, vegetation, unicellular organisms, and aquatic ecosystems, especially plankton (Fahey et al., 2011).

To measure the quantity of ozone at a certain point on the globe, Dobson unites (DU) are used. Needless to say, the distribution of atmospheric ozone is heterogenous, with higher concentrations found at middle-high latitudes, but also varying seasonally, or even daily.

Naturally, ozone forms in the stratosphere when ultraviolet radiation breaks oxygen molecules into two oxygen atoms, each of which can collision with another oxygen molecule and bind to form ozone.

$$3\,O_2 + UV \rightarrow 2\,O_3 \qquad \textit{Eq. 36}$$

Despite the largest production of ozone being found in areas with high insulation, the tropics have lower ozone concentrations (as stated above) due to the movements of stratospheric air (Fahey et al., 2011).

As ozone molecules form from the interaction between oxygen and UV light, they can be destroyed when exposed to ozone-depleting substances (ODSs) which are halogens containing chlorine and bromine. ODSs only include gases from anthropogenic provenance, even though there are also natural gases that contribute to stratospheric chlorine and bromine. The most important ODSs are CFCs, Halons, CCl_4, CH_3CCl_3 and CH_3Br (Fahey et al., 2011). When these gases, both from human and natural sources (named halogen source gases) reach the stratosphere, they are exposed to high UV radiation and converted into radioactive halogen gases. Some of these do not react directly with O_3 (and are called reservoir gases) but can still be transformed into other gases that do and are highly radioactive, the most relevant of which are ClO and BrO. These react with ozone in catalytic cycles (i.e., they react and re-form), the first one of which happens all around the planet and has a final result of the conversion of one ozone molecule into two diatomic oxygen molecules (*Eq. 39*).

Ozone destruction cycle 1:

$$Cl + O_3 \rightarrow ClO + O_2 \quad \textit{Eq. 37}$$

$$ClO + O \rightarrow Cl + O_2 \quad \textit{Eq. 38}$$

$$O + O_3 \rightarrow 2O_2 \quad \textit{Eq. 39}$$

In Polar regions, however, radioactive halogens are more abundant and react with each other to destroy ozone, having a final net reaction that transforms two ozone molecules into three diatomic oxygen molecules (Fahey et al., 2011). The higher presence of radioactive gases in the Polar Stratosphere is caused by the low temperatures in the Arctic and Antarctic, which allow Arctic Polar Stratospheric Clouds (PSCs) to form. This happens when water vapor present in the stratosphere condenses due to the low temperatures (Piana, 2020). PSCs form when temperatures are below -78ºC, a limit frequently reached during several months especially in Antarctica, where the temperatures are the lowest during winter. On the surface of these clouds, ClO is easily formed from reservoir gases. PCSs also contribute to the removal of nitrogen oxides and nitric acid from the stratosphere, which would otherwise help lower the impact of chlorine (Molina, 1991; NASA, 2017). This is the reason why the most severe ozone depletion happens in the Antarctic during late winter and spring.

Ozone destruction cycles in Polar regions (cycles 2 and 3):

$$ClO + ClO \rightarrow (ClO)_2 \quad \textit{Eq. 40}$$

$$(ClO)_2 + sunlight \rightarrow ClO_2 + Cl \quad \textit{Eq. 41}$$

$$ClO_2 + ClO \rightarrow Cl + O_2 \quad \textit{Eq. 42}$$

$$2(Cl + O_3 \rightarrow ClO + O_2) \quad \textit{Eq. 43}$$

$$2O_3 \rightarrow 3O_2 \quad \textit{Eq. 44}$$

$$ClO + BrO \rightarrow BrCl + O_2 \quad \textit{Eq. 45}$$

$$BrCl + sunlight \rightarrow Cl + Br \quad \textit{Eq. 46}$$

$$Cl + O_3 \rightarrow ClO + O_2 \quad \textit{Eq. 47}$$

$$Br + O_3 \rightarrow BrO + O_2 \quad \textit{Eq. 48}$$

$$2O_3 \rightarrow 3O_2 \quad \textit{Eq. 49}$$

In the 1980s, the ozone hole in the Antarctic was first reported and reached alarming points, which lead to the Montreal Protocol (1987). The use of around 100 ODSs from human sources was prohibited (United Nations, 2020b) due to their high ozone depletion potential (ODP), and widespread use. Thanks to this global effort in reducing polluting substances, the ozone layer has been recovering and all principal ODSs were phased out. However, the emissions already present in the stratosphere remain there and can still cause ozone depletion due to their long lifetime. The boundary set for stratospheric ozone depletion is surpassed seasonally during spring in the Antarctic (Steffen et al., 2015), and in some cases like in May 2020 or 2011 particularly cold winters cause the hole to open alarmingly. The 2020 event resulted in a hole in the ozone layer of unprecedented size (Witze, 2020). Still, in both cases the hole closed during the later spring, and the ozone layer is expected to have recovered by 2050, when the effect of the ozone depleting substances emitted before the Montreal Protocol should cease (World Meteorological Organization, 2018; Andrady et al., 2009).

The climate change and the stratospheric ozone depletion boundaries have various and complex interactions (Andrady et al., 2009). From ozone being the third most important GHG produced by humans (Simpson et al., 2014) to the reduction in radiative forcing that a healthy ozone layer represents (McKenzie et al., 2011), many aspects are to be considered when studying the relationship between both Earth Systems. The increase of temperatures in the Arctic zones due to climate change also reduce the risk of the ozone hole opening. Moreover, ozone depletion could also be linked to the biogeochemical cycles, as a result of more UV-B reaching the Earth’s surface (Zhang et al., 2018; Zepp et al., 2003).

The boundary defined for the stratospheric ozone depletion Earth System was not framed around the ozone hole phenomenon but the thinning of the extra-polar ozone layer. The reason for this choice is the seasonality and dependence of the ozone hole on cold climates, nitric acid, and PSCs, to which humans do not contribute directly entirely (Rockström et al., 2009). The limit established, and employed in this research,h is set at a decrease lower than 5% in column ozone levels with respect to pre-industrial values (1964-1980), for any latitude (Rockström et al., 2009; Steffen et al. 2015) while the uncertainty range is that proposed by *Steffen et al.* (2015) and stands at a 10% decrease.

6.4 Biogeochemical flows

Biogeochemical cycles, or flows, are fluxes of different chemical elements that are transformed and recycled while passing through biotic and abiotic elements in the Earth's ecosystems (Zavarzin, 2008). Various biological, chemical, and geological processes are included in the pathways of chemicals, such as weathering, erosion or photosynthesis. Overall, Earth does not receive or eliminate matter, but instead it follows a closed cycle through all its compartments, including the biosphere, lithosphere, atmosphere, and hydrosphere (The Environmental Literacy Council, 2020). Sometimes, elements are retained in reservoirs (or exchange pools) instead of moving through their pathway, a clear example of this could be animals, where the cycle is put in pause and matter is stored. The most important biogeochemical cycles are those of carbon, sulfur, hydrogen, oxygen, nitrogen, and phosphorus, and each of them runs at a different pace depending on its reactivity, state or processes that requires.

Biogeochemical cycles can be altered and accelerated by human activities through the input of additional matter in the fluxes (Schlesinger, Bernhardt, 2013). For the nitrogen, phosphorus, and sulfur cycles, significant increases in global fluxes have been attributed to human actions (Schlesinger, 2013). Moreover, the increase of CO_2 emissions does not only represent the principal cause of climate change, but also disturbs the carbon cycle (IPCC, 2007a; King et al. 2012). The biogeochemical cycles associated with a PB are those of nitrogen and phosphorus, since these are the two which have been heavily altered by human activities.

Regarding the nitrogen boundary, the control variable is the input of N-compounds to the Earth System (fixation of otherwise atmospheric N_2) resulting from anthropogenic activities, mainly including industrial (e.g., Haber-Bosch process for ammonia production) and biological (e.g., from agriculture and the combustion of fossil fuels and biomass) sources. This control variable addresses the eutrophication of aquatic ecosystems though the flow of nitrogen from soil to Fresh Water (FW) systems (Steffen et al., 2015). The emission of NOx from human activities, primarily transport and industry, is also a source of nitrogen

fixation. They are principal GHGs which contribute directly to climate change, and therefore are already included in its PB, so the effects of said compounds are not considered in the biogeochemical flows PB to avoid double-counting (Rockström et al., 2009; Steffen et al., 2015). Instead, their impact is quantified in terms of maximum increase in radiative forcing caused by anthropogenic emissions that can be sustained by the climate change Earth System.

The effects of an alteration of the nitrogen cycle can cause negative effects on the environment and human health through the eutrophication of terrestrial aquatic and marine ecosystems causing a decrease in biodiversity, the increase in atmospheric ammonia and tropospheric ozone concentration while a decrease in stratospheric ozone is also induced by N_2O, the contamination of ground water (GW) and the acidification of soils and crop yield reduction (de Vries et al., 2013; Ryberg et al., 2018b). However, nitrogen in ground does not just have adverse environmental effects but it can also positively increase the growth of plants, which act as a principal natural CO_2 sink, consequently helping reduce climate change. Furthermore, it also fertilizes ground, which is incredibly important in terms of food security and agriculture that does not require an unsustainable amount of land (De Vries et al., 2013). When setting a numeric value to the nitrogen cycle boundary, all of these factors have to be considered to find a point in-between nitrogen scarcity and nitrogen overuse. The aim is not to return to a Holocene level of fixation of nitrogen, since this would entail the inability to feed the present population of the Earth, which has since grown.

An important point to consider is that the variation of fixed nitrogen from fertilizer application has a high variability across the globe, being highly overused in regions with rich agriculture (mainly Europe, North America, and China) but insufficient in Africa, South America and Central Asia (Steffen et al., 2015). Besides that, in many wild regions of the world there is no agriculture whatsoever, and crop species from different regions may have different demands for nitrogen. This uneven distribution of human applied nutrients requires regional boundaries for the nitrogen cycle Earth System. In some areas, an increase in nutrients would potentially damage land and crop yields, while in some others, it would even positively affect the environment and food production (de Vries et al., 2013). Consequently, redistributing the nitrogen present around the globe would make

it possible to both keep environmental impacts of nitrogen use at a sustainable level but also maintain or even enhance current agriculture practices (Steffen et al., 2015).

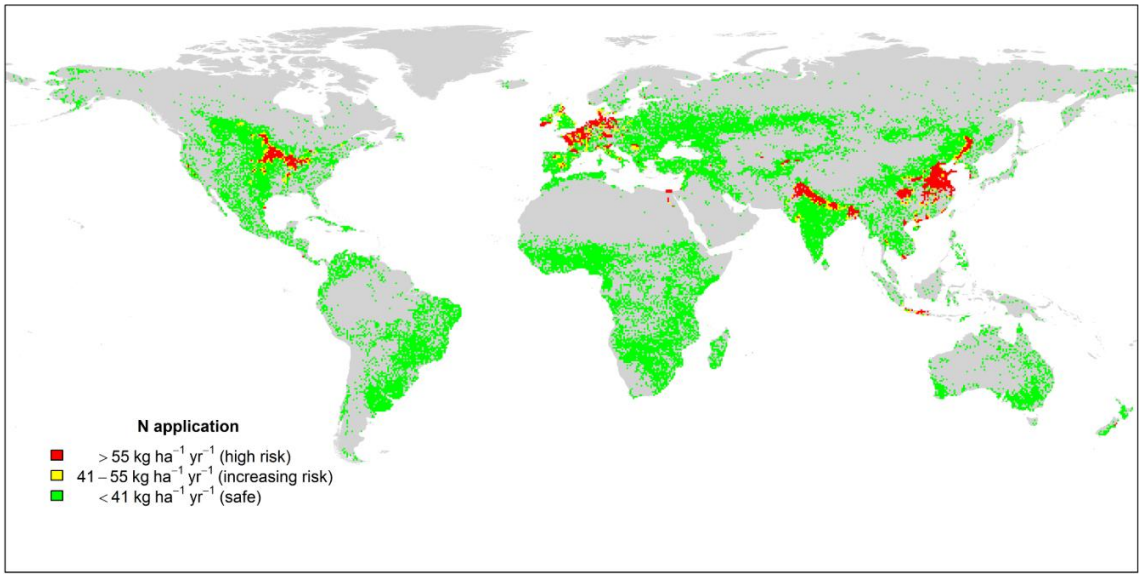

Fig. 6-1: Distribution of nitrogen (Steffen et al., 2015).

The desired level of N_2 fixation initially set by *Rockström et al*. has been reviewed (de Vries et al., 2013) to consider the need to fertilize soils for agriculture besides the necessity to reduce the environmental impacts of nutrient use.

To obtain the PB for nitrogen, *de Vries et al.* (2013) identified the three principal control variables quantifying the presence of nitrogen in the environment (i.e., (i) atmospheric NH_3, inorganic nitrogen and N-derived compounds concentration in (ii) fresh and (iii) ground water systems). The critical intended inputs of nitrogen from human activities into these three compartments are calculated using a risk indicator and given a threshold (de Vries et al., 2013). The substances monitored as human-caused nitrogen losses are NO_3^-, NH_3, N-tot, N_2O, Nitrogen Organic Bound and Nitrogen compounds (Ryberg et al., 2018b). Since N_2O already has an effect on climate change, the limit for the tolerable emissions of N_2O is calculated depending on allowed maximum radiative forcing goals.

de Vries et al. (2013) also calculated the PB for nitrogen fixation considering the nitrogen required for food safety, dietary individual requirements (which imply nitrogen soil, animal, and crop requirements), efficiency of fertilizer use and the losses of nitrogen and wastes from the alimentary sector.

The resulting values at a global scale from these calculations indicate that if environmental factors are considered, the threshold should be found from 20 to 130 Tg N*yr^{-1}. The lowest values correspond to those of radiative forcing, which is not included in the nitrogen cycle boundary but the climate change one to avoid double-counting, so the values left range from 62 to 130 Tg N*yr^{-1}.

Considering the worst-case scenario (the nitrogen inputs for the environmental compartment allowing the lowest alteration), the boundary would be set at 62 Tg N*yr^{-1} with an uncertainty zone up to 82 Tg*yr^{-1}. The results for the need to feed a global population of nine billion people indicate a value of 50-80 Tg N*yr^{-1} for the boundary, which is well within the environmental requirements limit. Therefore, the new threshold is set at 62-82 Tg N*yr^{-1} for anthropogenic eutrophication of aquatic ecosystems (de Vries et al., 2013; Steffen et al., 2015; Ryberg et al., 2018b).

As explained, some regions of the world are responsible for transgressing the nitrogen cycle boundary. The threshold developed and applied to this study serves as a “global valve” regulating the flow of new reactive nitrogen.

As for the phosphorus boundary, two control variables are considered. A distinction is made between the outflow of phosphorus to marine waters, and to soil (and freshwater systems). The control variable for the phosphorus boundary is human-induced phosphorus inputs to either oceans or soil, with this phosphorus being extracted straight from mined phosphate rock.

When high concentrations of nutrients such as phosphorus are found in water, organisms increase their productivity until they consume all available oxygen. Therefore, in the background of oceans and seas, the principal scenario that is aimed to be avoided is the trigger of a global oceanic anoxic event (OAE). That would deploy oceans of dissolved oxygen causing waters to become anoxic and in some cases even euxinic (containing high levels of hydrogen sulfide and no oxygen), becoming soon uninhabitable for many forms of marine life. These of events also involve the formation of sediments rich in organic carbon cause by the death of phytoplankton and other organisms as in eutrophication (Schlanger et al., 1986).

OAEs have been proved to have happened in numerous occasions throughout the planet's history, linked with periods of sudden increase in temperatures and CO_2 presence in the atmosphere, when nutrient influx to the oceans and seas also rises due to more intense weathering. All these conditions lead to the trigger of anoxic events, while the dynamics between these and the shift to oxic conditions are believed to be regulated by feedbacks between biogeochemical cycles and ocean productivity (Bush et al., 2017). Marine productivity refers to the cycle in which phytoplankton and other autotrophs (primary productivity) and heterotrophic organisms (secondary productivity) produce new organic matter (Sigman & Hain, 2012).

Currently, more than 400 dead zones are present in different water bodies worldwide, most of them being found near highly populated cities, which indicates how human activities can induce the formation of anoxic zones (Diaz & Rosenberg, 2008). However, it is uncertain whether it is possible that anthropogenic phosphorus influx into marine waters can cause a global OAE. The reason for this is that a high, sustained influx of phosphorus would have to be directed to the oceans, and the phosphate rock reserves mined for industrial or agricultural use are limited. In addition, the dynamics between oxic and anoxic states have really large time scales. Still, the time scale is also slow on the reverse side, so even drastically reducing the current levels of phosphorus directed to the oceans, anoxic zones would still appear for longer than 1000 more years (Rockström et al., 2009).

The aim of the PB is to keep the anoxic fraction of marine waters far from one (global OAE scenario) in the long-term. For that, the sustained flow of phosphorus from freshwater systems to marine waters in TgP/yr should be reduced. The original threshold was offset to keep the flow under approximately 10 times the natural background rate of inflow from phosphorus into oceans, based on the study of historical anoxic events. Later, *Steffen et al.* proposed to fix the value at 11 TgP/yr with an uncertainty zone ranging from 11 to 100 TgP/yr (Steffen et al., 2015). This global threshold is the phosphorus boundary used in this study.

In addition, a regional threshold of 6.2 TgP/yr with an uncertainty from 6.2-11.2 TgP/yr has been proposed for the inflow of phosphorus to soils and freshwater, with the aim to avoid the eutrophication of freshwater systems (Carpenter et al.,

2001; Steffen et al., 2015). This boundary includes the flows of phosphorus from land to freshwater, to erodible soils and the total mass of phosphorus already present in soil. Each of these flows and quantities of phosphorus being present in soil and freshwater systems have different levels of impact to final water quality. The control variable that is defined as principal is the flow of phosphorus to soils, since it is easier to measure and manage than phosphorus to freshwaters or in soil, but all three contribute to the final value in a proportional way to their impact. The flows of phosphorus to soil due to weathering are subtracted from the PB value, while the assumed flow of phosphorus to the sea influences the result as well. Insufficient data is available for the quantification of this regional boundary since the studied chemical plants are not geo-localized.

An alternative to phosphorus fertilizers is manure because it does not represent new phosphorus applied to soils but the recycle of phosphorus already in soil. A better use of manure would reduce the risk of exhaustion of phosphorus deposits and of transgressing the phosphorus boundary since phosphorus (as nitrogen and other nutrients) is mainly used as a fertilizer. That creates a conflict between food security and environmental impacts of nutrient use as in the nitrogen boundary. Since some areas of the world have more croplands than others, there is an irregular distribution of phosphorus in soils. The areas with higher agriculture contribute to the trespassing of the phosphorus boundary in a higher degree. Consequently, the control variable for phosphorus flow to soil, freshwaters and in soil is established as a regional boundary, and as for nitrogen, a redistribution of phosphorus would allow to steer away from the transgression of the phosphorus boundary while also having a positive effect in crop yields and agricultural productivity at a global scale. That would secure and most likely even increase food production while also reducing eutrophication and maintaining better water quality.

However, it must be noted that despite correctly redistributing nitrogen and phosphorus at a global level, the flows of these nutrients must also be reduced, since both limits are currently already being globally transgressed.

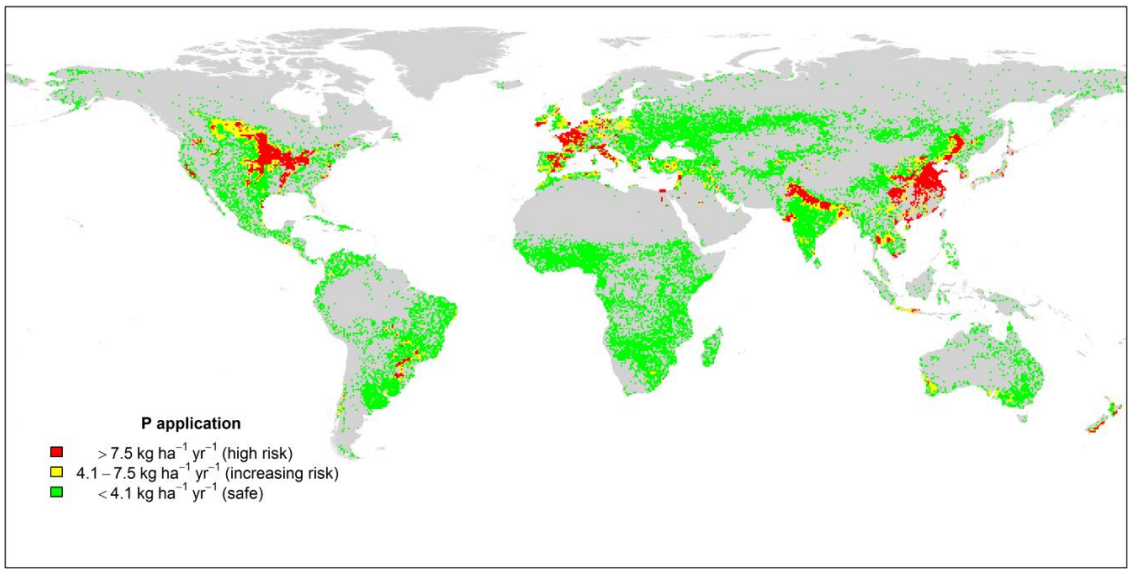

Fig. 6-2: Distribution of phosphorus (Steffen et al., 2015).

The values given to the nitrogen and phosphorus boundaries can be revised by using the ratio in which these nutrients as used as fertilizers. Nitrogen and phosphorus concentrations for optimal plant growth have been studied in order to avoid nutrient deficiency and find the most efficient way to fertilize crops. The N:P ratio has been proven to directly affect the specific growth rate of plants. Even if the optimum relationship can be calculated for each species, the ratio for many of them is about 11.83 (Greenwood et al., 2008). Despite small variations, the consistency of the values established independently for each threshold can be seen when calculating them through the N:P ratio.

Table 6-1: Relationship between the original nitrogen and phosphorus threshold values (in green) and those obtained through the N:P ratio (in black).

Reference PB (column)	**N boundary (Tg N*yr^{-1})**	**P boundary (Tg P*yr^{-1})**
N boundary	62	5.2
P boundary	6.2	73.3

As described, in this study, only one control variable for phosphorus is to be evaluated, with that being the phosphorus flow from freshwater systems into the ocean. The regional boundary set for phosphorus flow from fertilizers (i.e., mined P) to erodible soils is not included for the sake of reducing estimations, since the threshold defines the amount of mined phosphorus applied to erodible agricultural soils. Available data do not provide such level of detail on the origin of the described flows or the type of soil to which they are applied, thus, the calculated impact would carry too much uncertainty.

6.5 Land system change

Human action has altered the Earth's biomes causing the loss of biodiversity and destabilization of ecosystems. This could lead to much further disequilibrium and prevent the planet's natural regulation of climate through the exchange of water, momentum and energy between land and the atmosphere (Steffen et al., 2015) to function correctly. The loss of biodiversity can also facilitate the spreading of diseases and the appearance of zoonosis. The principal causes of land use are large-scale agriculture, resource extraction and construction, all having both regional and global effects. Even though the dynamics of these changes are slow, in most cases once a limit of disturbance is crossed, effects appear in abrupt and irreversible ways. One well-known case would be the conversion to savanna of the Amazon rainforest, which is believed would take place if more than 40% of the region is deforested (Nobre et al., 2016). The Amazon rainforest hosts around 15% of the world's terrestrial biodiversity, acts as a major regulator for river waters, and is also one of the world's greatest natural carbon sinks.

The biodiversity loss, biogeochemical flows, and freshwater use Earth systems are all affected by land use. As these PBs are, any threshold set for land system changes is tightly related to food security. Land system science's aim is to obtain the best ways to distribute land change worldwide in a way that allows to preserve the Earth's ecosystems and mitigate the environmental impacts of land use while ensuring enough productive land for agriculture (Erb et al., 2013; Verburg et al., 2013). High-productivity regions should therefore be used for agriculture, and not lost to urbanization or other activities, which would lead to the marginalization of croplands to probably lower-yield lands, where more exploitation of soil would be needed to achieve the same level of production that a higher productivity soil would have offered. Meanwhile, carbon-rich soils and sensitive forests should remain undisturbed.

In the context of the PBs, the control variable is the percentage left of unaltered forested land compared to the potential forest land in the Holocene. A global threshold is proposed, which is a weighted aggregate of three biome-specific limits for tropical, temperate, and boreal forests. Changes in these three principal forest biomes have an impact on climate and trigger further alterations on larger

areas at different levels. Those biomes that are more sensitive have more demanding land preservation requirements. The three forest biomes are defined as a control variable since they have greater influence on the climate than other biomes such as taiga, tundra, steppe, and others. They influence atmospheric, hydrologic and energy cycles, represent some of the world's largest natural carbon sinks and could therefore mitigate climate change effects if preserved correctly or amplify them even more if destroyed.

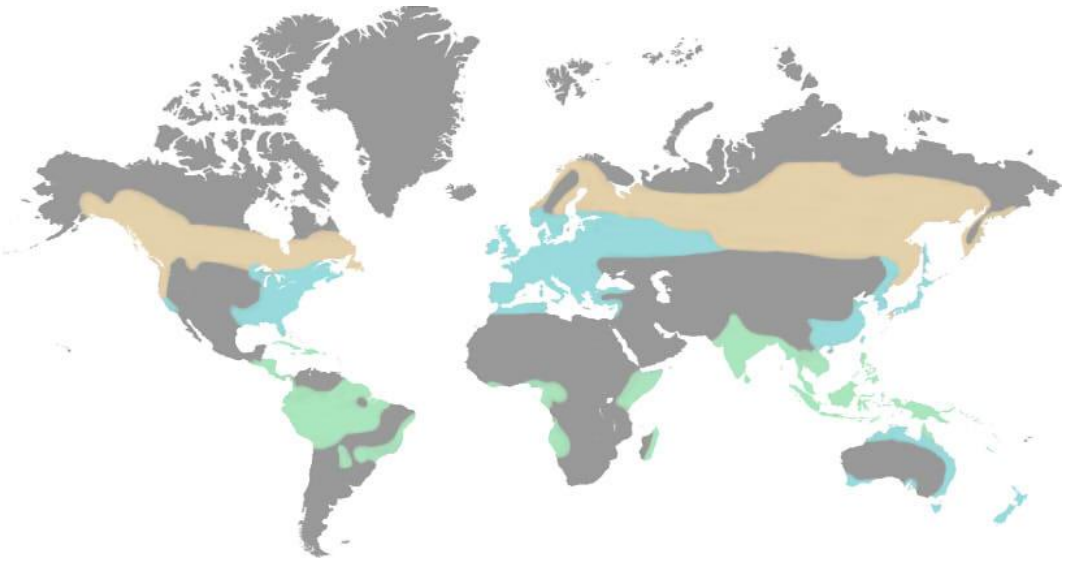

Fig. 6-3: Tropical (green), temperate (blue) and boreal (brown) forest biomes distribution.

The most vulnerable forest biome is the tropical forest, including areas such as Amazon rainforest, India, and New Guinea – all known for hosting some of the richest ecosystems on Earth. As stated before, the Amazonian rainforest plays an important role in the global water cycle since it is the largest tropical forest worldwide and contributes hugely to land surface evapotranspiration. It also has a major impact on global atmospheric circulation (global movements of air and their regulation, also known as the wind systems of the planet), and so do the other rainforest blocks that can be found in Africa and Asia. The loss of these biomes to savanna would entail a reduction of tropical vegetation and therefore transpiration, leading to only a more severe reduction of rainfall worldwide and further land-change. Studies strongly suggest a critical threshold of lost rainforest exists, over which rapid transformation of the whole biome would be triggered (Hasler & Avissar, 2007; Werth & Avissar, 2004). Said boundary is currently believed to lie around 15% alteration of tropical forest biomes (Rockström et al.,

2009; Steffen et al., 2015). Present levels of deforestation are already around this percentage, causing more frequent wildfire and drought, huge biodiversity loss and regional regime shifts (Steffen et al., 2015).

As for boreal forests, the same limit is set (15%). Their main contribution to global climate is through energy exchange between land and atmosphere through the regulation of the fraction of sunlight reflected (Steffen et al., 2015). Boreal forests, as all forests, have low reflection rates, contributing to the mitigation of global temperature increase. Their presence is especially important, though, since they are located at cold regions with frequent snow, which has a high albedo if not masked by forest cover. They are also a large storage of carbon in soil and permafrost. Even though these forests are very vulnerable to global warming due to their location and nature, their current state is not as properly studied as that of tropical forests due to their much larger size and distribution (Wang et al., 2019). In fact, they compose the largest forested area worldwide.

Finally, regarding temperate forests and based on their lower impact on global climate and hydrologic systems, the threshold is set at a ratio of 50/50 preserved/altered potential forest. Even though their influence to climate is believed to be lower than that of other biomes, they do function as a large carbon sink and hold more than 20% of the world's biomass (Bonan, 2008). Even so, they have been generally highly altered, which causes their natural functions to work less effectively (Wohlleben, 2020).

The global boundary for land system change in forested land (weighted aggregate of these three biomes) is set at 75% of preserved forest cover with an uncertainty zone of 75% to 54% (Steffen et al., 2015). Current values already transgress the boundary (~62% remaining forest) but remain within the uncertainty zone, triggering the previously discussed effects.

6.6 Freshwater use

As with land use, over-consumption of freshwater can alter the global hydrological cycle. On the one hand, river flows are altered by the withdrawal of water (especially irrigation) and the construction of dams and other obstacles, reducing the total river discharge into marine waters and internal sinks. The decrease of

average river discharge has led to biodiversity loss and a reduction of discharge amplitude. In addition, even though human interference reduces the natural seasonal variability of river flows, interannual variability has grown larger in many parts of the world (Doell et al., 2009). On the other hand, vapor flows have also been anthropogenically modified due to land use and deforestation (as discussed in the land system changes section). The vapor cycle suffers from highly heterogeneous changes, with some regions of the world being especially threatened with the transgression of regional thresholds. An example would be the Indian tropical forest, where the alteration of vapor flows could trigger a shift in the behaviour of the continental monsoon system (Gordon et al., 2005). Rivers, lakes, and other water bodies also work as carbon sinks and climate regulators. Their degradation will lead to a decline in precipitations, in both global and regional scales, and threaten water availability and biomass production.

A differentiation is made between green water and blue water. The former refers to soil moisture which transpires though vegetation, while the latter is water present in surface and underground reservoirs. Blue water is influenced by green water through moisture feedback, which generates rainfall, and habitat transformations such as the previously discussed drought of the Amazon region would be caused by the crossing of thresholds related to green water. Meanwhile, if blue water is drastically reduced, river and lake ecosystems are at risk.

The PB for freshwater use should ensure three conditions: (i) water availability for humanity and aquatic ecosystems, (ii) that freshwater ecosystems can develop their natural regulative functions correctly, and (iii) that there is enough rainfall (thus, enough green water for a normal behaviour of the vapor cycle). Hence, the connection between vapor flows and runoff must be considered when defining the value of the boundary, which is expressed as maximum global consumptive blue water use. The proposed value for this boundary is 4000 km^3/yr of freshwater with an uncertainty zone up to 6000 km^3/yr (Rockström et al., 2009).

Still, *Steffen et al.* proposes different thresholds adapted to seasonal changes in river flow or changes due to the type of river basin (some rivers have stable flows while there are also monsoon or unpredictable-flow rivers). By defining the amount of water that can be withdrawn from rivers according to their flow rate, all these variables are encompassed. Thus, the control variable in this case is the

amount of consumptive blue water use allowed as an average percentage of the normal monthly flow for each river basin type. There are three different regimes, those being (i) high flow (ii) intermediate-flow and (iii) low flow seasons. Mean monthly flow (MMF) defines the average flow a river carries during each season, and environmental water flow (EWF) is the minimum amount of flow that is needed for the river's ecosystem to survive, and for the river to develop its regulating services normally. EWF can also be expressed as a % of MMF, with a 15% of uncertainty according to *Steffen et al., 2015* (*Eq. 50*, Table 6-2).

$$Allowed\ withdrawal\ (\%\ of\ MMF) = \frac{MMF - (EWF \pm 0.15 * MMF)}{MMF} * 100 \qquad \textit{Eq. 50}$$

Table 6-2: Calculated maximum amount of freshwater withdrawal (%).

Flow regime	**Average EWF (%)**	**Withdrawal boundary (%) (15% uncertainty)**	
		Low: $EWF + 0.15 * MMF$	**High:** $EWF - 0.15 * MMF$
Low	60%	25%	55%
Intermediate	45%	40%	70%
High	30%	55%	85%

The resulting maximum withdrawals reflect the previously discussed variation in the eco-hydrologic characteristics of different river basins. Each PB is set at the lower end of the uncertainty range shaded in grey.

As for the ozone depletion boundary, the state of the freshwater use boundary undergoes many variations throughout the year due to changes in the normal flow of rivers (EWF remains the same but not MMF). This leads to the seasonal transgression of the boundary in certain regions. A risk index can be calculated for each river basin which is the product of the duration and intensity of water deficiency (Fig. 6-4).

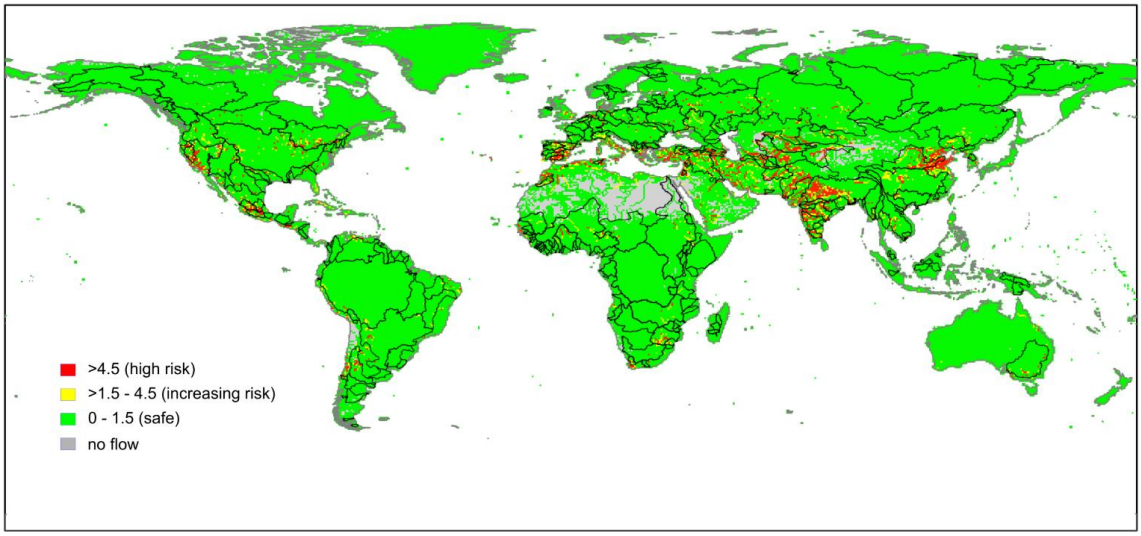

Fig. 6-4 Current state of the freshwater use risk index (Steffen et al., 2015).

Using this approach and applying it to a global scale, it results into an average value of 2800 km^3/yr with an uncertainty range from 1100-4500 km^3/yr. This includes the originally proposed global value of 4000 km^3/yr, but highlights that if strict EWF requirements are considered, the threshold may need to be lower. Despite this, *Steffen et al*. (2015) maintains the boundary given by *Rockström et al*. (2009) of 4000-6000 km^3/yr. The regional approach is not applied to this study since the studied production plants are not geo-localized and no information of the types of river basins that they have influence on is provided; thus, only the global limits are used.

6.7 Atmospheric aerosol loading

Atmospheric aerosol loading can not only alter the climate system but also directly deteriorate human health. The presence of aerosols (suspended particles measuring from 0.1 millimetres to nanometres excluding the vapor that forms clouds) can alter the hydrological and vapour cycles, produce changes in energy balance (Pösch, 2005), and cause acidic rain. Regarding human health, they are the cause of severe respiratory problems such as infections, cancer and cardiopulmonary diseases (Rockström et al., 2009).

The system is measured calculating the change in aerosol optical depth (AOD; i.e., the alteration on the absorption or scattering of light associated with suspended particles) that annual emissions of aerosols produce. The definition of a global threshold for aerosol loading is complex due to the huge spatial

variation in the distribution of these substances and the particular sensitivity of some localities. The south Asian monsoon is an example of a natural process which is highly sensitive to the presence of aerosols, since carbonaceous aerosols resulting mainly from petrochemical activities spread around India could reduce rainfall and lead the subcontinent to a drier climate (Steffen et al., 2015). The boundary proposed by *Steffen et al.* (2015) is that of an anthropogenic total AOD of 0.25-0.5.

For this study, CFs developed specifically for the European region are used (Ryberg et al., 2018b), since they allow for a more adequate assessment given the boundaries of the research than if global averages were employed. *Ryberg et al*. (2018b) assumed that emitted aerosols were evenly distributed over the studied region for every regional CF, thus giving more importance to regionally emitted aerosols and less weight to aerosols which are transported to other regions. They undertook two sensitivity analysis the results of which indicate that for Europe the circulation of aerosols between regions is highly limited and that emitted aerosols primarily have an impact within the region. Therefore, the regional CFs are considered adequate and applied in this study. For consistency with regional CFs, the regional threshold proposed by *Steffen et al.* (2015) is used for Europe. Note that this threshold was originally calculated for South Asia (as a case-study), yet it has already been used for Europe in *Ryberg et al.* (2018a).

6.8 Included planetary boundaries

Table 6-3 shows the PBs that are selected for the present study together with their control variables and units as a summary of the section.

Table 6-3: Briefing of the Earth-system processes linked to a PB considered in the present study.

Earth-system process	Control variable(s)	Boundary	Unit
Climate change	Atmospheric CO_2 concentration	1.0-1.5	ppm
	Energy imbalance at top-of-atmosphere	350-500	$W*m^{-2}$
Stratospheric ozone depletion	Stratospheric O_3 concentration	275-261	DU
Ocean acidification	Carbonate ion concentration: average global surface ocean aragonite saturation state	2.75-2.41	Ω_{arag}
Biogeochemical flows	N Global: Industrial and intentional biological fixation of N	62-82	$Tg\ N*yr^{-1}$
	P Global: P flow from freshwater systems into the ocean	11-100	$Tg\ P*yr^{-1}$
Land-system change	Global: Area of forested land as fraction of potential forest	75-54	%
Freshwater use	Global: Maximum amount of consumptive blue water use	4000-6000	km^3*yr^{-1}
Atmospheric aerosol loading	Regional: AOD as seasonal average over a region	0.25-0.5	AOD

7 Life Cycle Assessment

Life Cycle Assessment (LCA) is a tool used for quantifying the impacts of anthropogenic processes and activities not only on the environment but also on the Earth's resources and humans. Given a well-defined scope for the activity to be assessed, energy and material flows exchanged between the activity and the environment (i.e., emissions and resource extractions or uses) are identified and quantified. System boundaries are not limited to the in-plant process, but can also encompass the whole supply chain, including feedstock generation or the usage phase. Different assessment methods allow for the translation of these energy and material flow into pressures exerted onto various impact categories, such as ecosystems integrity, human health, or resource availability.

This environmental assessment tool was concepted around 1960-1970, when the first studies conducting (at least partial) LCA were developed, but it was not until the 1990s that it evolved widely. A variety of assessment methods covering multiple impact categories (Hauschild et al., 2013) were developed by different research centres, universities, and enterprises. Even up to this date, specific LCA methods are being developed, still causing the range of LCA applications to broaden. Regardless, the creation of many LCA methods led to the appearance of discrepancies, which called for a standardization process. Between 1990 and 2000, international societies, workshops, and journals (such as the *Journal of Cleaner Production*) around LCA appeared, leading to greater harmonization of the existent methods and therefore more reliable and comparable results (Bengtsson, 2011). LCA also started to appear in legislation, and it currently contributes to two of the United Nations' sustainable development goals (SDGs), including the responsible consumption and production and the climate action ones (United Nations, 2012).

SETAC (the Society of Environmental Toxicology and Chemistry) has been developing and harmonizing LCA methods, and the ISO (International Organization for Standardization) has also been involved since 1994. Thus, specific LCA ISO standards have been released and revised. The newest versions are *ISO 14040: Environmental management - Life cycle assessment - Principles* and *ISO 14044: Environmental management - Life cycle assessment*

- *Requirements and guidelines*. The latter was last reviewed in 2016 and a new update is currently under development. The standard specifies which requirements are demanded for LCA assessments and provides guidelines for facilitating its use. It also offers support through the application of all LCA phases, encourages a critical review and report of the LCA, informs of its limitations and the relationship between all its phases, and includes the conditions for use of value choices and optional elements. The report also includes examples of interpretation and data collection (International Standard Organization, 2006).

Currently, the interest in LCA has grown even more, especially in both European (though the United Nations and SETAC) and American (though the US Environmental Protection Agency) Policy. New databases provide information on which exchanges happen during the production process of a wide range of products, including chemical compounds. The life cycle concept has also been applied to other fields, such as economy (with life cycle costing) or social studies (with social LCA).

LCA is, thus, well established and used for evaluating the environmental pressures associated with a good or service throughout its life cycle. The scope of the study determines which phases of the production of the subject under study are included in the LCA. These include feedstock obtainment, production, use and end-of-life, which can involve recycling, a treatment or disposal. The scope of the assessment depends on its aim. LCA enables decision makers to identify the critical stages of a life cycle of a product and provides the information for required for supporting new technologies or procedures with better environmental performance. In this context, LCA is used for informing about a product not only to the people in charge of planning or designing its manufacturing process but also for underpinning an environmental claim or an environmental product declaration in marketing. It is a relevant and useful tool for facilitating the implementation of good environmental practices in businesses, for research on life cycle impacts of products and how to improve them and for helping develop effective environmental polices (Huijbregts et al., 2017).

7.1 Phases of LCA

To ensure transparency and reliability, LCA has four standardized main phases, which are described by *ISO 14040* and *14044*. In LCA, all phases are interconnected. The results and their interpretation may lead to a revision of the methodology followed in previous steps in an iterative process. In Fig. 7-1, the relations between each phase are shown. The following sections describe and discuss the decisions taken and the criteria followed in each phase for this specific study.

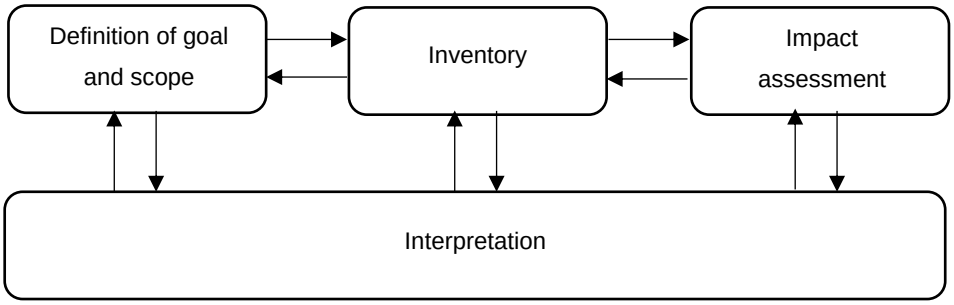

Fig. 7-1: Links between LCA phases.

7.1.1 Goal and scope definition

7.1.1.1 LCA goals

LCA was originally used to compare the environmental impacts of different products or processes. Currently, it has a wide range of applications, including ecolabeling, process design and decision and policy making at much higher levels. When combined with the PBs framework, LCA is used to evaluate the absolute sustainability of an activity, and if that level of impact is acceptable in the long-term considering the Earth's ecological capacity. In this study, however, the contribution of each selected chemical to the PBs is also analysed.

The goal of the LCA for the present study is exactly that of identifying and analysing the environmental impacts of the European chemical industry to propose improvement measures which would increase the sustainability level of the sector. Therefore, as stated before in the project report, the LCA carried out adopts an attributional approach.

Quantifying LCA impacts in terms of the PBs helps portray the severity of the environmental damage in a clearer and more direct way. The approach is therefore especially suitable for the communication of the results with a broad audience.

7.1.1.2 Scope and system boundaries

During the initial stage of LCA, the scope, the commonly named functional unit and allocation criterion of the study need to be defined, all according to the purpose of the study.

In terms of the scope, system boundaries and level of detail are of upmost importance. The boundaries define which parts of the complete life-cycle of the product are to be considered, with the possibility of including impacts derived from the activities upstream the plant, also known as cradle (implications of feedstocks and energy requirements) to the activities downstream, called grave (use/consumption and end-of-life of a product's life). In between, we find the production process itself, the boundaries of which would be defined as gate-to-gate. The aforementioned possible scopes for LCA are shown in Fig. 7-2.

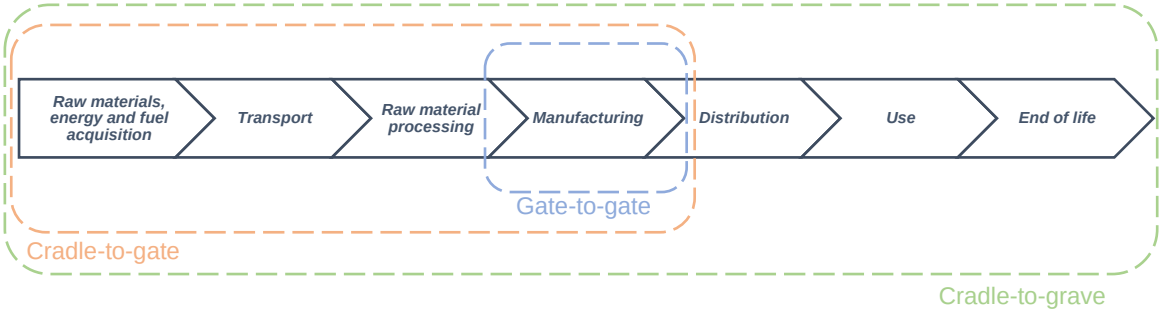

Fig. 7-2: Scope definition in LCA.

As shown, a cradle-to-grave scope would include the life of the product once it leaves the production plant. However, since this study is production-based (and not consumption-based), a cradle-to-gate scope is adopted, including the acquisition of required feedstocks and their transport to plant, energy generation and ending with the production of the chemical (gate-to-gate) (Wernet et al., 2016). Thus, the performance of strictly the chemical industry is assessed. However, for the base chemicals within the study's boundaries, the "distribution" stage is quantified since they are used as feedstocks within the industry.

Specifically, cradle-to-gate system boundaries include:

- Acquisition of non-renewable resources (e.g., natural gas or other fossil fuels).
- Acquisition of renewable resources (e.g., biomass).
- Transformation of the acquired resources into energy.
- Processing into feedstock and storage of all resources and raw materials.
- Recycling (in production) of wastes and other materials.
- Production process of the chemical.
- All transport required until the chemical is produced, including transport of resources, raw materials, and intermediate products.
- Management and treatment of wastes and emissions produced within the cradle-to-gate boundaries.

In this study, the application of the LCA tool is applied to a sector (chemical industry) instead of a single individual product (e.g., benzene production) (Goedkoop et al., 2008). This is done by consistently combining individual cradle-to-gate LCAs for each of these products, while ensuring impacts are not double-counted in the process (see section entitled Interrelations between processes).

Therefore, as the search for links between activities within the system boundaries could be a never-ending task, a threshold for the number of “backwards steps” or “chain echelons” that will be studied when analysing the input flows for each activity. In this study, the threshold is set at one “iteration”, so the manufacture of every direct input for each process are analysed, but any inputs before that are not. This approach studying direct inputs (foreground processes) but disregarding indirect ones (background processes) is often adopted in the literature (Bojarski, 2010). It is agreed to be conservative in the sense that overlooked connections (if any) will always lead to an overestimation of impacts owing to a certain degree of double counting.

Ammonia and styrene can serve as examples for clarifying the significance of studying only foreground activities when calculating volumes to avoid double-counting (the LCA does include background processes since data is provided by *ecoinvent*).

In one of the studied processes, ammonia is obtained as a by-product in the manufacturing of cocamide DEA, which is in turn produced from DEA. Meanwhile, DEA is synthetized by reacting ethylene oxide (International Agency for Research on Cancer, 2013). The dataset for ammonia from cocamide DEA production is therefore linked with ethylene oxide if we move two steps backwards, and with DEA if we apply the decided criteria. Thus, using the one-echelon criterion, ethylene oxide is not identified as an input in the supply chain of ammonia, and therefore, its impact is counted twice.

As for styrene, it can be obtained by the dehydrogenation of ethylbenzene, which is in turn produced by the catalytic alkylation of benzene with ethylene (ICIS, 2010b). Therefore, the study of foreground processes neglects the fact that ethylene and benzene are (indirect) inputs for the styrene production process, for which only ethylbenzene is detected. In this case, if ethylbenzene were one of the studied processes, further links would be detected.

Fig. 7-3 shows these two examples illustrated in a Sankey diagram to depict the significance of system boundaries. The studied activity constitutes the main process, while the activities supplying the necessary direct feedstocks, energy, resources, or auxiliaries (in this example, the depicted fluxes are those of chemical products) are the foreground processes. Background activities are those which contribute to the foreground and therefore indirectly to the main process as well (Sonesson et al., 2010).

Note that the link between ethylene oxide and ammonia (both included in the study) is not detected when only the study of foreground processes (in addition to the main process) is undertaken. Similarly, the use of ethylene and benzene as indirect feedstocks of the styrene production process is also neglected.

Additionally, the diagram helps better visualize how if ethylbenzene and DEA were included in the study, the relationship between these chemicals and the feedstocks needed for their production would be included.

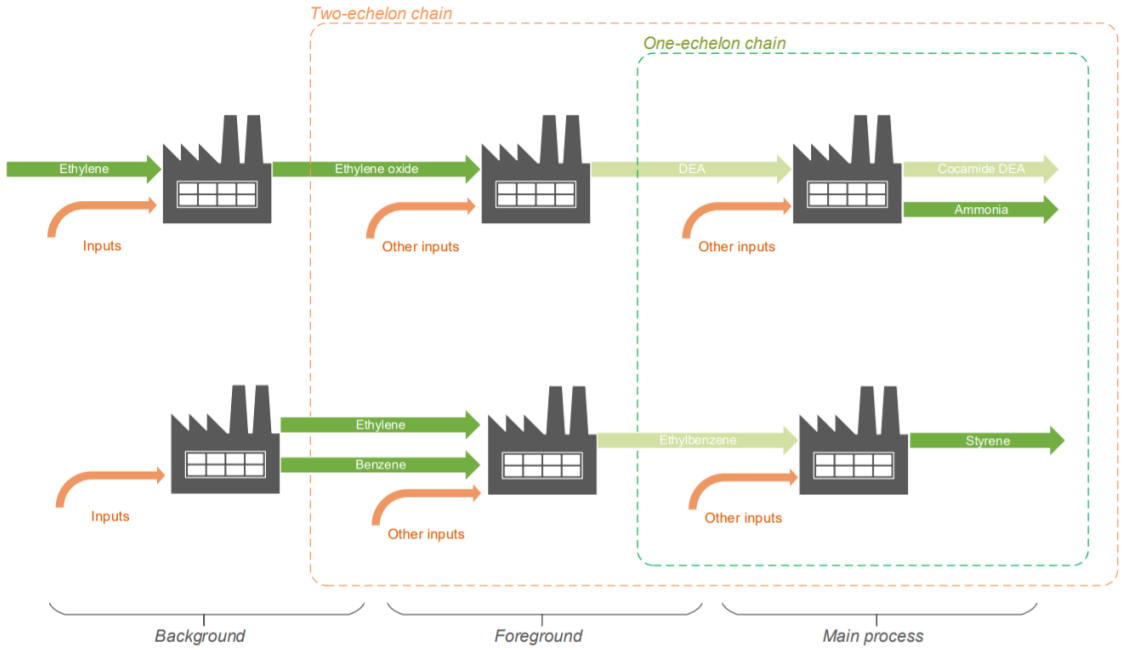

Fig. 7-3: Sankey diagram depicting the comparison between one- and two-echelon chains.

In order to detect all interrelationships between the studied processes, the complexity of the connections would call for the analysis of thousands of activities as in beyond the scope of any work in the literature (e.g., the generation of energy for a certain process might use equipment or machinery containing plastic pieces which may be generated from another one of the studied chemicals).

Even if the study of the relationships between processes takes the study of only foreground processes as a boundary, the quantification of the impacts of the industry does include background processes, since datasets provide such information (often modelled from average industry data) incorporated in the LCIs of each process.

The relationships detected between the studied chemicals by systematic analysis of foreground processes have been discussed in sections Selected chemicals and processes and Interrelations between processes, however, Table 7-1 shows a briefing the connections in Fig. 4-21.

Table 7-1: Interlinks between the studied chemicals.

ID	Chemical	Main feedstocks	Linked to
1	Acrylonitrile, Sohio process	Propylene	17,1,2
2	Ammonia, partial oxidation	Coal heavy fuel oil	
3	Ammonia steam reforming	Methane or higher hydrocarbons, catalyst (Ni)	
4	Ammonia, from cocamide DEA production	DEA, methyl cocoate / coconut oil / coconut acids / stripped coconut fatty acids, alkaline catalyst	8
5	Benzene	Chain hydrocarbons	
6	Benzene, coking	Coal	
7	Cumene	Benzene and propylene	3,4,17
8	Ethylene glycol	Ethylene oxide	8
9	Ethylene oxide	Ethylene	9,17
10	Ethylene, average	Chain hydrocarbons	
11	HDPE, granulate	Ethylene	9,17
12	HDPE, granulate, recycled to generic market for HDPE	Ethylene	9,17
13	LDPE, granulate	Ethylene	9,17
14	LLDPE, granulate	Ethylene	9
15	Methanol	Natural gas, coal, CO_2, other natural resources (e.g., wood, solid waste, etc.)	
16	PP, granulate	Propylene	17
17	Propylene oxide	Propylene, chlorine	17
18	Propylene	Chain hydrocarbons	
19	Purified terephthalic acid	Xylene, acetic acid	23
20	Styrene	Ethylbenzene	9, 3, 4
21	Toluene, liquid	Chain hydrocarbons	
22	Vinyl chloride	Ethylene, chlorine	9
23	Xylene	Chain hydrocarbons	

7.1.1.3 Functional unit

Finally, the functional unit (FU) of the study (the calculation basis) must be defined according to the object of study in a way that ensures it can be used thought the analysis as a reference. In this case, a multiproduct functional unit based on the production volumes for each product or activity of a particular year is used [kg/yr]. Expressing the FU in an annual basis allows the Application of the PB-LCIA damage assessment model.

7.1.1.4 Data Quality Goals

The reliability of the results depends in great measure of the quality of the data employed. In this context, quantifying data uncertainty according to the goals of the study is crucial, especially if relying on databases as in the present study. On

the one hand, acknowledging the inherent uncertainty that is associated with databases increases the study's credibility, quality, and transparency. On the other hand, the quantification of uncertainties allows for drawing more reliable conclusions when interpreting the results (Baker & Lepech, 2009).

In this study, nominal (i.e., deterministic) impacts are be accompanied by error bars providing the ranges of values that an apparent impact in one PB may take. This variability may the limit to be transgressed or not, depending on the realization of the uncertainty. Furthermore, large uncertainties in certain impacts of processes could reduce or even outweigh the differences when comparing between two or more alternatives.

In this study, the analysis of the extent to which the data quality goals are met and the calculation of uncertainties for every result is carried out through the completion of a pedigree matrix, a rubric to determine the adequacy of LCA datasets to the aims of the carried study. As will be discussed in the Data Quality Analysis section, it is of critical interest to determine what are the data quality requirements of the study for the five parameters appearing in the pedigree matrix, those being (i) data reliability, (ii) completeness, (iii) temporal, (iv) geographical and (v) technological accuracy.

For this work, the data quality goals (DQGs, presented in Table 7-2) are defined for each of the aforementioned categories. The data quality analysis is the section which requires higher specificity in terms of definition of DQGs. Therefore, a detailed description of the decisions made before reaching the goals provided in Table 7-2 is given in the Data Quality Indicators.

Table 7-2: Data Quality Goals.

Data Quality Goals	Applied to this study
Reliability	Verified data (reviewed data in *ecoinvent*)
Completeness	Representative % production sites (<20)
Temporal coverage	LCA recommendation: one year min (-2018)
Geographical coverage	Level C (Sub-region, EU-28)
Technological coverage	Match with IEA, 2013

The main decisions made during the initial phase of LCA are briefed in Table 7-3.

Table 7-3: Initial phase of LCA.

	Applied to this study
Scope	Cradle-to-gate
Goal	Sectoral study
Functional unit	Multiproduct, kg chemical/yr

7.1.2 Life cycle inventory

The second phase of LCA is the Life Cycle Inventory (LCI) phase. It entails the elaboration of an inventory of all the inputs and outputs involved in the assessed system, to the level of detail desired and in concordance to the study's scope. These inputs include raw materials, energy, and other auxiliary necessities, while outputs comprise emissions, effluents, and wastes released to air, land, surface water and ground water (ISO, 2006). LCIs need to be found for every considered activity, and the functional units need to be homogenized to allow the aggregation of results.

At this point, it is convenient to introduce two new terms: the ecosphere and the technosphere. Natural resources and energy carriers are extracted from the ecosphere, while if the materials used come from another process, it is said they are an exchange with the technosphere. For this study, all LCIs are fluxes coming from or emitted to the environment (i.e., the ecosphere), as exchanges with the technosphere are ultimately transformed into flows from and to the environment by studying the corresponding upstream process.

Eq. 51 shows the calculations made in LCA to obtain the LCI values for each element *i* exchanged between the process and the ecosphere (or technosphere) for product or chemical *j*.

Later, LCIs are characterized into a contribution to each PB using the equation presented in the section for the Characterization of LCIs in terms of their contribution to the planetary boundaries (LCIA phase).

$$LCI_{i,j} = \sum_{Stages} LCI_{i,j}^{Stages} \quad \forall i,j \qquad \textit{Eq. 51}$$

In *Eq. 51*, *i* represents the specific flow exchanged (e.g., CO_2 emissions or water uptake) while *j* is the final product (i.e., chemical). The sum of the exchanges of a certain flow (*i*) required to produce *j* during the different stages of its life cycle yields the total exchanged volume of *i*.

In practice, this information is usually sensitive and confidential, and companies seldom disclose it, forcing LCA practitioners to resort to environmental databases. These databases provide LCI inventories for selected processes. Such inventories are based on measurements of existing plants and account for all LCIs exchanged between the activity assessed and the technosphere from a cradle-to-gate perspective (i.e., they are already $LCI_{i,j}$). They are typically expressed per unit of output of the main product, as defined by the corresponding FU of the dataset (e.g., per kg of ethylene or kWh of electricity).

Available LCA databases can either be public (e.g., *European Life Cycle Database*, *CPM LCA Database*, *US Life Cycle Inventory Database*) or private (e.g., *ecoinvent*, *GaBi* and *SimaPro*). Among them, *ecoinvent* v3.5 is held in high regard by the research community, and other LCA modelling tools use its data (Hollerud & Bowyer, 2017). Additionally, all datasets submitted to *ecoinvent* go through a revision process, and the database is constantly updated. Therefore, in this work, LCIs for every assessed product have been collected from the version of this database that fits the year under study according to the DGQ, that being *ecoinvent* v3.5. In order to model the connections between processes, inputs from the technosphere for PE, PP, and vinyl chloride were obtained from the same datasets but from v.3.7.1, since the information was not provided by v3.5. Environmental burdens were still modelled from v3.5. Datasets used for each specific chemical and information on the exact exchanges with the ecosphere of each dataset are provided in Table S2-1.

Ammonia's total production volume is given in kg N, not NH_3, so it has been duly modified to match *ecoinvent*'s unit of kg NH_3. The collected data for the rest of chemicals did not require any unit change.

7.1.3 Life cycle impact assessment

Once the complete inventory is prepared, the fluxes of materials and energy must be translated into impacts on the desired impact categories to understand their significance. This is carried out in the Life Cycle Impact Assessment Phase (LCIA). Not all substances contribute equally (if at all) to all environmental categories. Taking as an example the climate change category, a single tonne of CH_4 emitted has the same global warming potential (GWP) as 84 tonnes of CO_2 (Climate Change Connection, 2020), while non GHGs such as ammonia show no GWP at all. These numbers weighting the effect of each stressor (*i*) in each impact category (*b*; e.g., human health or environment health) are called characterization factors ($CF_{i,b}$) (Huijbregts, 2011).

Many methodologies and damage assessment models have been developed and updated. These provide the values of the characterization factors for the impact categories considering in the corresponding assessment model (as discussed later in this section). ECOPOINTS 1990 was the first ever proposed LCIA method, which was later updated to ECOPOINTS 97. Other former methods include CML 1992 and EPS1994. Later, newer models were created by merging, partially adapting or incorporating parts of the older ones. That is the case of ReCiPe, which was developed from CML 2001 (the reviewed version of CML 1992) and Eco-Indicator 99. Both the latter and ReCiPe have been widely used. Other currently relevant methods include Impact 2002+ and TRACI (Hauschild & Huijbregts s, 2015).

Among impact categories, a distinction is made whether they are midpoint or endpoint, with different LCIA methods built on just one of these two categories, or a combination of both. Midpoint categories focus on earlier stages in the cause-effect chain for the emission of a pollutant, while an endpoint category provides the impact of the pollutant at the end of the impact series. Endpoints are also called areas of protection. Fig. 7-4 shows a small section of the impact chain for global warming, and how LCIs (in this case, emissions of CO_2 and CH_4) are related to final impacts on more than one impact category. Other midpoint impact category examples could be freshwater eutrophication, terrestrial acidification, or water use, while damage to resource availability is also one of the three main endpoints (Huijbregts et al., 2016).

In addition to midpoint and endpoint categories, single scores also exist, although they are not widely. The reason is that single score indicators require impacts on endpoints categories to be rated according to their importance or severity, which could lead to unethical or subjective evaluation (i.e., is the extinction of a species more “acceptable” than the appearance of a new human disease and should therefore contribute less to the final weighted score?). In the same line, endpoint categories are considered more likely to be subject to interpretation, while midpoint approaches are associated with higher scientific robustness as their quantification entail modelling fewer environmental mechanisms.

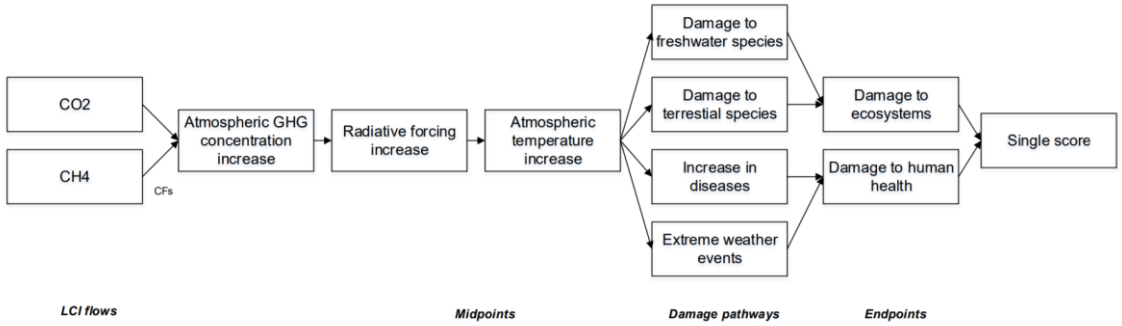

Fig. 7-4: Section of the impact pathway for global warming (adapted from Hauschild & Huijbregts, 2015; Li et al., 2019).

Many authors provide recommendations for choosing the best fitting LCIA methodology for an LCA study. *Hauschild et al., 2013* compare and analyse the suitability of the models available for each impact category and choose the most satisfactory ones. Both stakeholders and specialists were involved in this study, with the aim of providing reliable conclusions. The relevance of geographical differentiation in characterization factors was pointed out, as well as the need for further research in the characterization modelling at endpoint impact categories and the uncertainties associated with some CFs.

Since LCA is continuously developing field, all these points have been addressed. The ReCiPe 2016 model was one to tackle these challenges. Characterization factors were given for a European level and adapted them to the global scale while still permitting their characterization to a more precise level. Moreover, they also added more impact categories and overall described a reliable method for moving from the LCI to the LCIA phase for some impact categories on midpoint and endpoint level (Huijbregts et al., 2017). Consistency between all the different

categories was considered a priority, since some of them such as ecotoxicity present additional challenges (van Zelm et al., 2009).

For this study, a PBs -based life-cycle impact assessment is done, and so LCIs must be quantified in terms of their impact towards the PBs. *Ryberg et al. (2018b)* presented an LCIA methodology called PB-LCIA which considers the Planetary boundaries as impact categories. The results that traditional LCA studies and the PB-LCIA framework offer were compared, and the PB-LCIA procedure was proved to be reliable. In PB-LCIA, the 85 elementary LCI flows that affect the different Earth Systems and therefore contribute the most to the transgression of the PBs are selected. The characterization factors developed for this methodology allow to express each of these 85 flows according to the control variables for every PB. This framework is used in the LCIA phase of the present study.

7.1.3.1 PB-LCIA

LCA's aim is to give a clearer vision on how resource use and emissions arising from a specific activity can alter the state of a final system, may it be human health, an ecosystem, or Earth Systems such as ocean acidification in the PB-LCIA framework. The main challenges of linking the LCA and PBs frameworks are the connection of two studies with different impact categories (damage on human health and ecosystems and resource availability in conventional LCIA and stable Earth Systems in the PB-framework) and the necessity to translate non-global processes or activities to a consumption of a global safe operating space (allocation of said impacts). Fig. 7-5 shows the concept of the PB-LCIA framework, which combines LCA and the PBs.

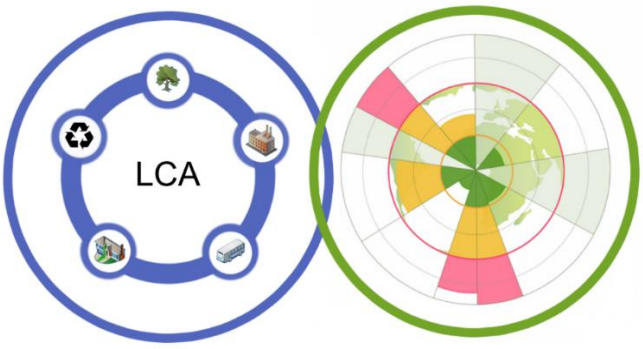

Fig. 7-5: PB-LCIA methodology linking LCA and the PBs framework.

The first approach (Tumoisto et al., 2012) to the combination of these two fields of study introduced weighting factors that related LCI impacts to the more relevant PBs based on the distance between each PB and their control variable value.

The next step (Bjørn & Hauschild, 2015; Sandin et al., 2015) was defining clear and normalized links between LCIA impact categories and PBs. The capacity of the environment and ecosystems to receive impacts in the studied regions was evaluated (Bjørn & Hauschild, 2015), since a PB is a quantification of how much stress the Earth System can withstand without irreversible damage being caused to its functioning and structure. Authors of each study calculated and expressed these capacities (called capacity normalization factors) in terms of LCIA midpoint impact indicators with the same metrics.

Later, *Ryberg et al.* refined the methodology by identifying (Ryberg et al., 2016) and addressing (Ryberg et al., 2018b) the principal challenges of expressing LCA impact scores as PBs.

They introduced CFs that allowed the desired conversion in the LCIA phase, and also addressed the fact that some impacts overlap, which is not problematic in PB-LCIA as the aim is to calculate the burdens put into every PB separately. In contrast, in LCA, impacts need to be weighted (Life Cycle Assessment) to obtain a combined score for the different impact categories. The third challenge addressed was the difficulty to obtain single scores for some PBs which had burdens irregularly distributed across the globe, such as land-system change (Planetary boundaries). To resolve the problem, the developed CFs allow for both global averages and region-specific results to be obtained (Ryberg et al., 2018b). This study uses the PB-LCIA framework as the damage assessment model in the LCIA phase of the LCA to quantify the impacts of the studied system on the PBs. The methodology followed for such calculations is described in the following section.

An additional challenge is the need to compare a safe operating space, defined at global (Earth) level, with the burdens caused by a single activity. Arguably, a single process should not have the right to consume all the environmental budget for human activities to develop. Therefore, an issue yet unsolved is how to allocate a certain share of sage operating space to an activity or system in such

a way that it is perceived as fair. *Sandin et al.* (2015) also noted the importance of the method chosen for the allocation of the general global safe space so as to obtain the impact allowed to the studied system. In the Allocation of the safe operating space section, the criteria adopted for this study are described and discussed.

Ryberg et al. (2018b) defined characterization factors for all PBs (Röckstrom et al., 2009; Steffen et al., 2015) except for biosphere integrity and introduction of novel entities. They took various considerations into account to ensure reliability, such as coherence in complexity between models and control variables and the maturity of said models. Additionally, all *Ryberg et al. (2018b)* followed a newly proposed path by *Huijbregts et al. (2011)* to derive CFs.

Some characterization factors are derived with models using linear cause-and-effect relationships (Huijbregts et al., 2008) for most impact categories. However, some do not show a linear relationship between the environmental burden and its effects (for example, the potentially disappeared fraction of species in the ecosystem) and there is a need to derivate the CFs from a curve. With a marginal change approach, the result depends on the point in the curve approximated, as seen in Fig. 7-6 (a) for the impact of phosphorus concentrations on macroinvertebrate diversity in freshwater systems. This model's critical weakness is that for situations of already existing high pollution, where the CF (as given by the slope of the curve) will approach zero. That said, the main advantages of such an approach are the possibility to identify the point where emission changes would have the greatest efficiency (where the slope is the steepest) and being able to calculate a specific cause-effect CF for the exact pollution situation the system is found at. Older studies use this methodology (Van Zelm et al., 2009; Strujis et al., 2011), which has also been typically supported in LCA.

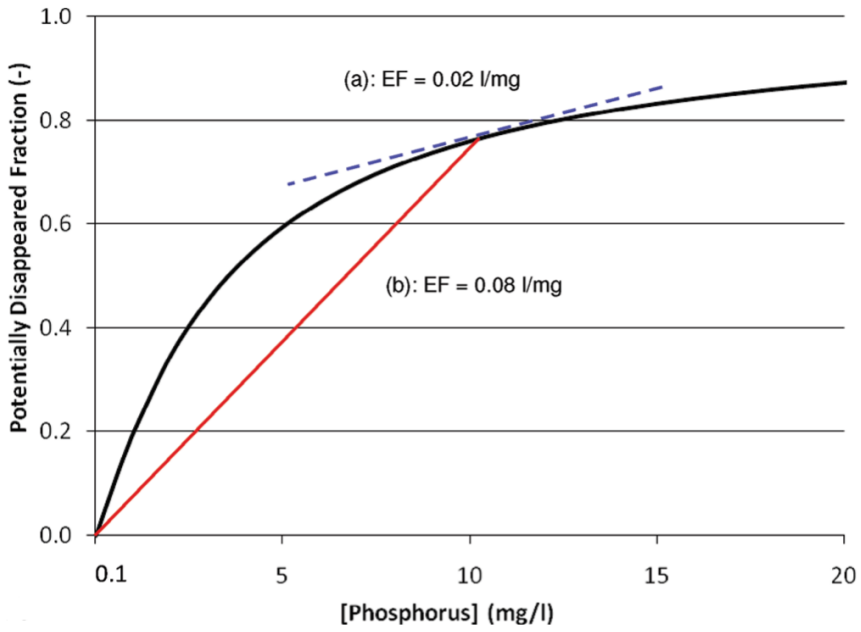

Fig. 7-6: Effect factor approaches zero if the current state is the same or below the target (Huijbregts, 2011). Example for the state of macroinvertebrate communities in freshwater ecosystems depending on the phosphorus concentration.

Nevertheless, when working with the PB-LCIA framework as in this study, focusing on a future target state instead of analysing marginal changes is key, and therefore following an average approach as seen in Fig. 7-6 (b) would make CFs reflect how the studied flow contributes to said preferred state in the long-term. This would involve deriving characterization factors between the target state and the current state calculating the average change in the distance between both and its slope.

7.1.4 Interpretation of results

In the final stage, the results of LCA are interpreted, and recommendations or improvement plans can be developed. ISO 14040 provides a guideline for which sections the interpretation phase of LCA should include. Besides the particular conclusions of each study, the quality of the data used should be evaluated, as well as the general level of completeness. In the Results section, the conclusions drawn, as well as the recommendations arising from them, are shown.

8 Application of the PB-LCIA damage assessment model

In this section, the methodology followed for the application of the PB-LCIA damage assessment model is described along with the calculations and consideration undertaken for the obtention of the impacts of the chemical industry in the PBs.

8.1 Collection of data on elementary flows (LCI phase)

Fig. 8-1 shows a general representation of the methodology followed during the data collection stage. The availability and quality of data needs to be considered and can lead to the refinement of the original data requirements with the aim to achieve the highest possible completeness of the final inventories.

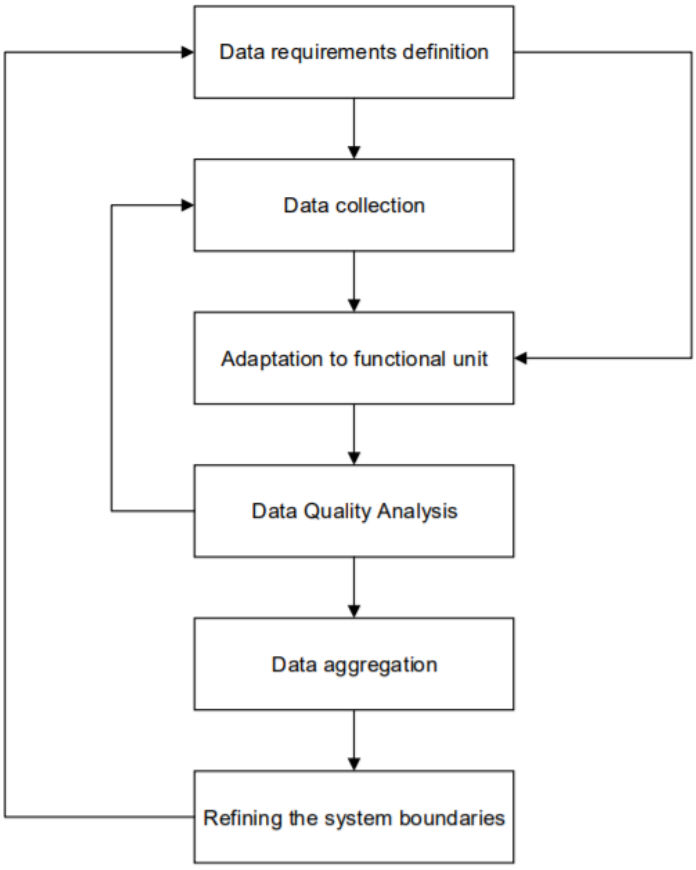

Fig. 8-1: Methodology of the LCI phase.

In many cases, more than one production route for the same chemical *j* is included in the study. For each LCI, the total input and output flows were calculated as a weighted aggregate of the contributions of all considered

processes. Therefore, the total quantity of each pollutant or resource *i* that is derived from all activities that produce *j* ($LCI_{i,j}$) [units of *i*/kg *j*] is the sum of the products of all LCIs and the market share (MS_a) of each process *a* (see *Eq. 52*).

$$LCI_{i,j} = \sum_{a} (LCI_{i,j,a} \cdot MS_a) \ \forall i,j \qquad \textit{Eq. 52}$$

8.2 Treatment of LCI data

Before the LCIA stage, the LCI data collected need to be transformed to adjust to the PBs (PB)-LCIA framework approach as follows.

The method used in LCIA considers the impacts of a pulse emission of each of the involved flows and integrates their exposure over time, as seen in *Eq. 53*. The interval of time considered can either be finite or infinite (if time tends to infinite) but does not account for or track the specific instant the emissions was released. In addition, the function includes the exponential of the product of the time passed after the pulse is emitted (*t*) and (*A*), a coefficient matrix that defines what kind of impact the flow has. After multiplying that by (Δm), the strict mass value of the pulse, everything is integrated. The result can be expressed in terms of impact to different impact categories when multiplied by the suitable effect factor ($CF_{i,b}$) (Heijungs, 1995), as previously described.

$$\gamma = mass\ time = \int_0^T (e^{t*A} * \Delta m) dt \qquad \textit{Eq. 53}$$

However, in the context of PB-LCIA, given the definition of the PBs as limit values the Earth can withstand and if we take them as impact categories, it is necessary to consider that single pulse emissions as given in the LCA method do not cause the transgression of these limits. Nevertheless, continuous pulse emissions or exploitation of resources do have an effect and provoke changes in environmental states, which is why in this case the impact scores should be expressed as constant (i.e., steady state) inputs instead of pulse emissions.

Applying the aforementioned calculations, *Eq. 53* changes into *Eq. 54*, that is, from an integral to a first order differential equation. This is achieved by substituting Δm with *S* - a constant annual flow expressed in [kg/yr] as in this

study. *Eq. 54* (Ryberg et al., 2018b) can be solved to obtain the mass remaining in the environment as a result of each annually expressed LCI (steady state mass or m_{ss}). How mass changes with time is also considered as expressed below ($\dot{m} = dm(t)/t$).

$$\dot{m} = -A * m(t) + S \rightarrow \lim_{t\to\infty}(\dot{m}) = 0 = -A * m(t) + S \rightarrow m_{ss} = A^{-1} * S \qquad \textit{Eq. 54}$$

With such adaptation, the PB-LCIA framework can focus on the inputs and outputs that come from diverse life cycles of the product, which are not necessarily in the same production chain, but happen within the studied time period. Traditional LCA, on the other hand, focuses on a discrete number of life cycles which end and finish during an indefinite extent of time (Ryberg et al., 2018b). Fig. 8-2 represents the two different concepts for better understanding.

This leads to a change in the functional units, from just mass (as in environmental databases) to mass/time. To adapt LCIs from *ecoinvent* (expressed as flux/kg chemical) to the suitable units for the PB-LCIA framework, annual total production values (TPV_j, expressed in [kg *j*/yr]) were acquired from the *Prodcom* database for each chemical *j* (European Union, 2020e). *Eq. 55* was then used to transform conventional LCIs for each pollutant or resource *i* and chemical *j* ($LCI_{i,j}$) expressed in [units of *i*/kg *j*] and obtained from *Eq. 51* and *Eq. 52* into LCI values in accordance with the PB-LCIA metrics ($LCI_{PB\text{-}LCIA,i,j}$, expressed in [kg *i*/yr]). Finally, the sum of production volumes of *j* destined to the manufacture of other chemicals (*j'*) in the study [kg *j*/yr] is subtracted from the total production volume in order to avoid double-counting impacts. This value ($V_{j,j'}$) is obtained through the characterization of the chemical industry described in Interrelations between processes.

Note that since the study is production-based, when calculating total flows of stressors ($LCI_{PB\text{-}LCIA,i,j}$) the exports are not subtracted from the total volume as appears in *Eq. 33*. OU_j was purely used to create the Sankey diagram presented in section 4.2.

$$LCI_{PB-LCIA,i,j} = LCI_{i,j} * \left(TPV_j - \sum_{j'} V_{j,j'} \right) \quad \forall i,j \qquad \textit{Eq. 55}$$

In order to be consistent with the DQGs of the study, and since LCI indicators (Wernet et al., 2016) are generally found for the RER (Continental Europe) area (the highest specificity *ecoinvent* provides in terms of geographic location for most datasets), the total production volumes are searched for the EU-28 area (European Union, 2020e). The scope of the study is, thus, maintained at EU-28. In the case some LCIs are not provided for the RER area, the severity of the geographical mismatch is evaluated in the Data Quality Analysis.

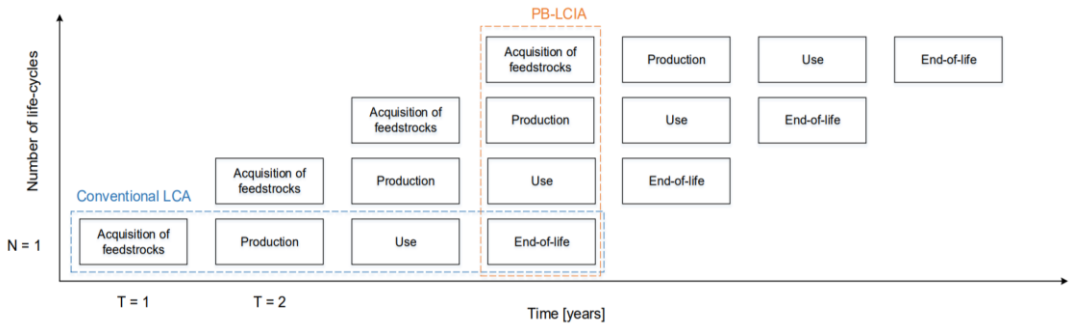

Fig. 8-2: Difference in derivation and modelling between conventional LCIA methods and PB-LCIA (Ryberg et al., 2018b).

8.3 Characterization of LCIs in terms of their contribution to the planetary boundaries (LCIA phase).

Characterization factors (CFs) for each LCI entry and PB are employed to link LCI values to each PB. However, a first selection of the LCIs needed for the study must be conducted, since not all flows impact on all (or any) PBs. Furthermore, the CFs developed by *Ryberg et al. (2018b)* might not match exactly the LCI entries available in the database employed, so there is a need to reconcile available LCIs, according with the energy/material flows or resource uses described in the CFs, together with the direction and compartment of the exchange (i.e., from the technosphere to air, freshwater, groundwater, or soil). To obtain more adequate results, the following considerations are made when selecting the adequate LCIs for each CF:

- Biogenic CO_2 and inorganic carbon to air are neglected since their neat balance is zero as they are retrieved from and emitted to air.
- *Ryberg et al. (2018b)* do not provide a CF for the effect of N_2O on stratospheric ozone depletion (OD), even when their impact on this system is not negligible.An additional CF is therefore calculated by transforming

the N_2O to CFC-11 equivalent emissions using *Eq. 56* (Algunaibet et al., 2019) and then multiplying by the CF of CFC-11.

$$CF_{N2O,OD} = CF_{CFC-11,OD} * \frac{0.018\ kg\ CFC - 11\ eq}{kg\ N_2O} \qquad \textit{Eq. 56}$$

- To avoid double-counting:
    - For the nitrogen fixation boundary, CFs are given for more than one N-containing compound (i.e., nitrogen oxides and ammonia to air, nitrates and total nitrogen to freshwater, and nitrates to groundwater). Using all the provided indicators together leads to an over-counting of the nitrogen runoff since the total applied amount and the impact on the PB would be three times larger as the PB is designed to quantify the amount of N from one flow (Ryberg et al., 2018b). Therefore, only the most relevant substance must be selected for the calculations (e.g., the one with the most reliable LCIs). Additionally, only *intended* nitrogen fixation has to be quantified in LCIs for consistency with the control variable of the nitrogen PB. In this study, loss of nitrogen to freshwater was used as it is the principal route for nitrogen fixation. This is the recommended approach according to previous research (Brentrup et al., 2000; Langevin et al., 2010;).
    - For the aerosol loading boundary, *Ryberg et al.* (2018b) provides CFs for NO_x and NO_2. To avoid double-counting the impact of NO_2, its specific flow is neglected. NO_3^-, on the other hand, is quantified since it is not an oxide but an ion coming from a salt.
- Emissions and uptakes whose compartments are labelled as “unspecified” in the database are included only if the CF for the LCI does not apply to a particular type of flow either (e.g., as in the CF for CO_2, which is linked to the flow for “CO_2, non-fossil – unspecified”). Conversely, if any requirement is indicated, these emissions are disregarded as they are assumed not to contribute towards this particular PB (e.g., the CF provided for NMVOCs from urban areas is linked to the LCI labelled as “NMVOCs – urban air close to ground” but not to “NMVOCs – unspecified”).

- *Ryberg et al.* (2018b) defined CFs for LCIs that are not available in the consulted datasets. This might lead to the underestimation of the impacts on some PBs (i.e., climate change, stratospheric ozone depletion, ocean acidification, and aerosol loading).
- LCIs labelled as *land transformation to forest* and clean *water effluent to water* are given a negative sign to represent the inverse direction of the environmental flow (i.e., resource uptake).

Once the LCI entries are selected, their contribution to the PBs is obtained by multiplying each LCI by the CF (Ryberg et al., 2018b) corresponding to flow *i* and PB *b* (*Eq. 57*).

$$FC_{b,j} = \sum_{i} LCI_{PB-LCIA,i,j} * CF_{i,b} \quad \forall b, j \qquad \textit{Eq. 57}$$

$FC_{b,j}$ refers to the total impact on PB *b* produced by product *j* [units *PB*], $LCI_{i,j}$ is the life cycle inventory *i* (flow or resource use in their corresponding units calculated with *Eq. 55* generated because of the manufacture of product *j*) [units *i*/yr], and $CF_{i,b}$ [units of *PB**yr/units of *i*] is the characterization factor for the impact of each LCI item *i* on the studied PB *b*.

8.4 Modelling impacts

It is important to note that some PBs have inverse proportionality, whereby an between increase in the value of the control variables values will be perceived as negative for the PB and vice versa. PBs exhibiting this behaviour are ocean acidification, stratospheric ozone depletion and land-system change.

Another consideration taken was the adaptation of units from kg/yr to just kg for specific flows that as a description only occur once, instead of being constant during the selected time (one year). An example would be an emission of CO_2 due to the removal of a tree or forest versus a constant emission of CO_2 from a process. In the first scenario, the carbon that was stored in the vegetation or soil is released as a single pulse, while in the second scenario there is a constant emission flow. However, it is still possible to compare land-transformation CO_2 emissions to constant CO_2 emissions as they both contribute to the global

increase of atmospheric CO_2 concentration and climate change (Ryberg et al., 2018b).

8.5 Allocation of the safe operating space

As previously discussed, a challenge for PB-LCIA studies is to successfully downscale PBs to the studied sector or geographic location since PBs are defined at a global scale. The threshold values given by the study of each Earth System are expressed as global maximum burden that can be sustained at a planetary level. In consequence, it is necessary to calculate which part of this environmental budget can be assigned to the activities studied.

8.5.1 Definition of the safe operating space

Initially, it is important to note that the planet itself has a natural contribution (called natural background level) towards each PB. The natural background level has to be subtracted from the corresponding threshold of each PB before obtaining the room actually available for all anthropogenic activities, which receives the name of safe operating space (SOS).

The natural background level for the land system change boundary is a clear example of the concept, since before any human activity, the altered fraction of forest was zero. Therefore, for a PB of a minimum percentage of preserved forest of 75%, the size of the SOS is that of a maximum of 25% of forest disturbance. In boundaries where the natural background level is not zero, the same calculation must be done. For instance, the global background natural level of phosphorus inflows into marine waters has a value of 8 Tg $P*yr^{-1}$. Meanwhile, the PB is set at a maximum of 11 Tg $P*yr^{-1}$. therefore leaving a SOS of 11 - 8 = 3 Tg $P*yr^{-1}$. For those boundaries that work inversely, the SOS is calculated analogously, as seen in Table 8-1. An example would be the ocean acidification boundary, where the calculus is reversed since a higher value indicates a better state of the Earth system.

For boundaries assessed at a regional level (e.g., aerosol loading), the values for all the categories must be downscaled to the proposed region as well.

Table 8-1: SOS assigned to each PB considering natural contributions.

Impact category	Units	Planetary boundary	Natural background level	Total SoS,PB
Climate change (energy imalance at top of atmosphere)	W m−2	1.000	0.000	1.000
Climate change (atmospheric CO2 concentration)	ppm CO2	350.000	278.000	72.000
Stratospheric ozone depletion	DU	275.500	290.000	14.500
Ocean acidification	Ω_{arag}	2.752	3.440	0.688
Biogeochemical flows (Nitrogen), global	Tg N yr-1	62.000	0.000	62.000
Biogeochemical flows (Phosphorus), global	Tg P yr-1	11.000	1.100	9.900
Land-system change, global	%	75.000	100.000	25.000
Freshwater use, global	km3 yr-1	4000.000	0.000	4000.000
Aerosol loading (regional boundary)	AOD	0.250	0.140	0.110

Similarly, it is possible to compute the remaining SOS by subtracting the current value of each control variable (natural and anthropogenic) from the PB. Today, some boundaries are already transgressed at a global level, which results in negative values for the remaining SOS (Table 8-2).

Table 8-2: Remaining SOS for each PB.

Impact category	Units	Planetary boundary	Current value (Steffen et al., 2015)	Current available SoS
Climate change (energy imalance at top of atmosphere)	W m−2	1.000	2.300	-1.300
Climate change (atmospheric CO2 concentration)	ppm CO2	350.000	398.500	-48.500
Stratospheric ozone depletion	DU	275.500	200.000	-75.500
Ocean acidification	Ω_{arag}	2.752	2.890	0.138
Biogeochemical flows (Nitrogen), global	Tg N yr-1	62.000	150.000	-88.000
Biogeochemical flows (Phosphorus), global	Tg P yr-1	11.000	22.000	-11.000
Land-system change, global	%	75.000	62.000	-13.000
Freshwater use, global	km3 yr-1	4000.000	2600.000	1400.000
Aerosol loading (regional boundary)	AOD	0.250	0.300	-0.050

The remaining SOS can be used to explore the current state of the boundaries, or how the introduction of a new activity would affect the present situation. Regardless, it does not evaluate the sustainability of any certain activity since it considers all current impacts on the Earth system. Moreover, when evaluating a new activity, negative values are found for many control variables given the limits are already transgressed, so even if the studied processes were sustainable, the total would still not be positive.

8.5.2 Assigning the share of safe operating space to the studied sector and region

Once the SOS has been defined for all anthropogenic activities, different principles can be used to further downscale the PBs to levels lower than the global one. The share of safe operating space (SoSOS) assigned to the sector, region or activity under study must reflect their impact to a selected parameter. The criterion chosen for this step can widely influence the results and the conclusions of the study, as different criteria will give rise to different SoSOS values (Sandin et al., 2015).

Two different approaches can be adopted when allocating SOS, one based on egalitarian principles and a second using non-egalitarian principles. Regarding the first equality-based principles, SOS is firstly downscaled to the corresponding region based on its population share, and then further specificity is achieved by using additional indicators, which are generally economic, for activities, sectors, or companies. Conversely, non-egalitarian or sovereignty-based principles assign the share that corresponds to an activity according to the environmental stress they cause. The latter allow to calculate the downscaled PB without requiring any further information but cannot provide the same level of specificity as the egalitarian method. Note that egalitarian principles assume that all people should have the same right to the ecological space (Häyhä et al., 2016).

For any sharing principle, the SoSOS is the result of the product of the total SOS_{PB} [control variable for each PB] and the allocation factor [$aS_{PB,SP}$; %], as described in *Eq. 58*, where $SoSOS_{PB,SP}$ is the assigned share to planetary boundary *PB* according to sharing principle *SP*.

$$SoSOS_{PB,SP} = SOS_{PB} * aS_{PB,SP} \qquad \textit{Eq. 58}$$

After calculating the SoSOS and having characterized the impact of the system under study according to the control variables for each PB (IS_{PB}), the occupied share of SOS [$occSoSOS_{PB,SP}$; control variable for each PB] can be determined through *Eq. 59*. Logically, if $occSoSOS_{PB,SP}$ is ≤1, the activity is within the assigned SoSOS and therefore can be considered environmentally sustainable from a PBs perspective.

$$occSoSOS_{PB,SP} = \frac{IS_{PB}}{SoSOS_{PB,SP}} \qquad \textit{Eq. 59}$$

This equation evidences the consequences of using different principles to obtain the SoSOS, since different denominators in the right-hand side of *Eq. 59* can cause the same numerator (i.e., impacts) to transgress or not a given PB.

For this study, an egalitarian distribution of the SOS is calculated using three criteria which sequentially narrow down the allocation to adjust to the specific data used for the development of the LCA. *Eq. 61* illustrates the calculations that

have been done to obtain the allocation factor for each step of the downscaling process. Fig. 8-3 graphically shows the steps followed for the downscaling of the PBs to the study.

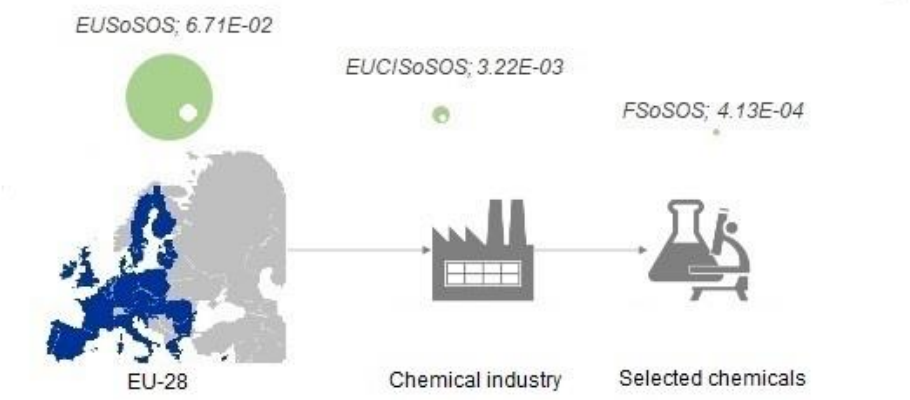

Fig. 8-3: Egalitarian allocation of the SOS narrowing down from global PBs to a European level, then the European chemical industry and finally the chemicals and processes under study.

Additionally, a non-egalitarian principle is also applied, so that the results can be compared and their sensitivity to the allocation method chosen can be analysed.

For the egalitarian principle, three levels of specificity are applied one after another until the final allocation factor is derived. This cascade allocation has the advantage of allowing the assessment of results at different levels of disaggregation, provider greater perspective on the magnitude of the impacts. On the other hand, it must also be acknowledged that each allocation criterion uses a ratio between two values to calculate the percentage of SOS that corresponds to the assessed activity, and therefore adds a supplementary degree of uncertainty to the final results (similarly as endpoint indicators are inherently more uncertain than midpoints). The disaggregation of the SoSOS assigned according to each criterion facilitates the analysis of results.

In the first place, an initial $aS_{PB,SP}$ is calculated taking into account the total number of inhabitants who reside within the studied area (EU-28), giving $aS_{PB,PP}$. Population data are taken from Eurostat and 2019's World Population Prospects for the year of study (2018), so the ratio between the area of study and the global population can be calculated. In *Eq. 61*, P_{EU-28} and P_{world} [population] refer to the 2018 populations of the countries conforming EU-28 (thus, before United

Kingdom's exit) and the world, respectively (European Union, 2020c; United Nations, 2020c). Thus, *Eq. 62* provides the **EUSoSOS**, which is the share of the global SOS assigned to Europe. Nonetheless, an egalitarian per capita division of SOS does not provide enough specificity to refer to the chemical industry, as other economic activities also take place within this region. Therefore, two more additional factors are added (Brejnrod et al., 2017; Sandin et al., 2015; Wolff et al., 2017).

First, a second sharing principle is defined based on the fraction of gross value added (GVA) that the chemical industry represents with respect to Europe's (EU-28) total GVA (**EUCISoSOS**). Both $GVA_{ChemInd}$ and $GVA_{EU\text{-}28}$ [€] data refer to the year of study. Total GVA is obtained from Eurostat (European Union, 2020b) while the fraction of it corresponding to the sector under study is calculated through WIOT Input-Output Tables (Timmer et al., 2015) and *Eq. 60*. Input-Output Tables contain economic information of different sectors of an economy, classified according to NACE (Statistical Classification of Economic Activities in the European Community) codes. In this case, the chemical industry is represented through category R-11 within the tables, which corresponds to NACE C20 (manufacture of chemicals and chemical products). Thus, the total GVA in 2014 US$ (WIOT still has not released more updated tables) is obtained. This value is transformed into euro and undergoes an adjustment to 2018 currency values, considering the cumulative inflation for the 2014-2018 period. The latter is calculated through harmonized consumer price indexes (European Union, 2020a). Finally, the resulting allocation factor ($aS_{PB,PP\&GVA}$, see *Eq. 61*) can be used to calculate the SoSOS occupied by the European chemical industry (*Eq. 63*).

Taula 8-1: Adjustment of GVA, GDP at market prices chain linked volumes; seasonally and calendar adjusted data.

Value adjustment	**HICP (index 2015 = 100)**
Q4, 2018	103.89
Q4, 2014	99.90
% inflation	4.00%

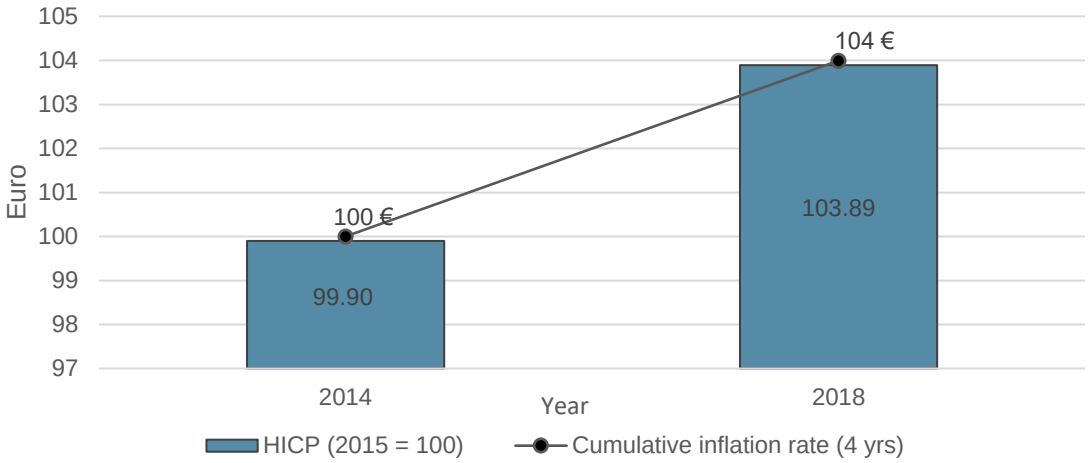

Fig. 8-4: Adjustment of GVA using harmonized consumer price indexes to calculate cumulative inflation.

$$GVA = Total\ output - Total\ intermediate\ consumption \qquad \textit{Eq. 60}$$

To narrow down the calculations even more, a third principle was added to account for the fact that the whole chemical industry is approximated here based on a subset of chemicals. Therefore, the SoSOS allocated to the selected chemicals (**FSoSOS**) is obtained based on the allocation factor $aS_{PB,PP\&GVA\&value}$ as shown in *Eq. 64*.

In *Eq. 61*, $Value_{NACE\text{-}C20}$ [€; for EU-28] refers to the total annual value (2018) of the C20 sector (i.e., the manufacture of chemicals and chemical products). Meanwhile, $Value_{SelChem}$ refers to the value of the specific chemicals selected. All data were extracted from the *Prodcom* database (European Union, 2020e).

$$aS_{PB,SP} = aS_{PB,PP\&GVA\&value} = \underbrace{\frac{P_{EU-28}}{P_{World}}}_{aS_{PB,PP}} * \underbrace{\frac{GVA_{ChemInd}}{GVA_{EU-28}}}_{aS_{PB,PP\&GVA}} * \underbrace{\frac{Value_{SelChem}}{Value_{NACE\ C20}}}_{aS_{PB,PP\&GVA\&value}} \qquad \textit{Eq. 61}$$

$$EUSoSOS_{PB} = SOS_{PB} * aS_{PB,PP} \qquad \textit{Eq. 62}$$

$$EUCISoSOS_{PB} = SOS_{PB} * aS_{PB,PP\&GVA} \qquad \textit{Eq. 63}$$

$$FSoSOS_{PB} = SOS_{PB} * aS_{PB,PP\&GVA\&value} \quad \textit{Eq. 64}$$

As for the second sharing principle, a non-egalitarian approach is employed. In line with *Ryberg et al. (2018b)*, the final SoSOS for the study is assigned according to the share of the current level of global impact on each boundary that stems from the sector under study (SQSoSOS, *Eq. 66*). In *Eq. 65*, $I_{EU,chemind,PB}$ and $I_{world,PB}$ are the contributions to the control variable for planetary boundary *PB*.

$$aS_{PB,SP} = aS_{PB,SQ} = \frac{I_{EU,chemind,PB}}{I_{world,PB}} \quad \textit{Eq. 65}$$

$$SQSoSOS_{PB} = SOS_{PB} * aS_{PB,SQ} \quad \textit{Eq. 66}$$

The allocation principles are presented in Table 8-3 along their resulting assigned shares. It is relevant to note that the egalitarian principle results in a single allocation factor which is applied to all PBs equally, and is calculated to allow a distribution of resources without further distinctions between people.

Meanwhile, the non-egalitarian principle is based on the *status quo*, thus being influenced by the level of development of the region and industry, its access to resources, and its current exploitation of those. The status quo (SQ) allocation is therefore a more conservative principle which does not imply a redistribution of natural goods and focuses on a BAU scenario. As seen in Table 8-3, the final allocation factor for the SQ principle is higher for those Earth systems being more greatly impacted by the sector, while it is closer or even inferior to the $aS_{PB,sp}$ of the final step of the egalitarian principle for systems already being under lower levels of stressors.

Table 8-3: Sectorial and national sharing principles for the allocation of the planetary SOS.

Sharing principle	**$aS_{PB,SP}$ (%)**	
***EU**SoSOS*	$6.71 \cdot 10^{+0}$	
***EUCI**SoSOS*	$3.22 \cdot 10^{-1}$	
***F**SoSOS*	$4.13 \cdot 10^{-2}$	
***SQ**SoSOS*	Climate change *(energy imbalance at top of atmosphere)*	$1.94 \cdot 10^{+0}$
	Climate change *(atmospheric CO2 concentration)*	$2.78 \cdot 10^{+0}$
	Stratospheric ozone depletion	$3.22 \cdot 10^{-4}$
	Ocean acidification	$1.86 \cdot 10^{+0}$
	Biogeochemical flows (Nitrogen), global	$1.10 \cdot 10^{-2}$
	Biogeochemical flows (Phosphorus), global	$1.97 \cdot 10^{-3}$
	Land-system change, global	$3.68 \cdot 10^{-5}$
	Freshwater use, global	$5.06 \cdot 10^{-3}$
	Aerosol loading, regional	$5.32 \cdot 10^{-1}$

Note that uncertainty zones defined for the different PBs, as described in section Planetary boundaries, can also be expressed in terms of their corresponding SoSOS. To do so, it suffices with recalculating the value of variable SOS_{PB} in *Eq. 64* subtracting the natural background level from the PB threshold. As a result, three different situations will be defined for the impacts from the activity assessed:

- If impacts lie below the lower bound of the uncertainty range for the SoSOS, the activity will be deemed sustainable.
- If impacts lie above the upper bound of the uncertainty range for the SoSOS, the activity is clearly unsustainable.
- If impacts lie within the uncertainty band for the SoSOS, no strong conclusion can be drawn for the sustainability level of the activity, although there is a high risk that it causes irreversible damage to the planet.

9 Data Quality Analysis

As previously stated, a critical point which influences the reliability of any scientific study is the quality of the data used. The uncertainty level associated with the results obtained must be evaluated, which requires methods for managing data in an objective way. Preferably, a common rubric or procedure should be followed for all similar studies to guarantee high reproducibility, that is, that equal results are obtained for the same data even when different analysts are carrying out the study. Therefore, these methods should prevent dependence on personal perspective or subjective ideas.

In the context of LCA, large sets of data are manipulated during the LCI phase. Consequently, efforts have been put into providing a standardized process for data quality assessment (DQA from this point forward). Since the first guidance document presented (Bakst et al., 1995), the methods applied have evolved to provide more systematic and consistent results. While probability functions can sometimes be obtained directly from databases or by comparing the retrieved information to historical data, a common approach, more appropriate for the present study, is the use of standardized DQA methods. In particular, the so-called pedigree matrix (Weidema & Wesnaes, 1996) is used here. According to this methodology, LCI entries are assumed to follow log-normal distributions whose standard deviation can be calculated from scores assigned to certain indicators described in the pedigree matrix. Therefore, the pedigree matrix allows to translate a qualitative assessment on a number of indicators into a quantitative estimation of data uncertainty, improving this way the quality of the results for the LCI and LCIA phases in LCA.

The matrix has been through several revisions to include previously neglected aspects such as cost data quality considerations for eco-efficiency measures (Ciroth et al., 2009), and to eliminate any misleading or ambiguous language that could lead to higher variance in the results from different institutions or individuals due to misunderstanding of the method. Alternative procedures for the analysis of data quality have been released as well, but the selected pedigree matrix is specifically developed for the database used in this study (ecoinvent).

In this study, the revised pedigree matrix by *Ciroth et al.*, (Table 9-2) is applied to quantify uncertainties of LCIs. The table shows the changes done in 2016 with respect from prior version of 2009. The pedigree matrix assigns scores ranging from 1 to 5 for five different categories called Data Quality Indicators or DQIs (those being (i) reliability, (ii) completeness, and (iii) temporal, (iv) geographical and (v) technological coverage). It must be kept in mind that low-ranking scores do not necessarily imply poor quality of the data but lower relationship with the goals and scope of a particular LCA study. Therefore, DQA must be consistent with the goals of the study (Data Quality Goals or DQG), as defined during the Goal and scope definition of LCA. Table 9-1 shows the criteria followed for the elaboration of the pedigree matrix with the DQIs that depend on each DQG presented in bold.

Table 9-1: Data Quality Goals.

DQIs	DQGs
Reliability	Verified data (reviewed data in *ecoinvent*)
Completeness	Representative % production sites (<15 threshold)
Temporal coverage	**LCA recommendation: one year min (-2018)**
Geographical coverage	**Level C (Sub-region, EU-28)**
Technological coverage	**Match with IEA, 2013**

Note that, among all the DQI included in the pedigree matrix, only the temporal, the technological, and the geographical correlation are affected by the DQG of the study. The scope of the LCA will directly impact the years, areas, and processes that the study is aimed at. Therefore, the scores for these indicators are specific for the study that is being undertaken and will be equal for all datasets. On the other hand, the reliability and completeness indicators are not related to the DQG but the data itself (Crioth et al., 2009; Weidema & Wesnaes, 1996). This implies that the scores designated in these categories would be equal for any other study, since any change in the aim of a particular study would not make the collected data any less reliable or representative.

Table 9-2: Pedigree matrix (Weidema et al., 1996 revised by Ciroth et al., 2008). Between brackets is the adapted version by (Ciroth et al., 2016) for ecoinvent v3.

Indicator score	1	2	3	4	5
Reliability of source	Verified data based on measurements	Verified data partly based on assumptions **or** non-verified data based on measurements	Non-verified data partly based on assumptions	Qualified estimate e.g., by industrial expert	Non-qualified estimate or unknown origin
Completeness	Representative data from a sufficient sample of sites (*from all sited relevant for the market considered*) over an adequate period to even out normal fluctuations	Representative data from a smaller number of sites (*> 50% of the sites relevant for the market considered*) but for adequate periods to even out normal fluctuations	Representative data from an adequate number of sites but from shorter periods (*from only some sites: <<50% relevant for the market considered, or >50% of sites but from shorter periods*)	Representative data but from a smaller number of sites and shorter periods or incomplete data from an adequate number of sites and periods (*from only one relevant site for the market considered or some sites but from shorter periods*)	Representativeness unknown or incomplete data from a smaller number of sites and/or (*only and*) from shorter periods
Temporal differences	Less than 3 years of difference to year of study (*to the time period of the dataset*)	Less than 6 years of difference (*to the time period of the dataset*)	Less than 10 years of difference (*to the time period of the dataset*)	Less than 15 years of difference (*to the time period of the dataset*)	Age of data unknown or more than 15 years of difference (*to the time period of the dataset*)
Geographical differences	Data from area under study, same currency	Average data from larger area in which the area under study is included, same currency	Data from area with slightly similar cost conditions, same currency, or with similar cost conditions and similar currency	Data from area with slightly similar cost conditions, different currency	Data from unknown area or area with very different cost conditions
Further technological differences	Data from enterprises, processes, and materials under study	Data from processes and materials under study from different enterprises, similar accounting systems	Data from processes and materials under study but from different technology, and/or different accounting systems	Data on related processes or materials but same technology	Data on related processes or materials but different technology

In this study, all categories have been reviewed individually for every chemical included in the study. In case of lack of data or doubt, a worst-case scenario policy has been considered. Accordingly, the highest score among all possible options has been assigned, which translated into higher variance values and, thus, lower reliability. This ensures that the variance reported for the results is not optimistically lower than what could be expected form a realistic point of view. For all *ecoinvent* datasets used, the technologies studied are at a current level.

9.1 Data Quality Indicators

9.1.1 Geographical coverage

Geographical data coverage indicates the area required to be under study so enough data are collected to reach the desired reliability. (ISO, 2006).

Rather than focusing on strict geographical regions, the pedigree matrix focuses on levels of geographic specificity surrounding the studied area. Seven levels of specificity or resolution are defined by expanding the four proposed by the United Nations geo-scheme (United Nations, 2013; Weidema & Wesnaes, 1996) as shown in Table 9-3. For this specific study, a C category is used since the field of study is the European chemical industry. The chosen region from which data should apply is therefore defined as EU-28.

Table 9-3: Levels of geographical specificity UN (United Nations, 2013; Weidema & Wesnaes, 1996).

Specificity level	
A	Global
B	Continental
C	Sub-region
D	Nation
E	Province/ State/ Region
F	Country/City
G	Site specific

9.1.2 Technological coverage

The technological data quality goal considers four categories and assigns a score depending on how many of them match the case of study. These categories include (i) process design and (ii) scale, (iii) operating conditions, and (iv) materials. These are all correlated with the inputs and outputs of a process and therefore determine the quality and characteristics of the final product, which is

why they are evaluated. (ISO, 2006; Edelen et al., 2016). Thus, this category includes potential technological variances that are not a result of a different temporal or geographical setting, since these are already evaluated in their respective categories (Weidema & Wesnaes, 1996).

As explained in section Selected chemicals and processes, the chemicals selected as proxies for the whole chemical industry are based on a list from the IEA Roadmap (IEA, 2013). Therefore, *ecoinvent* data on the process considered for the production of each chemical is evaluated to assess how much (if at all) it matches with the technologies considered in the IEA Roadmap. As an example, the technological coverage score will be lower if some processes considered in the IEA Roadmap are being neglected in *ecoinvent*.

In many cases, data collectors in *ecoinvent* do not provide the level of detail required to assess all four categories of this DQUI, which causes the score for the technological differences section to be particularly high owing to the worst-case scenario policy. However, this difficulty can sometimes be overcome by resorting to related patents which do describe the route followed to obtain the chemical with enough detail.

9.1.3 Temporal coverage

Temporal coverage is defined as the shortest time required to provide reliable results considering there will be fluctuations in time and they should be evened out (ISO, 2006). The DQG should express the defined period of time that the study aims to cover, and the pedigree matrix evaluates the difference between this DQG and the end date of collection of data used. The data should be able to reflect the dates that the study chooses to include. For LCA, no original recommendation had been set as for what length of time is necessary to achieve such goals, meaning different studies could lead to different scores. Following recent guidance documents released (Edelen, 2016), this study takes the recommended value of at least one year of data collection to meet the DQG.

9.1.4 Completeness

The completeness uncertainty category defines which part of the total value of the production for each chemical is being considered in the LCI data. The factors

that influence completeness are the number of sites studied, the coverage of the complete production of each chemical and whether the time span allows for data to eliminate normal fluctuations and therefore be representative enough (Crioth et al., 2016; Crioth et al., 2013). For the assessment of the datasets in the study, the following criteria has been applied:

Since the total number of relevant plants manufacturing each product within the region is unknown, score 1 can already be discarded. Therefore, it is needed to assess whether each dataset receives a score of 2, 3, 4 or 5. For datasets providing the number of sites (>1) and knowing the time period assessed is representative in all cases (therefore category 4 is also discarded), the scores are granted between 2 and 3. Contrarily, if the number of sites covered is not specified or data are reported to be a European average, representativeness is unknown and therefore a score of 5 is assigned.

The differentiation between score 2 and 3 lies in the % of coverage of the total plants, according to *ecoinvent* and the pedigree matrix. Specifically, in *Ciroth et al.*'s (2016) version, it is specified that score of 2 applies to data covering more than 50% of the total production sites, while a score of 3 refers to data which cover less than 50% of relevant sites.

However, due to industrial confidentiality, the number of plants within the studied region is usually not available. Datasets for methanol and benzene from coking already report data on coverage, but for the remaining datasets, due to the difficulty to ensure all datasets are assessed according to equal criteria, the following procedure has been applied:

1. For datasets providing the exact number of sites studied for data collection, a threshold of 15 sites has been established.
2. For datasets above this threshold, the number of plants considered for data collection has been compared with the total number of production plants for that chemical. This latter value has been researched in the literature and allows to compute the % of actual coverage of the dataset, to ultimately ensure no dataset is assigned a high-ranking score when it does not meet the pedigree matrix standards.

The only datasets reporting the number of sites and meeting the threshold are those of ethylene, propylene, vinyl chloride, granular HDPE and LDPE, and PP. The total number of industries involved in their production in Europe was consulted to ensure the threshold of 15 sites was representative in each case. For PE and PP, no data on the number of production sites was found, preventing a clear assessment of whether the coverage of the datasets is representative or not. Therefore, they have been assigned a score of 3, which corresponds the worst-case scenario for these datasets (ICIS, 2020). The information on the rest of datasets for which data could be found is summarised in Table 9-4.

Table 9-4: Specifications for the completeness category.

Chemical	Number of sites in the RER area	Number of sites covered in the dataset	Covered production sites (%)	Final score
Ethylene	55 (Ecofys, 2009)	19	34.5	3
Propylene	>91 (Boulamanti & Moya, 2017a)	19	20.9	3
Vinyl Chloride	35 (Cherrie et al., 2011)	18	51.4	2

9.1.5 Reliability

Similar to the completeness one, the reliability category does not depend on the DQG since the information evaluated relates to how data was acquired and verified, and to which sources were used (Weidema & Wesnaes, 1996). In the *ecoinvent* database, data are subject to review by experts and, therefore, can be classified as verified. In most cases, the score assigned will be 2, since data come from literature based on measurements or plant reports; however, the fact that assumptions or approximations are made prevents the possibility of assigning a score equal to 1.

9.2 Assigned scores for all studied chemicals

A section providing the complete reasoning behind the scores assigned to every chemical can be found in the annex (Section S3). For some chemicals, more than one dataset was used for calculating LCIs so as to include all existent markets and processes. In these cases, the data quality study is applied to each dataset individually.

9.3 Uncertainty study

The completed pedigree matrix is presented below in Table 9-5.

Table 9-5: Completed pedigree matrix (RS: Reliability of Source; C: Completeness; TD: Temporal Differences; GD: Geographical Differences; FTD: Further Technological Differences).

Indicator score	RS	C	TD	GD	FTD
Methanol	2	2	1	5	4
Ethylene	2	3	1	2	5
Propylene	2	3	1	2	5
Cumene	4	5	1	2	4
Ethylene glycol	2	5	1	2	2
Styrene	2	5	1	2	4
Purified terephthalic acid	2	5	1	2	5
Propylene oxide, liquid	4	5	1	2	5
Vinyl chloride	2	2	1	2	2
Acrylonitrile through the Sohio process	2	5	1	2	2
Ammonia through partial oxidation, liquid	1	3	1	2	2
Ammonia through cocamide diethanolamine production	2	5	1	2	2
Ammonia through steam reforming, liquid	1	3	1	2	2
Polyethylene, high density, granulate	2	3	1	2	4
Polyethylene, high density, granulate, recycled to generic market for HDPE granulate	5	5	1	2	5
Polyethylene, low density, granulate	2	3	1	2	4
Polyethylene, linear low density, granulate	2	3	1	2	4
Polypropylene, granulate	2	3	1	2	4
Benzene, general	2	3	1	2	5
Benzene through coking	2	2	1	3	2
Toluene production, liquid	2	2	1	2	5
Xylene	2	5	1	2	5
Ethylene oxide	2	3	1	2	2

Each score for all evaluated categories (*n*) is linked to a default uncertainty factor (σ_n^2) which represents the variance of the underlying normal distribution and is used to calculate the total variance of dataset. Additionally, a sixth factor (referred to as basic uncertainty factor or σ_b^2) is added relative to the specific uptake or emission, given that some exchanges carry greater uncertainty than others because they depend on a wider range of factors (e.g., CO_2 emissions are usually easier to calculate than CO emissions, since the latter may vary according to state and characteristics of the engine that produces them, among other variables). The basic uncertainty is thus defined for each LCI depending on the type of environmental burden it represents.

σ_b^2 variances are provided for specific emissions originating from (i) combustion (ii) processes or (iii) agriculture (e.g., CO as a combustion or a process emission). In this study, to comply with the general criterion of adhering to the worst-case scenario, the largest uncertainty factor is assigned when the origin of an exchange is unknown.

Eq. 67 gives the total variance corresponding to each LCI value (e.g., 0.05 for CO_2 emissions to urban air from ethylene oxide production) calculated as the summation of all six uncertainty factors (Weidema et al., 2013). In this equation, σ_1^2 is the basic uncertainty of the LCI, and $\sigma_{2\text{-}5}^2$ are the additional variances associated with each DQI for every dataset. Note that a different variance value is obtained for each of the 112 LCI entries (i.e., fluxes) in each of the 23 processes (or datasets), which results in total of 2576 uncertainty values. These variance values, together with the nominal LCIs provided in *ecoinvent* are then used to characterize (quantitatively) the probability distribution of every LCI as follows.

$$\sigma_{g,LCI}^2 = \sum_{n=1}^{6} \sigma_n^2 \qquad \textit{Eq. 67}$$

A lognormal distribution can be assumed to model uncertainties for LCI values in *ecoinvent*, that is LCI~Lognormal(μ,σ) (Weidema & Wesnaes, 1996). Logrnomal distributions are characterized by the fact that the log-transformed data show a normal distribution (i.e., ln(X)~N(μ,σ)), which is referred to as the underlying normal distribution. Indeed, lognormal distributions are typically defined based on the underlying normal distribution through parameters μ and σ. On the one hand, μ is the geometric median of the underlying normal distribution and can be obtained by log-transforming the median of the original lognormal distribution (μ*) (Limpert et al., 2001).). In turn, μ* is assumed to correspond to the nominal value provided for the LCI in *ecoinvent* (i.e., the one that would be used straight ahead if uncertainties were neglected, see *Eq. 68*). On the other hand, σ is the standard deviation of the underlaying normal distribution and can be calculated from the geometric variance obtained with the pedigree matrix ($\sigma^{*2}_{g,LCI}$) by means of *Eq. 69*, *Eq. 70* (Albrecht et al., 2021). All calculations are performed in Matlab.

Note that the choice of lognormal distributions to characterise uncertainties in LCIs avoids the appearance of negative values during the simulation.

$$\mu = \ln(\mu^*) \qquad \textit{Eq. 68}$$

$$\sigma^* = e^{\sqrt{\sigma^2_{g,LCI}}} \qquad \textit{Eq. 69}$$

$$\sigma = \ln(\sigma^*) \qquad \textit{Eq. 70}$$

Once characterised through the corresponding values of μ and σ, the 2576 probability distributions are discretised into a set of scenarios, each illustrating a potential realization of the uncertainty in the data. In particular, 100 scenarios for each LCI are generated using Monte Carlo sampling in Matlab for all PBs and chemicals. Uncertainty in LCIs is then propagated through the damage assessment model (*Eq. 52*, *Eq. 55*, and *Eq. 57*) which is solved for each scenario. As a result, 100 different values are obtained for variable $FC_{b,j}$ each denoting the total impact on PB *b* produced by product *j* in each of the 100 scenarios. To factilitate data manipulation, results for the 23 chemicals, nine PBs and 100 scenarios were stored in a three-dimensional matrix A = (23,9,100), as seen in Fig. 9-1.

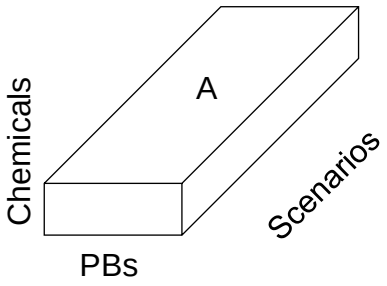

Fig. 9-1: Matrix containing the 100 potential contributions of each of the 23 chemicals in each of the 9 PBs.

This information is reported in the upcoming results by means of error bars, providing the best and worst performances attained among the 100 scenarios. This representation of all potential outcomes allows to evaluate the reliability of the conclusions (i.e., whether the conclusions of the study depend or not on the realization of the uncertainty). Fig. 9-2 shows the 100 generated scenarios in terms of the total contribution to each PB.

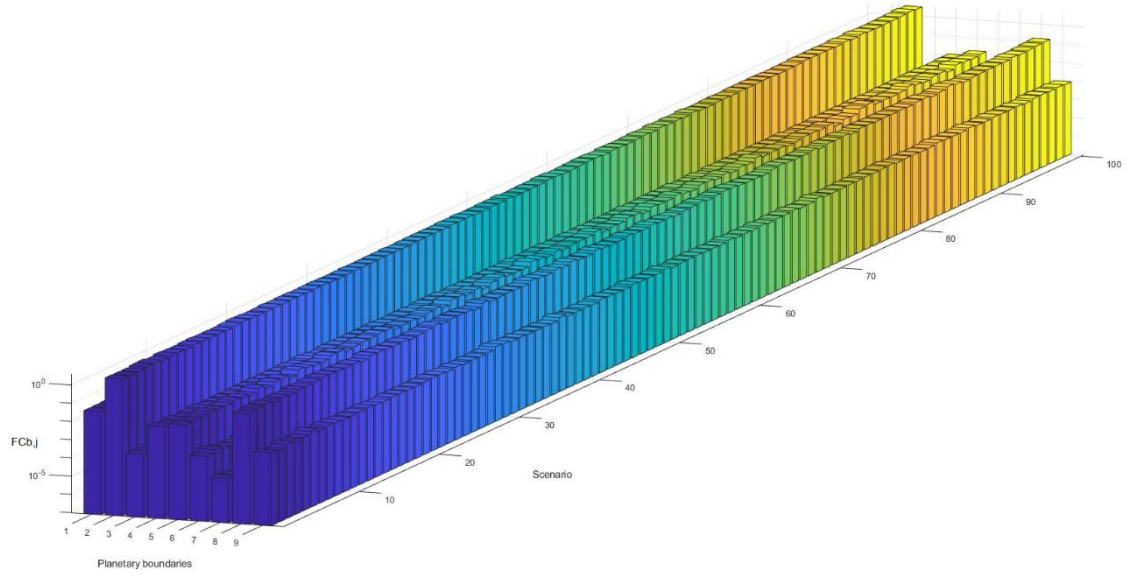

Fig. 9-2: Matlab figure representing the generated impact scenarios for all PBs, where 1: Climate change (energy imbalance at top of atmosphere); 2: Climate change (atmospheric CO2 concentration); 3: Stratospheric ozone depletion; 4: Ocean acidification; 5: Biogeochemical flows (Nitrogen); 6: Biogeochemical flows (Phosphorus); 7: Land-system change; 8:Freshwater use; 9: Aerosol loading.

10 Results and discussion

10.1 Environmental performance of the European chemical industry

In this section, the results on the contribution of the chemical industry on the PBs are initially presented for the two aforementioned allocation principles (i.e., egalitarian, and non-egalitarian), including the three levels of specificity calculated for the former. This results in a total in four different graph plots: a first showing the fraction of SOS which is being occupied when the allocation is done at a European level, a second narrowing down the allocated SOS to the European chemical industry, a third showcasing the final impacts of the egalitarian allocation once the SoSOS is downscaled to the studied fraction of the industry, and a fourth where the SQ sharing principle is adopted.

The allocation criteria and the abbreviations used to refer to each of them are found in the Allocation of the safe operating space section. With the representation of the impact of the chemical industry as the occupied share of assigned SOS ($occSoSOS_{PB}$), the absolute sustainability of the studied activities can be assessed by checking whether the different boundaries are exceeded or not. Note that, although the contribution of the chemical industry to the PBs is unique, it results in different values once it is expressed as occSoSOSPB; thus, different values can be expected for each individual allocation.

The figures presented in the discussion were elaborated using MATLAB by polishing and coding the results obtained mainly in Microsoft Excel (Fig. 10-3, Fig. 10-4, Fig. 10-5, and Fig. 10-6 found in pages 148, 149, 150, and 154). Each bar plot shows the total contribution of all considered chemicals and processes (blue bar) together with the uncertainties associated with the collected LCIs (black error bar). The quality of data is proved to be high since short error bars are obtained for all PBs. Red error bars are used indicate the uncertainty zone designated for each PB as discussed in the Planetary boundaries section. The results are presented in a logarithmic scale so that all PBs can we viewed in one figure despite the different magnitudes of the values. Thus, the y axis represents the occSoSOSPB (*Eq. 59*) and all contributions to a PB exceeding a value of $1 = 10^0$ are surpassing the limit and found, in the best case, within the uncertainty zone of the boundary. This means that there is a risk for the activity to cause

irreversible damage as feedbacks of the Earth system are unclear within this region. Once the occSoSOS$_{PB}$ also transgresses the red uncertainty zone of a PB, the impact of the chemical industry can be clearly classified as critically unsustainable. Only in cases where occSoSOS$_{PB}$ lies below a value of one can the chemical industry be deemed sustainable. Fig. 10-1 shows a preliminary polar plot where these three zones of the PBs and the contribution of the industry on each limit are shown (according to the FSoSOS allocation principle).

Additional figures aiding the discussion, and providing insight to mechanisms behind the obtained results, the environmental burdens considered, how they were classified, and the role of each of them in the final contribution values to each PB (whether each PB is transgressed or respected) can be found in the annex and along the discussion. Finally, the numerical values of the average SOS occupied by the industry (average value out of the generated scenarios) can be consulted in the annexes (Table S4-1).

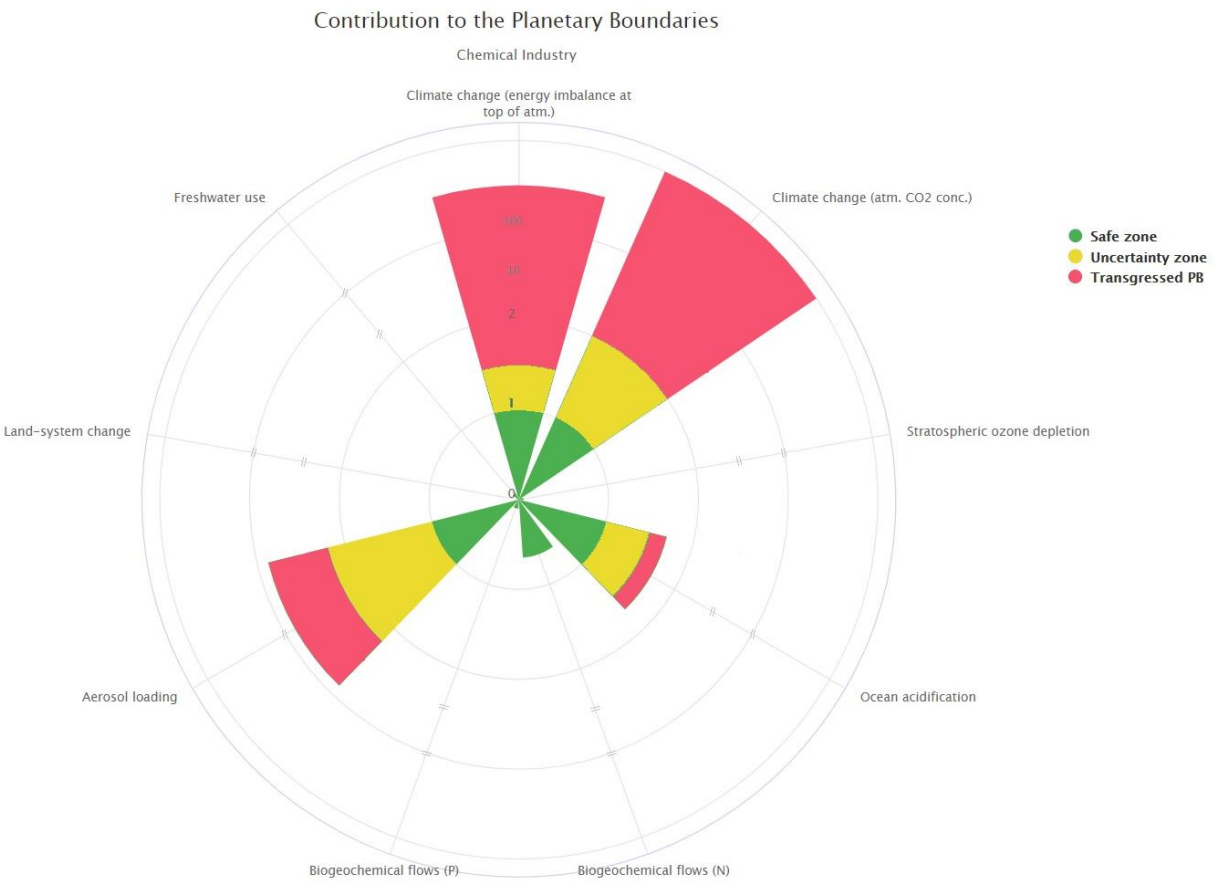

Figure 10-1: Contributions of the chemical industry on the PBs (depicted is the occSoSOS). Figure elaborated in JSFiddle.

10.1.1 Egalitarian allocation

The results for the egalitarian allocation principle are firstly discussed, since they provide the principal and most adequate downscale of the PBs of the study, adapting the SoSOS to exactly the assessed chemicals. The results yielded when the non-egalitarian allocation system is applied are later evaluated, together with the adequacy of the approach.

Fig. 10-3 (page 148) shows the fraction of SOS assigned to solely the EU-28 region (according to the EUSoSOS allocating principle) consumed by the chemical industry. Even if no boundaries are transgressed, the results already hint at a potential surfeit of environmental burdens posed by the sector. For the climate change Earth system, the studied part of the chemical industry alone takes up between 66.29 and 69.20% of the SoSOS corresponding to Europe, despite representing only a 0.6% of Europe's GVA. Taking the economic value of the sector as a proxy for its contribution to human wellbeing and following an equality of welfare approach to egalitarianism (where a fair distribution of resources is achieved when it brings people the same level of welfare (Dworkin, 1981)), it is obvious that the stressors put on the boundaries are excessive.

The ocean acidification and aerosol loading limits are also under threat of being transgressed once more adjusted allocation methods are applied, since the contributions are already at 22.13% and 11.53% of total EUSoSOS, respectively. The level of stressors directed towards the other five boundaries appear to be reasonable when considering the weight of the sector in Europe's economy (always below 0.04%, the final $aS_{PB,SP}$ representing the weight of the studied system, see Table 8-3).

Once the SOS correspondent to the study is narrowed down using the downscaling of the boundaries not only to the European region but also to the chemical industry, the formerly predicted issues become evident. Even though the allocation is not yet completed, Fig. 10-4 (page 149) shows how three boundaries (i.e., energy imbalance at top of atmosphere, atmospheric CO_2 concentration, and ocean acidification) are being widely transgressed. The impact to a fourth (i.e., aerosol loading) falls within the uncertainty zone of the PBs, even if the uncertainty of the LCIs indicates the contribution to the boundary

may be slightly above the limit of the uncertainty range of the PB (the upper bound of the range is transgressed in 2% of the scenarios). It is important to note that, up to this point, the uncertainty associated with the contribution of the chemical industry to the PBs does not affect any conclusion drawn for any PB except for this last one.

Once the egalitarian principle for allocation is completely applied (Fig. 10-5, page 150), the results indicate that under the modelled scenario which considers BAU activity of the chemical sector, four and potentially five of the nine studied PBs are transgressed.

As predicted by the hypothesis of the study, the sector is energy intensive and a primary emitter of GHG emissions, thus undoubtedly trespassing both climate change boundaries. The gap between the assigned SoSOS and the real impact of the industry can be calculated and shows how the energy imbalance boundary is exceeded by 108% (the value of the fraction of occSoSOS which should be at most 1 is 108; since the contribution to the PB is 0.0445 while the available SOS is 0.0004) while the CO_2 concentration limit (which is usually used as the reference threshold for climate change as described in the Climate change PB section) is even more critical and transgressed by 112% (contribution of 3.34 vs an available SOS of 0.03). These percentadges are calculated for only 19 chemicals, even if these are responsible for around 75% of the industry's GHG emissions (IEA, 2013), it is relevant to note that still around 25% of GHG emissions that could be associated with the sector are not quantified and would increase the final impacts even more.

Further insight can be obtained by analysing gases responsible for the impact on the two climate change boundaries. It is known the chemical industry is a great emitter of CO_2 but also of other GHGs such as fugitive methane (CH_4), nitrous oxides (NO_x), hexafluoride (SF_6), hydro fluorocarbons (HFCs) being the most relevant (Suding, 2013). More tracked GHGs include non-methane volatile organic compounds (NMVOCs), carbon monoxide (CO), nitrogen fluoride (NF), and chlorofluorocarbons (CFCs). Intuitively, one may think that the sector's contribution to the atmospheric CO_2 PB would be lower than the impact on the energy imbalance limit, since the latter considers CO_2 and all additional GHGs, while the former only quantifies CO_2. However, the CO_2 appears to be more

affected than the energy imbalance PB. This is due the fact that different control variables and concepts are involved. As described in the Climate change section, aerosols can have a cooling effect that diminishes the energy imbalance caused by other GHGs, thus reducing the total contribution on the energy imbalance PB. Additionally, the available SOS for CO_2 concentration is reduced when the natural background level for this PB is discounted, while the energy imbalance boundary has no natural background level associated, suffering no space reduction, and leaving more room for humanity to manoeuvre. Finally, if the environmental flows of the studied activities are examined, the present study finds that even if 45 types of GHGs have been analysed and considering the total volumes of the chemicals, from 98 to 99.77% of all GHG emissions in kilograms correspond to CO_2, and 99.85-100% of these come from the combustion of fossil fuels (Figure S5-17). Out of these emissions, fluxes of fossil CO_2 to urban and non-urban air at different heights of the atmosphere predominate, while CO_2 from soil, biomass stock or fossil that reaches higher layers (stratosphere and troposphere) are much lower (Fig S5-1 and S5-2). The GHGs which follow CO_2 in terms of emission volume are methane, CO, and NMVOCs, but their total mass emitted is three to four orders of magnitude smaller (while GWP is only three to 28 times larger than CO_2's) (Fry et al., 2013; Myhre et al., 2013). Therefore, since the largest contribution is suffered because of CO_2, the boundary which refers to the maximum concentration of this gas allowed in the atmosphere is principally threatened.

The ocean acidification boundary, which is heavily related to the climate change boundary, is also transgressed. The increment in pH of marine waters is due to the absorption of CO_2 (and similar GHG gases such as CH_4, CO, and NMVOCs), thus a high atmospheric CO_2 concentration leads to higher accumulation of the compound in the ocean and more acidic waters (see Ocean acidification boundary). As seen in Fig S5-3 and S5-4, 24 types of emissions are assessed, from which the dominant in terms of total emitted mass are again three (out of the four) fossil CO_2 fluxes (those emitted to urban and non-urban air, closer or further from ground, and other unclassified fossil CO_2 emissions). When the total production of all included chemicals is considered, fossil CO_2 emissions account for 99% of total GHG emissions in kilograms, while the remaining 1%

corresponds to fossil CH_4 emissions. Plots shown in the supplementary material with the breakdown of total GHG emissions for every chemical reveal negligible differences between the contributions of each GHG to the total tracked for the ocean acidification boundary and those for the climate change boundaries. This is because, even if the climate change PBs consider the contribution of a higher number of emissions, both PBs seem to be affected mostly and similarly by CO_2 and CH_4.

Since the emission of large volumes of CO_2 is the main cause of the transgression of the climate change and ocean acidification boundaries, one of the proposed solutions to transition towards a sustainable chemical industry will be the incorporation of carbon capture storage (CCS) technologies (see section for Carbon capture and storage (CCS)).

The prediction that the aerosol loading boundary could potentially be transgressed was also in line with the obtained results, which indicate the sector is 18.7 times above the limit (value of the occSoSOS, contribution of $8.52 \cdot 10^{-4}$ vs an available SOS of $4.54 \cdot 10^{-5}$). The min aerosols emitted vary depending on the process; however, the dominant ones include NMVOCs, sulfur dioxide, and nitrogen oxides (Figures S5-5 and S5-6).

Overall (Figure S5-17), sulfur dioxide emissions account for 39% of overall emissions in terms of mass, followed by nitrogen oxides (29%) and NMVOCs (24%). On the one hand, NMVOC emissions typically stem from the use, combustion, and manufacture of organic solvents and chemicals, which are in turn directly attributable to the chemical industry and especially to some of the assessed processes, as the Impact breakdown section addresses. On the other hand, the energy industry is responsible for a great fraction of SOx and NOx emissions, while an additional 60% of NOx emissions are attributable to road transport, as well as most particulate matter emissions (European Commission, 2014b). The scope of the LCA conducted in the present study follows a cradle-to-gate approach, meaning it includes the obtention of raw materials, energy, infrastructure use and all emissions and resources produced and consumed during the manufacturing process. However, transport of the product from gate to final consumers does not fall within the LCA's scope, and therefore, aerosol

emissions produced during this phase are not reflected in the results. Thus, the boundaries of the LCA may explain the dominance of sulfur dioxide over nitrogen oxides as identified aerosol emissions.

Considering the industry itself is not a principal aerosol emitter and attributing its poor performance over the aerosol loading boundary to its energy use, a scenario where the business-as-usual energy mix is substituted by a more sustainable energy mix will be studied.

The impact of the chemical industry on the four previously discussed PBs (i.e., energy imbalance at top of atmosphere, atmospheric CO_2 concentration, ocean acidification and aerosol loading) are greatly beyond the zone of uncertainty, therefore being highly unsustainable and threatening these four Earth systems.

Off the initial hypothesis of which limits could be transgressed, the ozone depletion limit was the only one showing surprising results: unexpectedly, the limit is respected, with the sector lying at 95.2 points below the limit with an occupation of the final assigned SoSOS of only 4.8%. Out of all ODS that contribute to the damaging of the ozone layer (including dinitrogen monoxide, HCFC-140, CFC-113, CFC-114, Halon 1001, Halon 1211, Halon 1301, HCFC-22, CFC-12, R-40, R-10, and CFC-11), dinitrogen monoxide is the main substance emitted by nearly all of the considered activities (Figures S5-7 and S5-8), accounting for 99% of overall ODS emissions (Figure S5-17) once total volumes are considered. Despite these substances being employed as solvents in the chemical industry (e.g., tetrachloromethane, R-10) (Environmental Protection Agency, 2021) their use has been controlled by recent regulations and become very limited. According to the *European Council Regulation (EC) No. 1005/2009* (2009), the production, use, trade, recovery, recycling, and destruction of all assessed ODS except for dinitrogen monoxide is controlled by law. The results are thus understandable, since most of the impact on the PB comes from unregulated compound, while the rest are currently phased out. The coming into effect of regulations protecting the ozone layer has been referred to as one of the most successful acts for environmental protection (United Nations, 2016; Word Meteorological Organization, 2018), even if the long lifetimes of CFCs and other ODS still restrain its recovery. As for current emissions (2018 as the focus of this study), the chemical industry is operating well below the PB.

The sector remains below the threshold for all other boundaries (i.e., nitrogen and phosphorus biogeochemical cycles, land system change and freshwater use) as expected except for the case of the nitrogen cycle. Both the nitrogen and the phosphorus cycles are primarily altered by the use of these nutrients in fertilizers in the agriculture industry (see the Biogeochemical flows section). However, for the chemical industry, the standard deviation of the LCIs causes the contribution to enter the zone of uncertainty of the nitrogen PB (Fig. 10-5), hinting at the possibility that the limit is being put under excessive pressure. The source of the nitrate emissions to water is discussed in the Impact breakdown section. All impacts associated with the waste management activities that are required to treat the produced wastes are included in the LCA. Thus, part of these nutrient fluxes to water are most likely attributed to the industry because of the treatments that some of the generated wastes require rather than because the processes cause direct emissions. Nevertheless, industrial activity is also directly responsible for nitrate point source pollution due to wastewater effluents poured to surface waters (Zhang et al., 2015) when no or insufficient treatment is applied. The chemical industry has an average contribution to the nitrogen cycle boundary which takes up 64.5% of the total SoSOS; however, 1% of the generated scenarios surpasses the SoSOS (i.e., there is a 1% probability that this PB is transgressed).

The maximum value of the occSoSOSPB attained among all the scenarios is 1.06 (6.54% over the limit), which falls within the PB's zone of uncertainty (a maximum nitrogen runoff of 63-82 Tg N*yr^{-1}, or 0.026-0.034 Tg N*yr^{-1} for the SoSOS of the FSoSOS principle). Even if the changes and feedbacks of nitrogen biogeochemical cycle when pressures are found in the uncertainty zone are unclear, the boundary is globally transgressed (Rockström et al., 2009; Steffen et al., 2015). Despite the chemical industry apparently not being a large contributor to this transgression, the results act as a warning sign indicating that it is especially necessary to carefully control nitrate concentrations in plant effluents in order to reduce the sector's impact on the nitrogen cycle.

Contrarily, the impact on the phosphorus cycle remains under the limit and takes up only 10.1% of the allocated SoSOS after the last downscale is performed (Fig. 10-5). Phosphorus runoff to surface water deriving from chemical plants can

originate from the use of this element as a raw material or in auxiliary compounds in manufacturing processes (Toama, 2017), but as with nitrogen fluxes, it can also be attributed to the treatment of chemical plant wastes. Regardless, the results show how phosphorus leaks in the chemical industry, although not negligible, are not a threat for the environment.

It is relevant to highlight how processes manufacturing chemicals deriving from propylene account for mostly all phosphorus emissions and a great fraction of nitrate emissions (see the Impact breakdown section for further discussion).

Finally, neither the land-system change, nor the freshwater use limits are transgressed. The chemical industry occupies only 0.13540% of the allocated SoSOS for the first one, which is the Earth system receiving the smallest pressure out of the nine boundaries included in the study.

The land system is mostly threatened by the need to feed a growing global population causing large-scale deforestation and land change from forest to pasture or crops (Lambin et al., 2001). Agriculture is therefore the primary cause of land use (Food and Agriculture Organization, 2016), which has no link with the chemical industry. Another important cause of land change, however, is biomass consumption. Despite helping reduce the use of fossil fuels, it also leads to land use (Verburg et al., 2015) and could be indirectly caused by the most energy-intensive industries within the chemical sector if biomass becomes more important in the future energy mix. The land use derived from the obtention of fossil fuels (e.g., natural gas) and other energy sources is also part of the total contribution to this PB. Other deforestation causes originating from the sector's activity include the conversion of forest land during the construction of chemical plants and related infrastructure, as well as the roads that enable access to them, and land use for the production or mining of specific raw materials used by the sector. It is important to note that the studied plants were not geo-localized, but ideally, these impacts should be assessed based on measurements for each new plant being constructed.

Since vegetation plays a vital role as a natural carbon sink, reforestation, and afforestation (i.e., the transformation to forest of a previously open area) projects were endorsed by environmental institutions as the planted trees aid climate

change mitigation by capturing atmospheric carbon through bio sequestering (UNFCCC, 2013). The Kyoto Protocol introduced the Clean Development Mechanism (CDM) as a flexibility measure through which private or public entities in developed countries could compensate their GHG emissions by financing tree plantation in developing countries (Kätelhön et al., 2019; Thomas Ledig & Kitzmiller, 1992; Thomas et al., 2010; UNFCCC, 2013). The CDM was expected to be operative until 2020, when the Paris Agreement substituted the Kyoto Protocol (thus, during the year of the study, 2018, the CDM was in effect). Beyond 2020, it is unsure whether countries will still be able to resort to the CDM to stay below their emission limits, since the concept of carbon trading may undermine the goals of the Paris deal. The coronavirus pandemic has added uncertainty to the future of the CDM since the 26th conference of parties (COP26), where the CDM was to be discussed has been postponed (Farand, 2020). Until then, temporary measures extending the CDM's operability into 2020 have been accorded (UNFCC, 2020). Many companies rely on flexibility mechanisms like the CDM to comply with GHG emission requirements. Additionally, enterprises use reforestation programmes as environmental marketing techniques to increase the public acceptance of their activities.

Reforestation projects for industrial activities are reflected in LCI entries labelled "land transformation to forest", and total 21.27 km^2 of land in 2018. Fig. 10-1 shows the comparison between deforested and reforested area calculated per activity and separated by type of transformation. Ammonia production accounts for the highest land change and based on the study's calculations reforests around 40% of the transformed land. Overall, the impact on the land system change boundary is reduced through reforestation. Reforested or afforested areas are counted as negative contributions (i.e., environmental credits) to the land-system change PB. Figures S5-9, S5-10 and S5-18 show how the deforestation caused by the chemical industry is mainly intensive rather than extensive. Reforestation projects are also based predominantly on intensive transformation (Figures S5-11 and S5-12), that being emphasized once total reforested areas are calculated using total volumes (Figure S5-18).

As for freshwater use, the occupied fraction of SOS is that of 7.96% of the total. Results indicate that the use of freshwater derived from chemical plants does not

pose a threat to the water cycle. Pressures on the Earth cycle stem from the overconsumption of this resource, the lack of efficient management and performance of water treatment facilities and infrastructures, together with the global alteration of the climate (Arora et al., 2015; Damania et al., 2017; Doell et al., 2009). In the chemical industry, water is used as a thermal fluid, as a solvent, in absorption and extraction processes, for cleaning or rinsing, and for vacuum creation, among many other uses. Chemical processes involving additional water use (i.e., when water or steam are required for the reaction), such those that produce styrene or ammonia, account for larger impacts on the PB, as discussed in the Impact breakdown section. As seen in figures S5-13 and S5-14, rivers are the principal water source for the chemical industry, even though groundwater is also collected by cumene, styrene, and vinyl chloride production plants. Water from lakes is more rarely used, most likely because of its lower availability and capacity. Once the volumes of the manufactured chemicals are considered, Fig S5-18 evidences that rivers provide 71% of the total water withdrawn by the sector, while another 28% is groundwater.

As in the land-system change boundary, industries can, in some cases, return the borrowed resource back to the environment if adequate treatment of water effluents is carried out. Fig. 10-2 shows the difference between withdrawn and returned water in m^3 for every chemical. As with reforestation, the treatment and return of water has been quantified as a negative contribution to the PB. Figures S5-15 and S5-16 show how, logically, processes' treated effluents are directed to surface water bodies (a category encompassing rivers and lakes) rather than to underground reservoirs. Total numbers indicate that 89% of water is returned to rivers and lakes and 11% to ground (Fig S5-18).

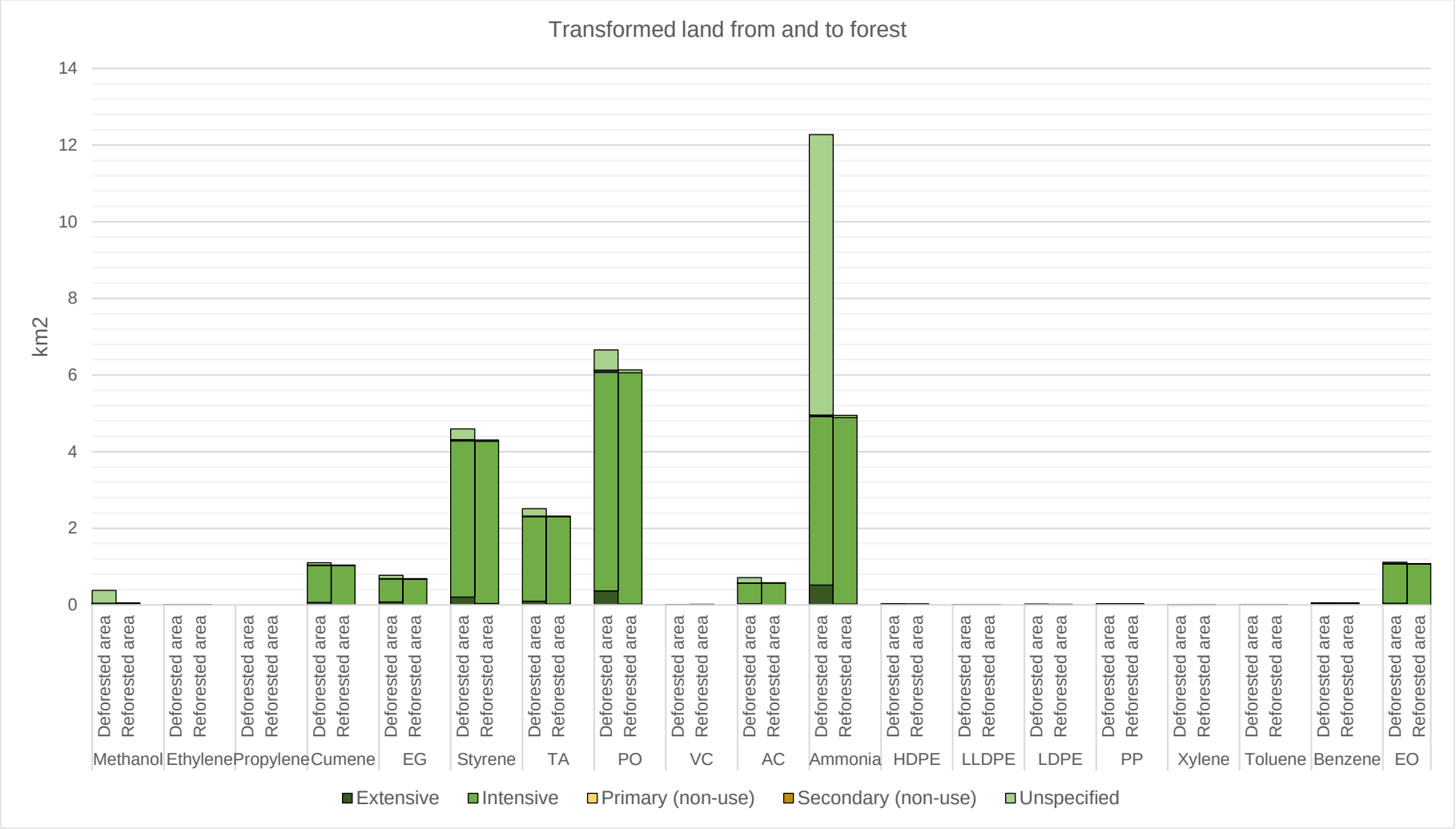

Fig. 10-1: Fractions of deforested and reforested land as a consequence of the chemical industry's activity, where EG: ethylene glycol; TA: terephthalic acid; PO: propylene oxide; VC: vinyl chloride; AC: acrylonitrile; EO: ethylene glycol.

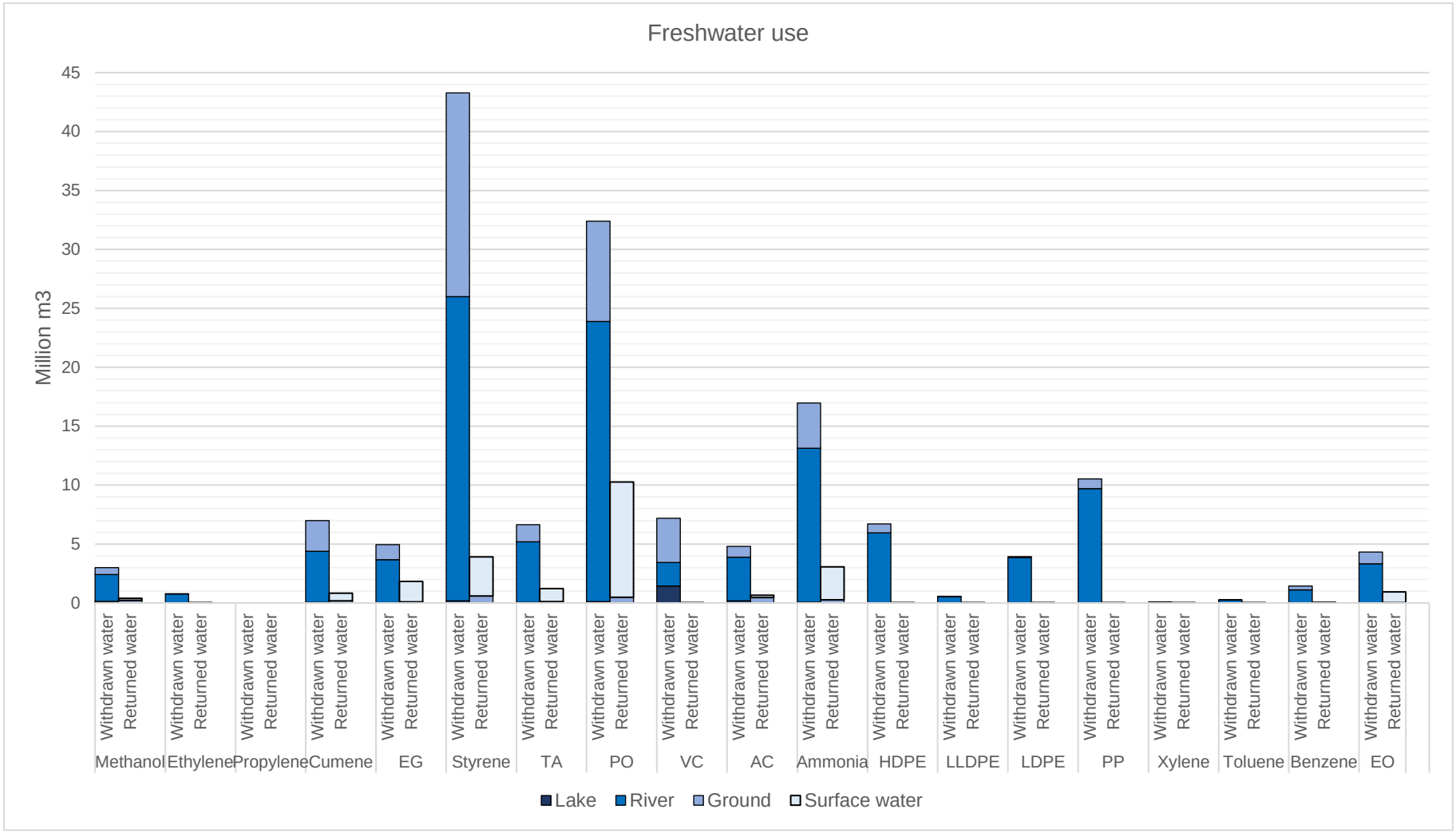

Fig. 10-2: Freshwater withdrawal and return as a consequence of the chemical industry's activity, where EG: ethylene glycol; TA: terephthalic acid; PO: propylene oxide; VC: vinyl chloride; AC: acrylonitrile; EO: ethylene glycol.

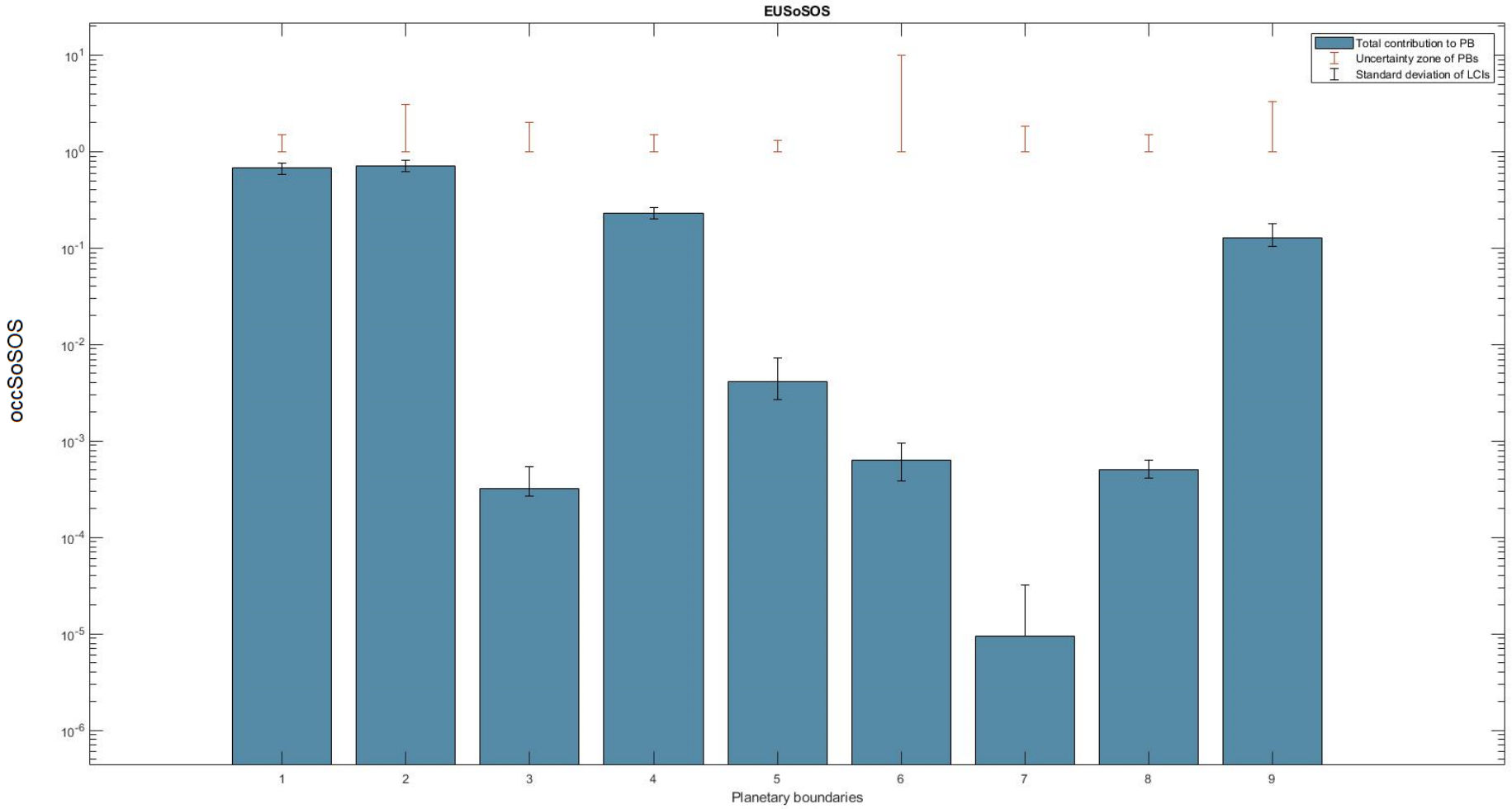

Fig. 10-3: Contributions of chemicals to the nine PBs (EUSoSOS) where 1: Climate change (energy imbalance at top of atmosphere, Wm^{-2}); 2: Climate change (atmospheric CO_2 concentration, ppm); 3: Stratospheric ozone depletion (DU); 4: Ocean acidification (Ω_{arag}); 5: Biogeochemical flows (Nitrogen, Tg N yr^{-1}); 6: Biogeochemical flows (Phosphorus, Tg P yr^{-1}); 7: Land system change (%); 8:Freshwater use (km^3yr^{-1}); 9: Aerosol loading (AOD).

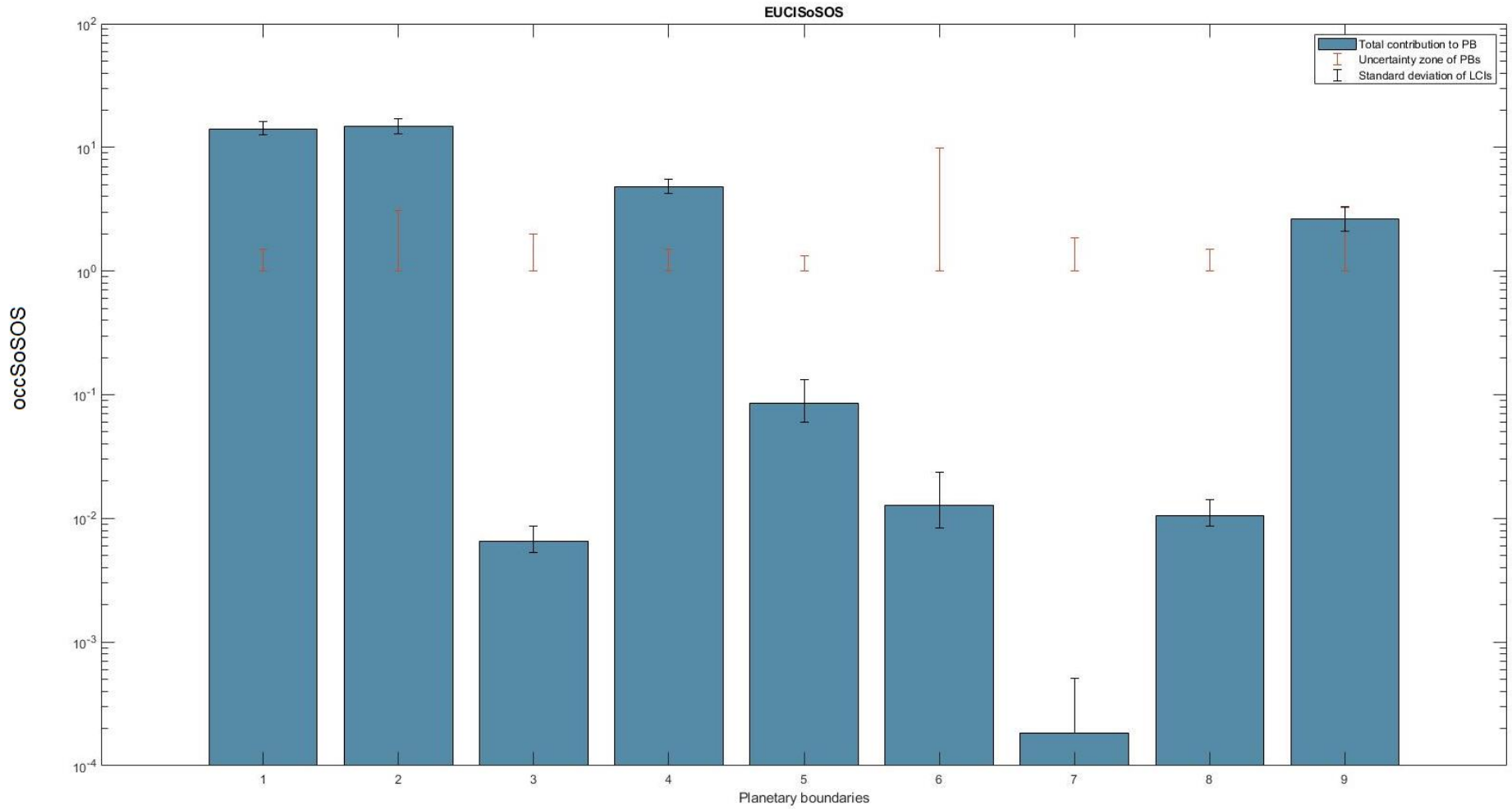

Fig. 10-4: Contributions of chemicals to the nine PBs (EUCISoSOS) where 1: Climate change (energy imbalance at top of atmosphere, Wm^{-2}); 2: Climate change (atmospheric CO_2 concentration, ppm); 3: Stratospheric ozone depletion (DU); 4: Ocean acidification (Ω_{arag}); 5: Biogeochemical flows (Nitrogen, Tg N yr^{-1}); 6: Biogeochemical flows (Phosphorus, Tg P yr^{-1}); 7: Land system change (%); 8:Freshwater use (km^3yr^{-1}); 9: Aerosol loading (AOD).

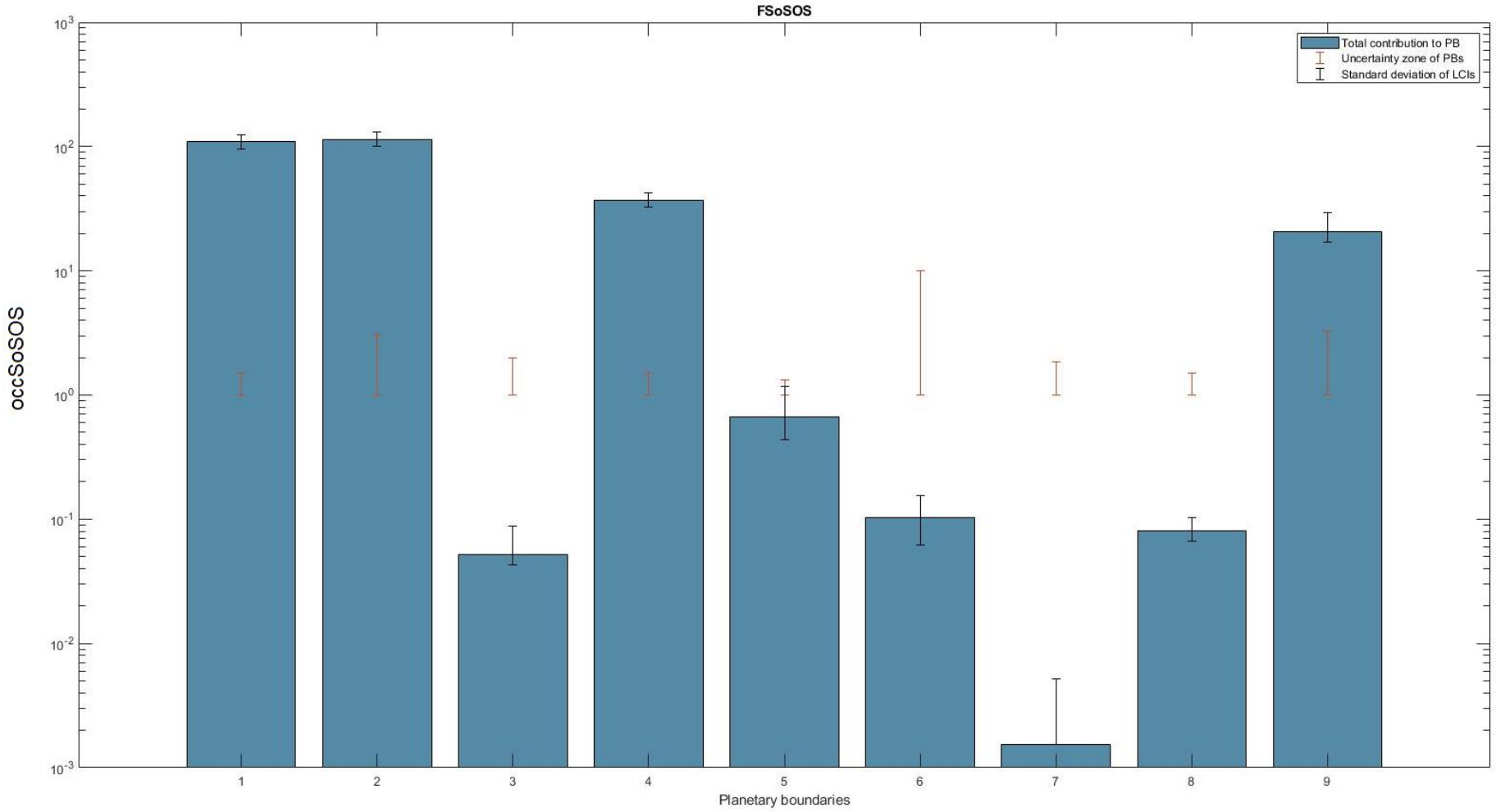

Fig. 10-5: Contributions of chemicals to the nine PBs (FSoSOS) where 1: Climate change (energy imbalance at top of atmosphere, Wm^{-2}); 2: Climate change (atmospheric CO_2 concentration, ppm); 3: Stratospheric ozone depletion (DU); 4: Ocean acidification (Ω_{arag}); 5: Biogeochemical flows (Nitrogen, Tg N yr^{-1}); 6: Biogeochemical flows (Phosphorus, Tg P yr^{-1}); 7: Land system change (%); 8:Freshwater use (km^3yr^{-1}); 9: Aerosol loading (AOD).

10.1.2 Non-egalitarian allocation

The SQ (or grandfathering) principle assigns the SOS according to the current level of impact of the assessed system (*Eq. 65* and *Eq. 66*). Thus, when a non-egalitarian approach is taken for the allocation of the SOS, activities using traditional or outdated technologies with high environmental impact are inevitably assigned a larger SoSOS, and thus being benefited in contrast with more modern or sustainable processes. The application of this principle requires no additional information and is simpler than the use of egalitarian methods, however, it fails to challenge the system towards environmental action or to reflect its characteristics (i.e., how many people it affects or whether it has a high or low economic importance). Additionally, it has been long known that the BAU performance of anthropogenic activities is unsustainable (Solomon et al., 2007). Regardless, the SQ principle is sometimes used by stakeholders and decision-makers due to its directness and pragmatism (Hjalsted et al., 2021) and to allow comparison in PB-LCIA studies (Ehrenstein et al., 2020; Lucas et al., 2020; Ryberg et al., 2018b).

The two factors with influence the SoSOS assigned by the SQ method are (i) the available SOS, and (ii) the current contribution of the assessed system to the boundary. The closeness of the values of both factors determines the assigned SoSOS (*Eq. 65*). Table 10-1 compares the values for both factors.

Thus, this allocation is highly sensitive to the *current global state of the PBs*. Fig. 10-6 (in page 154) shows how when using the SQ principle, only two PBs are completely respected, those being ocean acidification and freshwater use. As seen in Table 8-2 and Fig. 10-6, the two globally non-transgressed boundaries are the same two that remain within the limit when using the SQ approach. Meanwhile, the PBs for which the sector's contribution exceeds the upper limit of the uncertainty zone correspond to those which have a higher percentage of global occupation of the SOS.

It is thus important to note that boundaries receiving higher pressures according to the egalitarian method which are also under high stress globally see their contribution reduced when the SQ principle is used, since the latter principle assigns a larger SoSOS to these PBs. For example, this is the case of the climate

change PBs (Table 10-1), which are the two receiving the largest pressure from the system. Conversely, smaller contributions according to the egalitarian principle might be amplified in the SQ approach if the global contribution to the PBs is large, due to being assigned a smaller SoSOS. A clear example would be the land-system change PB (Table 10-1). $aSPB_{,SP}$ values in Table 8-3 also show this relationship.

Table 10-1: Large differences between both values cause a small SoSOS to be assigned to the PB.

PB	System contribution to the PB	Available SOS
Climate change (energy imbalance at top of atmosphere)	0.0071	2.3000
Climate change (atm. CO_2 concentration)	3.3457	120.5000
Stratospheric ozone depletion	0.0003	90.0000
Ocean acidification	0.0102	0.5504
Biogeochemical flows (N)	0.0165	150.0000
Biogeochemical flows (P)	0.0004	20.9000
Land-system change	0.0000	38.0000
Freshwater use	0.1315	2600.0000
Aerosol loading	0.0009	0.1600

Results suggest that, if the persistence of current technologies and distribution of emissions is desired, the SQ methodology helps to direct actions towards this direction and may thus reward inaction (European Commission, 2006a).

However, even with high impacts on critically endangered PBs being palliated in all cases (climate change and aerosol loading PBs) except for the ocean acidification PB, the method indicates that BAU practice leads to the transgression of seven boundaries, including those for both climate change limits, stratospheric ozone depletion, both biogeochemical flows, land-system change and aerosol loading. The freshwater use boundary is respected by both allocation principles.

The uncertainties linked to the LCIs appear larger than in the figures for the egalitarian allocation since the variations in scale of the impacts are smaller, however, they do not affect the conclusions drawn for any PBs (i.e., they do not

change any decision when classifying impacts between the un-transgressed, uncertainty zone, and transgressed states of any PB) except for the land-system change PB. In this case, the contribution exceeds the higher bound of the uncertainty range of the PB in 41% of the modelled scenarios.

The stratospheric ozone depletion is the boundary suffering the most change, from being totally under control according to the egalitarian principle to being over the zone of uncertainty through the lens of SQ. Table 8-2 reveals that the cause of this change is the level of perturbation suffered by the PB (compared to the contribution of the system, see Table 10-1), since the highest possible perturbance the limit seasonally suffers is taken as the value used for the calculations. As discussed before (Stratospheric ozone depletion; Egalitarian allocation), the emissions of ODS have been recently regulated, thus current emissions are low (hence the boundary not being transgressed when the egalitarian principle is applied), but the long-lasting effects of past emissions cause the ozone layer to still be recovering, therefore the available SOS is still seasonally exceeded by a factor of six (Table S5-1). The same happens with the nutrient cycles and land-system change: the originally not transgressed boundaries see their limits exceeded since they suffer from two downsides of the SQ principle: a low system contribution to current global impacts and high occupation of the available SOS at the global level.

Conversely, the ocean acidification boundary shifts from being transgressed to staying below the limit. This happens because the assigned SoSOS yielded by the relationship of the globally available SOS and the contribution of the industry to the PB is larger than that of the egalitarian principle.

The remaining limits (i.e., both for climate change, and aerosol loading) cannot stay at a sustainable level despite seeing their SoSOS widened by the SQ allocation, although the PBs are transgressed by lower factors than those yielded by the egalitarian method.

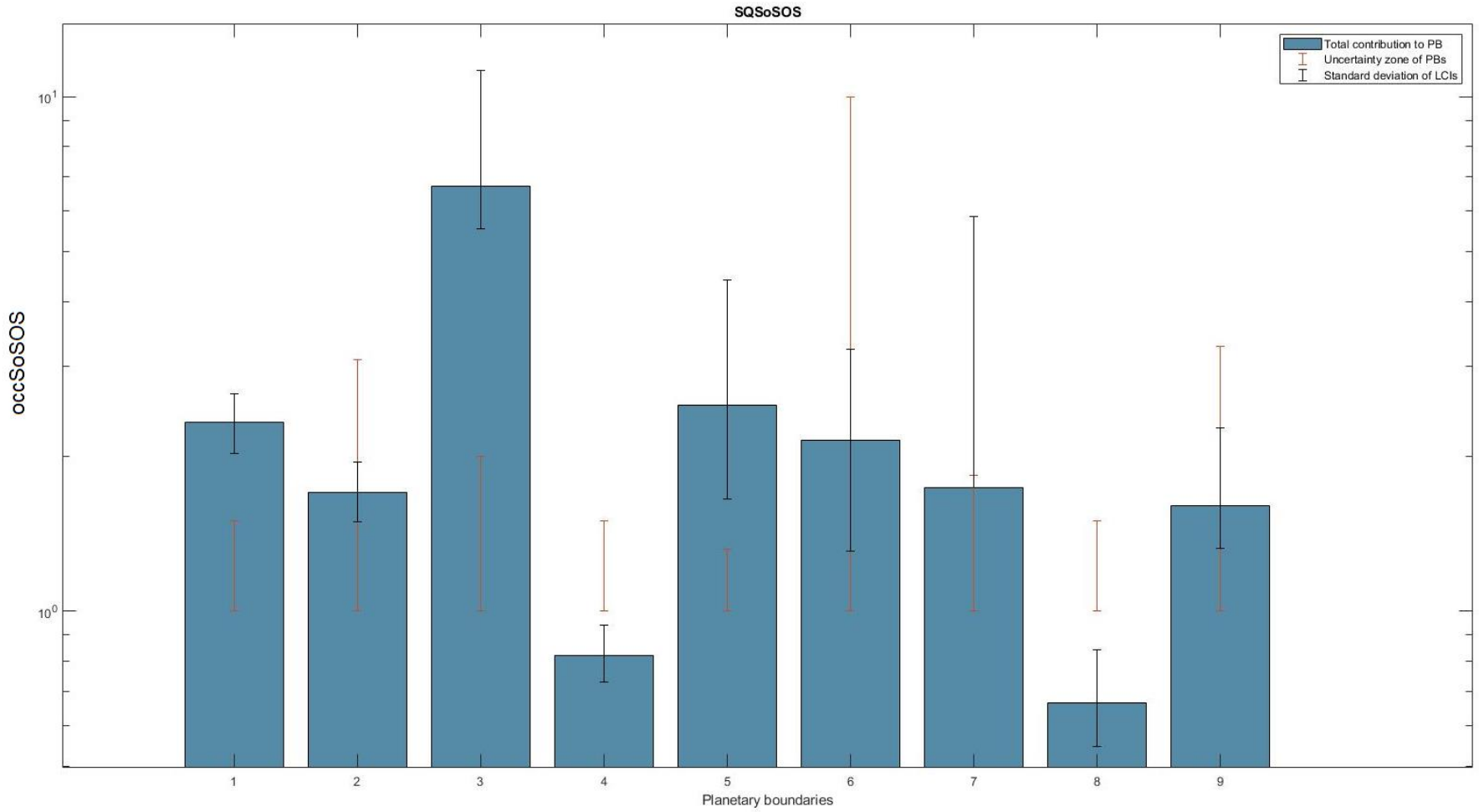

Fig. 10-6: Contributions of chemicals to the nine PBs (SQSoSOS) where 1: Climate change (energy imbalance at top of atmosphere, Wm-2); 2: Climate change (atmospheric CO2 concentration, ppm); 3: Stratospheric ozone depletion (DU); 4: Ocean acidification (Ωarag); 5: Biogeochemical flows (Nitrogen, Tg N yr-1); 6: Biogeochemical flows (Phosphorus, Tg P yr-1); 7: Land system change (%); 8:Freshwater use (km3yr-1); 9: Aerosol loading (AOD).

10.1.3 Criteria for the downscaling of the planetary boundaries

The uncertainty linked to the selection of the allocation principle has been found to be larger than that of the LCIs and the PBs, in accordance with previous studies (Ryberg et al., 2018). Thus, the need for a homogenized procedure or standard that regulates the methodology for the downscaling of the PBs is key for the future application of the PB-LCIA methodology.

In this study, an egalitarian perspective has been taken as the principal approach for he distribution of the SOS, since it is the most common practice in current studies working with the PB-LCIA framework (Algunaibet et al., 2019; Dao et al., 2018; Fang et al., 2015; Fanning & O'Neill, 2016; O'Neill et al., 2018; Ryberg et al., 2018; van den Berg et al., 2020) and it is capable of adapting to any system assessed. These egalitarian perspectives are based off economic or populational factors, as well as hybrids combining both as in the present study. The egalitarian method, has been, however, complemented with a non-egalitarian SQ (or grandfathering) principle in order to highlight the sensitivity of the results to the chosen principle, as previously done by various authors (Ehrenstein et al., 2020; Lucas et al., 2020; Ryberg et al., 2018b).

The per capita approach has been found to be the most favourable in terms of number of transgressed boundaries; nevertheless, the total impacts to the boundaries which are widely transgressed when using the egalitarian method surpass the limit by lower factors when the SQ principle is applied.

The decision on which allocation principle to use is ultimately linked with the concept of distributive fairness. Environmental research and polices have been requiring and applying allocation approaches in various situations, such as the distribution of emission rights and budgets, as well as reduction targets. The distribution criteria are based on different concepts, including: (i) equality between people, (ii) national and sectorial responsibility, (iii) capacity to act and contribute to global improvement (iv) cost effectiveness, and (v) sovereignty (Lucas et al., 2020). On the one hand, the SQ principle in this study is based on the sovereignty equity principle since it bases the distribution of SOS on current resource use. On the other hand, the applied egalitarian approach focuses on

equality, capability, and sectorial responsibility, by limiting a system's impact based on the people it affects (population) and its ability to pay (GVA).

Another factor that must be considered is that, as discussed in the Planetary boundaries section, the PBs can be classified as those with faster or slower control variables and feedbacks. Fast control variable thresholds (i.e., climate change, ocean acidification, and stratospheric ozone depletion) have global thresholds and therefore their allocation is more direct. However, slow control variable thresholds (i.e., biogeochemical flows, freshwater use, land-system change and aerosol loading boundaries) usually start giving feedbacks at a regional scale and then these cause global consequences. The allocation of the global SOS is thus, less intuitive, yet useful, especially when international trade is considered through exports and will fain further importance when scientific knowledge about the relationships between Earth systems improves. Downscaling is especially important for these boundaries as environmental impacts and resource distribution are different for each geographic area but the responsibility to preserve the Earth's resources is shared (Häyhä et al., 2016; Lucas et al., 2020).

It is acknowledged that despite egalitarian "per capita" allocations being widely used and yielding the most study-adapted results, they have various weaknesses, primarily: (i) they neglect regional conditions such as resource availability or necessity, (ii) they do not consider historical responsibility for past impacts caused by the system or future scenarios (Dao et al., 2018; Häyhä et al., 2016).

However, an accepted method for optimizing the allocation has not been developed yet. Additionally, such drawbacks are specifically relevant when assessing, for example, a country's general environmental performance (i.e., consumption and resource use carried out by the country's inhabitants). In this case, the SoSOS should reflect resource needs. An example would be that in countries where temperatures are higher, the population will make more use of air conditioners and thus their electricity consumption may be larger, or how contrarily, in countries where temperatures are generally lower, higher heating requirements for households should be considered. Regardless, the present study is centred at the activity of the European chemical industry, thus, the

allocation of the impacts according to their economic value is the most straight-forward approach.

The temporal dimension, currently overlooked in present allocation methods, is not to be taken lightly. From an egalitarian perspective, the per-capita share of each PB will decrease as global population increases. This is in addition to the need to allocate impacts from larger production volumes unless per-capita consumption of chemicals is reduced. Indeed, the demand for chemical products will probably increase with population unless a paradigm shift is experience in per-consumption rates. Meanwhile the allocation factor, calculated as a share of global population, will remain similar for many regions but could increase or reduce furthers owing to different factors (e.g., despair birth rates, migration, appropriate nourishment).

To assess how the sustainability of the industry might be affected by these factors in the future, three potential scenarios have been studied. In all of them, current consumption patterns are maintained (i.e., the consumption of chemicals per capita does not vary). The difference between the three scenarios stems from the global and regional populations, which are set at values predicted for years 2030, 2050 and 2100 in the World Population Prospects (United Nations, 2019). Since Europe's population predictions were given for EU-27, values for the UK have been added to obtain the population of the complete studied region (EU-28). Therefore, the change in the assigned SOS considers only changes in population shares, while the proportion of GVA corresponding to the chemical industry is maintained equal to 2018's as prospects for this variable were not available.

Fig. 10-7 compares current results (panel a) with those obtained for these three future scenarios (panels b-d), using the egalitarian allocation method in all the cases. Population predictions indicate that, opposite to the rest of the world, Europe will suffer a decrease in population. If nothing else changes, this would reduce the internal consumption of chemical products, but this effect would be offset by a larger reduction in the SoSOS for Europe. As a result, pressures on most of the PBs would increase. In other words, the slight drop in consumption stemming from a decreasing population will not be enough to counteract the effect of the reduction that the SoSOS assigned to the region will suffer.

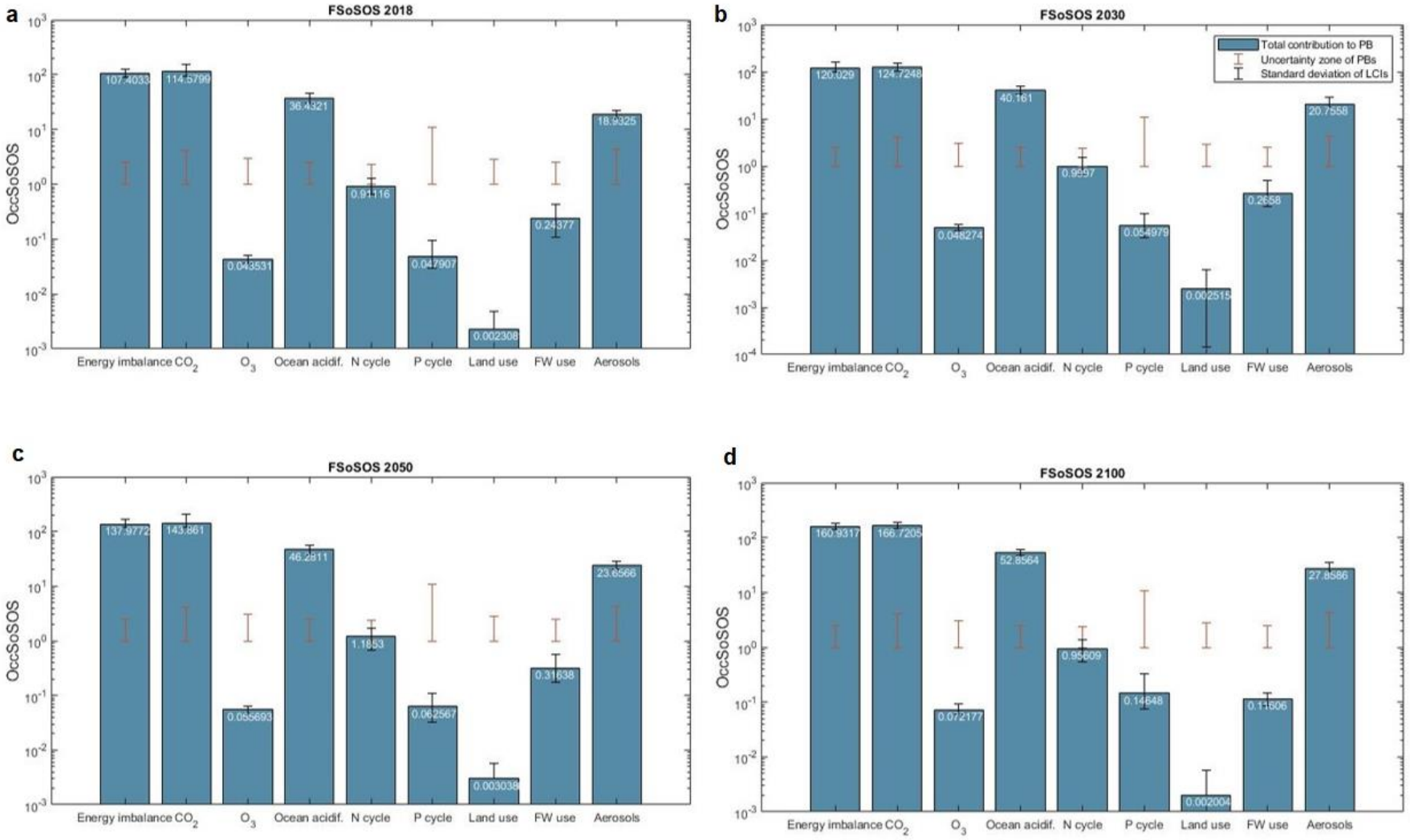

Fig. 10-7: Predictions on the state of the PBs assuming the current consumption patterns are maintained for the years 2030, 2050 and 2100.

It cannot be neglected that per-capita consumption or exports may also increase, adding yet more pressure on the PBs. As seen in Fig. 10-7, the occSoSOS will increase gradually for all boundaries, indicating that as time goes by, improvement measures will become even more urgent and will need to be more effective in order to achieve the same results. According to the undertaken calculations (i.e., if consumption is indeed maintained or has not increased significantly), the impacts on the N-cycle, land-use change, and freshwater use boundaries may slightly decrease between 2050 and 2100, since the predicted reduction of Europe's population is greater than that estimated between 2030 and 2050.

After the adopted considerations and out of the two applied downscaling methods (SQ or egalitarian allocation), the egalitarian approach can be classified as the most adequate allocation principle for the SOS in the present study, yielding the highest adaptation to the assessed activities and results which are independent from the contributions of other systems to the boundaries. Regardless, the differences in the results obtained through both principles highlight the importance of the study's transparency in terms of how the allocation of the SOS has been carried out. Besides, the dependence of the allocation factor on annual data regarding population and GVA highlights the importance of periodically updating the calculations obtained through the PB-LCIA methodology.

As suggested by *Ryberg et al.* (2018b), if the most conservative approach is taken, it could be considered that the chemical industry's performance is only sustainable in terms of freshwater use, since it is the only PB which is respected regardless of what allocation principle is applied.

Table 10-2 provides a heat map showing the results of the different allocation methods to facilitate comparison and summarize the results obtained. The PBs lying within the safe zone are shaded in different tones of green depending on the distance from the limit, while those found within the uncertainty range appear in yellow and those meeting the PBs are shown in red according to the severity of the transgression. The values refer to the occupied fraction of SoSOS for each principle.

As discussed, the choice of the allocation principle vastly affects the results. Note how the status quo principle yields much similar results for all PBs than the egalitarian by attenuating the values of some PBs and increasing the impacts on others according to the relationship between the contribution of the system and the global pressure exerted on the PBs. Even if the limits are transgressed by lower values, less PBs are respected than in the egalitarian method (only 2 PBs versus 5 PBs under the final egalitarian allocation).

Table 10-2: Summary heat map of the results (occSoSOS) obtained using the different allocation procedures.

occSoSOS	EUSoSOS	EUCISoSOS	FSoSOS	SQSoSOS
Climate change (energy imbalance at top of atmosphere)	$66.29 \cdot 10^{-2}$	13.8346	107.755	2.30
Climate change (atmospheric CO_2 concentration)	$69.21 \cdot 10^{-2}$	14.4425	112.490	1.67
Stratospheric ozone depletion	$0.029 \cdot 10^{-2}$	0.0062	0.048	6.21
Ocean acidification	$22.13 \cdot 10^{-2}$	4.6185	35.973	0.80
Biogeochemical flows (Nitrogen)	$0.39 \cdot 10^{-2}$	0.0828	0.645	2.42
Biogeochemical flows (Phosphorus)	$0.062 \cdot 10^{-2}$	0.0129	0.101	2.11
Land-system change	$0.00083 \cdot 10^{-2}$	0.0002	1.354E-03	1.52
Freshwater use	$0.049 \cdot 10^{-2}$	0.0102	0.080	0.65
Aerosol loading	11.53·10-2	2.4068	18.746	1.45

Safe zone *Uncertainty zone* *Above PB*

The freshwater use is the only PB respected under both allocations, while the energy imbalance is met also in both cases.

However, the impacts on the CO_2 concentration and aerosol loading PBs, which fall in the high-risk zone under the egalitarian allocation, are damped until they fall in the uncertainty range due to the high impacts these boundaries are receiving both from the system and globally, which causes the values to be closer and the SoSOS to be larger when the SQ allocation is applied. An improvement

caused by the relationship between the globally available SOS and the contribution of the industry is also seen for the ocean acidification PB.

Contrarily, the stratospheric ozone depletion, nitrogen cycle, land-system change, and phosphorus cycle PBs see their impacts enlarged since the system's contribution is low but the boundaries are under high global pressure. The former two limits go from not being transgressed to falling within the risk zone, while the latter change to the uncertainty zone.

10.2 Impact breakdown

In this section, impacts are broken down to identify the processes and chemicals with highest responsibility on the damage caused to each Earth system, in line with the study's goals. A summary of the chemicals with the highest absolute and unitary (i.e., per kg) impacts on each boundary is provided in Table 10-3: Top contributors to all boundaries.

Fig. 10-8 complements the information in Fig. 10-3, Fig. 10-4, Fig. 10-5, and Fig. 10-6 by providing insight on the contribution of each chemical to the total impact on PBs by means of a percentage stacked bar plot. Since impacts depend on production volumes, chemicals are sorted from higher (ammonia from steam reforming) to lower (propylene) total volumes (including exports). The points where the colour code starts again are marked for better understanding both in the bars and in the legend. The values of the average net contributions among all LCI scenarios represented in the figures (expressed in each PB's control variable), as calculated through LCIs (Wernet et. al., 2016), CFs (Ryberg et. al., 2018b), and total volumes (European Union, 2020e) can be found in Table S5-2. Note that in the land-system change PB, some contributions are negative due to the reforestation projects discussed in the previous section.

As seen, the breakdown for the three CO_2-based boundaries (i.e., energy imbalance at top of atmosphere, atmospheric CO_2 concentration, and ocean acidification), shows a similar pattern, with impacts being highly proportional to total production volumes. These similarities are due to the fact that the controlled stressors affecting these three boundaries are GHG emissions (see figures S5-1 to S5-6), and as discussed in the Environmental performance of the European chemical industry section, 99% of these correspond to the same LCIs (i.e., fossil CO_2 emissions to three different compartments). Additionally, since all the studied processes emit GHGs, the final impacts are strongly correlated with each chemical's total volume (even if the magnitude of these emissions varies mostly depending on the energy demand of the specific activity and on whether it has direct emissions or not).

For other boundaries, such as those for the biogeochemical flows or land-system change, the distribution of impacts among the processes is not as intuitive since

the weight of contributions is more independent from the produced volumes, thus revealing that some activities are especially responsible for the alteration of these Earth mechanisms. These will be discussed in further detail in the ensuing section, while results will be summarised in section entitled Impact distribution.

Fig. 10-9 depicts the final impacts in a distribution that allows to show the percentage contribution of each chemical. For the sake of simplicity, percentage labels have been excluded for processes contributing less than 1%.

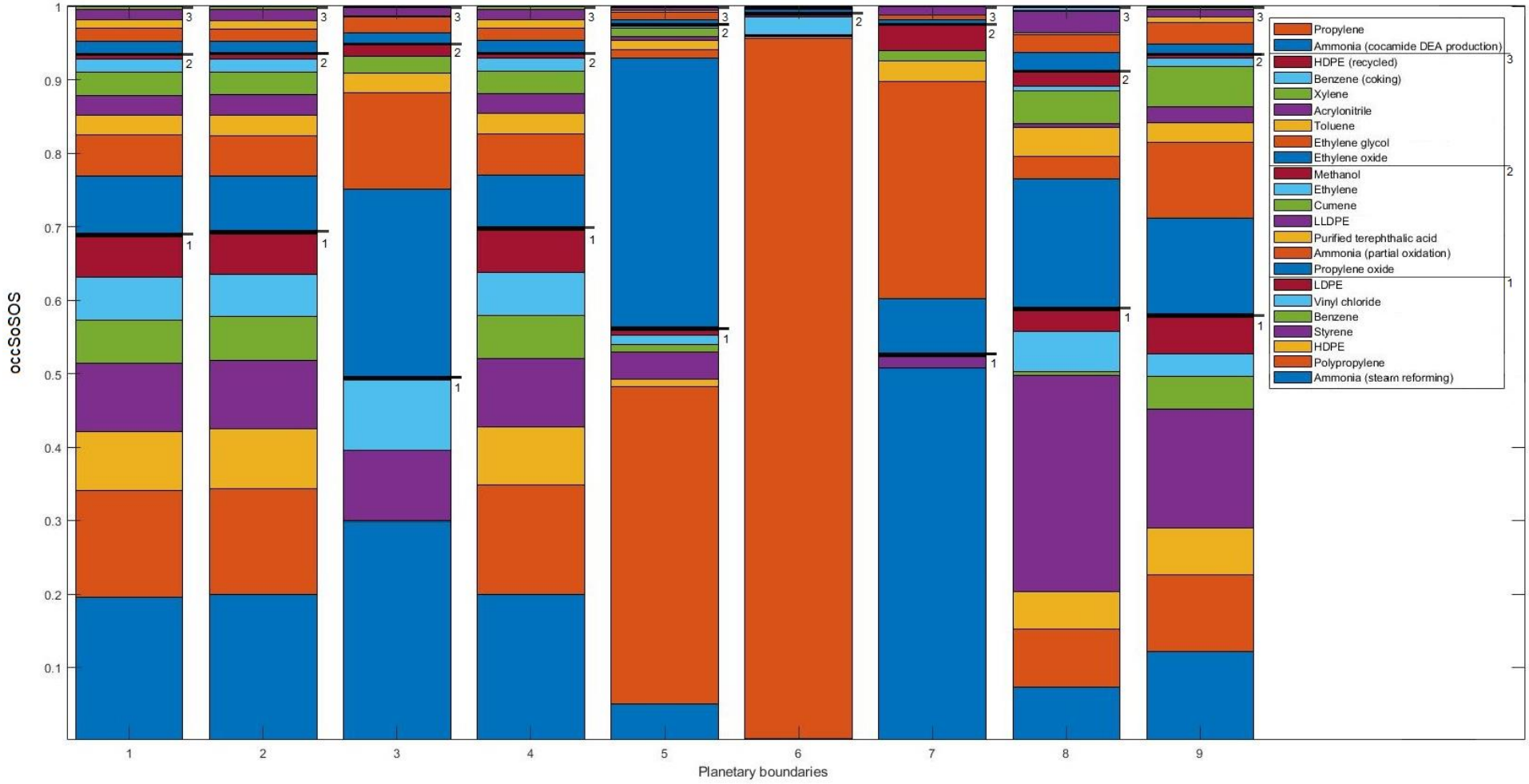

Fig. 10-8: Breakdown of the impacts to the nine studied PBs with chemicals sorted according to their production volume, where 1: Climate change (energy imbalance at top of atmosphere, Wm^{-2}); 2: Climate change (atmospheric CO_2 concentration, ppm); 3: Stratospheric ozone depletion (DU); 4: Ocean acidification (Ω_{arag}); 5: Biogeochemical flows (Nitrogen, Tg N yr^{-1}); 6: Biogeochemical flows (Phosphorus, Tg P yr^{-1}); 7: Land system change (%); 8:Freshwater use (km^3yr^{-1}); 9: Aerosol loading (AOD).

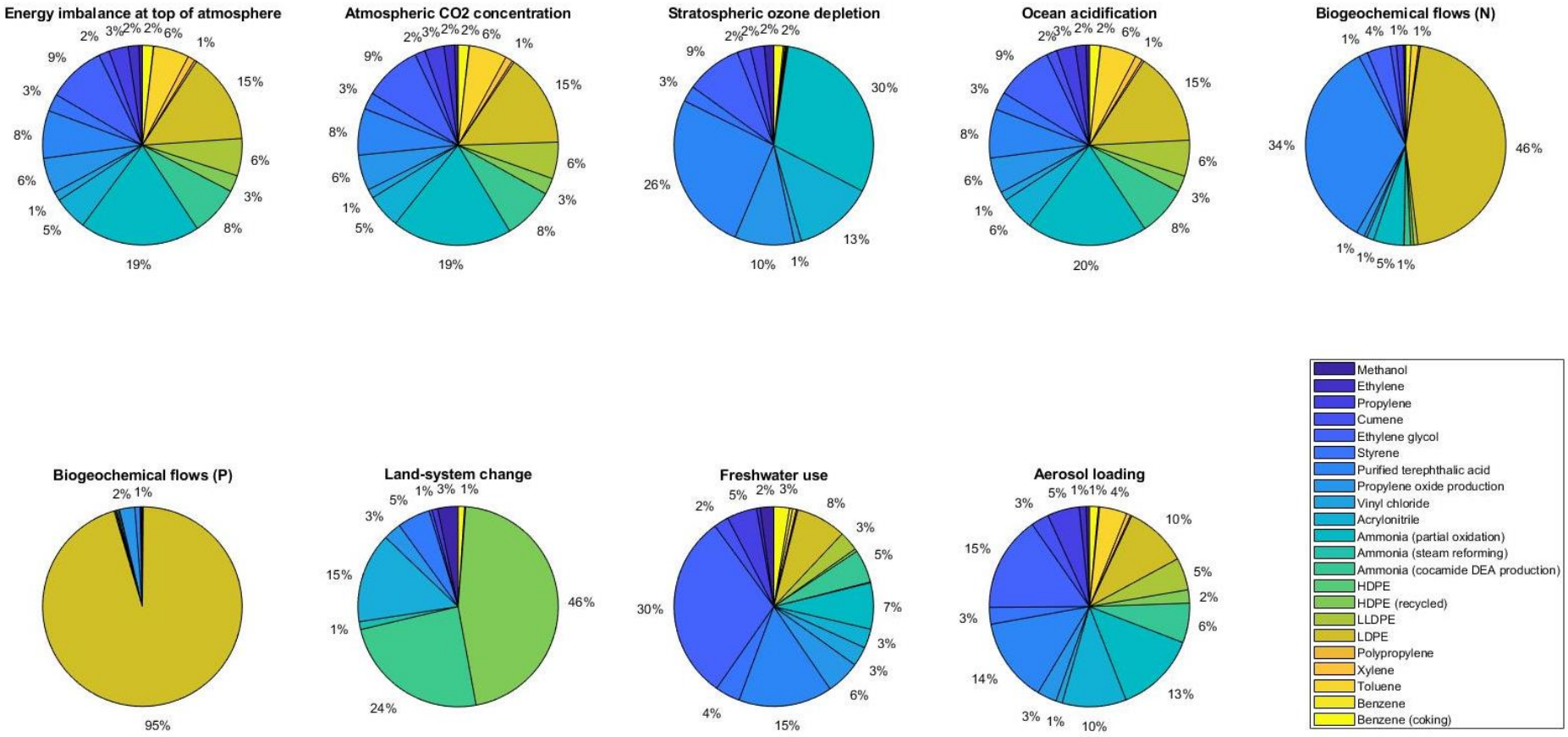

Fig. 10-9: Breakdown of the impacts on the nine studied PBs where the percentages over the total contribution to each threshold are shown for all activities with a burden representing ≤1% of the total.

10.2.1 Climate change and ocean acidification

As seen in Fig. 10-8 and Fig. 10-9, the climate change and ocean acidification boundaries are affected the most by those chemicals with higher production volume, since the distribution of emissions is more homogeneous between processes than for other PBs (as seen in Fig. 10-10).

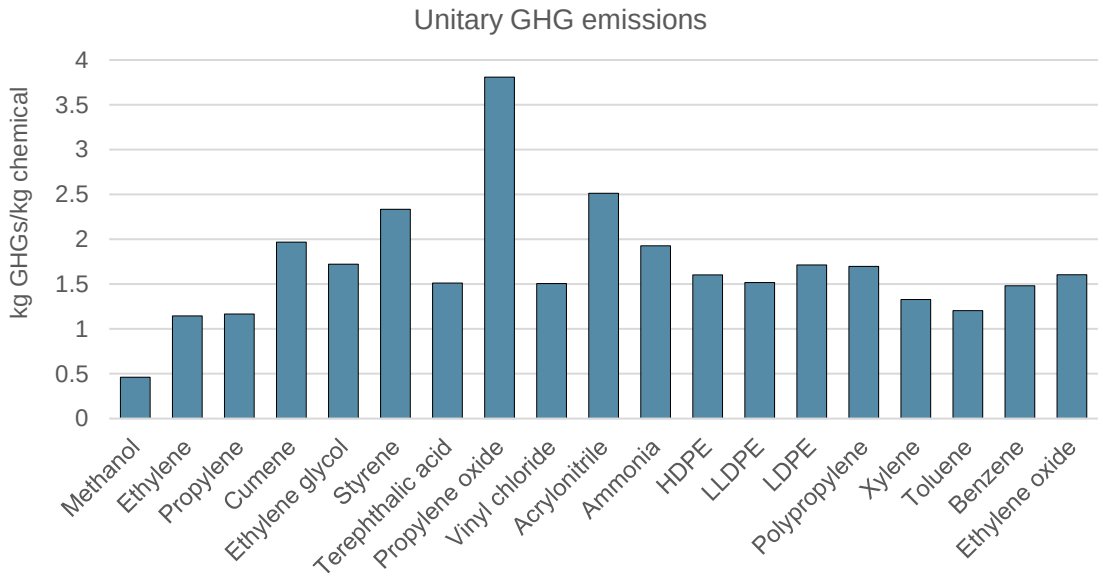

Fig. 10-10: Total GHG emissions (kg) per kg of chemical.

99% of GHG emissions affecting both the energy imbalance at top of atmosphere and the CO_2 concentration boundaries, as well as ocean acidification, stem from the same three LCI fluxes (see Environmental performance of the European chemical industry), Unitary emissions (i.e., kg of CO_2 emitted per kg of chemical produced) are also presented in order to analyse the marginal contribution of each chemical when total volumes do not influence the results (Fig. 10-11: CO2 emissions (kg) per kg of chemical).

Out of the total emissions, 35-99% are fossil CO_2 to urban air close to ground, the emissions of which show an incredibly uniform distribution within processes. On the one hand, results in Fig. 10-11 confirm that acrylonitrile and ammonia are the compounds with highest emissions of this type; this is in agreement with findings during the characterization of the chemical industry and selection of processes (Fig. 4-2). On the other hand, propylene oxide plants (operating with the chlorohydrin process) are revealed as the principal emitters of CO_2 to rural air and from high stacks, which is the second most relevant GHG emission type.

Fig. 4-2 already presented propylene oxide as one of the three principal chemicals in terms of tCO_2/t product, hence these initial estimations are confirmed by these new results. Note that CO_2 emissions from the chlorohydrin technology can be attributed either to the obtention of the reagents, the electricity and thermal energy, the production process itself or the waste treatment.

Regarding the latter, the chlorohydrin process is known for producing waste streams requiring extensive treatment (ICIS, 2009b; Nexant, 2009). Even if no explicit data is provided by *ecoinvent*, the internal treatment of wastewater is included and, thus, it is possible that some of the impacts associated with the process stem from it.

Then, the analysis of the electricity (Fig. S5-19) and heat demand of the process, propylene oxide shows average requirements compared to other chemicals. This leaves the reagents (propylene, Cl2 and NaOH) and the production process itself as main candidates for producing the impacts.

Propylene has a high energy consumption, accounting for 23% of propylene oxide's total fossil CO_2 emissions (Fig S5-20).

Environmental data for the obtention of Cl_2 and NaOH has been researched. Three technologies have been found to produce these two chemicals through the chlor-alkali electrolysis: one using diaphragm, another based on membrane and a last one using mercury cells. Impacts from these three methods have been weighted using market shares to supply 1.28 kg of chlorine and 1.38kg NaOH per kg of propylene oxide (Wernet et al, 2016). Results reveal that 52% of total fossil CO_2 emissions of propylene oxide (in the life cycle) originate from the chlor-alkali process (Fig. S5-20), namely mostly because of its energy consumption, which is larger than that for any of the studied chemicals. Among the three technologies, the membrane route is the one incurring lower environmental damage, while diaphragm technology is the one with the largest energy demand.

Thus, a significant part of propylene oxide's total emissions CO_2 emissions to the three aforementioned compartments can be attributed to its baseline reagents. The direct emissions from the production of propylene oxide represent 25% of the total value, including heat and electricity.

Opposite to former predictions, styrene also appears to have high CO_2 emissions per kg of product. The energy consumption of the process has been evaluated, revealing that the dehydrogenation of ethylbenzene is one of the most energy demanding processes (Fig. S5-19).

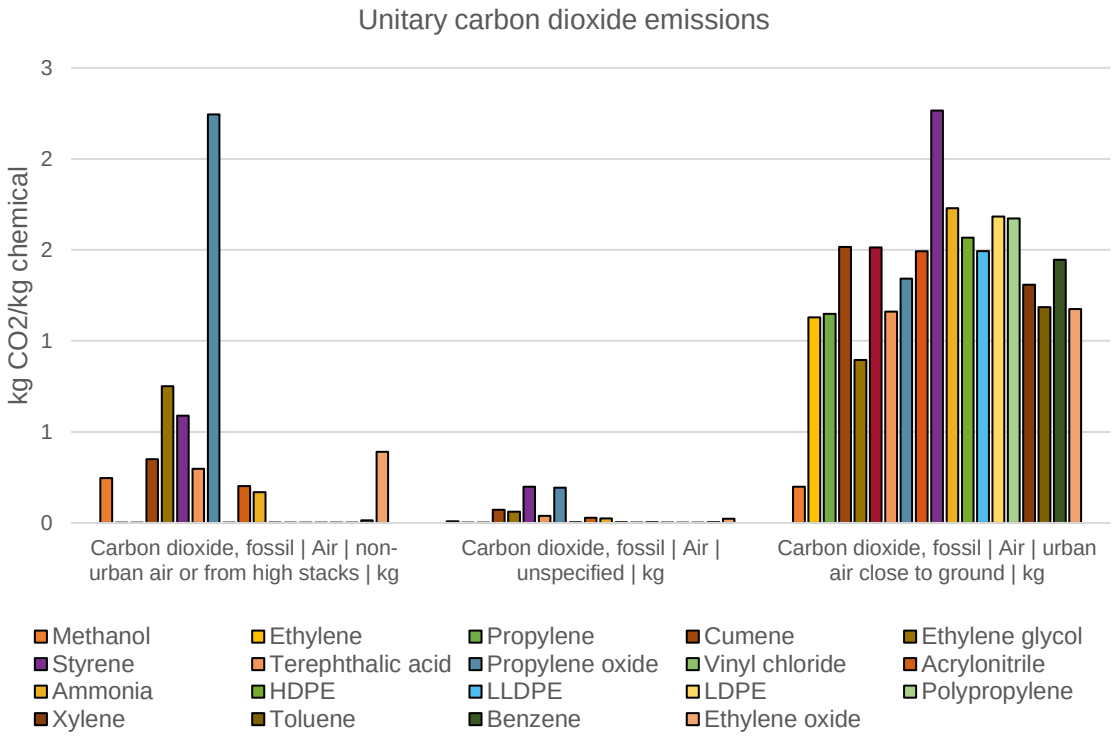

Fig. 10-11: CO_2 emissions (kg) per kg of chemical.

Once real demands for these chemicals are considered, the low production volume of acrylonitrile in comparison with other chemicals reduces its final impact on the energy imbalance and CO_2 concentrations boundary to only 1.5%. Inversely, ammonia production ends up accounting for nearly 25% of all emissions in the three boundaries (Fig. 10-9). 19% of those are attributed to the steam reforming process and 5% to the partial oxidation route, while less than 1% are due to the cocamide DEA manufacturing process. Despite the steam reforming process being attributed a higher fraction of total emissions (because of market shares), the CO_2 emitted per kg of ammonia produced through this process is lower than that of the partial oxidation route. This is in concordance with the descriptions of the processes, which indicated that the partial oxidation route is more energy intensive and therefore has higher CO_2 emissions (Partial oxidation and Steam reforming).

Despite the discovery of the industrial synthesis of ammonia being one of the most important breakthroughs in chemical engineering, the manufacturing of ammonia through the Steam reforming (and the Partial oxidation) process produces CO_2 as part of the reaction sequence in more than one stage. The gas is not included in the final product, which means that it is removed before the synthesis happens, generating high quantities of residual CO_2. Given the high impact of ammonia in the climate change and ocean acidification boundaries, it is expected that improvements in its manufacturing would significantly reduce the global impact of the chemical industry. Since ammonia is produced from hydrogen and following recent exploration of the possible routes for its production, a straightforward improvement measure would be to replace the steam reforming process with a cleaner route for the obtention of H_2, as will be explored later (Green hydrogen production and chlor-alkali electrolysis powered with renewable energy).

Additionally, GHG emissions attributed to the Sohio process are most likely due to the impacts of the manufacturing of its raw materials, which include ammonia. Thus, if ammonia production were to be improved, acrylonitrile's impact would be reduced as well.

The analysis of Fig. 4-2 in section 4 indicated that ethylene, propylene and LLDPE were also potential environmental threats in terms of GHGs emissions. However, once the whole analysis has been completed, they have not been found to show an especially high carbon footprint, neither per kg of chemical nor when their production volumes are considered. Ethylene's contribution to all three boundaries is around 2%, while LLDPE's is closer to 3%. Out of all PE types, HDPE shows a higher contribution due to its higher production volume, since unitary (i.e., per kg) emissions are very similar for LLDPE, LDPE and HDPE (they are all around 1.6 kg of CO_2/kg PE). Ethylene is around (1.13 kg CO_2/kg ethylene) and since its impacts are included in all its derivatives, the impact of strictly manufacturing PE is left at around 0.47 kg CO_2/kg PE. The same situation is repeated for propylene (1.15 kg CO_2/kg propylene) and PP (1.67 kg CO_2/kg PP, thus only 0.52 kg CO_2 being attributed directly to the manufacturing process of PP).

It is important to note that propylene does not explicitly appear in Fig. 10-8 and Fig. 10-9 because its impacts are accounted for as burdens of its derived products (Interrelations between processes). Therefore, improvements in the production process of propylene would repercuss on other chemicals' impacts. PP, for example, is the second largest contributor to the climate change and ocean acidification PBs because of its large production volume, accounting for 15% of the overall impacts on all three boundaries (Fig. 10-8 and Fig. 10-9), 69% of which can be attributed to propylene production.

The impact of PE would greatly decrease by reducing its production volume, since its carbon footprint is not greater than that of other chemicals. An alternative to producing new plastics would be the mechanical recycling of polymers or waste products after their use life. PP has been proved to maintain its tensile mechanical properties, even if its elongation-at-break and fracture toughness do decrease with every recycling step (Achilias et al., 2007; Aurrekoetxea et al., 2001), evidencing that mechanical recycling cannot solve the problem. Conversely, recycling through pyrolysis has been recognized as a potential route for the recovery of otherwise discarded plastics, showing promising environmental and economic performance (Somoza-Tornos et al., 2020).

The substitution of PP with other biodegradable or bio-based polymers such as PLA, TPS, or even the combination of both, would help gate-to-grave impacts and recycling would still be feasible since PP hybrids containing low amounts of more biodegradable plastics do not show worse performances when recycled (Samper et al., 2018). Biofiber composites are also emerging potential substitutes to PP and other petroleum-based plastics (Mohanty et al., 2002). Plastic sorting and mechanical recycling processes also have environmental impacts, and their performance must be studied before assuming their implementation would positively affect the sector. In this study, recycled PE is compared with manufactured PE, yielding impacts 5, 3, 0.9 and 2.9 times smaller for the climate change, ocean acidification, freshwater use, and aerosol loading PBs. However, as for nitrogen losses and ODS emissions, recycled PE had contributions 40 and 16 times larger.

As previously discussed (Environmental performance of the European chemical industry), and in addition to actions made towards the processes causing the

most impact in terms of carbon footprint (ammonia and PP), the switch to a greener electricity mix could benefit the industry as a whole and improve its sustainability level.

10.2.2 Stratospheric ozone depletion

When analysing the impacts on the stratospheric ozone depletion boundary, ammonia and propylene oxide stand out again, dwarfing the impacts from all other chemicals. Ammonia and propylene oxide account for 43% (30% from the steam reforming process plus 15% attributed to partial oxidation) and 25.6% of the total impacts, respectively (Fig. 10-8 and Fig. 10-9).

Turning the attention to unitary impacts, propylene oxide widely outweighs all other chemicals (Fig. 10-12), while ammonia has a modest contribution, only amplified by its large production volume. Similar to the origin of propylene oxide's CO_2 emissions, the chlor-alkali electrolysis is found to account for nearly 80% of all N_2O oxide (Fig S5-20).

Fig. 10-12 depicts the total unitary (per kg of chemical) ODS emissions and unitary dinitrogen monoxide emissions, showing the high correlation between both (since N_2O represents 99% of all ODS emissions). Vinyl chloride and ethylene glycol plants operating with the direct chlorination and oxychlorination of ethylene and the hydrolysis of ethylene oxide appear to have high ODS emissions per kg of chemical produced compared to other compounds.

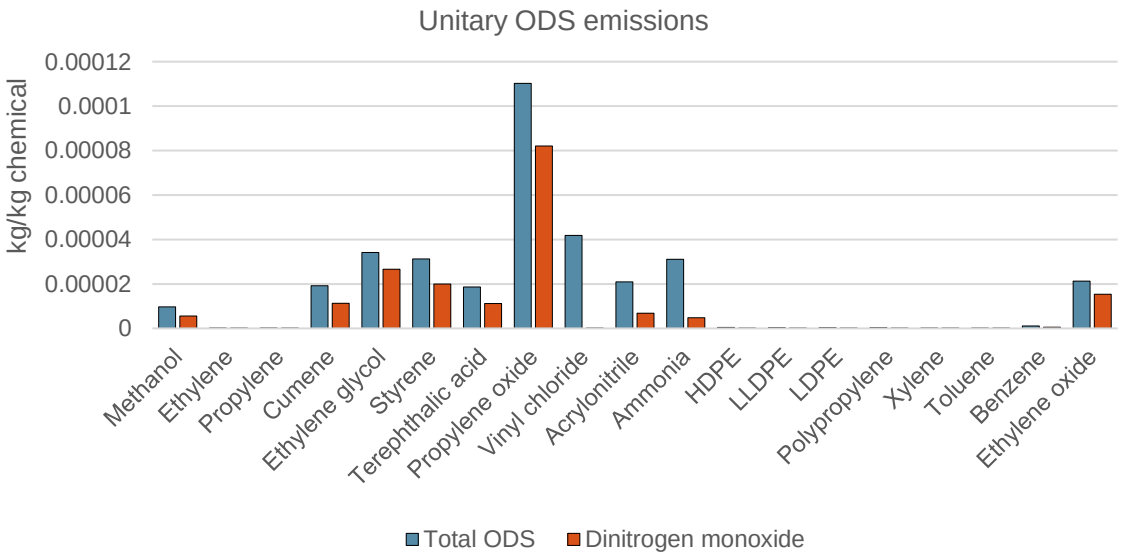

Fig. 10-12: Total emissions of ODS (kg) and dinitrogen monoxide per kg of chemical.

As for vinyl chloride, its nitrous oxide emissions are likely to originate from waste treatment, since the vinyl chloride production process is responsible for large volumes of waste. LCIs for the principal waste types produced by chemical plants (i.e., average incineration residue, coal slurry, municipal solid waste, spoil from hard coal mining, waste plastic, and waste wood) were all the highest for vinyl chloride. Additionally, since the chlorination and oxychlorination processes require chlorine as a baseline reagent, the high N_2O emissions are also due to the obtention of chlorine, as in the case of propylene oxide.

Regarding the hydrolysis of ethylene oxide, the process has a relatively high energy demand which is further increased when excess water is used (Yang et al., 2010). However, this practice increases the selectivity of the reaction (Hydrolysis of ethylene oxide). The use of catalysts could help narrow the energy needs of the process while maintaining the selectivity at low ethylene oxide-water ratios.

10.2.3 Biogeochemical flows (N and P)

Since the impact on the nitrogen boundary oscillates around the limit it is of special relevance to identify possible improvement routes.

As seen in Fig. 10-8 and Fig. 10-9, PP and propylene oxide are the main contributors to the boundary, producing 43% and 36% of the total impacts, respectively. If nitrate emissions per kilogram of product are analysed, the same two chemicals stand out, especially propylene oxide, which emits $4.4 \cdot 10^{-4}$ kg of nitrates to freshwater per kg of product. Fig. 10-13 shows how this value is particularly high when compared with the emissions of other chemicals. However, the larger production volume of PP positions it as the main contributor to the final impacts.

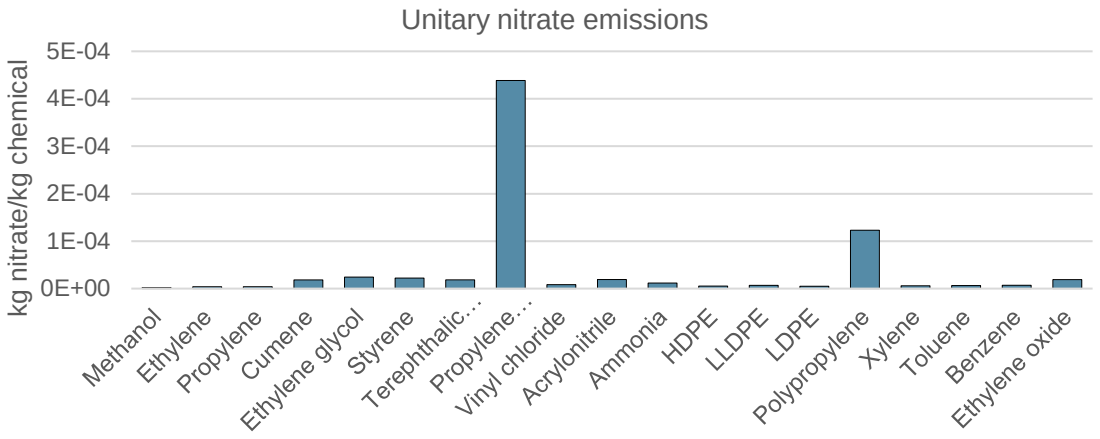

Fig. 10-13: Nitrate emissions to surface water (kg) per kg of chemical.

As for the phosphorus boundary, Fig. 10-8 and Fig. 10-9 show how PP dominates with up to 95% of the total impacts and only marginal contributions from all other chemicals. Nevertheless, since the boundary is not transgressed and the total contribution is low, it is important to note that even if the production of PP and its associated activities seem to have a high effect on the phosphorus cycle, the flux of phosphorus originating from the system is neither critical nor especially high. The second chemical having a noticeable contribution to the total in comparison with the rest is vinyl chloride, even if it is far behind PP, at only 2.5% of the overall impacts. PP also takes the lead in phosphorus emissions per kg of chemical, followed at great distance by vinyl chloride and propylene oxide (Fig. 10-14).

Thus, altogether, PP and propylene oxide make up for 80% and 96% of the impacts on the nitrogen and phosphorus boundaries, respectively.

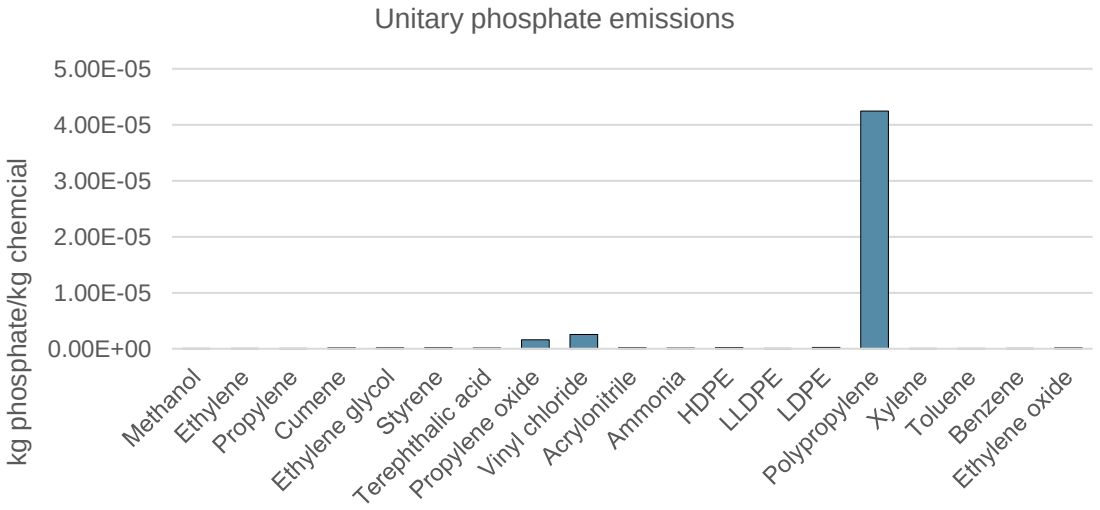

Fig. 10-14: Phosphate emissions to surface water (kg) per kg of chemical.

The reason behing of PP's exceptionally high nitrate and phosphorus emissions is uncertain. Despite contacting the author of the *ecoinvent* dataset, no additional information on the source of the LCIs (or on which of the included activities within the system's boundaries they could be attributed to) could be provided due to confidentiality issues. The original dataset from PlasticsEurope was consulted (PlasticsEurope, 2016); however, even if they report PP to have a higher aquatic eutrophication potential (calculated with the PP system's phosphate emissions to water) than other chemicals (e.g., toluene, xylene, vinyl chloride, propylene, ethylene, ethylene oxide), no further details are given. The fluxes could have been attributed to the process as a result of the boundaries that the authors of the dataset established when analysing the emissions of the studied plants.

As for propylene oxide, 95% of nitrate emissions (Fig S5-21) stem from the electrolytic production of chlorine and NaOH, where they originate from impurities found in the raw materials (European Commission, 2014a). However, phosphorus emissions cannot be attributed to the obtention of its baseline reagents (Fig S5-21); instead, the high phosphorus flows are most likely to be attributed to wastewater management since the chlorohydrin process requires intense post-treatment of waste effluents. For example, waste from plants operating with the chlorohydrin process containing dilute calcium chloride brine can be treated with phosphate compounds (Chinese Patent No. CN1006222B, 1996).

10.2.4 Land system change

Since the land system change boundary is not transgressed, no impacts caused by any manufacturing process are critical or large. Even so, the main contributors at a final impact scale can be identified as ammonia (85%), methanol (4%) and propylene oxide (5%), as shown in Fig. 10-8 and Fig. 10-9.

Ammonia is once more positioned as one of the most critical process. However, when chemicals are sorted in decreasing order of its unitary impacts, ammonia falls to the sixth place, with impacts of $7.6 \cdot 10^{-4}$ transformed m^2 per kg of product, falling behind propylene oxide ($2.7 \cdot 10^{-3}$), terephthalic acid ($1.1 \cdot 10^{-3}$), acrylonitrile and styrene ($1 \cdot 10^{-3}$ and $9.3 \cdot 10^{-4}$), and ethylene oxide ($8.3 \cdot 10^{-4}$).

As additionally shown in Fig. 10-15, methanol does not have a high land demand, however, the industry producing it is also barely involved in reforestation projects. Recall that the final impact each activity has on this boundary is calculated considering the possibility to counteract deforestation practices with reforestation projects. Once evaluating the impacts of an activity, these environmental actions are attributed to plants and reduce the total area transformed by the action of the different enterprises. Chemicals such as terephthalic acid, acrylonitrile, and styrene, despite associated with higher land transformation, are also accredited for contributing to the recovery of other areas back to forest (Fig. 10-1).

For some chemicals, negative impacts were found because their participation in reforestation programmes offsets the deforestation they incur. These are the cases of ethylene and PE, PP, vinyl chloride, xylene, and toluene (Fig. 10-5). These practices do not fully recover the initial ecosystems that the industry perturbs, since old, undisturbed forests hold environmental functions and present characteristics that young plantations may take years to achieve and develop.

Since reforestation practices are associated with carbon sequestering objectives, one obvious downside of deforesting and replanting young trees (thus replacing old-growth forests with new ones) is the vast quantity of CO_2 that old trees store, which is released into the atmosphere once they are disturbed. Moreover, contrary to previous belief that old forests are carbon-neutral (i.e., they are in steady state, capturing as much carbon as they release due to biomass natural decay), it has been found that old trees do in fact continue to accumulate CO_2. Therefore, protecting an old forest may be better than planting a new one in terms of CO_2 capture (Wohlleben, 2020; Luyssaert et al., 2008). Nonetheless, current practices allow to counterweigh ecosystem disturbance with the reconversion of the same or other areas, and thus, the calculations have been performed to reflect these actions.

Since the impacts derived from the construction of the chemical plants and their associated infrastructures are of the same magnitude for all chemicals (Fig S5-22), the disturbed surface of forest was analysed for the reagents of the four chemicals which have the highest impact per kilogram of product (i.e., propylene oxide, terephthalic acid, acrylonitrile, and styrene) to determine whether the impacts could stem from the obtention of feedstocks.

For terephthalic acid, acrylonitrile and styrene, the fraction of land use that can be attributed to their reagents is low. For the former, the studied inputs from the technosphere include nitrogen, water, acetic acid and NaOH, which take up 7.73% of the total land use of terephthalic acid. Then, as for acrylonitrile, sulfuric acid, and water only account for 1.25% of the land use. Finally, for styrene, nitrogen and water represent 1.14% of the overall disturbed surface. Therefore, the land use arising from the production of these chemicals may be due to the use of biomass in the plants, the transportation, or the fact that plants may be located at forest-rich regions. For propylene oxide, however, the production of chlorine and NaOH causes almost 84% of its total deforestation (Fig S5-23).

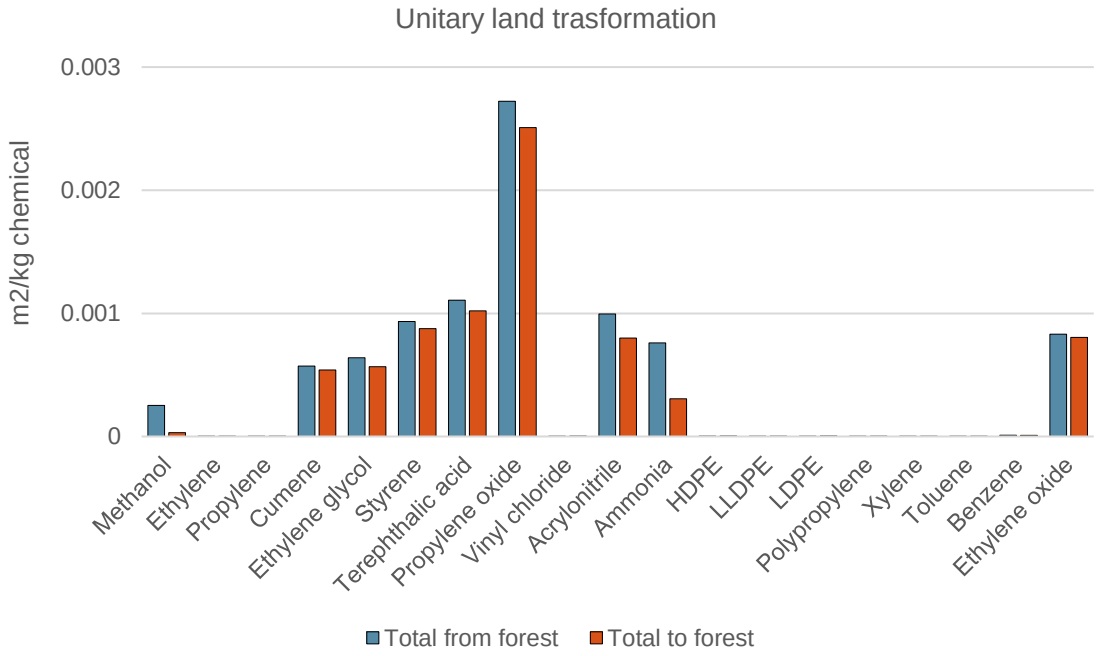

Fig. 10-15: Deforested land (m^2) and reforested land (m^2) per kg of chemical.

10.2.5 Freshwater use

As for the land use boundary, the consumption of freshwater in chemical plants has not been found to be an environmental issue. The total impacts once production volumes and characterization factors are considered indicate a much more homogeneous distribution of water use between processes, even if styrene and propylene oxide do take up 30% and 18% of the impacts, respectively. Ammonia (10%) and polypropylene (8%) are next in terms of contribution to the freshwater use PB, as shown in Fig. 10-8 and Fig. 10-9. Once the impacts are broken down to unitary contributions (L of water needed/kg chemical; Fig. 10-16),

propylene oxide is again the studied product with the largest impact, being followed more closely than in other boundaries by styrene, acrylonitrile, and ethylene glycol.

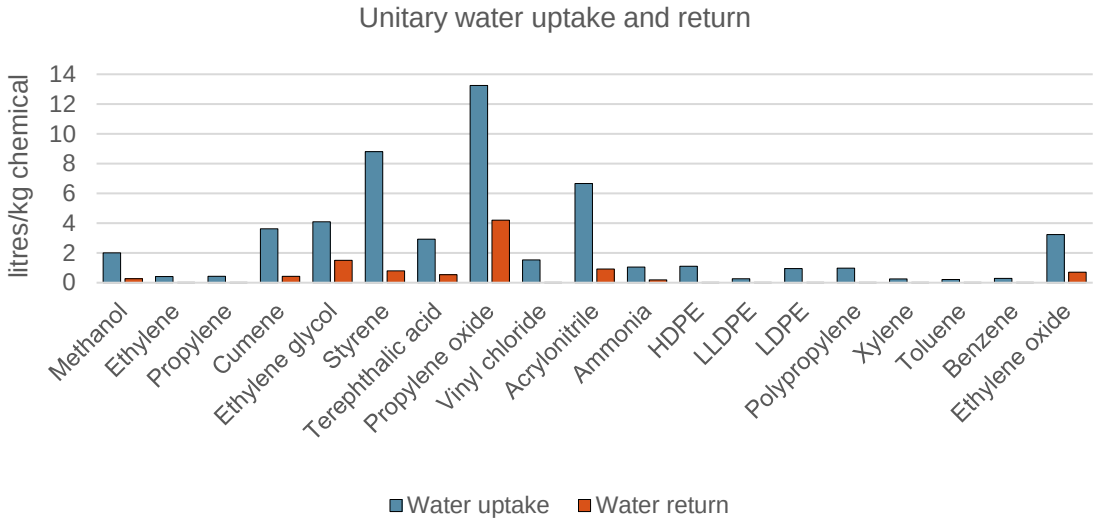

Fig. 10-16: Total withdrawn water (L) and returned water (L) per kg of chemical.

In the case of acrylonitrile, the high water consumption stems from the need to constantly refrigerate the reactor to keep its temperature constant (Sohio process), while for propylene oxide, styrene, and ethylene glycol, the requirements are due to the use of water as a reagent, directly from the environment or as steam.

In the Chlorohydrin process, water, propylene, and chlorine are fed to the reaction section to produce a chlorohydrin intermediate (*Eq. 20* and *Eq. 21*) which is then reacted with sodium hydroxide to obtain propylene oxide (*Eq. 22*; Fig. 4-15: Process flow diagram of the chlorohydrin process (adapted from Matar & Hatch, 2001; Nijhuis et al., 2006).). Additionally, this second reaction is carried out in a stripping column, which requires steam.

Ethylene glycol obtained through the Hydrolysis of ethylene oxide uses an excess of water in the reactor (*Eq. 15*) as a measure to increase the conversion (Fig. 4-7: Process flow diagram for the production of ethylene glycol by the hydrolysis of ethylene oxide (adapted from Rebsdat & Mayer, 2012a).). This could cause not only the energy demand of the process to rise (as seen in the Stratospheric ozone depletion boundary) but also results in larger amounts of water being used compared to other processes. Nevertheless, since the freshwater use boundary

is not put under pressure, the consumption can be considered sustainable, and so the benefits of an enhanced conversation rate outweigh the impacts in terms of water use.

Finally, for the production of styrene *via* Dehydrogenation of ethylbenzene, large quantities of steam are required to maintain the reaction temperature (Fig. 4-16: Process flow diagram of the dehydrogenation of ethylbenzene process (adapted from Chadwick, 2000; Zarubina, 2015).). One recursive observation is that steam production is one of the main uses of water in the chemical industry.

The fraction of water returned to the environment is also represented in Fig. 10-16. No processes return more water than they withdraw, even when in some, such as the chlorohydrin process and the direct oxidation of ethylene, water is formed as a by-product in the reaction (*Eq. 63* and *Eq. 22*).

10.2.6 Aerosol loading

Analogously to the climate change and ocean acidification boundaries, the impacts on aerosol loading are really dependent on the production volume of chemicals since unitary emissions are similar for all chemicals. Moreover, some of the flows are classified as both GHGs and aerosols (e.g., NMVOCs) thus yielding a final distribution of impacts (Fig. 10-8) similar to the other three boundaries (Fig. 10-8 and Fig. 10-9).

In the aerosol loading case, ammonia (23%), styrene (15%), propylene oxide (14%), and PP (10%) are the four principal contributors to the total impacts. On the one hand, ammonia and PP (the first and second chemicals with highest production volume) see their impacts amplified by their high demands. On the other hand, despite being in the top ten of highest volume chemicals, styrene and propylene oxide show higher contributions than benzene or HDPE, which are above them in terms of kilograms produced.

Once the unitary emissions of all investigated aerosols are shown, propylene oxide, styrene, cumene and LDPE show the highest pollution rates (Fig. 10-17), even if the distribution is fairly even.

Since propylene oxide and styrene are the two chemicals showing slightly larger pollution rates and the chlor-alkali process has been proved to widely contribute

to the total impacts of the former on numerous PBs, the analysis of the emissions of the reagents has been carried out for this boundary as well. The LCIs corresponding to aerosol emissions of the feedstocks have been collected and processed to calculate the percentage of the total they represent, standing at 71.5% for chlorine and NaOH in the chlorohydrin process and only 0.4% for nitrogen and water in the dehydrogenation of ethylbenzene. Therefore, the energy use of the chlor-alkali electrolysis process is the cause of the high aerosol emissions of propylene oxide, while, as

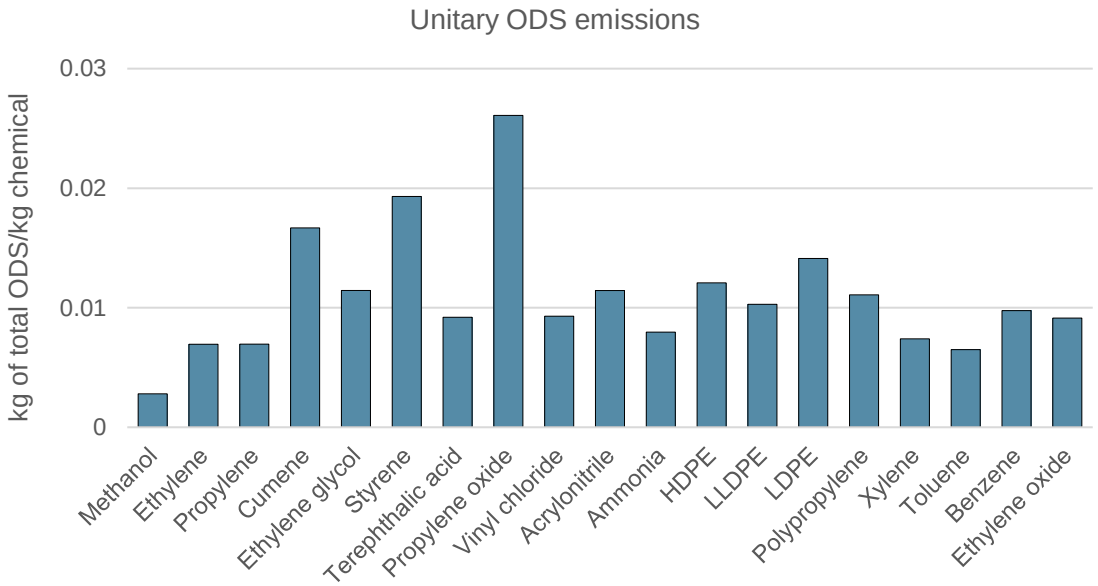

Fig. 10-17: ODS emissions (kg) per kg of chemical.

10.3 Impact distribution

Since one of the study's goals was to identify those activities which contribute the most to the occupation of the allocated SOS, Table 10-3 presents a summary of the impact breakdown section showing the top four chemicals with the highest contribution to each PB in terms of both absolute final and unitary impacts.

Table 10-3: Top contributors to all boundaries.

	Absolute impact	**Per kg of chemical**
Climate change: energy imbalance at top of atmosphere	Ammonia	Propylene oxide
	Polypropylene	Acrylonitrile
Climate change: atmospheric CO_2 concentration	Propylene oxide	Styrene
	HDPE	Ammonia
Stratospheric ozone depletion	Ammonia	Propylene oxide
	Propylene oxide	Vinyl chloride
	Vinyl chloride	Ethylene glycol
	Styrene	Styrene
Ocean acidification	Ammonia	Propylene oxide
	Polypropylene	Acrylonitrile
	Propylene oxide	Styrene
	HDPE	Ammonia
Biogeochemical flows: N cycle	Polypropylene	Propylene oxide
	Propylene oxide	Polypropylene
	Ammonia	Ethylene glycol
	Styrene	Styrene
Biogeochemical flows: P cycle	Polypropylene	Polypropylene
	Vinyl chloride	Vinyl chloride
	Propylene oxide	Propylene oxide
	Ammonia	LDPE
Land-system change	Ammonia	Propylene oxide
	Propylene oxide	Acrylonitrile
	Methanol	Terephthalic acid
	Styrene	Styrene
Freshwater use	Styrene	Propylene oxide
	Propylene oxide	Styrene
	Ammonia	Acrylonitrile
	Polypropylene	Ethylene glycol
Atmospheric aerosol loading	Ammonia	Propylene oxide
	Styrene	Styrene
	Polypropylene	Cumene
	HDPE	LDPE

10.4 Potential improvement pathways

In this section, potential scenarios to enhance the environmental performance of the chemical industry deemed promising according to the results are investigated. The aim is to determine the magnitude of the improvement they could allow for, whether burden shifting occurs due to the collateral impacts of their deployment, and the capacity and resource use they would require.

The first action proposed is the switch to a more sustainable electricity mix (yet not carbon-free, since an absolutely carbon-free mix is not realistic currently). This would allow to reduce GHG emissions and hopefully mitigate the impacts of the sector on the CO_2-based boundaries (i.e., climate change and ocean acidification), but also to reduce ODS and aerosol emissions. A general improvement is expected on the performance of the industry and its contribution on all PBs. However, the measure may not be sufficient, and the possibility of burden-shifting must be studied.

Additionally, the implementation of carbon capture and storage technologies is assessed since they have been proposed as potential aids for the mitigation of the effects of GHG emissions. If the emitted carbon is sequestered and stored in geologic deposits, the industry could continue its BAU operation, so this measure could help during the transitioning of the sector towards a more sustainable model. The required carbon capture and storage capacity to position the chemical industry within the safe zone of the climate change and ocean acidification boundaries is investigated, as well as the impacts on resource use and on other PBs that this route would entail.

Another scenario where the sustainable production of H_2 is implemented is analysed, since ammonia has been found to be one of the top contributors to all PBs. The production of hydrogen from fossil fuels is switched to its obtention through the electrolysis of water powered by wind power. Additionally, the chlor-alkali process has been found to cause high impacts on all PBs and position propylene oxide as one of the top polluters of the industry (both in terms of unitary and absolute contributions to the boundaries) due to its high energy demand. Therefore, the electricity mix of the chlor-alkali electrolysis is changed to the sustainable mix presented in the first scenario. These two actions not only affect

ammonia and propylene oxide production, but also the manufacturing processes of methanol, vinyl chloride, PP, all types of PE, benzene from coking and terephthalic acid.

It must be noted that most of the improvements suggested must be accompanied by the generation of renewable energy, which takes place beyond the boundaries of the chemical industry.

10.4.1 Energy mix

Energy production constitutes one of the main threats to the environment and especially the climate, causing around three quarters of the world's GHG emissions (Ritchie, 2020). The shift towards a mix based on renewable sources that would allow to decarbonise the power sector is a key and ineluctable step towards a sustainable economy.

As the results of the present study indicate, the chemical industry is exerting an enormous pressure on all PBs which are affected by GHGs due to the large energy demand of the majority of manufacturing routes. The activities with higher energy demand were found to be the chlorohydrin, steam cracking, and dehydrogenation of ethylbenzene processes. Thus, the change from the current (i.e., BAU) electricity mix considered in the study to an alternative mix based on renewable energy sources is expected to help reduce the emissions of the sector.

The shares with which different power technologies are combined in these two mixes are shown in Fig. 10-18. The BAU mix corresponds to one used so far to calculate the results in all previous figures. It was obtained by tracing back the activities supplying electricity for the manufacture of the chemicals studied (in a direct or indirect way) and aggregating them by technology. The *ecoinvent* datasets include losses occurring during transmission and storage of the energy and are based on data from 2014. Thus, the energy mix is not updated to current policies or adapted to climate change mitigation roadmaps. As a result, a great fraction of the total electricity is found to be obtained from coal (14%) and natural gas (34%). However, hydropower and nuclear energy, both considered low-carbon energy sources and therefore clean from a GHG emissions point of view (Lau et al., 2019) also contribute generating 36% of the total electricity (Fig. 10-18).

The mix adopted using the shares presented in the World Energy Outlook 2019 (IEA, 2019) in accordance with the Sustainable Development scenario (SDS, 2040) is mostly composed of renewable energies, while carbon capture and storage is installed in some coal and natural gas plants as an aid to reduce their CO_2 emissions. In order to model this mix, *ecoinvent* datasets for every technology are collected and a weighted to obtain the environmental burdens derived from the generation of one kWh of electricity with the new mix. The transformation of LCIs to change the part proportional to the energy production to a new set of impacts modelled for a different mix is a consequential LCA, since the effects of an action, which in this case involves electricity, are assessed.

Coal and natural gas plants with CCS are not available in *ecoinvent* and thus are modelled by combining data for traditional coal and natural gas plants, with those of the CCS system. In turn, the CCS system is modelled based on data in *Galán-Martín et al.* (2021), by adapting the inventories therein for the capture of 1 kg of CO_2 in coal and natural gas plants with CCS to 1 kWh of electricity delivered at plant. In this regard, a CCS system with a capture rate of 90% (i.e., capturing 90% of the CO2 in the off-gases) is assumed to capture 1.29 kg of CO_2 in coal plants while in natural gas plants the ratio is lower, at 0.31 kg of CO_2, per kWh produced. This is because natural gas plants show lower carbon emissions than coal plants per kWh generated. Impacts of transporting and storing the captured CO_2 in geologic deposits are also included in these activities, as modelled according to the inventories shown in Table S5-4. The new mix allows for a reduction of CO_2 emissions of 67.8% and of total GHGs of 67.7%. The inventory of all technologies which conform the renewable mix can be found in the annexes (Table S5-1, S5-2, and S5-3).

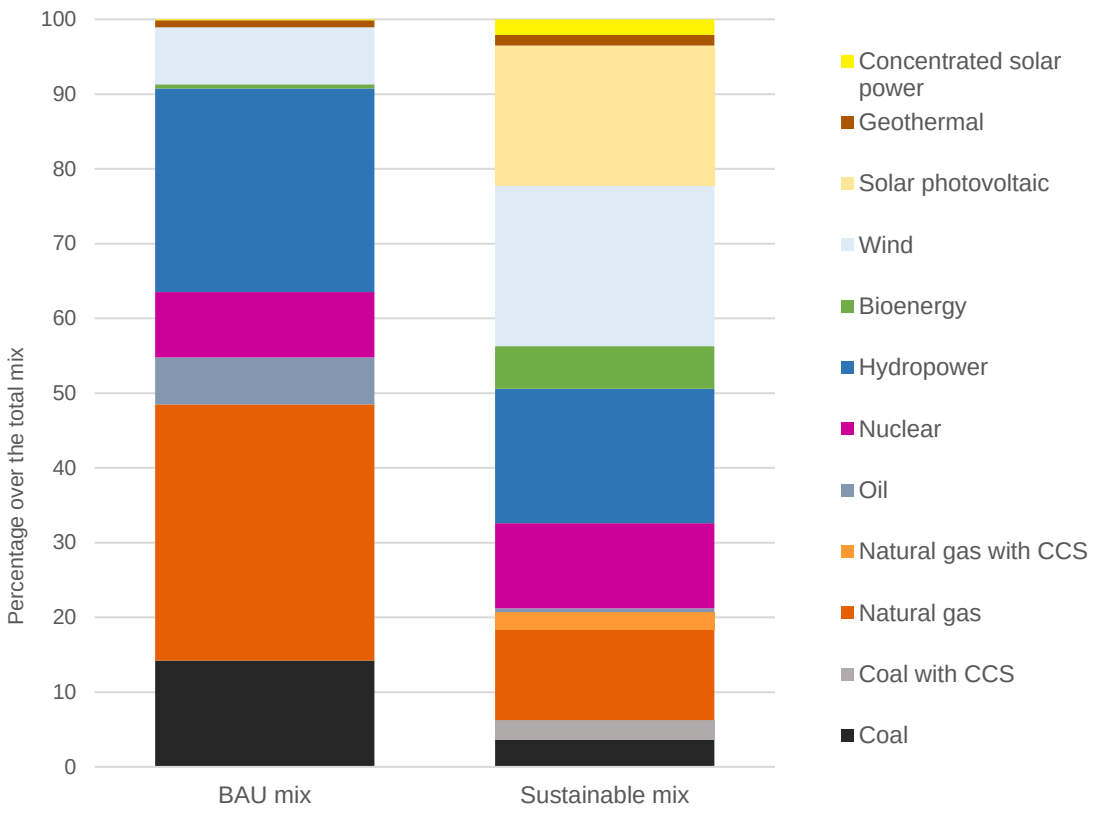

Fig. 10-18: High voltage electricity mix for the European region (average technology mix used by ecoinvent) as compared with the proposed renewable mix.

With the LCIs of the sustainable mix at hand, this improvement scenario is constructed by replacing contribution of the BAU mix with an analogous contribution (i.e., same amount of electricity generated) from the sustainable mix (Eq. 71).

$$FC_{b,j,SM} = FC_{b,j,BAU} + \left(\sum_{i} CF_{i,b} * \left(LCI_{PB-LCIA,i,j,SM} - LCI_{PB-LCIA,i,j,BAU}\right)\right) * ED_j \quad \forall b,j \qquad \text{Eq. 71}$$

Here, $FC_{b,j,SM}$ is the total impact on PB *b* caused by product j in the scenario using the new mix, while $FC_{b,j,BAU}$ is the impact previously calculated (*Eq. 57*). $LCI_{PB-LCIA,i,j,SM}$ and $LCI_{PB-LCIA,i,j,BAU}$ are the LCIs for flow *i* generated because of the manufacture of *j*, $CF_{i,b}$ is the characterization factor for the impact of each LCI item *i* on PB *b*, and ED_j is the energy demand of the process for the production of *j*.

A challenge is faced when trying to identify ED_j since ecoinvent does not provide information on the total life-cycle electricity demanded by activities but only the

electricity consumed directly at the production plant of the relevant chemical (i.e., foreground process). Therefore, the electricity consumed by the foreground processes is used as a proxy for ED_j. This is a conservative approach, since impacts derived from electricity generation for the background processes (e.g., acquisition of reagents, waste treatment, etc.) are still based on the less-clean BAU mix.

The switch to a mix based on renewable energies results in a significant reduction of the impacts on the PBs. However, since only the mix of the electricity used by foreground processes can be changed with the available data, the improvement is insufficient for placing the chemical industry below the PB limits. Improvements in the contributions to the PBs are range from 0.26 to 22.80% in the cases of the alteration of the phosphorus cycle and freshwater use, respectively, as shown in Table 10-4.

Table 10-4: Final contributions to the PBs when the renewable energy mix is used.

Planetary boundary	**$occSoSOS_{PB}$ BAU mix**	**$occSoSOS_{PB}$ Renewable energy mix**	**% reduction**
Energy imbalance at top of atmosphere	$1.08 \cdot 10^{2}$	$1.01 \cdot 10^{2}$	6.12
Atmospheric CO_2 concentration	$1.12 \cdot 10^{2}$	$1.06 \cdot 10^{2}$	5.14
Stratospheric ozone depletion	$4.83 \cdot 10^{-2}$	$3.88 \cdot 10^{-2}$	19.58
Ocean acidification	$3.60 \cdot 10^{1}$	$3.40 \cdot 10^{1}$	5.63
Biogeochemical flows (N)	$6.45 \cdot 10^{-1}$	$6.87 \cdot 10^{-1}$	-6.58
Biogeochemical flows (P)	$1.01 \cdot 10^{-1}$	$1.01 \cdot 10^{-1}$	0.26
Land-system change	$1.35 \cdot 10^{-3}$	$1.32 \cdot 10^{-3}$	1.96
Freshwater use	$7.96 \cdot 10^{-2}$	$6.15 \cdot 10^{-2}$	22.80
Aerosol loading	$1.87 \cdot 10^{1}$	$1.72 \cdot 10^{1}$	7.86

As seen in the Climate change and ocean acidification section, the four chemicals with higher GHG emissions per kg were found to be propylene oxide, ammonia, acrylonitrile, and styrene. In many cases, GHG emissions stem from energy-

demanding background processes such as the chlor-alkali one. These processes still obtain their electricity from the BAU mix, causing the emissions of propylene oxide (the main emitter of GHGs per kg of chemical produced) to remain similar as in the BAU, with a reduction of only 3%. As for ammonia (and consequently, acrylonitrile), CO_2 emissions were mainly due to the obtention of H_2 and notto their energy requirements. Therefore, neither of the two species see their emissions reduced in this scenario. Conversely, styrene, which was found to have a high energy demand, sees a reduction of 11% in its total CO_2 (and thus, total GHG) emissions.

Secondly, the change in energy mix cuts down and even cancels in many cases the emissions of GHGs such as carbon monoxide, methane, and dinitrogen monoxide; however, the reduction of CO_2 emissions is more modest (from 0.4 kg CO_2 to 0.13 kg CO_2 per kWh of electricity). Considering CO_2 accounts for around 99% of total GHG emissions, final impacts on the climate change and ocean acidification boundaries are hardly affected by the avoidance of the emissions of other GHGs (Climate change and ocean acidification). As expected, the change affects all three boundaries similarly. However, the reduction of methane and dinitrogen monoxide emissions (from $7 \cdot 10^{-4}$ to $4 \cdot 10^{-4}$ and $1.85 \cdot 10^{-5}$ to $3.7 \cdot 10^{-6}$ kg per kWh, respectively) has a higher effect on the stratospheric ozone depletion limit (19.58%, compared to 6.12%/5.14% and 5.63% for both climate change PBs and for the ocean acidification PB, respectively). Additionally, the emissions of some aerosols are also cancelled, including sulfur dioxide, sulfate, and particulate matter, causing a small reduction of the impact on the aerosol loading boundary (7.86%).

As for resource uptake, Table 10-4 indicates how the greatest improvement is made on the freshwater use boundary. Coal, natural gas, and nuclear energy were found to require water volumes from 1 to 6 order of magnitude larger than any other energy type included in the renewable mix. Therefore, the substitution of these technologies causes the water requirements of the processes to drop dramatically.

The only boundary which is impaired by the change in the energy mix is that of the nitrogen cycle. Nitrate emissions to surface water of concentrated solar power

plants are significantly higher than those of the conventional mix ($1.42 \cdot 10^{-5}$ versus $6.4 \cdot 10^{-6}$ m^3 of water per kWh). These emissions are most likely due to the salt mixtures containing nitrates utilized as energy storage media in concentration solar power installations (Villada et al., 2019; Fernández, 2019). Thermal energy storage is used to enable plants to produce electricity when solar radiation is low, even during the night. Molten salts commonly used for this purpose include potassium and sodium nitrate. The results indicate that, while concentrating solar power is seen as an attractive alternative to fossil fuels (Villada et al., 2019), its widespread use could damage the nitrogen cycle and may thus require attention. Additionally, wind and solar photovoltaic installations, and natural gas plants operating with CCS also have nitrate emissions one order of magnitude above the conventional mix. These arise from the use of sorbent to collect CO_2, which is typically an amine (DEA, or ethanolamine).

The two energy production technologies with the lowest CO_2 emissions have been found to be hydropower and bioenergy (including the combustion of wood chips, pellets, other biomass, biofuels, waste, and biogas). Both have high installed capacities which have been further increasing during recent years. To compel with the Sustainable Development Goals, an increase in global hydropower capacity of 3% per year is required until 2030, while bioenergy should see an annual increase of 6% (IEA, 2020a, 2020b). The further development of bioenergy and hydropower must consider the impacts of their extensive deployment, especially the disturbance of dwells on rivers and their biodiversity, and the possible social issues arising from the use of biomass as an energy source instead of food. However, both technologies hold high potential as renewable energy sources that could help decarbonise the energy sector, bringing ancillary benefits to the chemical industry.

10.4.2 Carbon capture and storage (CCS)

Carbon capture and storage (CCS) technologies are recognised as potential aids for tackling of climate change through mitigative action. They would allow for current practices to be maintained while avoiding emissions to the atmosphere and thus keeping impacts lower (Boot-Handford et al., 2014; Haszeldine, 2009).

The capture of CO_2 is usually implemented at point sources producing large volumes of emissions. Three main configurations can be identified: post- and pre-combustion capture, and oxyfuel capture. Post-combustion capture avoids CO_2 from combustion gases to reach the atmosphere with the use of solvents in scrubbing columns. Pre-combustion capture requires the treatment of the fossil fuel prior to its combustion through its gasification, partial oxidation, or reforming followed by its reaction with water, to produce CO_2, which is then captured. Finally, a fraction of the captured gases is recycled in the process in oxyfuel (or recycle) capture. In the last two processes, the air is also treated before entering the combustion unit to separate oxygen from hydrogen (Bui et al., 2018; Gibbins & Chalmers, 2008). Point source technologies are limited by their removal efficiencies, since it is not possible to remove 100% of the produced CO_2, although capture rates of 99% can be achieved at certain costs (Brandl et al., 2021).

Additionally, can be combined with certain technologies to ensure a net withdrawal of CO_2 from the atmosphere, thus allowing for Carbon Dioxide Removal (CDR). CDR technologies relaying on CCS include mainly Direct Air Capture with Carbon Storage (DACCS) and Bioenergy with Carbon Capture and Storage (BECCS) and can help reach the climate goals of many energy-intensive industries.

On the one hand, DACCS also employs solvents to absorb CO_2, but uses a different technological configuration compared to CCS at point sources. DACCS plants can be installed anywhere and operate with large capture devices (air contractors), which use fans to draw air inside the system, where CO_2 is chemically removed from the air flow and trapped in an absorbent solution (Lehtveer & Emanuelsson, 2021). The solution is later purified and compressed so the resulting CO_2 stream can be geologically stored. DACCS allow to extract

CO_2 from the atmosphere creating a flow from air to the process, which is set as negative using conventional sign criterion for emissions.

On the other hand, BECCS have lower costs than DACCS and allow for power generation, arguably as a by-product. They are based on adding a CCS system to a conventional bioenergy power plant. In this case, CDR is attained in the life cycle as follows. Biomass absorbs CO_2 from the atmosphere during photosynthesis. This CO_2 is fixed as biogenic carbon in the plant and will be oxidized back to CO_2 during biomass combustion at the power plant. In traditional bioenergy plants, these results in an (almost neutral) cycle, with all the CO2 absorbed by the plant being released again to the atmosphere. However, when a CCS systems prevents the release of, e.g., 90% of the CO_2, the overall balance can be negative in the life cycle, thus removing more CO_2 from the atmosphere than released back to it (Anderson & Newell, 2004; Fridahl & Lehtveer, 2018; Gambhir & Tavoni, 2019).

The CO_2 captured must be kept from returning to the atmosphere. Therefore, it can either be reused as a feedstock in processes which need it (e.g., methanol from CO_2), or stored in geologic deposits, ensuring it will not escape. In the presented scenarios, the CO_2 is assumed to be stored.

Even if the use of DACCS, BECCS or CCS at point-source, have limitations (mainly, their energy requirements, potential land use conflicts and removal efficiency, respectively), the use of CCS combined with CDR technologies can help provide the means to meet climate goals, especially if these systems are powered with renewable energies.

The performance of DACCS and BECCS are assessed in this section in order to determine how much capacity would need to be deployed to achieve climate neutrality and assess how this deployment would affect the state of the PBs. Four scenarios are presented for each CCS method, (i) a nominal scenario where the electricity mix is not changed and the aim is to obtain net zero emissions of CO_2, (ii) an improvement over the first scenario considering the renewable mix is used, and two additional scenarios where the aim is to cancel, not only CO_2, but the total contribution on the energy imbalance PB by capturing the equivalent amount of CO_2 using both the (iii) BAU electricity mix and the (iv) sustainable mix.

10.4.2.1 Direct Air Capture with Carbon Storage (DACCS)

To apply direct air capture to the assessed system, a scenario where all CO_2 produced by the chemical industry is captured using DACCS technologies and stored in geologic deposits is presented. The air capturing systems can be installed anywhere and sequester CO_2 directly from air for its geologic storage, as depicted in Fig. 10-19.

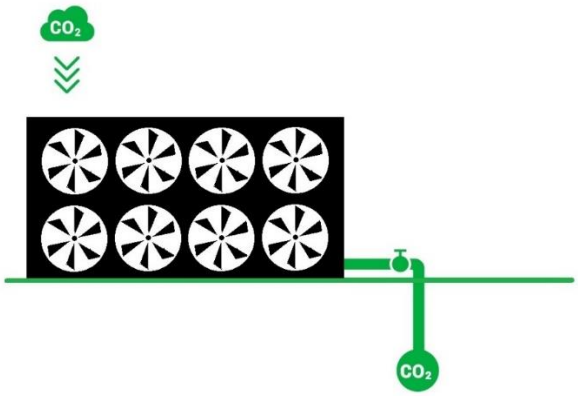

Fig. 10-19: Schematic representation a DACCS system (adapted from Fridahl et. al., 2020).

DACCS is a very novel technology which cannot be found in environmental databases yet. Hence, DACCS was modelled as an individual process with a negative LCI for CO_2 emissions, with the remaining LCIs based on inputs and outputs from *Galán-Martín et al.* (2021) and provided in Table S5-5. Then, the transportation and storage of the CO_2 captured is modelled as previously done for the coal and natural gas plants operating with CCS (Table S5-4). Two variants of the DACCS model are developed. In the first one, the electricity required by the DACCS plant is obtained from the BAU mix in order to adopt a conservative approach. In this scenario, the assessed processes would continue operating without further modifications, and DACCS facilities would be deployed in parallel to remove from the atmosphere the emissions associated with the chemical industry.

The DACCS capacity that has to be installed to cancel out all fossil CO_2 emissions has been calculated considering the positive emissions from DACCS as well. It was found that 300,000,000 net tonnes of CO_2 had to be removed from DACCS in order to obtain a net balance equal to zero and achieve a significant reduction of the impacts from industry on the climate change and ocean acidification boundaries.

The impact of the deployment of DACCS to counteract the industry's emissions is illustrated in Fig. 10-20, where the BAU situation is represented with stacked bars showing the contribution on each process on the total (up to 100%). The additional bars in orange represent the impacts of the DACCS system. As appreciated, DACCS provide negative contributions to some PBs (e.g., ocean acidification) which counteract the rest of impacts, but also increase the total pressure on others by adding an additional contribution (e.g., freshwater use).

The total values of the net contributions to the PBs considering all processes and the DACCS system are shown in green markers, while the limit of each PB is depicted using red markers. This representation allows to compare the state of the PBs before and after the deployment of DACCS and see which PBs are transgressed in each scenario. Note that the y axis is cut at several points to correctly include the limits of some PBs. Additionally, the changes are quantified in Table 10-5.

Table 10-5: Impact reduction with respect to the current situation achieved by the implementation of DACCS (conservative scenario: BAU mix and cancellation of CO_2 emissions).

Planetary boundary	**$occSoSOS_{PB}$ BAU practice**	**$occSoSOS_{PB}$ DACCS**	**% reduction**
Energy imbalance at top of atmosphere	$1.08 \cdot 10^{2}$	$5.18 \cdot 10^{0}$	95.20
Atmospheric CO_2 concentration	$1.12 \cdot 10^{2}$	$2.99 \cdot 10^{0}$	97.33
Stratospheric ozone depletion	$4.83 \cdot 10^{-2}$	$7.28 \cdot 10^{-2}$	-50.64
Ocean acidification	$3.60 \cdot 10^{1}$	$9.54E \cdot 10^{-1}$	97.35
Biogeochemical flows (N)	$6.45 \cdot 10^{-1}$	$8.05 \cdot 10^{-1}$	-24.80
Biogeochemical flows (P)	$1.01 \cdot 10^{-1}$	$1.01 \cdot 10^{-1}$	-0.35
Land-system change	$1.35 \cdot 10^{-3}$	$2.07 \cdot 10^{-3}$	-53.03
Freshwater use	$7.96 \cdot 10^{-2}$	$4.13 \cdot 10^{-2}$	-418.99
Aerosol loading	$1.87 \cdot 10^{1}$	$2.28E \cdot 10^{1}$	-22.11

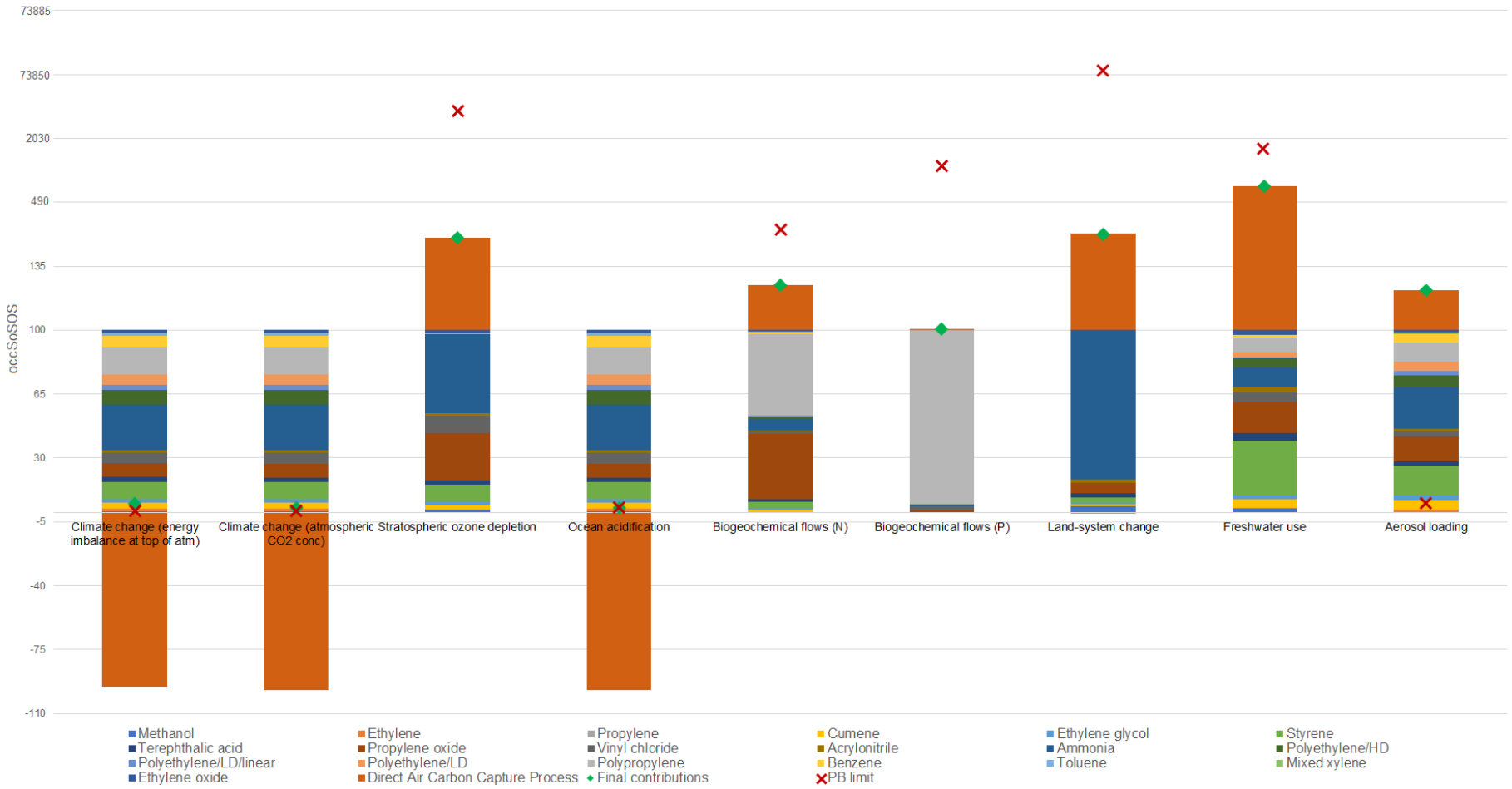

Fig. 10-20: Impact reduction with respect to the current situation achieved by the implementation of DACCS in terms of % over the total contribution to each PB in the current scenario (conservative scenario: BAU mix and cancellation of only CO_2 emissions).

As expected, the withdrawal of CO_2 impacts positively on Earth Systems which are damaged by this species (i.e., energy imbalance at top of atmosphere, atmospheric CO_2 concentration, and ocean acidification). The total capture of CO_2 causes reductions of above 95% for the three PBs, which are sufficient to bring the pressure on the ocean acidification boundary below the threshold, but not enough to position the chemical sector within the safe zone of the climate change boundaries. Nevertheless, these boundaries are now transgressed by lower values of 5.2% and 3%, instead of 108% and 112% as in the current situation. The remaining contribution is due to the impact of all GHGs which are not CO_2, which, even if emitted in lower volumes, often have higher global warming potential than CO_2. Hence, the emissions from these GHGs are enough to exceed the CO_2-based PBs and, therefore, are not to be taken lightly.

In addition, the implementation of DACCS (including both the plants and the transport and storage of the collected CO_2) is not exempt of impacts, with repercussion on the rest of PBs, thus causing the phenomenon known as burden-shifting. The consequences of DACCS deployment in terms of resource use and electricity demand are important factors to consider when investigating the potential of this technology (Bassetti, 2019; Gambhir & Tavoni, 2019; Lebling et al., 2021; Realmonte et al., 2019). Thus, the quantification of the impacts that DACCS facilities would have on land and water use are especially relevant.

As observed in Table 10-5, the freshwater use boundary takes the greatest hit, since DACCS technologies using liquid solvents have a high water demand. Additionally, the manufacture of these solvents (in this case, calcium carbonate) requires also important water inputs. However, the PB is still not met even when the water withdrawal of all processes plus that of the deployment of DACCS is considered, so the impacts still fall within the safe zone. Another drawback associated with DACCS is land use (Table 10-4, Fig. 10-20). The space requirement of DAC plants and CO_2 storage, even if not excessive compared with the rest of processes, is amplified by the large capacity required to remove all emissions. It has been reported that DACCS facilities need to be located at least 250m apart from each other to prevent dual depleted air intake (McCollum & Ogden, 2006). The impact on the land-use change boundary is therefore increased by 53% in this case, yet it also remains well below the limit.

The stratospheric ozone depletion suffers an impact increase of 50% also due to the level of intervention required, which causes the need for a large number of DACCS plants to be installed. The main ODS emitted by DACCS is also dinitrogen monoxide, mainly due to the electricity used and the manufacture of solvents. The same situation is repeated with the aerosol loading boundary, which was already surpassed in the original scenario and suffers an additional increase of 22% mainly due to the sulfur dioxide and nitrogen oxide emissions from DACCS. The boundary ends up being transgressed by 22.8% instead of the current 18.7%.

Finally, nitrates and phosphorus emissions to water, even if not significantly high per kg of captured CO_2, cause an increase of the final impacts on the nitrogen and phosphorus boundaries of 24.8 and 0.35% respectively. However, neither boundary is met (note that the N boundary was only met in 1 out of the 100 modelled scenarios).

The deployment of DACCS yields promising results in terms of reduction of impacts on the climate change and ocean acidification boundaries while not causing the transgression of any additional PB. In this scenario, the model is optimized using excel solver to find the DACCS capacity that would allow to compensate, not only for CO_2 emissions, but also for the impact of all GHGs on the energy imbalance PB. Among the three CO_2-based PBs, the cancellation of the contribution to the energy imbalance at top of atmosphere boundary is set as the objective since it is the PB receiving the highest pressure out of the three and better representing the impact of all non-CO_2 GHGs. The capture and sequestration of 243,000,000 tonnes of CO_2 is found to be necessary in order to cancel 100% of the impacts on this boundary and achieve an occupied fraction of SOS of 0 (Table 10-6).

In turn, this action would allow the chemical industry to set its impact on the CO_2 concentration and ocean acidification boundaries within the safe zone. Negative values in the occupied fraction of safe operating space for these PBs indicate that the sector would need to remove more CO_2 than it releases in order to cancel the energy imbalance PB. This additional removal would offset the emissions of the subset of GHGs considered in the two less demanding carbon-based PBs (i.e.,

the energy imbalance and the CO_2 concentration PBs), causing them to be especially benefited and obtain negative values, as seen in Table 10-6. The extra CO_2 emissions captured would derive from other economic activities.

Table 10-6: Impact reduction with respect to the current situation achieved by the implementation of DACCS (BAU mix and aiming for the fraction of occupied SoSOS for the energy imbalance PB to be equal to zero).

Planetary boundary	**$occSoSOS_{PB}$ BAU practice**	**$occSoSOS_{PB}$ DACCS**	**% reduction**
Energy imbalance at top of atmosphere	$1.08 \cdot 10^{2}$	$0.00 \cdot 10^{0}$	100.00
Atmospheric CO_2 concentration	$1.12 \cdot 10^{2}$	$-2.55 \cdot 10^{0}$	102.27
Stratospheric ozone depletion	$4.83 \cdot 10^{-2}$	$7.40 \cdot 10^{-2}$	-53.19
Ocean acidification	$3.60 \cdot 10^{1}$	$-8.15 \cdot 10^{-1}$	102.26
Biogeochemical flows (N)	$6.45 \cdot 10^{-1}$	$8.13 \cdot 10^{-1}$	-26.05
Biogeochemical flows (P)	$1.01 \cdot 10^{-1}$	$1.01 \cdot 10^{-1}$	-0.38
Land-system change	$1.35 \cdot 10^{-3}$	$2.10 \cdot 10^{-3}$	-55.69
Freshwater use	$7.96 \cdot 10^{-2}$	$4.30 \cdot 10^{-1}$	-440.16
Aerosol loading	$1.87 \cdot 10^{1}$	$2.30 \cdot 10^{1}$	-23.21

The impact difference between just cancelling the CO_2 emissions or those equivalent for the compensation of the impact on the energy imbalance PB does not cause the transgression of any additional PBs.

Finally, the combination of DACCS and the switch to the renewable energy mix is considered. The scenario is modelled by changing the electricity used by all foreground processes, including the DACCS system. A significant improvement is seen since less CO_2 has to be captured (316,000,000 tonnes) to obtain net zero CO_2 emissions. As observed in Table 10-7, the capture of all CO_2 is enough to position the sector within safe space in the climate change and ocean acidification boundaries (opposite to what happened in the scenario where the BAU mix was used). In this scenario, negative side effects of DACCS are also mitigated by the change in the electricity mix, showing the most significant

improvements in the aerosol loading and the stratospheric ozone depletion boundaries. The increase in the impacts on these planetary boundaries is reduced by more than 95%, resulting in a worsening of only 1.1% and 0.65%, respectively. The nitrogen boundary is however impaired by the mix change due to the inclusion of solar concentrated power.

Table 10-7: Impact reduction with respect to the current situation achieved by the implementation of DACCS (sustainable mix and cancellation of CO_2 emissions).

Planetary boundary	**$occSoSOS_{PB}$ BAU practice**	**$occSoSOS_{PB}$ DACCS**	**% reduction**
Energy imbalance at top of atmosphere	$1.08 \cdot 10^{2}$	$3.67 \cdot 10^{0}$	96.60
Atmospheric CO_2 concentration	$1.12 \cdot 10^{2}$	$2.59E \cdot 10^{0}$	97.69
Stratospheric ozone depletion	$4.83 \cdot 10^{-2}$	$4.86 \cdot 10^{-2}$	-0.65
Ocean acidification	$3.60 \cdot 10^{1}$	$8.27 \cdot 10^{-1}$	97.70
Biogeochemical flows (N)	$6.45 \cdot 10^{-1}$	$8.77 \cdot 10^{-1}$	-36.01
Biogeochemical flows (P)	$1.01 \cdot 10^{-1}$	$1.01 \cdot 10^{-1}$	-0.04
Land-system change	$1.35 \cdot 10^{-3}$	$1.91 \cdot 10^{-3}$	-41.61
Freshwater use	$7.96 \cdot 10^{-2}$	$3.32 \cdot 10^{-1}$	-316.59
Aerosol loading	$1.87 \cdot 10^{1}$	$1.89 \cdot 10^{1}$	-1.10

The capture of additional CO_2 to compensate for the rest of impacts on the energy imbalance boundary becomes unnecessary since the switch to a renewable-energy based mix already cancels most carbon monoxide, methane, and dinitrogen monoxide emissions (Energy mix). However, the use of DACCS powered by the renewable mix would yield the same results requiring less DACCS installed capacity. In this case, 253,000,000 tonnes of CO_2 would need to be captured (a reduction of 15.5% from the last scenario), to achieve the results shown in Table 10-8.

Table 10-8: Impact reduction with respect to the current situation achieved by the implementation of DACCS (sustainable mix and aiming for the fraction of occupied SoSOS for the energy imbalance PB to be equal to zero).

Planetary boundary	**$occSoSOS_{PB}$ BAU practice**	**$occSoSOS_{PB}$ DACCS**	**% reduction**
Energy imbalance at top of atmosphere	$1.08 \cdot 10^{2}$	$0.00 \cdot 10^{0}$	100.00
Atmospheric CO_2 concentration	$1.12 \cdot 10^{2}$	$-1.31 \cdot 10^{0}$	101.17
Stratospheric ozone depletion	$4.83 \cdot 10^{-2}$	$4.90 \cdot 10^{-2}$	-1.41
Ocean acidification	$3.60 \cdot 10^{1}$	$-4.20 \cdot 10^{-1}$	101.17
Biogeochemical flows (N)	$6.45 \cdot 10^{-1}$	$8.84 \cdot 10^{-1}$	-37.12
Biogeochemical flows (P)	$1.01 \cdot 10^{-1}$	$1.01 \cdot 10^{-1}$	-0.05
Land-system change	$1.35 \cdot 10^{-3}$	$1.93 \cdot 10^{-3}$	-43.25
Freshwater use	$7.96 \cdot 10^{-2}$	$3.42 \cdot 10^{-1}$	-329.36
Aerosol loading	$1.87 \cdot 10^{1}$	$1.90 \cdot 10^{1}$	-1.43

Overall, the implementation of DACCS technologies acts as a mitigation measure for the chemical industry to reduce its impacts on the climate change and ocean acidification boundaries, at the expense of increasing its contribution on the rest of boundaries, especially those related to resource use. Still, the deployment of sufficient DACCS capacity to achieve the desired reduction of the emitted CO_2 do not cause the transgression of any other PBs in any of the considered scenarios and should therefore be considered a valid option to transition towards a more sustainable chemical industry. If combined with the switch to a renewable mix, results are improved even further and allow to position the sector within the allocated SoSOS it has been assigned according to the FSoSOS principle. Even negative contributions on the CO_2 concentration and ocean acidification boundaries can be achieved, indicating that the sector could be capturing carbon present in air which does not derive from its activity.

10.4.2.2 Bioenergy with carbon capture and storage (BECCS)

As with DACCS, BECCS is an emerging technology not yet present in environmental databases such as *ecoinvent*. Therefore, the viability and impact of BECCS deployment is assessed by modelling the activity as an additional process providing net negative CO_2 emissions, according to the inputs and outputs shown in Table S5-6. A BECCS system consists of the infrastructure for energy production from biomass, considering a co-generation plant using wood chips, plus a CCS unit for the capture of emissions working with monoethanolamine solvent. The biomass burned in the plant is grown capturing CO_2 in air, while the emissions from the plant are captured and stored geologically as seen in Fig. 10-21.

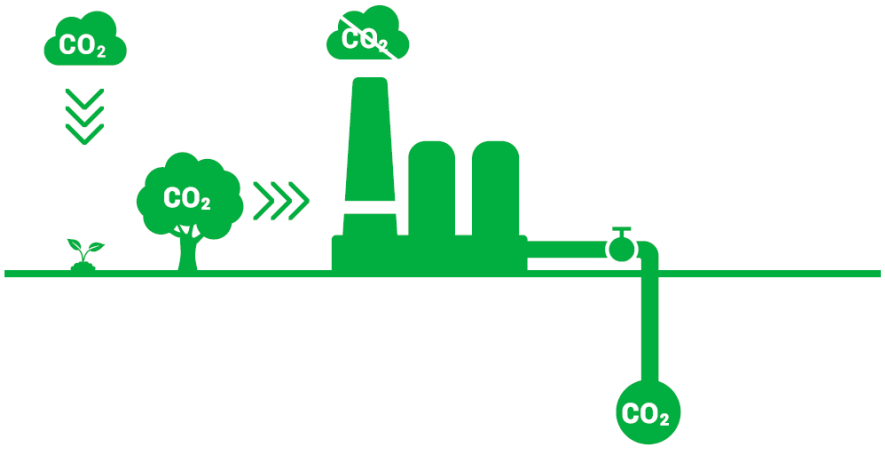

Fig. 10-21: Schematic representation of the concept behind BECCS (Fridahl et. al., 2020).

The input CO_2 emissions modelled as negative (captured by biomass during photosynthesis) are calculated assuming 0.841 kg of wood chips are required for the production of one kWh in the modelled plant and using the carbon content of the biomass, which is that of 49.4% (Galán-Martín et al., 2021). The electricity demanded by the CCS unit is firstly assumed to be acquired using the BAU electricity mix. Finally, the transport and storage of the captured CO_2 is also included and modelled according to the inventories in Table S5-4.

It is to be noted that, opposed to DACCS facilities which are single product (i.e., CO_2), BECCS plants generate electricity on top of CO_2. There are different ways to deal with multiproduct units in LCA. However, since electricity production is not the focus of this scenario, the total impacts of BECCS are allocated between the two products. Without loss of generality, impact allocation is done based on

economic criteria, considering prices of 60 USD/t CO_2 and 50 USD/MWh (Iribarren, 2013; Petrakopoulou, 2014). With this method, only a fraction of the total impact of the BECCS plant is attributed to the CO_2 captured.

As was done for DACCS, it is first necessary to obtain the installed capacity of BECCS required to attain net emissions of CO_2 equivalent to zero. In this case, the volume to sequester is 22% higher than with DACCS, of 383,000,000 tonnes. The net balance for CO_2 once inputs and outputs for the capture process are considered is lower for DACCS. The CO_2 emissions produced by the carbon capture process itself are higher for BECCS than for DACCS, giving a higher removal efficiency. Fig. 10-22 shows the how impact on the PBs is modified with respect to the current situation when deploying BECCS using the same format as Fig. 10-20. Table 10-10 shows the results of the implementation of BECCS for every PB in comparison with the current situation, where no mitigation techniques are applied.

Table 10-9: Impact reduction with respect to the current situation achieved by the implementation of BECCS (conservative scenario: BAU mix and cancellation of CO_2 emissions).

Planetary boundary	**$occSoSOS_{PB}$ BAU practice**	**$occSoSOS_{PB}$ BECCS**	**% reduction**
Energy imbalance at top of atmosphere	$1.08 \cdot 10^{2}$	$-7.69 \cdot 10^{0}$	107.14
Atmospheric CO_2 concentration	$1.12 \cdot 10^{2}$	$-9.74 \cdot 10^{0}$	108.66
Stratospheric ozone depletion	$4.83 \cdot 10^{-2}$	$5.34 \cdot 10^{-2}$	-10.37
Ocean acidification	$3.60 \cdot 10^{1}$	$-3.11 \cdot 10^{0}$	108.66
Biogeochemical flows (N)	$6.45 \cdot 10^{-1}$	$3.38 \cdot 10^{0}$	-423.44
Biogeochemical flows (P)	$1.01 \cdot 10^{-1}$	$1.01 \cdot 10^{-1}$	-0.07
Land-system change	$1.35 \cdot 10^{-3}$	$1.38 \cdot 10^{-3}$	-1.97
Freshwater use	$7.96 \cdot 10^{-2}$	$8.23 \cdot 10^{-2}$	-3.33
Aerosol loading	$1.87 \cdot 10^{1}$	$1.95 \cdot 10^{1}$	-3.81

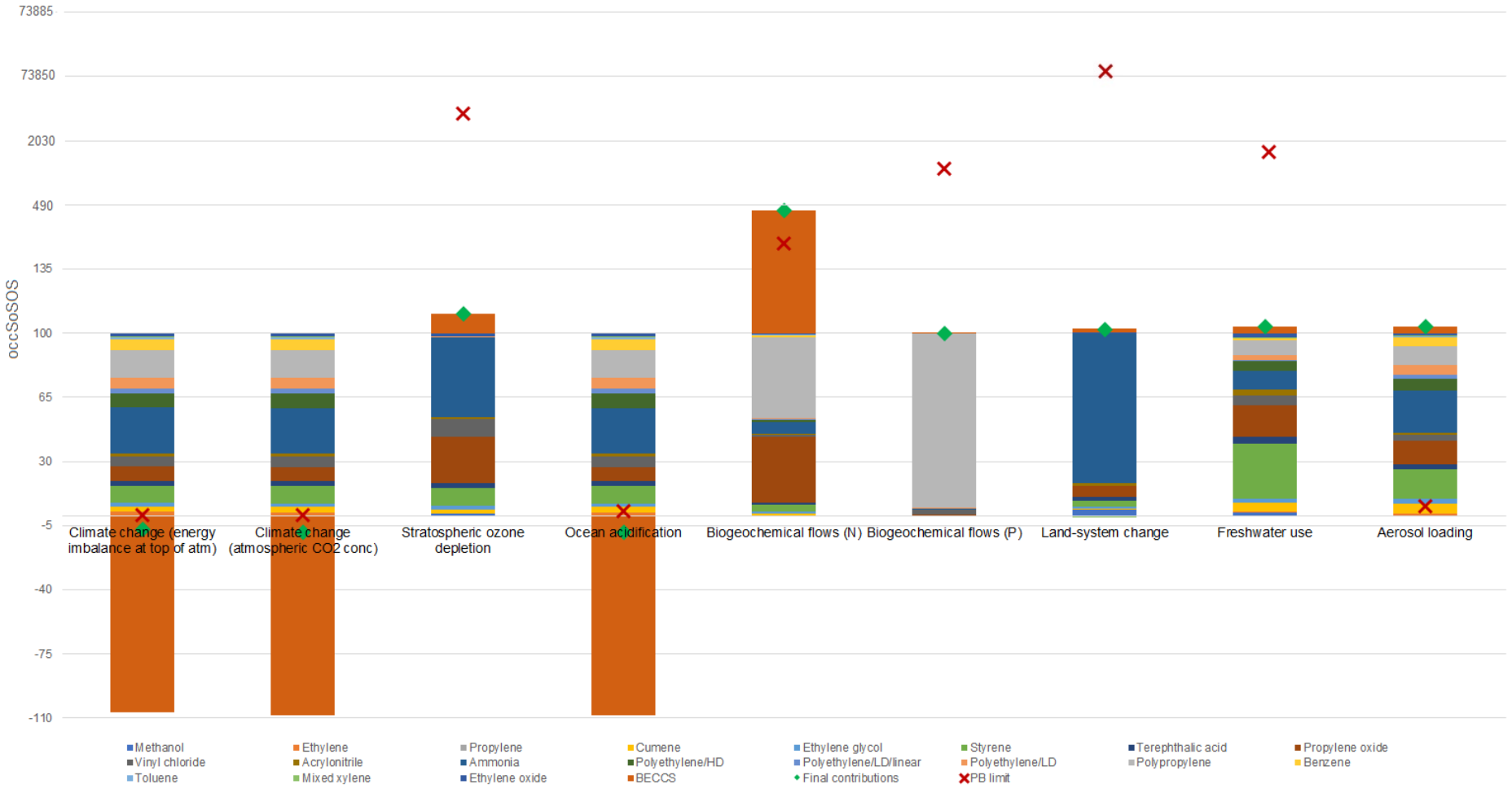

Fig. 10-22: Impact reduction with respect to the current situation achieved by the implementation of BECCS in terms of % over the total contribution to each PB in the current scenario (conservative scenario: BAU mix and cancellation of only CO_2 emissions).

Note that, in addition to environmental benefits, this scenario would result in the generation of 227 TWh. That would account for 8.1% of Europe's electricity demand, which was that of 2800 TWh in 2018 (the year of the study, European Union, 2020f). The obtained electricity could also be used to totally cover the industry's demand (25 tWh/yr), while the surplus could be sold.

Table 10-10: Impact reduction with respect to the current situation achieved by the implementation of BECCS (conservative scenario: BAU mix and cancellation of CO_2 emissions).

Planetary boundary	**occSoSOS$_{PB}$ BAU practice**	**occSoSOS$_{PB}$ BECCS**	**% reduction**
Energy imbalance at top of atmosphere	$1.08 \cdot 10^{2}$	$-7.69 \cdot 10^{0}$	107.14
Atmospheric CO_2 concentration	$1.12 \cdot 10^{2}$	$-9.74 \cdot 10^{0}$	108.66
Stratospheric ozone depletion	$4.83 \cdot 10^{-2}$	$5.34 \cdot 10^{-2}$	-10.37
Ocean acidification	$3.60 \cdot 10^{1}$	$-3.11 \cdot 10^{0}$	108.66
Biogeochemical flows (N)	$6.45 \cdot 10^{-1}$	$3.38 \cdot 10^{0}$	-423.44
Biogeochemical flows (P)	$1.01 \cdot 10^{-1}$	$1.01 \cdot 10^{-1}$	-0.07
Land-system change	$1.35 \cdot 10^{-3}$	$1.38 \cdot 10^{-3}$	-1.97
Freshwater use	$7.96 \cdot 10^{-2}$	$8.23 \cdot 10^{-2}$	-3.33
Aerosol loading	$1.87 \cdot 10^{1}$	$1.95 \cdot 10^{1}$	-3.81

As seen in Table 10-10, the incorporation of BECCS allows for the reduction of the impact on the carbon-related boundaries and has low additional impacts on the others, with the exception of the nitrogen cycle limit. The energy requirement of the CCS unit and the need for fertilizers to grow biomass cause an increase of 423% of the system's contribution to the nitrogen PB. This is specially concerning as it causes the transgression of this boundary, even if just by 3.38%. The pressure exerted on the remaining PBs is much lower than in the DACCS scenario.

The capture of CO_2 using BECCS is enough to situate the chemical industry under the limit established by the PBs, since the BECCS process itself have much

lower emissions of other GHGs than DACCS. In the DACCS scenario, 173 million tonnes of other GHGs are emitted in order to obtain net zero emissions of CO_2, while in the BECCS scenario, only 21 million tonnes of other GHGs remain in the atmosphere once all CO_2 is removed. Since the aim to obtain net zero CO_2 emissions does not consider the rest of GHGs, this difference causes the variation in results.

Once the same BECCS capacity is combined with the renewable mix, the results follow the same direction they did with DACCS, achieving greater reductions in the targeted PBs, and also reducing the pressure on the ozone layer. The nitrogen boundary is the only PB still receiving a larger impact (Table 10-11). 252 million tonnes of CO_2 need to be captured in this scenario (34% lower than when using the BAU mix).

Table 10-11: Impact reduction with respect to the current situation achieved by the implementation of BECCS (renewable mix and cancellation of CO_2 emissions).

Planetary boundary	**$occSoSOS_{PB}$ BAU practice**	**$occSoSOS_{PB}$ BECCS**	**% reduction**
Energy imbalance at top of atmosphere	$1.08 \cdot 10^{2}$	$-7.57 \cdot 10^{0}$	107.03
Atmospheric CO_2 concentration	$1.12 \cdot 10^{2}$	$-7.73 \cdot 10^{0}$	106.87
Stratospheric ozone depletion	$4.83 \cdot 10^{-2}$	$1.59 \cdot 10^{-2}$	67.17
Ocean acidification	$3.60 \cdot 10^{1}$	$-2.47 \cdot 10^{0}$	106.87
Biogeochemical flows (N)	$6.45 \cdot 10^{-1}$	$2.96 \cdot 10^{0}$	-358.51
Biogeochemical flows (P)	$1.01 \cdot 10^{-1}$	$1.00 \cdot 10^{-1}$	0.35
Land-system change	$1.35 \cdot 10^{-3}$	$1.26 \cdot 10^{-3}$	7.07
Freshwater use	$7.96 \cdot 10^{-2}$	$1.21 \cdot 10^{-2}$	84.76
Aerosol loading	$1.87 \cdot 10^{1}$	$1.35 \cdot 10^{1}$	27.99

As with DACCS and to allow for final comparison between the two carbon capture routes, two additional scenarios have been modelled, both assuming the cancellation of all GHG emissions with BECCS, but one using the BAU mix and

the other using the sustainable mix. Table 10-12 and Table 10-13 show the resulting contributions to the PBs of both situations. Using the BAU mix, 359 million tonnes of CO_2 need to be removed from the atmosphere, which is less than the initial value found of 383. As previously discussed and seen in Table 10-10, the removal of all CO_2 not only cancels the effects of the industry on the target PBs, but also gives improvements of 7.1%, 9.7%, and 3.1% on the energy imbalance, atmospheric CO_2 concentration, and ocean acidification boundaries respectively. Thus, the removal of all CO_2 is not necessary in order to achieve an occupied fraction of SOS of 0% for the first mentioned PB. Since BECCS has lower non-CO_2 GHG emissions, the removal of 93.7% of total CO_2 is shown to be enough to achieve the results shown in Table 10-12.

Table 10-12: Impact reduction with respect to the current situation achieved by the implementation of BECCS (BAU mix and aiming for the fraction of occupied SoSOS for the energy imbalance PB to be equal to zero).

Planetary boundary	**$occSoSOS_{PB}$ BAU practice**	**$occSoSOS_{PB}$ BECCS**	**% reduction**
Energy imbalance at top of atmosphere	$1.08 \cdot 10^{2}$	$0.00 \cdot 10^{0}$	100.00
Atmospheric CO_2 concentration	$1.12 \cdot 10^{2}$	$-1.60 \cdot 10^{0}$	101.42
Stratospheric ozone depletion	$4.83 \cdot 10^{-2}$	$5.30 \cdot 10^{-2}$	-9.68
Ocean acidification	$3.60 \cdot 10^{1}$	$-5.11 \cdot 10^{-1}$	101.42
Biogeochemical flows (N)	$6.45 \cdot 10^{-1}$	$3.20 \cdot 10^{0}$	-395.23
Biogeochemical flows (P)	$1.01 \cdot 10^{-1}$	$1.01 \cdot 10^{-1}$	-0.06
Land-system change	$1.35 \cdot 10^{-3}$	$1.38 \cdot 10^{-3}$	-1.84
Freshwater use	$7.96 \cdot 10^{-2}$	$8.21 \cdot 10^{-2}$	-3.11
Aerosol loading	$1.87 \cdot 10^{1}$	$1.94 \cdot 10^{1}$	-3.55

Once the renewable mix is applied to the BECCS scenario aiming to cancel the occupation of SOS on the energy imbalance boundary, the needed CCS capacity out of all modelled scenarios is found, giving a result of 234 million tonnes of CO_2 to be removed. As seen in Table 10-13, the trespassing of all four target

boundaries is avoided. The ozone layer and the freshwater use PBs are again benefited the most by the renewable mix.

Table 10-13: Impact reduction with respect to the current situation achieved by the implementation of BECCS (sustainable mix and aiming for the fraction of occupied SoSOS for the energy imbalance PB to be equal to zero).

Planetary boundary	**$occSoSOS_{PB}$ BAU practice**	**$occSoSOS_{PB}$ BECCS**	**% reduction**
Energy imbalance at top of atmosphere	$1.08 \cdot 10^{2}$	$0.00 \cdot 10^{0}$	100.00
Atmospheric CO_2 concentration	$1.12 \cdot 10^{2}$	$1.91 \cdot 10^{-1}$	99.83
Stratospheric ozone depletion	$4.83 \cdot 10^{-2}$	$1.75 \cdot 10^{-2}$	63.87
Ocean acidification	$3.60 \cdot 10^{1}$	$6.09 \cdot 10^{-2}$	99.83
Biogeochemical flows (N)	$6.45 \cdot 10^{-1}$	$2.80 \cdot 10^{0}$	-334.05
Biogeochemical flows (P)	$1.01 \cdot 10^{-1}$	$1.01 \cdot 10^{-1}$	0.33
Land-system change	$1.35 \cdot 10^{-3}$	$1.26 \cdot 10^{-3}$	6.73
Freshwater use	$7.96 \cdot 10^{-2}$	$1.56 \cdot 10^{-2}$	80.45
Aerosol loading	$1.87 \cdot 10^{1}$	$1.38 \cdot 10^{1}$	26.61

The application of BECCS can also yield negative emissions and help reduce the impact of the sector even beyond the capture of its own GHGs. The combination with renewable energy gives positive results again. It must be kept in mind that both CCS units need a continuous energy source for their correct operation, thus, the mix cannot rely entirely on intermittent sources such as solar or wind energy. Even if the mix is thus not entirely based on renewable energies, its global increased sustainability yields positive results in all modelled scenarios.

10.4.2.3 Summary of CCS scenarios

Table 10-14 and Table 10-15 summarize the results of the carbon capture and storage scenarios for both DACCS and BECCS technologies, respectively, as well as the amount of CO_2 that must be captured in each of them. Note how the change to a renewable mix allows for a capacity reduction for BECCS and DACCS in all scenarios.

The application of DACCS results in higher removal efficiency in terms of CO_2 since the process itself has lower emissions of the pollutant (note how higher capacities are needed in both CO_2 removal scenarios). Regardless, they have been found to emit more non-CO_2 GHGs than BECCS. Thus, once all GHGs are considered, BECCS perform better if powered with renewable energies, which enhance their efficiency by reducing CO_2 emissions, and less capacity is required to obtain the same reduction in the occupation of SOS. Fig. 10-23 shows the volumes of CO_2 each technology needs to sequester (including its own) to achieve the goals proposed. On the one hand, in the CO_2 scenario, the aim is to obtain final zero emissions of this gas, which is the GHG emitted in higher volumes, and which has a PB of its own. On the other hand, the GHGs scenario aims to set the occSoSOS at zero by capturing enough CO_2 to also cancel the emissions of all other greenhouse gases.

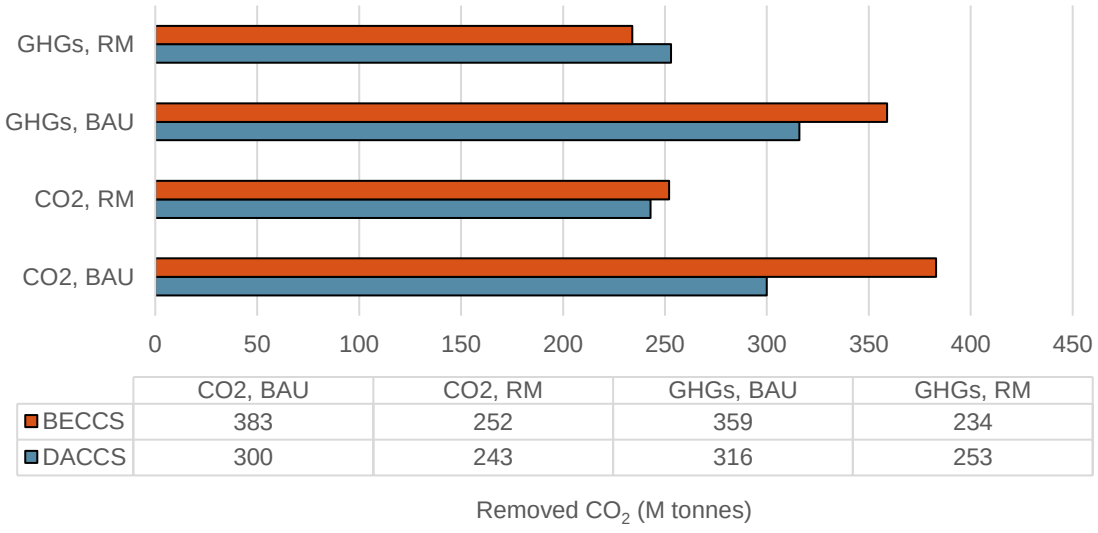

Fig. 10-23: Carbon capture and storage capacities required to fulfil the goals of the eight modelled scenarios (million tonnes CO2), where RM: renewable mix; BAU: business and usual mix.

*Table 10-14: Summary of DACCS scenarios. In each cell the symbol code shows if the boundary was transgressed in the current situation and its state after the implementation of CCS: * denotes the boundary is transgressed while – means it is not. The symbols are expressed as follows: BAU situation/scenario.*

$occSoSOS_{PB}$ / PB	**DACCS** *CO_2, BAU mix*	**DACCS** *CO_2, new mix*	**DACCS** *GHGs, BAU mix*	**DACCS** *GHGs, new mix*
Energy imbalance	$5.18 \cdot 10^{0}$ */*	$3.67 \cdot 10^{0}$ */*	$0.00 \cdot 10^{0}$ */-*	$0.00 \cdot 10^{0}$ */-*
CO_2 conc.	$2.99 \cdot 10^{0}$ */*	$2.59 \cdot 10^{0}$ */*	$-2.55 \cdot 10^{0}$ */-*	$-1.31 \cdot 10^{0}$ */-*
Ozone depletion	$7.28 \cdot 10^{-2}$ *-/-*	$4.86 \cdot 10^{-2}$ *-/-*	$7.40 \cdot 10^{-2}$ *-/-*	$4.90 \cdot 10^{-2}$ *-/-*
Ocean acidification	$9.54 \cdot 10^{-1}$ */-*	$8.27 \cdot 10^{-1}$ */-*	$-8.15 \cdot 10^{-1}$ */-*	$-4.20 \cdot 10^{-1}$ */-*
N cycle	$8.05 \cdot 10^{-1}$ *-/-*	$8.77 \cdot 10^{-1}$ *-/-*	$8.13 \cdot 10^{-1}$ *-/-*	$8.84 \cdot 10^{-1}$ *-/-*
P cycle	$1.01 \cdot 10^{-1}$ *-/-*	$1.01 \cdot 10^{-1}$ *-/-*	$1.01 \cdot 10^{-1}$ *-/-*	$1.01 \cdot 10^{-1}$ *-/-*
Land-system change	$2.07 \cdot 10^{-3}$ *-/-*	$1.91 \cdot 10^{-3}$ *-/-*	$2.10 \cdot 10^{-3}$ *-/-*	$1.93 \cdot 10^{-3}$ *-/-*
Freshwater use	$4.13 \cdot 10^{-1}$ *-/-*	$3.32 \cdot 10^{-1}$ *-/-*	$4.30 \cdot 10^{-1}$ *-/-*	3.42E-01 *-/-*
Aerosol loading	$2.28 \cdot 10^{1}$ */*	$1.89 \cdot 10^{1}$ */*	$2.30 \cdot 10^{1}$ */*	$1.90 \cdot 10^{1}$ */*
Captured CO_2 (million tonnes)	300	243	316	253

Notice how impacts on all PBs show the correspondent decrease that the switch to the sustainable mix grants, with the exception of the nitrogen cycle. As discussed, the nitrogen PB is the only boundary not benefited from the change fin the electricity, owing mostly to concentrated solar power and biomass.

In the DACCS scenario, the deployment of the technologies does not cause the transgression of any PB which was previously respected, while in the case of BECCS, the pressure increase on the nitrogen cycle causes the chemical sector to be clearly above the limit. However, BECCS not only require lower capacity as discussed but also allow for energy production. In the nominal case, the produced electricity could cover around 2.5% of Europe's demand. The decision on which technology to apply could widely depend on the region and the preferences established during the planning of the mitigation actions, since they both present benefits and drawbacks. With the correct management of nitrogen flows, the BECCS option could yield better results than the DACCS scenario. When aiming

to reduce the pressure on the target PBs and incorporating the renewable mix, BECCS require 7.5% less capacity than DACCS.

*Table 10-15: Summary of BECCS scenarios. In each cell the symbol code shows if the boundary was transgressed in the current situation and its state after the implementation of CCS: * denotes the boundary is transgressed while – means it is not. The symbols are expressed as follows: BAU situation/scenario.*

$occSoSOS_{PB}$ / PB	**BECCS** *CO_2, BAU mix*	**BECCS** *CO_2, new mix*	**BECCS** *GHGs, BAU mix*	**BECCS** *GHGs, new mix*
Energy imbalance	$-7.69\cdot10^{0}$ */-	$-7.57\cdot10^{0}$ */-	$0.00\cdot10^{0}$ */-	$0.00\cdot10^{0}$ */-
CO_2 conc.	$-9.74\cdot10^{0}$ */-	$-7.73\cdot10^{0}$ */-	$-1.60\cdot10^{0}$ */-	$1.91\cdot10^{-1}$ */-
Ozone depletion	$5.34\cdot10^{-2}$ -/-	$1.59\cdot10^{-2}$ -/-	$5.30\cdot10^{-2}$ -/-	$1.75\cdot10^{-2}$ -/-
Ocean acidification	$-3.11\cdot10^{0}$ */-	$-2.47\cdot10^{0}$ */-	$-5.11\cdot10^{-1}$ */-	$6.09\cdot10^{-2}$ */-
N cycle	$3.38\cdot10^{0}$ -/*	$2.96\cdot10^{0}$ -/*	$3.20\cdot10^{0}$ -/*	$2.80\cdot10^{0}$ -/*
P cycle	$1.01\cdot10^{-1}$ -/-	$1.00\cdot10^{-1}$ -/-	$1.01\cdot10^{-1}$ -/-	$1.01\cdot10^{-1}$ -/-
Land-system change	$1.38\cdot10^{-3}$ -/-	$1.26\cdot10^{-3}$ -/-	$1.38\cdot10^{-3}$ -/-	$1.26\cdot10^{-3}$ -/-
Freshwater use	$8.23\cdot10^{-2}$ -/-	$1.21\cdot10^{-2}$ -/-	$8.21\cdot10^{-2}$ -/-	$1.56\cdot10^{-2}$ -/-
Aerosol loading	$1.95\cdot10^{1}$ */*	$1.35\cdot10^{1}$ */*	$1.94\cdot10^{1}$ */*	$1.38\cdot10^{1}$ */*
Captured CO_2 (million tonnes)	383	252	359	234

Importantly, two additional factors need to be considered to assess the viability of DACCS and BECCS routes towards a more sustainable chemical industry.

On the one side, the capacity for underground storage of CO_2 in geological reservoirs is limited. Therefore, the capacity required to sequester all the CO_2 captured with DACCS and BECCS is next compared to Europe's storage capacity as given by the three main types of onshore geological formations: deep saline aquifers, depleted hydrocarbon fields, and depleted coal fields. Table 10-16 shows the percentage of Europe (EU-28) geological storage capacity (SUPER-Lab-repository, 2020) that would be occupied annually with the CO_2 collected in each of the proposed scenarios. Deep saline aquifers account for 79% of the total storage space, and are followed by hydrocarbon fields, which add another 20% to the total. Cold fields are minority storage sites which only represent 1% of the

total EU-28 capacity. The annual required space to store all the capture CO_2 mostly lies between 0.03% and 0.04% of the total.

Table 10-16: Occupation of EU-28's geological storage capacity taken up by the proposed scenarios.

Scenario	**CO_2 for storage (million tonnes/yr)**	**% of EU-28's capacity occupied (yr)**
DACCS (CO2, BAU mix)	300	0.0344
DACCS (CO2, renewable mix)	243	0.0279
DACCS (GHGs, BAU mix)	316	0.0363
DACCS (GHGs, renewable mix)	253	0.0290
BECCS (CO2, BAU mix)	383	0.0440
BECCS (CO2, renewable mix)	252	0.0289
BECCS (GHGs, BAU mix)	359	0.0412
BECCS (GHGs, renewable mix)	234	0.0269

Considering the CO_2 captured would be attributed solely to the chemical industry and is an annual requirement, it is clear that the volume of stored gas of the sector must be reduced either by using it as a raw material in the plants or by selling it to other industries also for its use. The recycling of CO_2 would additionally aid the shift towards a circular economy, instead of perpetuating the linear path of use and deposit of fossil CO_2. With the same downscaling method that was applied to assign the SOS correspondent to the EU-28's chemical industry, the fraction of total storage available is that of 0.04%. Thus, the chemical industry would consume that fraction in only one year if no measures were applied.

On the other side, the land necessary to grow biomass is not reflected in the calculations, since the land-use change boundary represents only the loss of forest area. However, one of the main drawbacks of BECCS stems precisely from its land occupation, which could interfere mainly with food production, and ecosystems in general. The required land surface to grow enough biomass to annually capture the volumes of CO_2 withdrawn in the BECCS scenario is thus calculated by using inventories for the production of one kg of wet poplar (Galán-

Martín et al., 2021; Gasol et al., 2009), considering 0.81 kg of biomass are required for each kWh produced by BECCS.

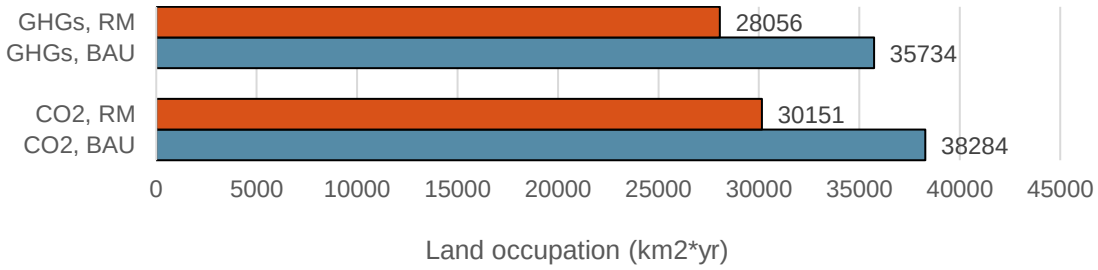

Fig. 10-24: Land requirements of all BECCS scenarios (land in km^2yr necessary to grow the biomass for the process).

The results of the land requirements to grow the biomass necessary for the sequestering of CO_2 and energy production in all BECCS scenarios are shown in Fig. 10-24. The total area of the EU-28 region is that of around four million square kilometres (World Data Bank, 2019). Thus, the required land would represent around 0.70% - 0.96% of the total. Biomass could be grown and harvested in the same regions annually. However, the transgression of the land-use PB by around 6% could be caused.

Additionally, the European Commission's Resource Efficiency Roadmap urges to keep the annual rate of new land use below 800 km^2 and to achieve a zero net land uptake by 2050 (EEA, 2018). The industry's requirements are broadly above this limit, so alternatives could be to grow BECCS biomass in recycled land, reduce the capacity by combining BECCS with DACCS and other CCS technologies, use agricultural and forestry residues to reduce land requirements, and weight if the negative impact in terms of land uptake is compensated by the benefits BECCS provide. Second generation biomass (i.e., grown on so-called marginal land, the one that is not suitable for agriculture) together with third generation biomass (algae) could also alleviate this burden (although the later also incurs in huge water use requirements).

Both DACCS and BECCS function as significantly efficient mitigation techniques in terms of reducing the pressure on the climate change and ocean acidification PBs exerted by the chemical sector. However, their deployment comes at the expense of elevated resource use and increased pressures on the rest of boundaries. The implementation of these technologies must therefore be coupled

with a general reduction of total emissions through prevention actions, and the switch to a carbon-free energy and electricity mix.

10.4.3 Green hydrogen production and chlor-alkali electrolysis powered with renewable energy

The results breakdown placed ammonia among the top four worst environmental performers for all PBs (Table 10-3), owing mainly to its large production volume. In this context, a cleaner production of the chemical could have a proportional positive impact on the performance of the chemical industry. Analogously, the chlor-alkali electrolysis for the obtention of chlorine and sodium hydroxide is highly energy-intensive, causing the contributions of every process using these chemicals as feedstocks to be vastly incremented, especially for propylene oxide but also for other chemicals, such as vinyl chloride or terephthalic acid, which obtain their reagents from this process.

With the aim to enhance the global sustainability of the chemical sector, a scenario is proposed where ammonia and the rest of chemicals using hydrogen as a baseline reagent use “green” hydrogen and where the chlor-alkali electrolysis is powered with the renewable mix, since its main environmental burdens stem from its electricity consumption (Liu & Elgowainy, 2019).

Besides propylene oxide, terephthalic acid, benzene from coking and vinyl chloride also rely on the chlor-alkali electrolysis to obtain sodium hydroxide, which is a direct input from the technosphere for all three processes. After the change, the electricity consumed by the electrolysis specifically (foreground process) is produced using the mix presented in Fig. 10-18, while the rest of activities continue (background processes) to use the BAU mix.

As for hydrogen, it has been obtained so far from the cracking of fossil fuels (i.e., grey hydrogen), but is produced in this new scenario by the electrolysis of water powered by wind energy (i.e., green hydrogen). The production of cleaner hydrogen is gaining momentum as it holds great potential as a fuel, and various routes exist receiving colour-coded names. The hydrogen obtained through the traditional route, described in the Partial oxidation and Steam reforming sections for the production of syngas, is referred to as “grey hydrogen”, since it is based on fossil fuels. If the CO_2 emissions of the process were to be captured, as

proposed in the Direct Air Capture with Carbon Storage (DACCS) and Bioenergy with carbon capture and storage (BECCS) scenarios, the hydrogen would receive the label of “blue hydrogen”. “Green hydrogen” is obtained when water electrolysis powered by renewable energies or gasified sustainable biomass is used to obtain the H_2 (Hydrogen council, 2021; Service, 2018). Additional labels, such as “pink”, “brown”, or “white” hydrogen describe other sources of H_2 (hydrogen produced by electrolysis powered by nuclear energy, extracted from the gasification of fossil fuels, or obtained as a byproduct of another process, respectively).

Unlike general plants, the electrolysis of water can be powered by intermittent energies such as solar or wind. For this scenario, wind energy was employed since it offers slightly better results than photovoltaic energy, even if their performances are similar (González-Garay et al., 2019; Hacatoglu et al., 2012).

The substitution of grey by green hydrogen impacts the production of different chemicals. The most important one is ammonia. It is conventionally produced by the Haber-Bosch process, which manufactures ammonia from nitrogen and hydrogen (syngas). However, up to this point, this syngas has been considered to be obtained from the steam reforming (or the partial oxidation) of hydrocarbons. These processes are now replaced by the obtention of hydrogen from water electrolysis. Other chemicals also benefitting from the new production route for hydrogen are methanol, all three PE types, PP, and vinyl chloride, which are also manufactured from hydrogen.

In all the cases, the main process for the synthesis of the chemical (e.g., the Haber-Bosch phase of the process) is maintained as in the database, while impacts from grey hydrogen (from the dataset for hydrogen cracking) are replaced by those associated with the production of the same amount of green hydrogen. Note that green hydrogen production, not available in *ecoinvent*, is modelled using the inventories in Table S5-7 (Gonzalez-Garay, 2019; Galán-Martín, 2021). The electricity needs therein include not only hydrogen production, but also the preparation of hydrogen for average feeding conditions of subsequent processes, as well as its compression for storage to ensure a continuous operation in plants (since wind energy is intermittent). The processes improved in this scenario are briefed in Table 10-17.

Table 10-17: Affected processes (green hydrogen and mix change for the chlor-alkali process scenario).

Direct inputs from the chlor-alkali process (energy mix change)
Chlorohydrin process (propylene oxide)
Coke production (benzene)
Oxidation of p-xylene (terephthalic acid)
Direct chlorination and oxychlorination of ethylene (vinyl chloride)
H_2 as direct input (change to green H_2)
Polymerization of ethylene (LDPE, LLDPE, and HDPE)
Polymerization of propylene (PE)
Direct chlorination and oxychlorination of ethylene (vinyl chloride)
Steam reforming and partial oxidation (ammonia)
Steam reforming (methanol)

The results of the consequential LCA for this scenario are shown in Table 10-18. Improvements are only seen in the climate change and ocean acidification boundaries (between 1.80% and 2.59%), while the rest are worsened. In line with findings in González-Garay et al. (2019), the freshwater use and nitrogen inputs are the main impaired PBs (30.70% and 48.64%, respectively) even if in this case none of them is transgressed. The slight improvements in the three benefited boundaries seem too small to counteract the large quantities of freshwater needed in the electrolysis process and the nitrogen flows associated with the renewable mix and wind energy (Energy mix). The pressure on the ozone depletion, land system change, aerosol loading, and phosphorus cycle PBs is also increased in comparison to the BAU scenario.

The main drawback of the process for the obtention of green hydrogen is its large energy consumption. Renewable energies, which seem carbon neutral, still have some CO_2 emissions associated to their life-cycle and are unable to improve the performance of the scenario significantly. In fact, according to the calculations

performed in this study, green hydrogen represents “only” an 11.7% reduction in GHGs in comparison with grey hydrogen. Therefore, despite the potential offered by alternative hydrogen production methods, improvements in energy efficiency are required any of them can be considered realistic routes towards the decarbonisation of the chemical sector. The availability of completely carbon-free energy sources would also represent a major improvement for the obtention of clean hydrogen. In addition, while the improvements in energy requirements for hydrogen production could mitigate the burden-shifting occurring to the ozone depletion, aerosol loading, and nutrient flows, the water boundary would still suffer large damage, since 11 kg of water are needed to produce 1 kg of H_2. Considering this boundary is far from being transgressed, the effect of the increased water uptake could be justified, but only if the improvement on other PBs was significant enough.

Table 10-18: Observed changes on the contributions to the PBs after the switch from grey to green H_2 and the powering of the chlor-alkali process with the renewable mix.

Planetary boundary	**occSoSOS$_{PB}$**	**occSoSOS$_{PB}$ green H_2**	**% reduction**
Energy imbalance at top of atmosphere	$1.08 \cdot 10^{2}$	$1.05 \cdot 10^{2}$	2.59
Atmospheric CO_2 concentration	$1.12E \cdot 10^{2}$	$1.10 \cdot 10^{2}$	1.80
Stratospheric ozone depletion	$4.83 \cdot 10^{-2}$	$4.96 \cdot 10^{-2}$	-2.73
Ocean acidification	$3.60 \cdot 10^{1}$	$3.52 \cdot 10^{1}$	2.30
Biogeochemical flows (N)	$6.45 \cdot 10^{-1}$	$9.59 \cdot 10^{-1}$	-48.64
Biogeochemical flows (P)	$1.01 \cdot 10^{-1}$	$1.02 \cdot 10^{-1}$	-0.90
Land-system change	$1.35 \cdot 10^{-3}$	$1.38 \cdot 10^{-3}$	-2.16
Freshwater use	$7.96 \cdot 10^{-2}$	$1.04 \cdot 10^{-1}$	-30.70
Aerosol loading	$1.87 \cdot 10^{1}$	$1.96 \cdot 10^{1}$	-4.58

Regarding the change of the electricity mix in the chlor-alkali electrolysis, a clear improvement can be seen in GHG emissions per kilogram of product owing to the new mix, which reduced CO_2 ad GHG emissions by 67.8% and 67.7%,

respectively, compared to the BAU mix (see Energy mix section). However, these improvements are diluted since only the direct consumption of electrolytic plants (and not the complete energy demand from cradle-to-gate) can be substituted by green energy. For example, 52% of propylene oxide's CO_2 emissions were attributed to the production of chlorine and sodium hydroxide, yet only a 23% reduction is seen despite a 35% (=0.52·0.678) could have been expected.

10.4.4 Summary of improvement pathways

Fig. 10-25 shows a visual summary of the improvements (in green) achieved or the deteriorations of the state of the PBs (in red) suffered by the application of the proposed actions. Green or red outlines indicate whether the boundary ends up being transgressed or not in each scenario (respectively). For the DACCS and BECCS case, only the models where the contribution to the energy imbalance PB is cancelled are represented in the figure. This figure shows how a global assessment of the repercussions on all environmental categories of any measure is needed before its implementation.

On the one hand, this representation allows to quickly identify if burden-shifting is occurring, and the magnitude of the repercussion of each measure. As discussed, in the BECCS scenarios, the state of the nitrogen cycle deteriorates by 395% and 334% in respect to the original situation, while in the DACCS cases, the freshwater use boundary takes the greatest hit (suffering a deterioration of 440% and 329%), even if it does not end up being transgressed. A change of the electricity mix or the production of hydrogen alone prove insufficient.

On the other hand, note how the improvement yielded by the sustainable mix is also clear. Since the electricity used by the DACCS and BECCS systems represents a significant percentage of the total electricity in both CCS scenarios, the general change seen from the mix switch in the DACCS and BECCS scenarios appears to be larger than in the model where only the mix is changed.

Finally, Fig. 10-25 evidences how none of the measures allow to respect the aerosol loading boundary, since most were focused on the principal environmental problem of the sector, which is GHG emissions. Thus, special measures for the reduction of aerosol emissions as well would need to be

considered to achieve a situation where all PBs were respected. As discussed during the analysis of the results (Egalitarian allocation), the energy sector is responsible for a high fraction of the total nitrogen and sulfur oxide emissions, which are two of the three main aerosols found to be emitted by the chemical industry. Additionally, as shown in the Aerosol loading section, styrene and propylene oxide are the chemicals showing slightly larger contributions to the aerosol loading PB due to their energy demand.

The modelling of the electricity mix change confirms how the switch to a more sustainable mix allows for significant reductions in the total impact on the aerosol loading PB, all in the specific scenario but also in the DACCS and BECCS cases. Therefore, if data on background processes was available and the electricity mix change could be entirely done, the aerosol loading PB would be benefitted. Further measures to improve the state of this PB would need to be focused on NMVOCs, for example by the reduction of the use of organic solvents.

Fig. 10-25: Summary of improvement pathways where the % of total improvement or worsening of the occSoSOS is represented for each included scenario.

11 Conclusions

The principal challenges of the study have been tackled, including the need to characterize the sector, the collection and adaptation of *ecoinvent* data to the PB-LCIA framework, the implementation of different allocation criteria to correctly downscale the PBs to the assessed system, and the development of a data quality and uncertainty analysis.

Therefore, the aims of the study have also been fulfilled, yielding the following conclusions (numbered in accordance with the goal of the study they refer to):

1) The development of a model of the chemical industry selecting a representative range of chemicals and identifying the interlinks between them to avoid the double-counting of impacts has been successful. The PBs have been downscaled accordingly (to the selected processes) so the results are in concordance with the analysed activities. The allocation of the available SOS for the chemical industry in general (EUCISoSOS) and for the selected chemicals (FSoSOS) through the egalitarian principle leads to the drawing of the same conclusions in terms of number of transgressed PBs.

2) The data necessary for the quantification of the impacts of the chemical industry on the PBs have been collected and the corresponding calculations have been performed using Microsoft Excel and Matlab. As a result, the contributions of the European chemical industry on the PBs have been obtained.

3) Following common practice, an egalitarian allocation has been taken as the principal approach for the downscaling of the PBs, and a non-egalitarian method has also been implemented for the sake of comparison. In compliance with similar studies, results are highly sensitive to the allocation method. The non-egalitarian approach, for instance, provides more homogeneous results across the PBs since it dampens the contributions to PBs which are already under high stress levels globally, while amplifying the rest. Despite this, the non-egalitarian method indicates that seven out of the nine PBs are met. Out of the two approaches, the egalitarian method is found to be the allocation principle providing more adequate results since it allows to set limits for the

PBs with total independence from the current situation of the PBs and to narrow the allocation down to the studied system. The differences in the results denote the importance of transparency regarding the choice of the allocation method in PB-LCIA studies.

The allocation factor of the egalitarian method is calculated using population and economic data, both bounded to change over the years. In order to incorporate the temporal dimension into this method, three future scenarios have been studied: 2030, 2050, and 2100. If current per-capita consumption patterns are maintained, the impacts on the PBs will still increase up to 2100. Europe's population is predicted to decrease in the following years, contrarily to the world's population, causing a lower fraction of the SOS to be assigned to Europe but also a lower internal consumption, which will however be insufficient to offset the reduction on the allocated SoSOS.

4) According to the principal allocation method applied (i.e., the egalitarian method), the European chemical industry transgresses four of the nine assessed PBs, including those for the energy imbalance at top of atmosphere, atmospheric CO_2 concentration, ocean acidification, and aerosol loading. A fifth boundary, corresponding to the Nitrogen cycle, is potentially under risk and is also surpassed in 1% of the modelled scenarios. The carbon-based PBs related to climate change (i.e., energy imbalance and atmospheric CO_2 concentration) suffer the greatest damage, with the contribution of the industry being two orders of magnitude larger than the established limit (108 and 112 times larger, respectively). In fact, the chemical industry alone is found to take up to 70% of Europe's GHG emission allowances (according to the PBs framework). Meanwhile, the ocean acidification and aerosol loading PBs receive an impact 36 and 19 times above the threshold. Land-use and stratospheric ozone receive the least pressure from the industry's activity, followed by freshwater use and the phosphorus cycle.

5) The top five highest volume chemicals (i.e., ammonia, PP, HDPE, styrene, and benzene) take up almost 50% of the impacts in all PBs despite not having especially high unitary (per kg) contributions (except for styrene, which does classify as one of the top contributors to eight out of nine boundaries). In fact,

the manufacturing of ammonia, PP, styrene, and HDPE alone locates the industry 27.0, 16.0, 10.2, and 8.0 times above the limit for GHG emissions and 3.0, 4.3, 1.3, and 1.2 times above the maximum volume of ODS allowed to stay below the aerosol loading PB. Benzene alone has a contribution to the carbon-based PBs of 6.5 times above the limit but does not transgress the aerosol loading PB.

Besides those processes associated with high production volume chemicals, the chlorohydrin technology for the manufacturing of propylene oxide yields especially high unitary impacts to all PBs, significantly standing out among all processes. The cause has been found to be the obtention of the baseline reagents (chlorine and sodium hydroxide) through the highly energy-intensive chlor-alkali electrolysis. Since high volumes of both chlorine and sodium hydroxide are required to produce a kilogram of propylene oxide, the global impact of their production is enlarged even more.

The top contributors to all PBs have been identified and are summarised both in terms of total and unitary impacts in Table 10-3: Top contributors to all boundaries.

6) The obtained results indicate that a significant amount of the impacts stem from sectors beyond the boundaries of the chemical industry. A clear example and the main underlying system responsible for the positioning of the industry above the PBs is the energy sector. The heavy dependence on Europe's energy mix, which currently relies widely on fossil fuels, results in significantly high GHG emissions which cause all carbon-related PBs to be transgressed. Therefore, any improvement measures in the chemical industry must be coupled and planned in accordance with progress made in related sectors.

   Besides specific actions targeted at critical processes described along the discussion such as the reduction of plastics production by the incorporation of recycled polymers in the loop (e.g., recycled PE shows lower impacts on all Earth processes except for the ozone layer and the nitrogen cycle) or the use of more specific catalysts or catalytic routes, the main actions identified that which could potentially improve the sustainability of the sector significantly

have been found to be the switch to a more sustainable electricity mix, the deployment of CCS technologies, the use of catalysts, and the manufacturing of hydrogen from water electrolysis instead of steam reforming.

7) The improvement pathways offering the highest potential for change have been modelled to size the required interventions. The effects of their implementation on all environmental categories have been assessed concurrently to identify episodes of burden-shifting (if any).

7.1) An electricity mix change is proposed where the BAU mix based mainly on coal, natural gas, and oil is replaced by a new mix which relies widely on hydropower, solar, wind and nuclear energy, and includes carbon capture at coal and natural gas plants. This causes causing CO_2 and total GHGs emissions per kWh of electricity to be reduced by 67.8% and 67.7%, respectively. The new mix, not available in environmental databases, has been modelled in the study.

Since the electricity change can only be applied to foreground activities due to data availability, the carbon-based boundaries see a pressure reduction of 5-6%. The greatest improvement is seen in the freshwater use and the stratospheric ozone depletion PBs, with reductions of 20 and 24% on the final impacts, respectively.

Even if the mix change does not cause the transgression of any new PBs, the nitrogen cycle is deteriorated by 6%.

7.2) The implementation of CCS technologies (DACCS and BECCS) powered by both the BAU and the renewable mix has also been assessed. The required capacity to attain the proposed goals is calculated when (i) the total amount of released CO_2 wants to be sequestered and (ii) the total impact on the energy balance PB wants to be cancelled.

CO_2 emissions stemming from the CCS process itself are lower for DACCS, thus offering a higher net CO_2 removal efficiency than BECCS. However, DACCS cause more non-CO_2 emissions and therefore require the capture of more CO_2 to compensate for their own emissions. When

BECCS are coupled with the renewable mix (which also reduces CO_2 emissions), a reduction between 3.6% and 7.5% on BECCS installed capacity is attained.

In fact, the combination of CCS with the obtention of electricity from the mix based on renewable energies allows for a capacity reduction of around 20% in DACCS and 35% in BECCS.

As for burden-shifting, the deployment of both technologies causes the pressure on all non-carbon related PBs to be incremented. While this increase does not cause the transgression of any PBs in the case of DACCS, the nitrogen cycle limit is met in all BECCS scenarios.

If a correct management of nitrogen losses is achieved, BECCS offer the most promising results. However, in the best-case scenario (BECCS using the renewable mix), 234 million tonnes of CO_2 would still need to be removed from the atmosphere in order to cancel the contribution on the climate change and ocean acidification PBs.

The storage of the captured CO_2 would imply the annual occupation of only 0.03-0.04% of EU-28's geological onshore storage capacity if no additional uses of CO_2 are considered.

Conversely, the land required to annually grow the biomass necessary in the BECCS scenarios would be that of 28,000-38,300 km^2, which is close to the entire size of Catalonia, or 5.5 million football fields.

The electricity produced from BECCS in the nominal scenario (where no changes are assumed in the electricity mix and the total volume of CO_2 emissions from the chemical industry is sequestered) could cover 2.5% of Europe's electricity demand.

7.3) Finally, the production of green hydrogen through electrolysis powered by wind energy and the powering of the chlor-alkali electrolysis by the renewable mix is assessed.

The measure would reduce the impacts on the energy imbalance, atmospheric CO_2 concentration, and ocean acidification PBs by 2.6%, 1.8%, and 2.3%, respectively.

The impacts on nitrogen and freshwater cycles would however be incremented by 48.6% and 30.7% due to burden-shifting, even if limits would not be transgressed. The other four PBs (stratospheric ozone depletion, the phosphorus cycle, land-system change, and aerosol loading) would suffer smaller yet appreciable pressure increases of 2.7%, 0.9%, 2.16%, and 4.6% with respect to the BAU scenario.

7.4) The results from the improvement pathways section put in evidence there is no “silver bullet” which would allow to solve the climatic problem alone without causing havoc in other environmental categories. Rather, a combination of the proposed improvement measures together with a portfolio of technological alternatives would be needed to attain a sustainable future. Parallelly, an assessment of the total impacts of any proposed action is needed to identify the potential shifts in burdens between environmental processes. Note that the need for improvements in other activities outside the industry such as the aforementioned energy sector also advocates for holistic approaches.

8) The uncertainties linked to the collected data have only influenced the final results in the cases of the final egalitarian allocation (FSoSOS) for the nitrogen cycle, where the PB is met in 1% of the proposed scenarios, the second level of the egalitarian allocation (EUCISoSOS), where the impacts on the aerosol loading boundary moved from the uncertainty zone of the PB to its transgression in 2% of the scenarios, and the land-use change of the non-egalitarian allocation, where 41 out of the 100 modelled scenarios led the contribution to the exceedance of the upper bound of the PB.

9) A recommendation for subsequent research on the case of the chemical industry would be to expand the study to cover the implications of the manufacturing of the assessed products not only on the environment, but also on human health.

Additionally, if data on background processes were available and incorporated in the improvement pathways section, larger changes in the total contributions to the PBs could we detected.

Finally, it is important to note that the contribution to the aerosol loading PB cannot be completely mitigated by any of the improvement measures, so special attention must be paid to this environmental issue. As found when examining the results, the energy industry is responsible for a high fraction of the chemical sector’s aerosol emissions. The modelling of the proposed pathways confirmed that an electricity mix change yields improvements in the aerosol loading PB. Therefore, the addition of data on background processes could especially help reduce the pressure on this PB, as well as the change of the complete energy mix (to include not only electricity but also heat). Measures for pollution control would need to focus on the three principal aerosols emitted, those being NMVOCs, sulfur dioxide, and nitrogen oxides.

12 Planning and budgeting

In this section, the planning and costs of the project are presented and broken down. The steps from the methodology introduced in the introduction section (Fig. 1-1: Methodology of the study) are shown and in a Gantt diagram where the start and end dates, together with the connections between tasks, are depicted.

12.1 Planning

Fig. 12-1 shows the Gantt diagram elaborated with Microsoft Project where the tasks undertaken for the development of this study are shown.

Note how the bibliographic research, the definition of the study's goals, and the data collection started during the month of July and continued until the start of the first semester of year 2020-2021 in order ensure a timely delivery of the project before the deadline. After the final exams of the first semester of the year, the work pace accelerated during the second semester. It must therefore be considered that some tasks took longer to finish since time availability varied during the whole project.

Especially when approaching the end of the study, some tasks were linked to others in the sense that they could not be started until the previous task had been finished. However, in other cases, more than one task was done parallelly. For example, the collection and quality analysis of data started at the same time, even if the quality analysis required more hours. Bibliographic research was needed throughout the whole project since a large range of topics was covered in this multidisciplinary study. The writing of the report also started during the second semester of the academic year and was done concurrently with the elaboration of each section.

EDT	Nombre de tarea	Predecesoras
1	**Final year project**	
1.1	**Project definition**	
1.1.1	Goal definition	
1.1.2	Bibliographic research	
1.1.3	**Scope definition**	**3**
1.1.3.1	Selection of the PBs	
1.1.3.2	Selection of the included processes	
1.2	**Development of the model**	**3**
1.2.1	Data collection and treatment	
1.2.2	Volumes calculation	7
1.2.3	Impact calculation	9;10
1.2.4	Allocation procedure	11
1.2.5	Data quality analysis	9CC
1.2.6	Uncertainty study	12
1.3	**Analysis of results**	**8**
1.3.1	Defniniton of improvement pathways	
1.3.2	Modelling of improvement pathways	16
1.4	Writing of the report	10CC

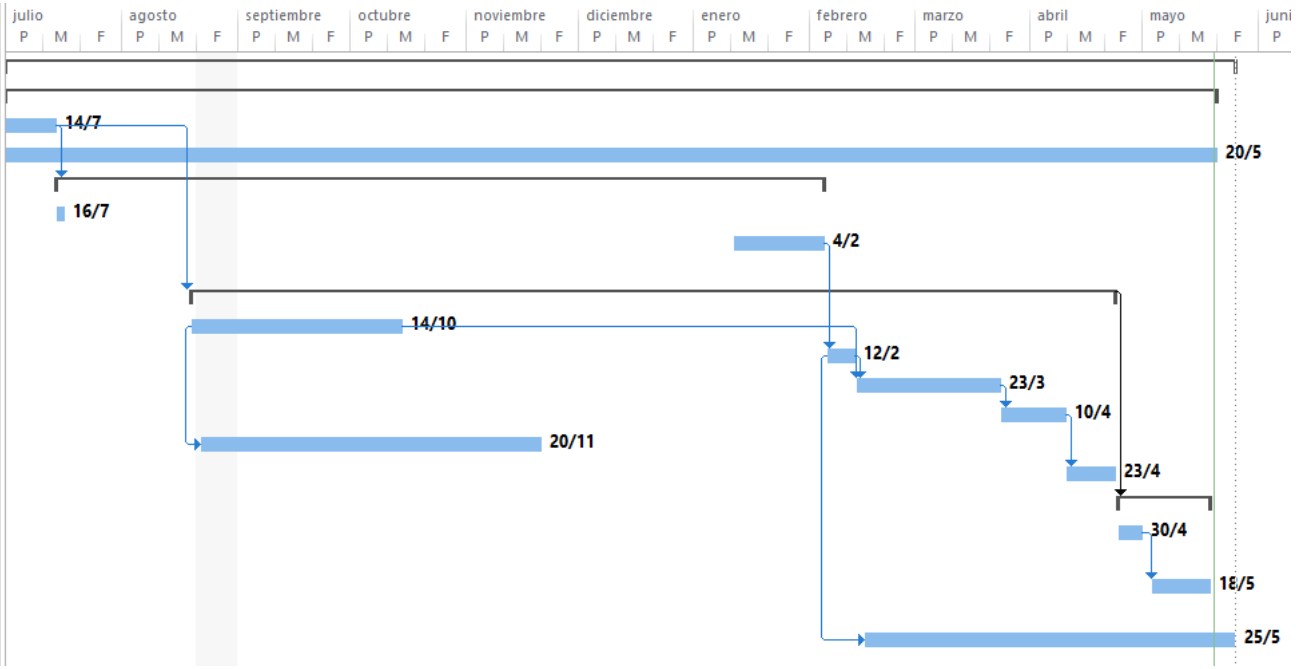

Fig. 12-1: Gantt diagram showing the planning of the study elaborated in Microsoft Project.

12.2 Costs

The costs of the project can be divided between three categories, including labour force, software purchase, and indirect costs. The cost assessment presented below breaks down each of these categories.

12.2.1 Labour force

The labour force costing obtained from Microsoft Project (using the program's costing tool) is presented in Table 12-1. Since no additional assistance was required, the two people involved in the development of the study were the author and the tutor.

Table 12-1: Labour costs.

	Hours	Cost (€/h)	Total cost (€)
Author	936.45	10	9364.5
Tutor	15	15	225.0
Total			9589.5

12.2.2 Software

Access to *ecoinvent* and Matlab was needed for the completion of the study. Table 12-2 provides the costs of both the database and the software. The access license to *ecoinvent* was annual and destined to educational users within the OECD. The Matlab pricing corresponds to the annual individual license for academic use. Since both licenses were annual and used solely during the development of the study, no inversions were made.

Table 12-2: Software costs.

	Cost (€)
Ecoinvent license	3800.0
Matlab	250.0
Total	4050.0

12.2.3 Indirect costs

A 5% of the labour costs of this project are taken as indirect costs generated by its elaboration. Therefore, these costs correspond to 468.2€.

12.2.4 Total cost

Table 12-3 shows the total costs of the project before and after adding the additional 21% corresponding to the value-added tax.

Table 12-3: Total costs.

	Cost (€)
Labour force	9589.5
Software	4050.0
Indirect costs	468.2
Total	14,107.7
Total (including VAT)	17,070.3

13 Bibliography

Abel, E. L., & DiGiovanni, J. (2015). Environmental Carcinogenesis. In *The Molecular Basis of Cancer* (pp. 103-128.e2). Elsevier. https://doi.org/10.1016/B978-1-4557-4066-6.00007-X

Achilias, D. S., Roupakias, C., Megalokonomos, P., Lappas, A. A., & Antonakou, E. V. (2007). Chemical recycling of plastic wastes made from polyethylene (LDPE and HDPE) and polypropylene (PP). *Journal of Hazardous Materials*, *149*(3), 536–542. https://doi.org/10.1016/j.jhazmat.2007.06.076

Albrecht, S., Fischer, M., Leistner, P., & Schebek, L. (2021). *Progress in Life Cycle Assessment 2019*.

Alghamdi, B., Alghazal, M., & Alsharif, A. (2019). *The Production of Cumene via the Alkylation of Benzene and Propylene*.

American Chemical Society. (1996). *SOHIO Acrylonitrile Process*.

Anderson, S., & Newell, R. (2004). Prospects for carbon capture and storage technologies. *Annual Review of Environment and Resources*, *29*(1), 109–142. https://doi.org/10.1146/annurev.energy.29.082703.145619

Andrady, A., Aucamp, P. J., Bais, A., Ballaré, C. L., Björn, L. O., Bornman, J. F., Caldwell, M., Cullen, A. P., Erickson, D. J., de Gruijl, F. R., Häder, D. P., Ilyas, M., Kulandaivelu, G., Kumar, H. D., Longstreth, J., McKenzie, R. L., Norval, M., Paul, N., Redhwi, H. H., ... Zepp, R. G. (2009). Environmental effects of ozone depletion and its interactions with climate change: progress report, 2008. *Photochemical & Photobiological Sciences: Official Journal of the European Photochemistry Association and the European Society for Photobiology, 8*(1), 13-22. https://doi.org/10.1039/b820432m

Arora, M., Malano, H., Davidson, B., Nelson, R., & George, B. (2015). Interactions between centralized and decentralized water systems in urban context: A review. *Wiley Interdisciplinary Reviews: Water*, *2*(6), 623–634. https://doi.org/10.1002/wat2.1099

Aurrekoetxea, J., Sarrionandia, M. A., Urrutibeascoa, I., & Maspoch, M. L. (2001). Effects of recycling on the microstructure and the mechanical properties of isotactic polypropylene. *Journal of Materials Science*, *36*, 2607–2631.

Bachari, H. (2019). *Monitoring of Marine Pollution* (H. Bachari Fouzia (ed.)). IntechOpen. https://doi.org/10.5772/intechopen.76739

Baker, J. W., & Lepech, M. D. (2009). Treatment of uncertainties in life cycle assessment. *International Congress on Structural Safety and Reliability*.

Bakst, J. S., Lacke, C. J., Weitz, K. A., & Warren, J. L. (1995). *Guidelines for Assessing the Quality of LCI Analysis*.

Bassetti, F. (2019). *Making the Case for Direct Air Capture for Carbon Storage*. https://www.climateforesight.eu/jobs-growth/direct-air-capture-for-carbon-storage-solutions/

BAT Nº 1. (1995). *Production of Ammonia, Best Available Techniques for Pollution Prevention and Control in the European Fertilizer Industry*.

Bengtsson, S. (2011). Life cycle assessment of present and future marine fuels. http://publications.lib.chalmers.se/records/fulltext/148820.pdf%5Cnhttp://ovidsp.ovid.com/ovidweb.cgi?T=JS&PAGE=reference&D=tspt&NEWS=N&AN=01448312

Bennett, E. M., Carpenter, S. R., Caraco, N. F. (2001). Human Impact on Erodable Phosphorus and Eutrophication: A Global Perspective: Increasing accumulation of phosphorus in soil threatens rivers, lakes, and coastal oceans with eutrophication, *BioScience, 51*(3), 227–234, https://doi.org/10.1641/0006-3568(2001)051[0227:HIOEPA]2.0.CO;2

Bertau, M., Offermanns, H., Plass, L., Schmidt, F., & Wernicke, H.-J. (Eds.). (2014). *Methanol: The Basic Chemical and Energy Feedstock of the Future*.

Bingham, E., Cohrssen, B., & Powell, C. H. (2001). *Patty's Toxicology Volumes 1-9 5th ed.* John Wiley & Sons.

Bibliography

Bjørn, A., Hauschild, M.Z. (2015). Introducing carrying capacity-based normalisation in LCA: framework and development of references at midpoint level. *The International Journal of Life Cycle Assessment, 20*, 1005–1018. https://doi.org/10.1007/s11367-015-0899-2

Blaas, H., & Kroeze, C. (2016). Excessive nitrogen and phosphorus in European rivers: 2000–2050. *Ecological Indicators*, *67*, 328–337. https://doi.org/10.1016/j.ecolind.2016.03.004

Bojarski, A. D. (2010). *Life cycle thinking and general modelling contribution to chemical process sustainable design and operat*ions.

Bonan, G. B. (2008). Forests and climate change: Forcings, feedbacks, and the climate benefits of forests. *Science, 320*(5882), 1444–1449. https://doi.org/10.1126/science.1155121

Boot-Handford, M. E., Abanades, J. C., Anthony, E. J., Blunt, M. J., Brandani, S., Mac Dowell, N., Fernández, J. R., Ferrari, M.-C., Gross, R., Hallett, J. P., Haszeldine, R. S., Heptonstall, P., Lyngfelt, A., Makuch, Z., Mangano, E., Porter, R. T. J., Pourkashanian, M., Rochelle, G. T., Shah, N., … Fennell, P. S. (2014). Carbon capture and storage update. *Energy Environ. Sci.*, *7*(1), 130–189. https://doi.org/10.1039/C3EE42350F

Boulamanti, A., & Moya, J. A. (2017). Production costs of the chemical industry in the EU and other countries: Ammonia, methanol and light olefins. *Renewable and Sustainable Energy Reviews, 68*, 1205–1212. https://doi.org/10.1016/j.rser.2016.02.021

Brandl, P., Bui, M., Hallett, J. P., & Mac Dowell, N. (2021). Beyond 90% capture: Possible, but at what cost? *International Journal of Greenhouse Gas Control*, *105*, 103239. https://doi.org/10.1016/j.ijggc.2020.103239

Brejnrod, K. N., Kalbar, P., Petersen, S., & Birkved, M. (2017). The absolute environmental per- formance of buildings. *Building and Environment*, *119*, 87–98.

Brentrup, F., Küsters, J., Lammel, J., & Kuhlmann, H. (2000). Methods to estimate on-field nitrogen emissions from crop production as an input to LCA studies in the agricultural sector. *The International Journal of Life Cycle Assessment*, 5(6), 349. https://doi.org/10.1007/BF02978670

Bui, M., Adjiman, C. S., Bardow, A., Anthony, E. J., Boston, A., Brown, S., Fennell, P. S., Fuss, S., Galindo, A., Hackett, L. A., Hallett, J. P., Herzog, H. J., Jackson, G., Kemper, J., Krevor, S., Maitland, G. C., Matuszewski, M., Metcalfe, I. S., Petit, C., … Mac Dowell, N. (2018). Carbon capture and storage (CCS): the way forward. *Energy & Environmental Science*, *11*(5), 1062–1176. https://doi.org/10.1039/C7EE02342A

Bush, T., Diao, M., Allen, R. J., Sinnige, R., Huisman, J., & Muyzer, G. (2017). Oxic-anoxic regime shifts mediated by feedbacks between biogeochemical processes and microbial community dynamics. *Nature Communications, 8*. https://doi.org/doi.org/10.1038/s41467-017-00912-x

Butler, J. R., Merrill, J. T. (1996). *Polymerization inhibitor process.* (Patent No. EP0747335B1). European Patent Office. https://patents.google.com/patent/EP0747335B1/en

Carr, C. (2020). Global Propylene Market. IHS Asia Chemical Conference. http://cdn.ihs.com/www/pdf/asia-chem-conf/Carr.pdf

Cespi, D., Passarini, F., Neri, E., Vassura, I., Ciacci, L., & Cavani, F. (2014). Life Cycle Assessment comparison of two ways for acrylonitrile production: the SOHIO process and an alternative route using propane. *Journal of Cleaner Production*, *69*, 17–25. https://doi.org/https://doi.org/10.1016/j.jclepro.2014.01.057

Chadwick, S. S. (2000). *Ullmann's Encyclopedia of Industrial Chemistry, 7th Edition*. Wiley-VCH. https://doi.org/10.1002/14356007

Challinor, A., Watson, J., Lobell, D. B.,Howden, S. M., Smith, D. R., Chhetri, N. (2019) A meta-analysis of crop yield under climate change and adaptation. *Nature Climate Change, 4*, 287–291. https://doi.org/10.1038/nclimate2153

Chenier, P. J. (1992). *Survey of Industrial Chemistry, 2nd revised edition*. Wiley-VCH.

Cherrie, J. W., Ng, M. G., Searl, A., Shafrir, A., Iom, M. V. T., Mistry, R., Sobey, M., Warwick, O., & Entec, C. C. (2011). *Health , socio-economic and environmental aspects of possible amendments to the EU Directive on the protection of workers from the risks related to exposure to carcinogens and mutagens at work Hexavalent Chromium. May,* 101.

Bibliography

Ciroth, A. (2009). Cost data quality considerations for eco-efficiency measures. *Ecological Economics, 68*(6), 1583-1590. https://doi.org/10.1016/j.ecolecon.2008.08.005

Ciroth, A., Muller, S., Weidema, B. P., Lesage, P. (2013). Refining the pedigree matrix approach in ecoinvent: Towards empirical uncertainty factors. In *LCA Discussion Forum*.

Ciroth, A., Muller, S., Weidema, B. P., Lesage, P. (2016). Empirically based uncertainty factors for the pedigree matrix in ecoinvent. *The International Journal of Life Cycle Assessment, 21*, 1338–1348. https://doi.org/10.1007/s11367-013-0670-5

Climate Change Connection. (n.d.). *No Title*. 2020. https://climatechangeconnection.org/emissions/co2-equivalents/

Clough, S. R. (2005). Toluene. In *Encyclopedia of Toxicology* (pp. 202–204). Elsevier. https://doi.org/10.1016/B0-12-369400-0/00955-8

Crawford, C. B., & Quinn, B. (2017). Physiochemical properties and degradation. In *Microplastic Pollutants* (pp. 57–100). Elsevier. https://doi.org/10.1016/B978-0-12-809406-8.00004-9

Crutzen, P. J. (2006). The “Anthropocene.” *In Earth System Science in the Anthropocene* (pp. 13–18). Springer-Verlag. https://doi.org/10.1007/3-540-26590-2_3

Dacey, J. W., Zemmelink, H.J. (2002). Sea Transfer: Dimethyl Sulfide, COS, CS2, NH4, Non-Methane Hydrocarbons, Organo-Halogens. In J. H. Steele (Ed.), *Encyclopedia of Ocean Sciences* (2nd ed., p. 157-162). https://doi.org/10.1016/B978-012374473-9.00063-1

Damania, R., Desbureaux, S., Hyland, M., Islam, A., Moore, S., Rodella, A.-S., Russ, J., & Zaveri, E. (2017). *Uncharted Waters: The New Economics of Water Scarcity and Variability*. World Bank, Washington, DC. https://doi.org/10.1596/978-1-4648-1179-1

de Vries, W., Kros, J., Kroeze, C., & Seitzinger, S. P. (2013). Assessing planetary and regional nitrogen boundaries related to food security and adverse environmental impacts. *Current Opinion in Environmental Sustainability, 5*(3), 392–402. https://doi.org/https://doi.org/10.1016/j.cosust.2013.07.004

Diamond, M. L., Sverker, M., de Wit, C. A., Scheringer, M., Backhaus, T., Lohmann, R., Arvidsson, R., Bergman, Å., Hauschild, M., NHoloubek, I., Persson, L., Suzuki, N., Vighi, M., & Zetzsch, C. (2015). Exploring the planetary boundary for chemical pollution. *Environmental International*, 78, 8–15. https://doi.org/https://doi.org/10.1016/j.envint.2015.02.001

Diaz, R. J., & Rosenberg, R. (2008). Spreading Dead Zones and Consequences for Marine Ecosystems. *Science, 321*(5891), 926–929. https://doi.org/10.1126/science.1156401

Dingwen, Y., Changhui, W. (1989). *Recovery of calcium chloride from waste liquid.* (Patent No. CN1006222B). https://patents.google.com/patent/CN1006222B/en

Doell, P., K, F., & J, Z. (2009). Global-scale analysis of river flow alterations due to water withdrawals and reservoirs*. Hydrology and Earth System Sciences, 13*(12). https://doi.org/10.5194/hess-13-2413-2009

Doell, P., K, F., & J, Z. (2009). Global-scale analysis of river flow alterations due to water withdrawals and reservoirs. *Hydrology and Earth System Sciences*, *13*(12). https://doi.org/10.5194/hess-13-2413-2009

Douglas, A. P., & Hoadley, A. F. A. (2006). A process integration approach to the design of the two- and three-column methanol distillation schemes. *Applied Thermal Engineering*, *26*(4), 338–349. https://doi.org/10.1016/j.applthermaleng.2005.07.001

Dry, J., Lawson, B., Le, P., Osisanya, I., Patel, D., & Shelton, A. (2003). Vinyl Chloride Production.

Dworkin, R. (1981). What is Equality? Part 1: Equality of Welfare. *Philosophy and Public Affairs*, *10*(3), 185–246. http://www.jstor.org/stable/2264894

ECI: The Essential Chemical Industry. (2016). *Polypropylene*. https://www.essentialchemicalindustry.org/polymers/polypropene.html

ECI: The Essential Chemical Industry. (2017). *Ethene (Ethylene)*. https://www.essentialchemicalindustry.org/chemicals/ethene.html

Bibliography

Ecofys. (2009). *Methodology for the free allocation of emission allowances in the EU ETS post 2012* (Issue November 2009).

Edelen, A., Ingwersen, W. (2016). *Guidance on Data Quality Assessment for Life Cycle Inventory Data*. U.S. Environmental Protection Agency, Washington, DC, EPA/600/R-16/096.

EEA. (2018). Environmental Indicator Report 2018: In Support to the Monitoring of the Seventh Environment Action Programme. In *European Environment Agency* (Issue 19). http://www.eea.europa.eu/publications/environmental-indicator-report-2014

Ehlers, E., Moss, C., Krafft, T. (2006). *Earth System Science in the Anthropocene: Emerging Issues and Problems*. Netherlands: Springer.

Encyclopædia Britannica. (2017). *Ziegler-Natta catalyst*. https://www.britannica.com/science/Ziegler-Natta-catalyst/additional-info#history

Environment Agency. (2016). *Business and environment report: Environmental outlook for the chemicals sector*. 1–12. www.gov.uk/environment-agency

Environmental Protection Agency. (2021). *The Ozone Layer*. https://www.epa.ie/air/airenforcement/ozone/

Erb, K.-H., Verburg, P. H., Mertz, O., & Espinadola, G. (2013). Land System Science: between global challenges and local realities. *Current Opinion in Environmental Sustainability, 5*(5), 433–437.

Eugster, M., Hischier, R., & Duan, H. (2007). Key environmental impacts of the Chinese EEE industry - a life cycle assessment study.

European Chemical Industry Council: CEFIC. (2020). 2020 Facts & figures of the European chemical industry. *Cefic*, 78.

European Commission. (2006a). *Harmonisation of allocation methodologies*.

European Commission. (2006b). *Life Cycle Assessment (LCA)*.

European Commission. (2014a). *Best Available Techniques (BAT) Reference Document for the Production of Chlor-alkali*. http://prtr-es.es/Data/images/BREF_Chlor_alkali_2014.pdf

European Commission. (2014b). *Contribution of industry to pollutant emissions to air and water*.

European Commission. (2015). *Paris Agreement.* https://ec.europa.eu/clima/policies/international/negotiations/paris_en

European Environmental Agency. (2020). *Ozone-depleting substances 2020*. https://doi.org/10.2800/388846

European Union. (2020a). Eurostat. *GDP and main components (output, expenditure and income).* [Data file]. shorturl.at/jvAFT

European Union. (2020b). Eurostat. *Gross value added and income A*10 industry breakdowns.* [Data file]. shorturl.at/fmHUY

European Union. (2020c). Eurostat. *Population on 1 January by age and sex.* [Data file]. shorturl.at/fhHN1

European Union. (2020d). *Member countries of the EU.* Retrieved September 10 from https://europa.eu/european-union/about-eu/countries_en

European Union. (2020e). Prodcom - NACE Rev. 2. [Data file]. Retrieved from https://ec.europa.eu/eurostat/web/prodcom

European Union. (2020f). Eurostat. Electricity production, consumption and market overview. https://ec.europa.eu/eurostat/statistics-explained/index.php/Electricity_production,_consumption_and_market_overview

Fahey, D.W., Hegglin, M.I. (2011). Twenty Questions and Answers About the Ozone Layer: 2010 Update. *Scientific Assessment of Ozone Depletion: 2010*. World Meteorological Organization, Geneva, Switzerland. https://www2.atmos.umd.edu/~rjs/class/spr2015/readings/WMO_Ozone_2010_QAs.pdf

Fernández, Á. G., & Cabeza, L. F. (2019). Molten salt corrosion mechanisms of nitrate based thermal energy storage materials for concentrated solar power plants: A review. *Solar Energy Materials and Solar Cells*, *194*, 160–165. https://doi.org/10.1016/j.solmat.2019.02.012

Ferreira, E. C., Lima, R., & Salcedo, R. (2004). Spreadsheets in chemical engineering education - A tool in process design and process integration. *International Journal of Engineering Education,* 20(6), 928–938.

Filippelli, G. (2002). The Global Phosphorus Cycle. *Reviews in Mineralogy and Geochemistry, 48*(1), 391-425 https://doi.org/10.2138/rmg.2002.48.10

Foglar, L., & Briški, F. (2003). Wastewater denitrification process—the influence of methanol and kinetic analysis. *Process Biochemistry*, *39*(1), 95–103. https://doi.org/https://doi.org/10.1016/S0032-9592(02)00318-7

Food and Agriculture Organization. (2016). *State of the world's forests*. http://www.fao.org/3/i5588e/i5588e.pdf

Fridahl, M., & Lehtveer, M. (2018). Bioenergy with carbon capture and storage (BECCS): Global potential, investment preferences, and deployment barriers. *Energy Research & Social Science*, *42*, 155–165. https://doi.org/10.1016/j.erss.2018.03.019

Fridahl, M., Bellamy, R., Hansson, A., & Haikola, S. (2020). Mapping Multi-Level Policy Incentives for Bioenergy With Carbon Capture and Storage in Sweden. *Frontiers in Climate*, *2*. https://doi.org/10.3389/fclim.2020.604787

Fry, M. M., Schwarzkopf, M. D., Adelman, Z., & West, J. J. (2014). Air quality and radiative forcing impacts of anthropogenic volatile organic compound emissions from ten world regions. *Atmospheric Chemistry and Physics*, *14*(2), 523–535. https://doi.org/10.5194/acp-14-523-2014

Gabrielli, P., Gazzani, M., & Mazzotti, M. (2020). The Role of Carbon Capture and Utilization, Carbon Capture and Storage, and Biomass to Enable a Net-Zero-CO2 Emissions Chemical Industry. *Industrial and Engineering Chemistry Research*, *59*(15), 7033–7045. https://doi.org/10.1021/acs.iecr.9b06579

Galán-Martín, Á., Tulus, V., Díaz, I., Pozo, C., Pérez-Ramírez, J., & Guillén-Gosálbez, G. (2021). Sustainability footprints of a renewable carbon transition for the petrochemical sector within planetary boundaries. *One Earth*, *4*(4), 565–583. https://doi.org/10.1016/j.oneear.2021.04.001

Galloway, J. N., Townsend, A. R., Erisman, J. W., Bekunda, M., Cai, Z. C., Freney, J. R., Martinelli, L. A., Seitzinger, S. P., Sutton, M. A. (2008). Transformation of the nitrogen cycle: Recent trends, questions, and potential solutions. *Science, 320*, 889-892, doi:10.1126/science.1136674

Gambhir, A., & Tavoni, M. (2019). Direct Air Carbon Capture and Sequestration: How It Works and How It Could Contribute to Climate-Change Mitigation. *One Earth*, *1*(4), 405–409. https://doi.org/10.1016/j.oneear.2019.11.006

Gasol, C. M., Gabarrell, X., Anton, A., Rigola, M., Carrasco, J., Ciria, P., & Rieradevall, J. (2009). LCA of poplar bioenergy system compared with Brassica carinata energy crop and natural gas in regional scenario. *Biomass and Bioenergy*, *33*(1), 119–129. https://doi.org/10.1016/j.biombioe.2008.04.020

Gibbins, J., & Chalmers, H. (2008). Carbon capture and storage. *Energy Policy*, *36*(12), 4317–4322. https://doi.org/10.1016/j.enpol.2008.09.058

Goedkoop, M., Heijungs, R., Huijbregts, M.A.J., De Schryver, A., Struijs, .J, van Zelm, R. (2009). ReCiPe 2008: a life cycle impact assessment method which comprises harmonised category indicators at the midpoint and endpoint levels.

González-Garay, A., Frei, M. S., Al-Qahtani, A., Mondelli, C., Guillén-Gosálbez, G., & Pérez-Ramírez, J. (2019). Plant-to-planet analysis of CO 2 -based methanol processes. *Energy & Environmental Science*, *12*(12), 3425–3436. https://doi.org/10.1039/C9EE01673B

Gordon, L. J., Steffen, W., Jönsson, B. F., Folke, C., Falkenmark, M., & Johannessen, A. (2005). Human modification of global water vapor flows from the land surface. *Proceedings of the National Academy of Sciences of the United States of America, 102*(21), 7612–7619. https://doi.org/10.1073/pnas.0500208102

Goswami, T. K., & Mangaraj, S. (2011). Advances in polymeric materials for modified atmosphere packaging (MAP). In *Multifunctional and Nanoreinforced Polymers for Food Packaging* (pp. 163–242). Elsevier. https://doi.org/10.1533/9780857092786.1.163

Green Car Congress (December 2009*). Devil In The Details: Is Copenhagen's 2 ºC "Guardrail" Obsolete?.* Retrieved 24 August 2020 from https://www.greencarcongress.com/2009/12/guardrail-20091216.html

Greenwood, D. J., Karpinets, T. V., Zhang, K., Bosh-Serra, A., Boldrini, A., & Karawulova, L. (2008). A Unifying Concept for the Dependence of Whole-crop N : P Ratio on Biomass: Theory and Experiment. *Annals of Botany, 102*(6), 967–977. https://doi.org/10.1093/aob/mcn188

Gulledge, B. (2021). *Products and Technology: ethylene glycol*. https://www.americanchemistry.com/ProductsTechnology/Ethylene-Glycols-2/What-is-Ethylene-Glycol/

Hacatoglu, K., Rosen, M. A., & Dincer, I. (2012). Comparative life cycle assessment of hydrogen and other selected fuels. *International Journal of Hydrogen Energy*, *37*(13), 9933–9940. https://doi.org/10.1016/j.ijhydene.2012.04.020

Haghighi, S. S., Rahimpour, M. R., Raeissi, S., & Dehghani, O. (2013). Investigation of ethylene production in naphtha thermal cracking plant in presence of steam and carbon dioxide. *Chemical Engineering Journal*, *228*, 1158–1167. https://doi.org/https://doi.org/10.1016/j.cej.2013.05.048

Han, I.S., Kim, M., Lee, C.H., Cha, W., Ham, B.K., Jeong, J.H., Lee, H., Chung, C.B., & Han, C. (2003). Application of partial least squares methods to a terephthalic acid manufacturing process for product quality control. *Korean Journal of Chemical Engineering*, *20*(6), 977–984. https://doi.org/10.1007/BF02706925

Hansen, J., Sato, M., Kharecha, P., Beerling, D., Berner, R., Masson-Delmotte, V., Pagani, M., Raymo, M., Royer, D. L., Zachos, J. C. (2008). Target atmospheric CO2: where should humanity aim? *Open Atmospheric Science Journal, 2*, 217–231. https://doi.org/10.2174/1874282300802010217

Hasler, N., & Avissar, R. (2007). What Controls Evapotranspiration in the Amazon Basin, *Journal of Hydrometeorology, 8*(3), 380–395. https://doi.org/10.1175/JHM587.1

Haszeldine, R. S. (2009). Carbon Capture and Storage: How Green Can Black Be? *Science*, *325*(5948), 1647–1652. https://doi.org/10.1126/science.1172246

Hauschild, M. Z., & Hujibregts. (2015). Life Cycle Impact Assessment. In LCA Compendium - The Complete World of Life Cycle Assessment, Life Cycle Impact Assessment. https://doi.org/10.1007/978-94-017-9744-3

Hauschild, M.Z., Goedkoop, M., Guinée, J., Heijungs, R., Huijbregts, M., Jolliet, O., Margni, M., De Schryver, A., Humbert, S., Laurent, A., Sala, S., Pant, R. (2013). Identifying best existing practice for characterization modeling in life cycle impact assessment. *The International Journal of Life Cycle Assessment, 18,* 683–697. https://doi.org/10.1007/s11367-012-0489-5.

Häyhä, T., Lucas, P. L., van Vuuren, D. P., Cornell, S. E., & Hoff, H. (2016). From Planetary Boundaries to national fair shares of the global safe operating space — How can the scales be bridged? *Global Environmental Change, 40*, 60–72. https://doi.org/10.1016/j.gloenvcha.2016.06.008

Heijungs, R. (1995). Harmonization of methods for impact assessment. *Environmental Science and Pollution Research, 2*, 217–224. https://doi.org/10.1007/BF02986769.

Herring, S. C., Christidis, N., Hoell, A., Hoerling, M. P., Stott, P. A. (2020). Explaining Extreme Events of 2018 from a Climate Perspective. *Bulletin of the American Meteorological Society, 101*(1), 1–128, https://doi.org/10.1175/BAMS-ExplainingExtremeEvents2018.1.

Hisham A. Maddah. (2016). Polypropylene as a Promising Plastic: A Review. *American Journal of Polymer Science*, *January*. https://doi.org/10.5923/j.ajps.20160601.01

Hjalsted, A. W., Laurent, A., Andersen, M. M., Olsen, K. H., Ryberg, M., & Hauschild, M. (2021). Sharing the safe operating space: Exploring ethical allocation principles to operationalize the planetary

boundaries and assess absolute sustainability at individual and industrial sector levels. *Journal of Industrial Ecology*, *25*(1), 6–19. https://doi.org/10.1111/jiec.13050

Hocking, M. B. (2005). Handbook of Chemical Technology and Pollution Control (Third Edition).

Hollerud, B., & Bowyer, J. (2017). A review of Life Cycle Assessment Tools.

Howarth, R. W., Jensen, H. S., Marino, R., Postma, H. (1995). Transport to and processing of P in near-shore and oceanic waters. *In Phosphorus in the global environment: Transfers, cycles and management* (pp. 323-346). John Wiley & Sons Ltd. SCOPE, No. 54

Huijbregts, M. A. J., Steinmann, Z. J. N., Elshout, P. M. F., Stam, G., Verones, F., Vieira, M., Zijp, M., Hollander, A., van Zelm, R. (2017). ReCiPe 2016: a harmonised life cycle impact assessment method at midpoint and endpoint level. *The International Journal of Life Cycle Assessment, 22*, 138–147.

Huijbregts, M.A.J., Hellweg, S., Hertwich, E. (2011). Do we need a paradigm shift in life cycle impact assessment?, *Environmental Science & Technology, 45*(9), 3833–3834. https://doi.org/201110.1002/ieam.141

Hwang, K. C., Sagadevan, A., & Kundu, P. (2019). The sustainable room temperature conversion of p - xylene to terephthalic acid using ozone and UV irradiation. *Green Chemistry*, *21*(22), 6082–6088. https://doi.org/10.1039/C9GC02095K

Hydrogen Council. (2021). *Hydrogen decarbonization pathways: a life-cycle assessment*. https://hydrogencouncil.com/wp-content/uploads/2021/01/Hydrogen-Council-Report_Decarbonization-Pathways_Part-1-Lifecycle-Assessment.pdf

ICCA. (2010a). *ICCA Annual Report*.

ICIS: Independent Commodity Intelligence Services. (2009a). *Ethylene Oxide (EO) Production and Manufacturing Process*. https://www.icis.com/explore/resources/news/2007/11/05/9075773/ethylene-oxide-eo-production-and-manufacturing-process/

ICIS: Independent Commodity Intelligence Services. (2009b). *Propylene Oxide (PO) Production and Manufacturing Process*. https://www.icis.com/explore/resources/news/2007/11/06/9076451/propylene-oxide-po-production-and-manufacturing-process/

ICIS: Independent Commodity Intelligence Services. (2010a). *Polyethylene - low density (LDPE) Production and Manufacturing Process*. https://www.icis.com/explore/resources/news/2007/11/06/9076158/polyethylene-low-density-ldpe-production-and-manufacturing-process/

ICIS: Independent Commodity Intelligence Services. (2010b). E*thylbenzene (EB) Production and Manufacturing Process*. https://www.icis.com/explore/resources/news/2007/11/02/9075695/ethylbenzene-eb-production-and-manufacturing-process

ICIS: Independent Commodity Intelligence Services. (2010c). E*thylene glycol (EG) Production and Manufacturing Process*. https://www.icis.com/explore/resources/news/2007/11/05/9075767/ethylene-glycol-eg-production-and-manufacturing-process/

ICIS: Independent Commodity Intelligence Services. (2020). *European chemical profiles*. https://www.icis.com/explore/

IEA. (2013). Technology Roadmap: Energy and GHG Reductions in the Chemical Industry via Catalytic Processes. https://www.iea.org/reports/technology-roadmap-energy-and-ghg-reductions-in-the-chemical-industry-via-catalytic-processes

IEA. (2019). *World Energy Outlook 2019*.

IEA. (2020a). *Hydropower*. https://www.iea.org/fuels-and-technologies/hydropower

IEA. (2020b). Bioenergy Power Generation. https://www.iea.org/reports/bioenergy-power-generation

International Agency for Research on Cancer. (2012). Coke production. In *Chemical Agents and Related Occupations*.

Bibliography

International Agency for Research on Cancer. (2013). *IARC Monographs on the Evaluation of Carcinogenic Risks to Humans, No. 101*.

International Standard Organization. (2006). *ISO 14044: Environmental management — Life cycle assessment — Requirements and guidelines.* https://www.iso.org/standard/38498.html

IPCC: Intergovernmental Panel on Climate Change. (2007). *Climate change 2007: the physical science basis*. *In* Solomon, S., Qin, D., Manning, M., Chen, Z., Marquis, M. C., Avery, K., Tignor, M., Miller, H. L. J., editors. *Contribution of Working Group I to the Fourth Assessment Report of the Intergovernmental Panel on Climate Change*. Cambridge University Press, Cambridge, UK. https://www.ipcc.ch/report/ar4/wg1/

IPCC: Intergovernmental Panel on Climate Change. (2013). *Climate Change 2013: The Physical Science Basis. Summary for Policymakers*., L. Alexander et al., editors. IPCC Secretariat, Geneva, Switzerland. https://doi.org/10.1017/CBO9781107415324

IPCC: Intergovernmental Panel on Climate Change (2018). Global warming of 1.5ºC.

Iribarren, D., Petrakopoulou, F., & Dufour, J. (2013). Environmental and thermodynamic evaluation of CO2 capture, transport, and storage with and without enhanced resource recovery. *Energy*, *50*, 477–485. https://doi.org/10.1016/j.energy.2012.12.021

IUCN Red List of Threated Species. (2020). List of Threated Species. https://www.iucnredlist.org/

Kamal, M. R., Jinnah, I. A., & Utracki, L. A. (1984). Permeability of oxygen and water vapor through polyethylene/polyamide films. *Polymer Engineering and Science*, *24*(17), 1337–1347. https://doi.org/10.1002/pen.760241711

Kandyala, R., Raghavendra, S. P., & Rajasekharan, S. (2010). Xylene: An overview of its health hazards and preventive measures. *Journal of Oral and Maxillofacial Pathology*, *14*(1), 1. https://doi.org/10.4103/0973-029X.64299

Kätelhön, A., Meys, R., Deutz, S., Suh, S., Bardow, A. (2019). Climate change mitigation potential of carbon capture and utilization in the chemical industry. *Proceedings of the National Academy of Sciences, 116*(23), 11187-11194. https://doi.org/10.1073/pnas.1821029116

Kehinde, A. J., Usman, M. A., Edoga, M. O., & Owolabi, R. (2012). Emerging Issues in the Mechanisms of High Pressure Free Radical Ethylene Polymerization: A Review. *American Journal of Polymer Science, 2*(5), 91–101. https://doi.org/10.5923/j.ajps.20120205.03

Khare, N. P., Seavey, K. C., Liu, Y. A., Ramanathan, S., Lingard, S., & Chen, C.-C. (2002). Steady-State and Dynamic Modeling of Commercial Slurry High-Density Polyethylene (HDPE) Processes. *Industrial & Engineering Chemistry Research*, *41*(23), 5601–5618. https://doi.org/10.1021/ie020451n

King, A. W., Hayes, D. J.,Huntzinger, D. N., Tristram, O., West, T. O.,Post, W. M. (2012). North America carbon dioxide sources and sinks: Magnitude, attribution, and uncertainty. *Frontiers in Ecology and the Environment, 10*, 512-519. https://doi.org/10.1890/120066

Klimesch, R., Littmann, D., & Mähling, F.-O. (2001). Polyethylene: High-pressure. In *Encyclopedia of Materials: Science and Technology* (pp. 7181–7184). Elsevier. https://doi.org/10.1016/B0-08-043152-6/01273-0

Koerner, G. R., & Koerner, R. M. (2018). Polymeric Geomembrane Components in Landfill Liners. In *Solid Waste Landfilling* (pp. 313–341). Elsevier. https://doi.org/10.1016/B978-0-12-407721-8.00017-6

Kolb, K. E., & Field, K. W. (n.d.). *Organic Industrial Chemistry.* http://www.chemistryexplained.com/Hy-Kr/Industrial-Chemistry-Organic.html

Kosek, J., & Ray, W.H (1999). Dynamics and Stability of Slurry Olefin Polymerization Processes. *Recent Progres En Genie Des Procedes*, *13*(69), 97–104.

Koval, Y., Skvortsevitch, Y., & Mayer, E. (2013). VLDPE Synthesis by Radical Ethylene Polymerization in Tubular Reactors–Negative Factor or Unrealized Opportunities. *Journal of Materials Science and Chemical Engineering*, *1*(1), 11–16. https://doi.org/10.4236/msce.2013.11003

Kroschwitz, J. I., Howe-Grant, M., Kirk, R. E., & Othmer, D. F. (Eds.). (1991). *Encyclopedia of Chemical Technology, Fourth edition*. John Wiley & Sons.

Kugler, E. L. (1995). *Cumene Production*.

Kumar, R., & Singh, R. (2020). Application of Nano Porous Materials for Energy Conservation and Storage. In *Encyclopedia of Renewable and Sustainable Materials* (pp. 42–50). Elsevier. https://doi.org/10.1016/B978-0-12-803581-8.11278-0

Kupolati, W. K., Ndambuki, J. M., Sadiku, E. R., Ibrahim, I. D., Adeboje, A. 0., Kambole, C., Ojo., O., Eze, A. A., & Paige-Green, P. (2017). The use of polyolefins in geotextiles and engineering applications. In *Polyolefin Fibres (Second Edition)*.

Lambin, E. F., Turner, B. L., Geist, H. J., Agbola, S. B., Angelsen, A., Bruce, J. W., Coomes, O. T., Dirzo, R., Fischer, G., Folke, C., George, P. S., Homewood, K., Imbernon, J., Leemans, R., Li, X., Moran, E. F., Mortimore, M., Ramakrishnan, P. S., Richards, J. F., … Xu, J. (2001). The causes of land-use and land-cover change: moving beyond the myths. *Global Environmental Change*, *11*(4), 261–269. https://doi.org/10.1016/S0959-3780(01)00007-3

Langevin, B., Basset-Mens, C., & Lardon, L. (2010). Inclusion of the variability of diffuse pollutions in LCA for agriculture: the case of slurry application techniques. *Journal of Cleaner Production, 18*(8), 747–755. https://doi.org/10.1016/j.jclepro.2009.12.015

Lau, L.-S., Choong, C.-K., Ng, C.-F., Liew, F.-M., & Ching, S.-L. (2019). Is nuclear energy clean? Revisit of Environmental Kuznets Curve hypothesis in OECD countries. *Economic Modelling*, *77*, 12–20. https://doi.org/10.1016/j.econmod.2018.09.015

Lebling, K., McQueen, N., Pisciotta, M., & Wilcox, J. (2021). *Direct Air Capture: Resource Considerations and Costs for Carbon Removal*. https://www.wri.org/insights/direct-air-capture-resource-considerations-and-costs-carbon-removal

Lee, W. J. (2005). *Ethylbenzene Dehydrogenation into styrene: kinetic modeling and reactor simulation*.

Lehtveer, M., & Emanuelsson, A. (2021). BECCS and DACCS as Negative Emission Providers in an Intermittent Electricity System: Why Levelized Cost of Carbon May Be a Misleading Measure for Policy Decisions. *Frontiers in Climate*, *3*. https://doi.org/10.3389/fclim.2021.647276

Lenton, T. M., Held, H., Kriegler, E., Hall, J. W., Lucht, W., Rahmstorf, S., & Schellnhuber, H. J. (2008). Tipping elements in the Earth's climate system. *Proceedings of the National Academy of Sciences*, *105*(6), 1786–1793. https://doi.org/10.1073/pnas.0705414105

Lenton, T. M., Rockström, J., Gaffney, O., Rahmstorf, S., Richardson, K., Steffen, W., & Schellnhuber, H. J. (2019). Climate tipping points — too risky to bet against. *Nature*, *575*(7784), 592–595. https://doi.org/10.1038/d41586-019-03595-0

Lewis, S. L., & Maslin, M. A. (2015). Defining the Anthropocene. *Nature*, *519*(7542), 171–180. https://doi.org/10.1038/nature14258

Li, C., Wang, N., Zhang, H., Liu, Q., Chai, Y., Shen, X., Yang, Z., & Yang, Y. (2019). Environmental Impact Evaluation of Distributed Renewable Energy System Based on Life Cycle Assessment and Fuzzy Rough Sets. *Energies*, *12*(21), 4214. https://doi.org/10.3390/en12214214

Li, L., Wang, X. (2012). Seasonal and Diurnal Variations of Atmospheric Non-Methane Hydrocarbons in Guangzhou, China. *International journal of environmental research and public health, 9*(5), 1859-73. https://doi.org/10.3390/ijerph9051859.

LIFE. (2013). Road Map Document for a Sustainable Chemical Industry. *LIFE Financial Instrument of the European Community*, *January*.

Lignell, D. (2015). *Possibilities of autoclave LDPE process*.

Limpert, E., Stahel, W. A., & Abbt, M. (2001). Log-normal Distributions across the Sciences: Keys and Clues. *Bioscience*, *51*(5), 341–352.

Linde. (2021). *Ethylene*. https://www.linde-gas.com/en/products_and_supply/packaged_chemicals/product_range/ethylene.html

Liu, X., & Elgowainy, A. (2019). Life-Cycle Analysis of Green Ammonia and its Application as Fertilizer Building Block. *Ammonia Energy Conference 2019*.

Loomis, D., Guyton, K. Z., Grosse, Y., Ghissassi, F. El, Bouvard, V., Benbrahim-Tallaa, L., Guha, N., Vilahur, N., Mattock, H., & Straif, K. (2017). Carcinogenicity of benzene. *The Lancet Oncology*, *18*(12), 1574–1575.

Luyssaert, S., Schulze, E.-D., Börner, A., Knohl, A., Hessenmöller, D., Law, B. E., Ciais, P., & Grace, J. (2008). Old-growth forests as global carbon sinks. *Nature*, *455*(7210), 213–215. https://doi.org/10.1038/nature07276

Ma, H., Wang, Y., Qi, Y., Rout, K. R., & Chen, D. (2020). Critical Review of Catalysis for Ethylene Oxychlorination. *ACS Catalysis, 10*(16), 9299–9319. https://doi.org/10.1021/acscatal.0c01698

Mace, G. M., Reyers, B., Alkemade, R., Biggs, R., Chapin, F. S., Cornell, S. E., Díaz, S., Jennings, S., Leadley, P., Mumby, P. J., Purvis, A., Scholes, R. J., Seddon, A. W. R., Solan, M., Steffen, W., & Woodward, G. (2014). Approaches to defining a planetary boundary for biodiversity. *Global Environmental Change*, *28*, 289–297. https://doi.org/10.1016/j.gloenvcha.2014.07.009

Maddah., H. A. (2016). Polypropylene as a Promising Plastic. *American Journal of Polymer Science*. https://doi.org/https://doi.org/10.5923/j.ajps.20160601.01

Maddah., H. A. (2016). Polypropylene as a Promising Plastic: A Review. *American Journal of Polymer Science*. https://doi.org/https://doi.org/10.5923/j.ajps.20160601.01

Malkan, S. R. (2017). Improving the use of polyolefins in nonwovens. In *Polyolefin Fibres (Second Edition)*.

Manal, N., & Marwan, H. (2013). *Polyethylene polymerization techniques and reactions*. Seminar held in Enppi.

Mao, R. L. Van, Yan, H., Muntasar, A., & Al-Yassir, N. (2013). Blending of Non-Petroleum Compounds with Current Hydrocarbon Feeds to Use in the Thermo-Catalytic Steam-Cracking Process for the Selective Production of Light Olefins. In *New and Future Developments in Catalysis*. https://doi.org/https://doi.org/10.1016/B978-0-444-53876-5.00007-6G

Matar, S., & Hatch, L. F. (2001). *Chemistry of Petrochemical Processes*. Elsevier. https://doi.org/10.1016/B978-0-88415-315-3.X5000-7

Maxwell, G. R. (2005). Uses of Ammonia. In *Synthetic Nitrogen Products*. Springer. https://doi.org/https://doi.org/10.1007/0-306-48639-3_7

McCollum, D. L., & Ogden, J. M. (2006). *Techno-Economic Models for Carbon Dioxide Compression, Transport, and Storage & Correlations for Estimating Carbon Dioxide Density and Viscosity*. https://escholarship.org/uc/item/1zg00532

McGill School of Computer Science. (2007). *Benzene*. https://www.cs.mcgill.ca/~rwest/wikispeedia/wpcd/wp/b/Benzene.htm

McKeen, L. W. (2009). Styrenic Plastics. In *The Effect of Creep and Other Time Related Factors on Plastics and Elastomers* (pp. 33–81). Elsevier. https://doi.org/10.1016/B978-0-8155-1585-2.50004-2

McKenzie, R. L., Aucamp, P. J., Bais, A. F., Björn, L. O., Ilyas, M., Madronich, S. (2011). Ozone depletion and climate change: impacts on UV radiation. *Photochemical & Photobiological Sciences, 10*, 182-198. https://doi.org/10.1039/C0PP90034F

Mclnerney, F., A., Wing, S. L. (2011). The Paleocene-Eocene Thermal Maximum: A Perturbation of Carbon Cycle, Climate, and Biosphere with Implications for the Future. *Annual Review of Earth and Planetary Sciences, 39*, 489-516. https://doi.org/10.1146/annurev-earth-040610-133431

Messages, K. (2014). *Key messages Key messages*. *27*(April), 1–8.

Mohammad, A., & Simon, G. P. (2006). Rubber-clay nanocomposites. In *Polymer Nanocomposites* (pp. 297–325). Elsevier. https://doi.org/10.1533/9781845691127.1.297

Mohanty, A. K., Misra, M., & Drzal, L. T. (2002). Sustainable Bio-Composites from Renewable Resources: Opportunities and Challenges in the Green Materials World. *Journal of Polymers and the Environment*, *10*, 19–26. https://doi.org/10.1023/A:1021013921916

Molina, M. (1991). Heterogeneous chemistry on polar stratospheric clouds. *Atmospheric Environment, 25*(11), 2535-2537. https://doi.org/10.1016/0960-1686(91)90170-C

Montoya, J. M., Donohue, I., & Pimm, S. L. (2018). Planetary Boundaries for Biodiversity: Implausible Science, Pernicious Policies. *Trends in Ecology & Evolution, 33*(2), 71–73. https://doi.org/10.1016/j.tree.2017.10.004

Montzka, S. A., Dlugokencky, E. J., Butler, J. H. (2011). Non-CO2 greenhouse gases and climate change. *Nature, 476*, 43-50. https://doi.org/10.1038/nature10322

Mucci, A. (1983). The solubility of calcite and aragonite in seawater at various salinities, temperatures, and 1 atmosphere total pressure. *American Journal of Science, 283*(7), 780–799. https://doi.org/10.2475/ajs.283.7.780

Myhre, G., Shindell, D., Bréon, F.-M., & Collins, W. (2013). *Climate Change 2013: The Physical Science Basis. Contribution of Working Group I to the Fifth Assessment Report of the Intergovernmental Panel on Climate Change*.

NASA. (Aug 7, 2017). *Polar Stratospheric Clouds*. Rertieved 26 August from https://www.nasa.gov/multimedia/imagegallery/image_feature_680.html

National Center for Biotechnology Information (2021b). PubChem Compound Summary for CID 1140, Toluene. Retrieved February 19, 2021 from https://pubchem.ncbi.nlm.nih.gov/compound/Toluene

National Center for Biotechnology Information. (2021a). *PubChem Compound Summary for CID 6378, Propylene oxide.* https://pubchem.ncbi.nlm.nih.gov/compound/Propylene-oxide

National Institute for Public Health and the Environment Ministry of Health, Welfare and Sport (2011, last revised February 2018). *LCIA: the ReCiPe model.* Retrieved 13 July 2020 from https://www.rivm.nl/en/life-cycle-assessment-lca/recipe

National Library of medicine. (2020). *Pubchem*. Retrieved 18 September 2020 from https://pubchem.ncbi.nlm.nih.gov/#query=Carbon%20dioxide

Neilen, M. G. M., & Bosch, M. S. (n.d.). *Tubular LDPE has the Extrusion Coating future.*

Neto, A. G., & Pinto, J. C. (2001). Steady-state modeling of slurry and bulk propylene polymerizations. *Chemical Engineering Science*, *56*(13), 4043–4057. https://doi.org/10.1016/S0009-2509(01)00076-8

Nexant. (2008). *Linear Low Density Polyethylene (LLDPE)*.

Nexant. (2009). *Industrial Organic Chemicals*.

Nexant. (2009). *Propylene Oxide*. https://engage.aiche.org/HigherLogic/System/DownloadDocumentFile.ashx?DocumentFileKey=a8300833-1d78-4d92-b692-1a1fd7548cfe&ssopc=1

Nijhuis, T. A., Makkee, M., Moulijn, J. A., & Weckhuysen, B. M. (2006). The Production of Propene Oxide: Catalytic Processes and Recent Developments. *Industrial & Engineering Chemistry Research*, *45*(10), 3447–3459. https://doi.org/10.1021/ie0513090

Niziolek, A. M., Onel, O., & Floudas, C. A. (2015). Production of benzene, toluene, and xylenes from natural gas via methanol: Process synthesis and global optimization. *AIChE Journal*, *62*(5), 1531–1556. https://doi.org/https://doi.org/10.1002/aic.15144

Nobre, C. A., Sampaio, G., Borma, L. S., Castilla-Rubio, J. C., Silva, J. S., & Cardoso, M. (2016). Land-use and climate change risks in the Amazon and the need of a novel sustainable development paradigm. *Proceedings of the National Academy of Sciences of the United States of Americatates of America, 113*(39), 10759–10768. https://doi.org/10.1073/pnas.1605516113

Nuttall, M. (2020). Water, ice, and climate change in northwest Greenland. *WIREs water, 7*(3), Article e1433. https://doi.org/10.1002/wat2.1433

O'Neill, D. W., Fanning, A. L., Lamb, W. F., & Steinberger, J. K. (2018). A good life for all within planetary boundaries. *Nature Sustainability, 1*(2), 88–95. https://doi.org/10.1038/s41893-018-0021-4

O'Neill, M. J. (Ed.). (2013). *The Merck Index - An Encyclopedia of Chemicals, Drugs, and Biologicals*. Royal Society of Chemistry.

OECD. (2001). *OECD Environmental Outlook for the Chemicals Industry*.

OECD. (2018). GDP long-term forecast (indicator). doi: 10.1787/d927bc18-en (Accessed on 01 September 2020)

OECD. (n.d.). *The Future Environmental Impact from the Chemicals Industry*. 2000. https://www.oecd.org/env/ehs/thefutureenvironmentalimpactfromthechemicalsindustry.htm

Bibliography

PasticsEurope. (2016). *Polypropylene (PP) Ecoprofile*. https://www.plasticseurope.org/es/resources/eco-profiles

Petrakopoulou, F., Iribarren, D., & Dufour, J. (2014). Life-cycle performance of natural gas power plants with pre-combustion CO_2 capture. *Greenhouse Gas Science and Technology*, *4*, 1–9.

Pharand-Deschênes, F. (2015). *Planetary boundaries (Globaïa)*.

Piana, M. E. (2020). *Harvard School of Engineering and Applied Sciences: Equable Climate Dynamics - Polar Stratospheric Clouds*. Retrieved 26 August from https://www.seas.harvard.edu/climate/eli/research/equable/index.html

Pilli, R. A., & Assis, F. F. De. (2018). Organic Synthesis: New Vistas in the Brazilian Landscape. *Anais Da Academia Brasileira de Ciências*, *90*(1 suppl 1), 895–941. https://doi.org/10.1590/0001-3765201820170564

Pistone, K., Eisenman, I., Ramanathan, V. (2019). Radiative Heating of an Ice-Free Arctic Ocean. *Geophysical Research Letters, 46*, 7474-7480. https://doi.org/10.1029/2019GL082914

Pizzol, M., Christensen, P., Schmidt, J., & Thomsen, M. (2011). Impacts of “metals” on human health: A comparison between nine different methodologies for Life Cycle Impact Assessment (LCIA). *Journal of Cleaner Production, 19*(6–7), 646–656. https://doi.org/10.1016/j.jclepro.2010.05.007

Plotkin, J. S. (2016). *The Propylene Quandary*. https://www.acs.org/content/acs/en/pressroom/cutting-edge-chemistry/the-propylene-quandary.html

Posch, W. (2011). Polyolefins. In *Applied Plastics Engineering Handbook*. Elsevier. https://doi.org/https://doi.org/10.1016/C2010-0-67336-6

Pöschl, U. (2005). Atmospheric Aerosols: Composition, Transformation, Climate and Health Effects. *Angewandte Chemie International Edition, 44*(46), 7520–7540. https://doi.org/https://doi.org/10.1002/anie.200501122

Quachio, R., Germiniani, D. S., Pinto, G. A., Pavanelli, P. E., & Tizzo, L. M. (2012). Improvements in Energy Efficiency of Polyethylene Autoclave Reactor using Advanced Process Control. *IFAC Proceedings Volumes*, *45*(15), 732–737. https://doi.org/10.3182/20120710-4-SG-2026.00061

RBN energy. (2014). *Changes In The US Reformate Market*. https://rbnenergy.com/don-t-fear-the-catalytic-reformer-changes-in-the-us-reformate-market

Realmonte, G., Drouet, L., Gambhir, A., Glynn, J., Hawkes, A., Köberle, A. C., & Tavoni, M. (2019). An inter-model assessment of the role of direct air capture in deep mitigation pathways. *Nature Communications*, *10*(1), 3277. https://doi.org/10.1038/s41467-019-10842-5

Rebsdat, S., & Mayer, D. (2012a). Ethylene glycol. In *Ullmann’s Encyclopedia of Industrial Chemistry*.

Rebsdat, S., & Mayer, D. (2012b). Ethylene oxide. In *Ullmann’s Encyclopedia of Industrial Chemistry*. https://doi.org/10.1002/14356007.a10_117

Ricke, K. L., Orr, J. C., Schneider, K., Caldeira, K. (2013). Risks to coral reefs from ocean carbonate chemistry changes in recent earth system model projections. *Environmental Research Letters, 8*(3), 034003. https://doi.org/10.1088/1748-9326/8/3/034003

Ritchie, H. (2020). *Energy mix*. https://ourworldindata.org/energy-mix

Rockström, J., Steffen, W., Noone, K., Persson, A., Chapin, F. S., Lambin, E., Lenton, T. M., Scheffer, M., Folke, C., Schellnhuber, H. J., Nykvist, B., de Wit, C. A., Hughes, T., van der Leeuw, S., Rodhe, H., Sörlin, S., Snyder, P. K., Costanza, R., Svedin, U., … Foley, J. (2009). Planetary boundaries: exploring the safe operating space for humanity. *Ecology and Society, 14*(2), Article 32. http://www.ecologyandsociety.org/vol14/iss2/art32/

Rosa, L., Sanchez, D. L., & Mazzotti, M. (2021). Assessment of carbon dioxide removal potential via BECCS in a carbon-neutral Europe . *Energy & Environmental Science*. https://doi.org/10.1039/d1ee00642h

Ryberg, M. W., Owsianiak, M., Clavreul, J., Mueller, C., Sim, S., King, H., Hauschild, M. Z. (2018a). How to bring absolute sustainability into decision-making: An industry case study using a Planetary Boundary-based methodology. *Science of The Total Environment*, *634*, 1406-1416. https://doi.org/10.1016/j.scitotenv.2018.04.075

Ryberg, M. W., Owsianiak, M., Richardson, K., Hauschild, M. Z. (2018b). Development of a life-cycle impact assessment methodology linked to the Planetary Boundaries framework. *Ecological Indicators, 88*, 250-262. https://doi.org/10.1016/j.ecolind.2017.12.065

Ryberg, M.W., Owsianiak, M., Richardson, K., Hauschild, M.Z. (2016). Challenges in implementing a planetary boundaries based life-cycle impact assessment methodology. *Journal of Cleaner Production, 139*, 450–459. https://doi.org/10.1016/j.jclepro.2016.08.074

Sabio, N., Pozo, C., Guillén-Gosálbez, G., Jiménez, L., Karuppiah, R., Vasudevan, V., Sawaya, N., Farrell, J. T. (2014). Multiobjective optimization under uncertainty of the economic and life-cycle environmental performance of industrial processes. *American Institute of Chemical Engineers, 60*(6), 2098-2121. https://doi.org/10.1002/aic.14385

Sadiku, R., Ibrahim, D., Agboola, O., Owonubi, S. J., Fasiku, V. O., Kupolati, W. K., Jamiru, T., Eze, A. A., Adekomaya, O. S., Varaprasad, K., Agwuncha, S. C., Reddy, A. B., Manjula, B., Oboirien, B., Nkuna, C., Dludlu, M., Adeyeye, A., Osholana, T. S., Phiri, G., … Ojijo, V. (2017). Automotive components composed of polyolefins. In *Polyolefin Fibres* (pp. 449–496). Elsevier. https://doi.org/10.1016/B978-0-08-101132-4.00015-1

Sala, S., Crenna, E., Secchi, M., & Sanyé-Mengual, E. (2020). Environmental sustainability of European production and consumption assessed against planetary boundaries. *Journal of Environmental Management, 269*(April). https://doi.org/10.1016/j.jenvman.2020.110686

Samper, C. (2009). Planetary boundaries: Rethinking biodiversity. Nature Climate Change, 1(910), 118–119. https://doi.org/10.1038/climate.2009.99

Samper, M., Bertomeu, D., Arrieta, M., Ferri, J., & López-Martínez, J. (2018). Interference of Biodegradable Plastics in the Polypropylene Recycling Process. *Materials*, *11*(10), 1886. https://doi.org/10.3390/ma11101886

Sandin, G., Peters, G. M., & Svanström, M. (2015). Using the planetary boundaries framework for setting impact-reduction targets in LCA contexts. *The International Journal of Life Cycle Assessment, 20*(12), 1684–1700. https://doi.org/10.1007/s11367-015-0984-6

Sastri, V. R. (2014). Commodity Thermoplastics. In *Plastics in Medical Devices* (pp. 73–120). Elsevier. https://doi.org/10.1016/B978-1-4557-3201-2.00006-9

Sawyer, G. (2015). *Propylene & Its Products*. https://www.aiche.org/academy/videos/basics-chemical-industry-propylene-its-products

Schlanger, S. O., Hilbrecht, H., & Arthur, M. A. (1986). The Cenomanian-Turonian boundary event: sedimentary, faunal and geochemical criteria developed from stratigraphic studies in NW-Germany Title. In Walliser O.H. (Ed.), *Global Bio-Events. Lecture Notes in Earth Sciences, vol 8*. Springer. https://doi.org/doi.org/10.1007/BFb0010217

Schlesinger, W. H, E. S. Bernhardt. (2013). Biogeochemistry: An Analysis of Global Change, 3rd Edition. https://doi.org/10.1016/C2010-0-66291-2

School of Ocean and Earth Science and Technology (SOEST). (2020). *Aragonite Saturation State of Seawater.* Retrieved 25 August 2020 from http://www.soest.hawaii.edu/mguidry/Unnamed_Site_2/Chapter%205/Figures/Box3SeawaterSaturationState.pdf

Sekerci, Y. (2020). Climate change effects on fractional order prey-predator model. *Chaos, Solitons & Fractals, 134,* 109690. https://doi.org/10.1016/j.chaos.2020.109690

Service, R. (2018). Ammonia—a renewable fuel made from sun, air, and water—could power the globe without carbon. *Science*. https://doi.org/10.1126/science.aau7489

Sheehan, R. (2011). Terephthalic Acid, Dimethyl Terephthalate, and Isophthalic Acid. In *Ullmann's Encyclopedia of Industrial Chemistry*. Wiley-VCH Verlag GmbH & Co. KGaA. https://doi.org/10.1002/14356007.a26_193.pub2

Sigman, D. M., & Hain, M. P. (2012). The Biological Productivity of the Ocean: Section 4. *Ature Education Knowledge, 2*(10), 1–19.

Simpson, D., Arneth, A., Mills, G., Solberg, S., Uddling, J. (2014). Ozone — the persistent menace: interactions with the N cycle and climate change. *Current Opinion in Environmental Sustainability, 9*, 9-19. https://doi.org/10.1016/j.cosust.2014.07.008

Somoza-Tornos, A., Gonzalez-Garay, A., Pozo, C., Graells, M., Espuña, A., & Guillén-Gosálbez, G. (2020). Realizing the Potential High Benefits of Circular Economy in the Chemical Industry: Ethylene Monomer Recovery via Polyethylene Pyrolysis. *ACS Sustainable Chemistry & Engineering*, *8*(9), 3561–3572. https://doi.org/10.1021/acssuschemeng.9b04835

Sonesson, U., Berlin, J., & Ziegler, F. (2010). *Environmental Assessment and Management in the Food Industry. Life Cycle Assessment and Related Approaches*.

Song, G., & Tang, L. (2018). Optimization Model for the Transfer Line Exchanger System. *Computer Aided Chemical Engineering*, *44*, 1015–1020. https://doi.org/https://doi.org/10.1016/B978-0-444-64241-7.50164-6

Speight, J. G. (2020). *The Refinery of the Future (Second Edition)*.

SPINE. (1999). *SPINE LCI dataset: Production of ammonia*. http://cpmdatabase.cpm.chalmers.se/Scripts/sheet.asp?ActId=CPMXFRTOOL1999-04-15835

Steffen, W., Richardson, K., Rockström, J., Cornell, S. E., Fetzer, I., Bennett, E. M., Biggs, R., Carpenter, S. R., de Vries, W. de Wit, C. A., Folke, C., Gerten, D., Heinke, J., Mace, G. M., Persson, L. M., Ramanathan, V., Reyers, B., Sörlin, S. (2015). Planetary boundaries: Guiding human development on a changing planet. *Science, 347*(6223), 1259855. https://doi.org/10.1126/science.1259855

Struijs, J., Beusen, A., De Zwart, D., Huijbregts, M. (2011). Characterization factors for inland water eutrophication at the damage level in life cycle impact assessment *The International Journal of Life Cycle Assessment, 16,* 59–64. https://doi.org/10.1007/s11367-010-0232-z

Suding, P. (2013). *Chemical Plant GHG Emissions, Technical Note No. IDB-TN-618*. *December*.

SUPER-Lab-repository. (2020). SUPER-Lab-repository/SUPER_Lab: Data for Figures on allocating national CDR quotas (Version v1.0). Zenodo. http://doi.org/10.5281/zenodo.3925151

SUPER-Lab-repository. (2020). *SUPER-Lab-repository/SUPER_Lab: Data for Figures on allocating national CDR quotas (Version v1.0). Zenodo.* https://doi.org/10.5281/zenodo.3925151

Tarrés, Q. (2019). *Química ecològica*.

Texas A&M University. (2012). *Catalytic Reforming*. https://www.chem.tamu.edu/class/majors/chem470/Catalytic_Reforming.html

Thakur, A. K., Gupta, S. K., & Chaudhari, P. (2020). Slurry-phase ethylene polymerization processes: a review on multiscale modeling and simulations. *Reviews in Chemical Engineering*. https://doi.org/10.1515/revce-2020-0048

The Environmental Literacy Council. (2020). *Biogeochemical Cycles.* Retrieved 26 August 2020 from https://enviroliteracy.org/air-climate-weather/biogeochemical-cycles/

The Institute for Industrial Productivity. (n.d.). *Ammonia*. http://www.iipinetwork.org/wp-content/Ietd/content/ammonia.html

The Royal Society. (2005). *Ocean Acidification Due to Increasing Atmospheric Carbon Dioxide* (Policy Document 12/05). https://royalsociety.org/~/media/Royal_Society_Content/policy/publications/2005/9634.pdf

Thomas, Z. A. (2016). Using natural archives to detect climate and environmental tipping points in the Earth System. *Quaternary Science Reviews, 152*, 60–71. https://doi.org/10.1016/j.quascirev.2016.09.026

Timmer, M. P., Dietzenbacher, E., Los, B., Stehrer, R. and de Vries, G. J. (2015), An Illustrated User Guide to the World Input–Output Database: the Case of Global Automotive Production, *Review of International Economics., 23*, 575–605

Toama, H. (2017). World Phosphate Industry. *Iraqui Bulletin of Geology and Mining*, *7*, 5–23.

Tolman, K. G., & Dalpiaz, A. S. (2013). Occupational and Environmental Hepatotoxicity. In Drug-Induced Liver Disease (pp. 659–675). Elsevier. https://doi.org/10.1016/B978-0-12-387817-5.00036-4

Tumoisto, H. L., Hodge, I. D., Riordan, P., Macdonald, D. W. (2012). Exploring a safe operating approach to weighting in life cycle impact assessment – a case study of organic, conventional and integrated farming systems. *Journal of Cleaner Production, 37*, 147-153. https://doi.org/10.1016/j.jclepro.2012.06.025

Udugama, I. A. (2017). *Improving Operations of Methanol Refining* [Technical University of Denmark]. https://doi.org/10.13140/RG.2.2.22538.47041

United Nations. (1972). *United Nations Conference on the Environment, 5-16 June 1972, Stockholm*.

United Nations. (2012). Sustainable Development Goals (SDGs). United Nations Conference on Sustainable Development, Rio+20. https://sustainabledevelopment.un.org/topics/sustainabledevelopmentgoals

United Nations. (2013). *Composition of macro geographical regions, geographical sub-regions, and selected economic and other groupings*. Retrieved September 14, 2020 from http://unstats.un.org/unsd/methods/m49/m49regin.htm

United Nations. (2016). *The Environmental Movement's Greatest Success Story: Ozone Layer Begins to Heal*. https://www.unep.org/news-and-stories/story/environmental-movements-greatest-success-story-ozone-layer-begins-heal

United Nations. (2017). Factsheet: Biodiversity. *In UN Ocean Conference: New York, United States*. Retrieved 25 August 2020 from https://sustainabledevelopment.un.org/content/documents/Ocean_Factsheet_Biodiversity.pdf

United Nations. (2019). *Probabilistic Population Projections Rev. 1 based on the World Population Prospects 2019.* Retrieved 1 September 2020 from http://population.un.org/wpp/

United Nations. (2020a). UN Ocean Conference. [Video]. https://www.un.org/en/conferences/ocean2020

United Nations. (2020b). *About Montreal Protocol.* Retrieved 26 August 2020 from https://www.unenvironment.org/ozonaction/who-we-are/about-montreal-protocol

United Nations. (2020c). World Population Pospects 2019. [Data file]. Retrieved from https://population.un.org/wpp/Download/Standard/Population/

United Nations. (2020d). *The Climate Crisis – A Race We Can Win*. https://www.un.org/en/un75/climate-crisis-race-we-can-win

University of London. (n. d.). *Environmental Science and Management: The Earth System and its Components*. Retrieved 24 August 2020 from https://www.soas.ac.uk/cedep-demos/000_P500_ESM_K3736-Demo/unit1/page_15.htm

van Leeuwen, P. W. N. M. (2003). Catalysis, Homogeneous. In *Encyclopedia of Physical Science and Technology* (pp. 457–490). Elsevier. https://doi.org/10.1016/B0-12-227410-5/00085-5

Van Zelm, R., Huijbregts, M. A. J., Posthuma, L., Wintersen, A., Van de Meent, D. (2009). Pesticide ecotoxicological effect factors and their uncertainties for freshwater ecosystems. *The International Journal of Life Cycle Assessment, 14,* 43–51, https://doi.org/10.1007/s11367-008-0037-5.

Verburg, P. H., Crossman, N., Ellis, E. C., Heinimann, A., Hostert, P., Mertz, O., Nagendra, H., Sikor, T., Erb, K.-H., Golubiewski, N., Grau, R., Grove, M., Konaté, S., Meyfroidt, P., Parker, D. C., Chowdhury, R. R., Shibata, H., Thomson, A., & Zhen, L. (2015). Land system science and sustainable development of the earth system: A global land project perspective. *Anthropocene*, *12*, 29–41. https://doi.org/10.1016/j.ancene.2015.09.004

Verburg, P. H., Mertz, O., Erb, K. H., Haberl, H., & Wu, W. (2013). Land system change and food security: Towards multi-scale land system solutions. *Current Opinion in Environmental Sustainability, 5*(5), 494–502. https://doi.org/10.1016/j.cosust.2013.07.003

Vetter, G. (2001). Chapter 1. In *High Pressure Process Technology: Fundamentals and Applications* (pp. 1–15). https://doi.org/10.1016/S0926-9614(01)80019-8

Villada, C., Jaramillo, F., Castaño, J. G., Echeverría, F., & Bolívar, F. (2019). Design and development of nitrate-nitrite based molten salts for concentrating solar power applications. *Solar Energy*, *188*, 291–299. https://doi.org/10.1016/j.solener.2019.06.010

Vitousek, P. M., Aber, J. D., Howarth, R. W., Likens, G. E., Matson, P. A., Schindler, D. W., Schlesinger, W. H., Tilman, D. G. (1997). Human alteration of the global nitrogen cycle: Sources and consequences. *Ecological Applications, 7*, 737-750, doi:10.1890/1051-0761(1997)007[0737:HAOTGN]2.0.CO;2

Wang, J. A., Sulla-Menashe, D., Woodcock, C. E., Sonnentag, O., Keeling, R. F., & Friedl, M. A. (2019). Extensive land cover change across Arctic–Boreal Northwestern North America from disturbance and climate forcing. *Global Change Biology, 26*(2), 807–822. https://doi.org/doi.org/10.1111/gcb.14804

Waters, C. N., Zalasiewicz, J., Summerhayes, C., Barnosky, A. D., Poirier, C., Ga uszka, A., Cearreta, A., Edgeworth, M., Ellis, E. C., Ellis, M., Jeandel, C., Leinfelder, R., McNeill, J. R., Richter, D. d., Steffen, W., Syvitski, J., Vidas, D., Wagreich, M., Williams, M., … Wolfe, A. P. (2016). The Anthropocene is functionally and stratigraphically distinct from the Holocene. *Science, 351*(6269), aad2622–aad2622. https://doi.org/10.1126/science.aad2622

Weidema, Bauer, C., Hischier, R., Mutel, C., Nemecek, T., Reinhard, J., Vadenbo, C. O., & Wernet, G. (2013). Overview and methodology. Data quality guideline for the ecoinvent database version 3.

Weidema, P. B., & Wesnaes, S. M. (1996). Data quality management for life cycle inventories-an example of using data quality indicators. In *J. Cleaner Prod* (Vol. 4, Issue 1).

Wernet, G., Bauer, C., Steubing, B., Reinhard, J., Moreno-Ruiz, E., Weidema, B. (2016). The ecoinvent database version 3 (part I): overview and methodology. *The International Journal of Life Cycle Assessment, 21*(9), pp.1218–1230. Available at: http://link.springer.com/10.1007/s11367-016-1087-8

Werth, D., & Avissar, R. (2004). The Regional Evapotranspiration of the Amazon. *Journal of Hydrometeorology, 5*(1). https://doi.org/10.1175/1525-7541(2004)005<0100:TREOTA>2.0.CO;2

Wittkoff, H. A., & Reuben, B. A. (1996). *Industrial Organic Chemicals*. John Wiley & Sons.

Witze, A. (2020). Rare ozone hole opens over the arctic. Nature, 580, 18-19. https://doi.org/10.1038/d41586-020-00904-w

Wohlleben, P. (2020). *La vida secreta dels arbres*. Cossetània Edicions.

Wolff, A., Gondran, N., & Brodhag, C. (2017). Detecting unsustainable pressures exerted on biodiversity by a company. Application to the food portfolio of a retailer. *Journal of Cleaner Production*, *166*, 784–797.

World Data Bank. (2019). Land area (sq. km), European Union. https://data.worldbank.org/indicator/AG.LND.TOTL.K2?locations=EU

World Meteorological Organization. (2018). *Scientific Assessment of Ozone Depletion Global Ozone Research and Monitoring Project*. https://ozone.unep.org/sites/default/files/2019-05/SAP-2018-Assessment-report.pdf

Yang, Z.-J., Ren, N., Zhang, Y.-H., & Tang, Y. (2010). Studies on mechanism for homogeneous catalytic hydration of ethylene oxide: Effects of pH window and esterification. *Catalysis Communications*, *11*(5), 447–450. https://doi.org/10.1016/j.catcom.2009.11.020

Youssef, A. (2019). *Solution & Bulk polymerization*. https://doi.org/10.13140/RG.2.2.16472.96001/2

Zarubina, V. (2015). *Oxidative dehydrogenation of ethylbenzene under industrially relevant conditions*.

Zavarin, G. A. (2008). *Encyclopedia of Ecology*. https://doi.org/10.1016/B978-008045405-4.00745-X

Zeebe, R. E. (2013). Time-dependent climate sensitivity and the legacy of anthropogenic greenhouse gas emissions. *Proceedings of the National Academy of Sciences of the United States of America, 110*(34), 13739-13744. https://doi.org/10.1073/pnas.1222843110

Zepp, R. G., Callaghan, T. V., Erickson, D. J. (2003). Interactive effects of ozone depletion and climate change on biogeochemical cicles. *Photochemical & Photobiological Sciences, 2*, 51-61. https://doi.org/10.1039/B211154N

Zhang, C., Shao, Z., Chen, X., Gu, X., Feng, L., & Biegler, L. T. (2016). Optimal flowsheet configuration of a polymerization process with embedded molecular weight distributions. *AIChE Journal*, *62*(1), 131–145. https://doi.org/10.1002/aic.15040

Zhang, L., Hoshika, Y., Carrari, E., Cotrozzi, L., Pellegrini, E., Paoletti, E. (2018). Effects of nitrogen and phosphorus imbalance on photosynthetic traits of poplar Oxford clone under ozone pollution. *Journal of Plant Research, 131*, 915-924. https://doi.org/10.1007/s10265-018-1071-4

Zhang, Q., Sun, J., Liu, J., Huang, G., Lu, C., & Zhang, Y. (2015). Driving mechanism and sources of groundwater nitrate contamination in the rapidly urbanized region of south China. *Journal of Contaminant Hydrology*, *182*, 221–230. https://doi.org/10.1016/j.jconhyd.2015.09.009

Zhong, X., Zhao, X., Qian, Y., & Zou, Y. (2017). Polyethylene plastic production process. *Materials Science: Materials Review*, *1*(1), 1–11.

Zhongqiong, Z., Qingbai, W., Guanli, J., Siru, G., Ji, C., Yongzhi, L. (2020). Changes in the permafrost temperatures from 2003 to 2015 in the Qinghai-Tibet Plateau. *Cold Regions Science and Technology, 169*, https://doi.org/10.1016/j.coldregions.2019.102904

Zimmerman, H. (2017). *Ullmann's Encyclopedia of Industrial Chemistry 7th ed.* John Wiley & Sons.